Peter Petrik

Structural investigation techniques in materials science

Ellipsometry

- Polarized light
- Hardver
- Modeling and evaluations
- Applications

Which photo was taken using a polarizing filter?

What is ellipsometry

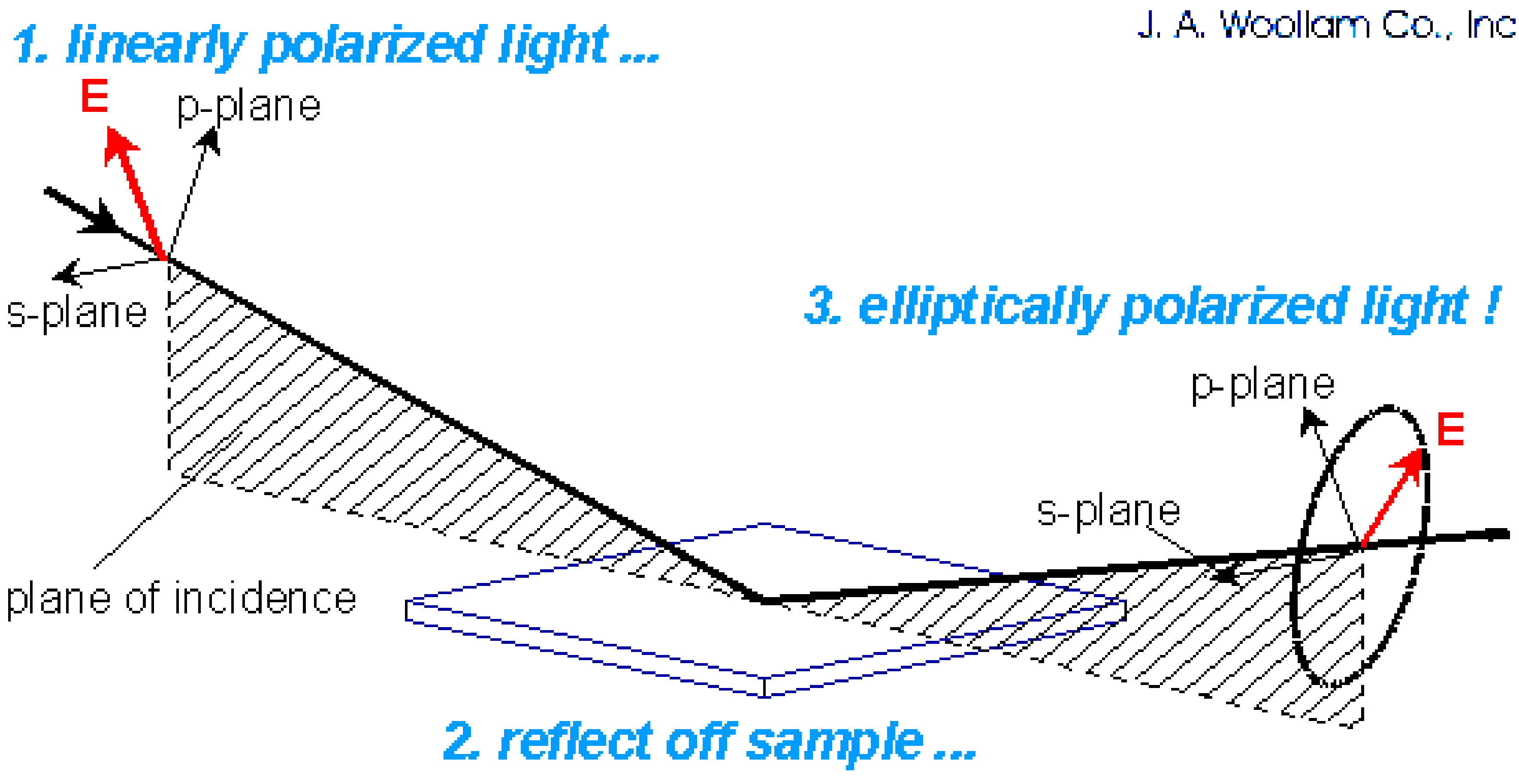

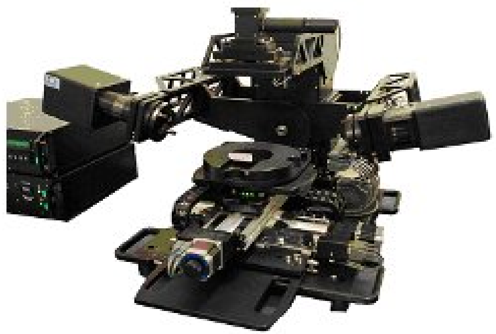

Woollam M2000DI

Forgókompenzátoros spektroszkópiai ellipszométer a 190-1700 nm hullámhossztartományban automatikus goniométerrel és mintamozgató asztallal. Fókuszálás minimálisan 0.15 mm-es folton. A mérési idő pontonként néhány másodperc.

SOPRA ES4G

Dupla-monokromátoros forgó-polarizátoros spektroszkópiai ellipszométer a 250-850 nm hullámhossztartományban. A foltméret kb. 1 mm. Különösen alkalmas nagy hullámhosszfelbontású precíziós mérésekre, ahol a sebesség nem annyira fontos követelmény.

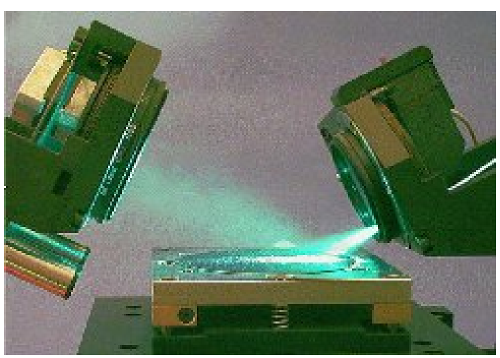

Divergens nyalábú térképező ellipszométer

Saját fejlesztésű térképező ellipszométer, amely számos hardver-változatban elkészült, többek között cluster-kamrára szerelve.

Papers with "ellipsometry" in the title or in the abstract

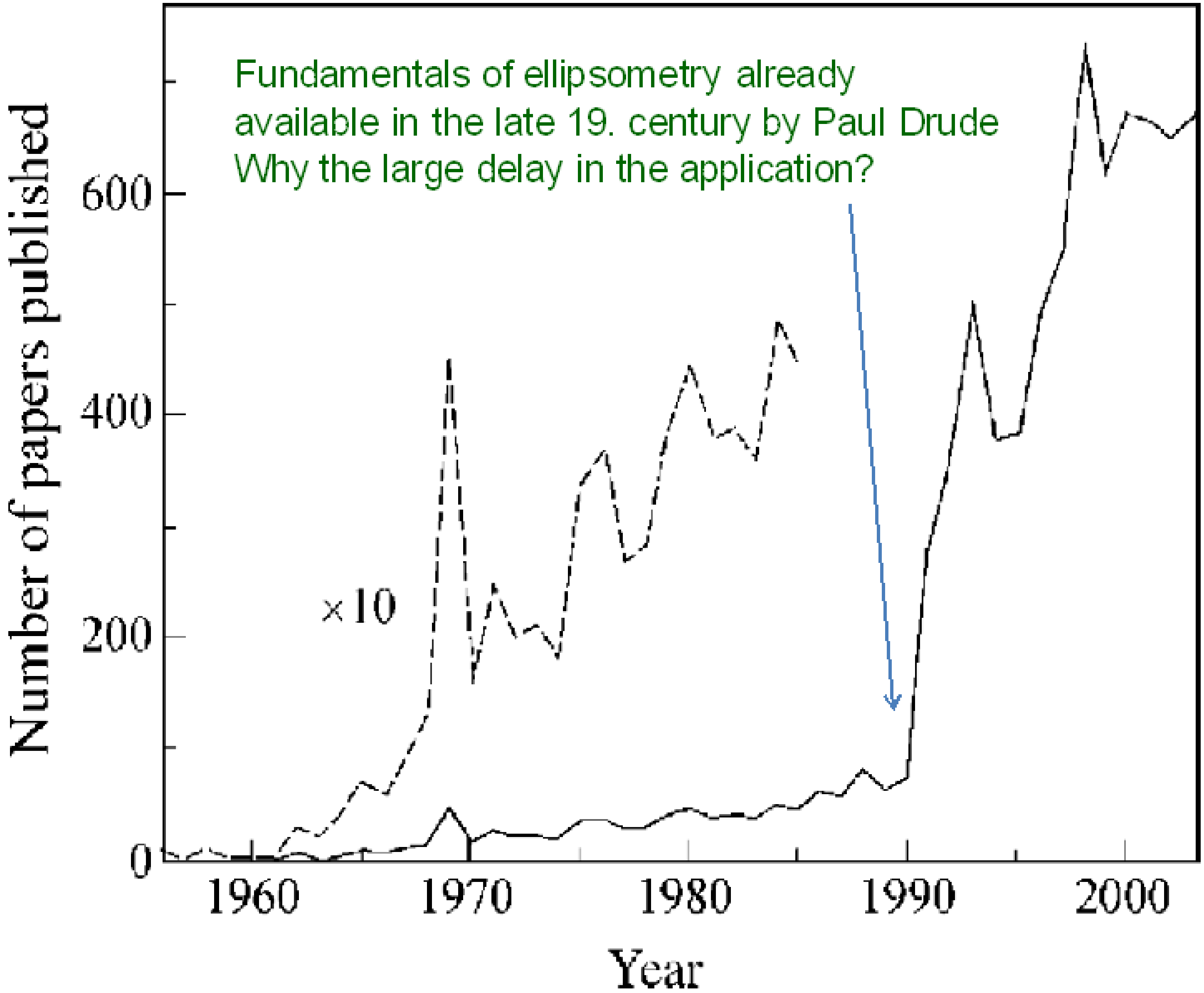

Propagation of electromagetic waves

$$E(z,t) = E_0 \sin\left(-\frac{2\pi}{\lambda}(z - \mathrm{v}t) + \xi\right)$$

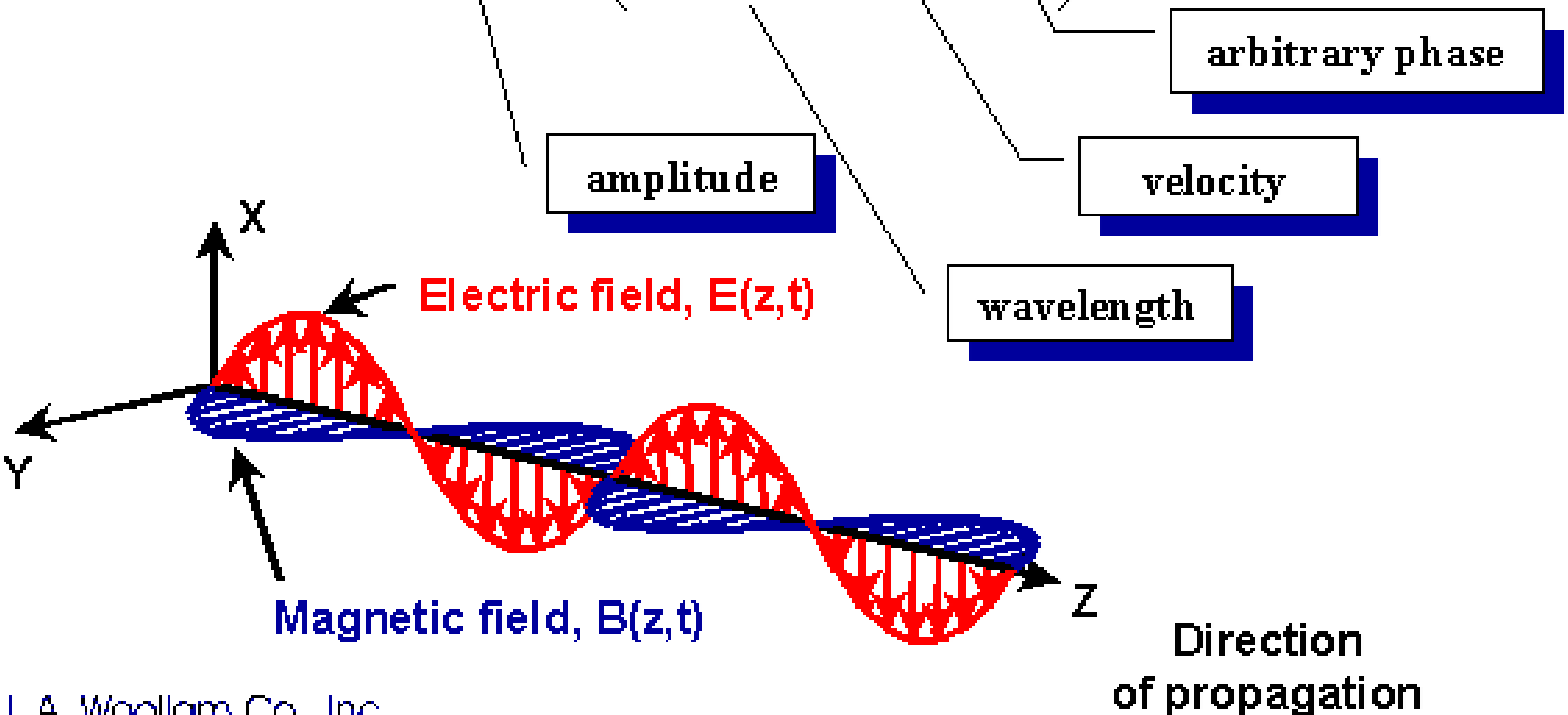

J. A. Woollam Co., Inc.

Polarization states

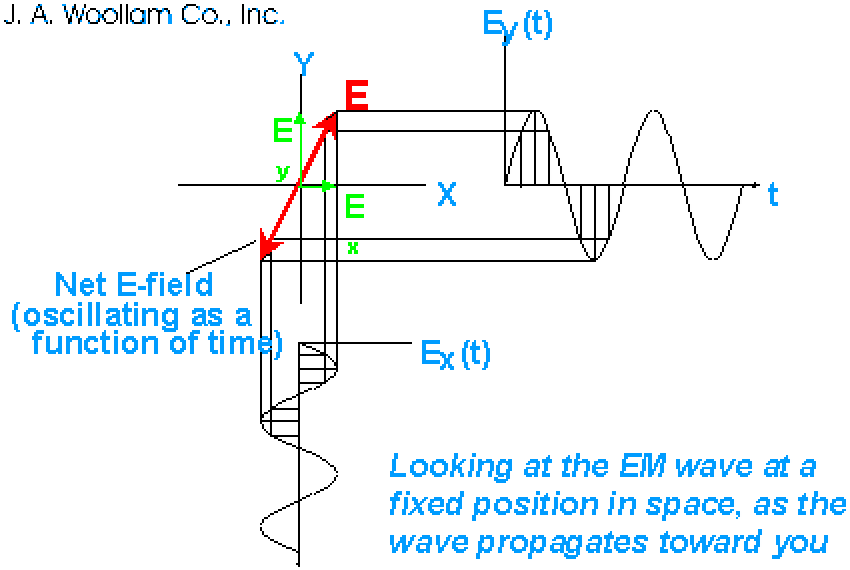

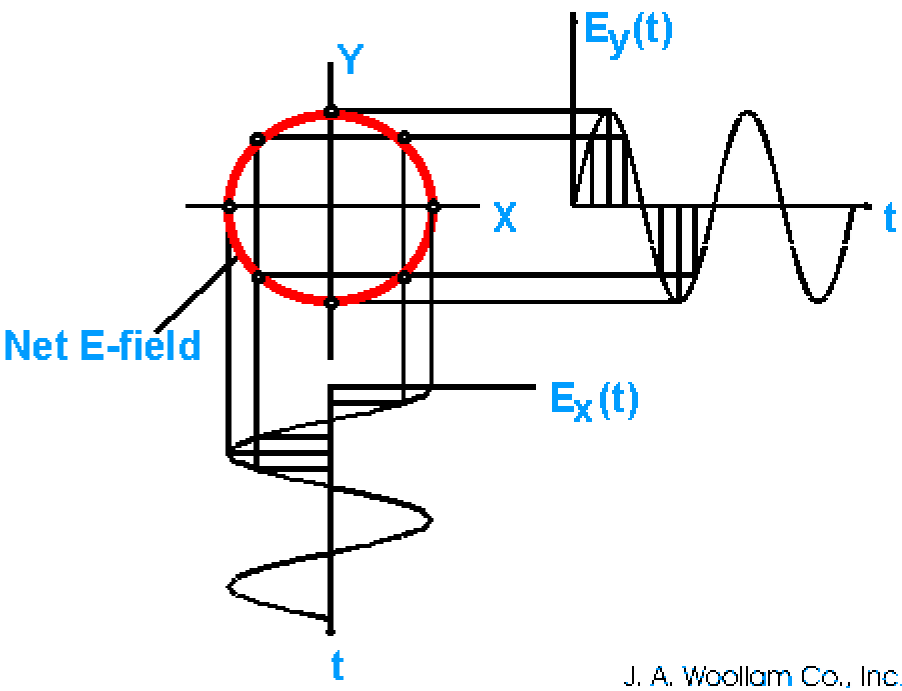

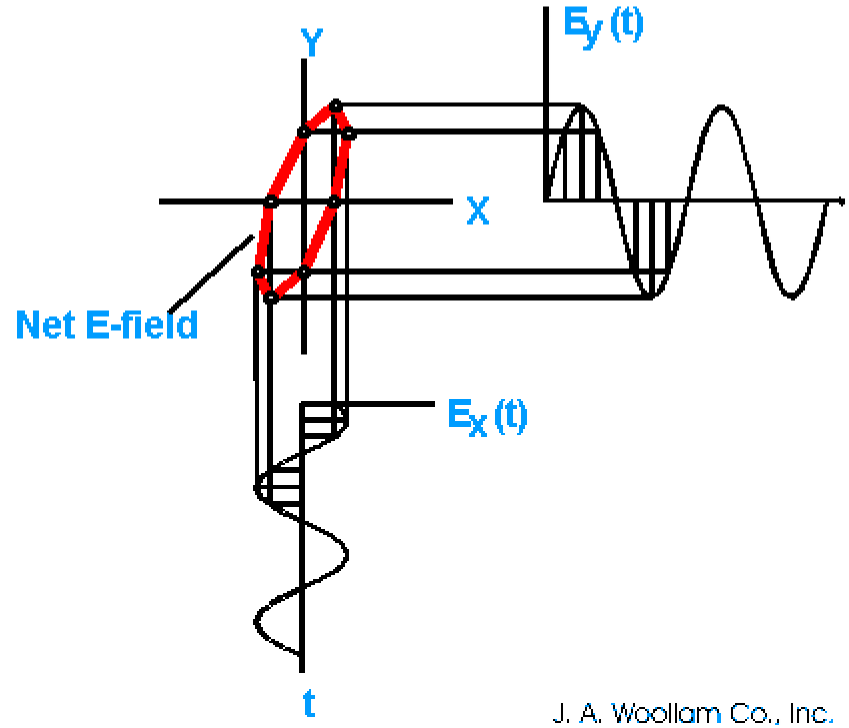

$$n_0 \sin(\Phi_i) = n_1 \sin(\Phi_t)$$

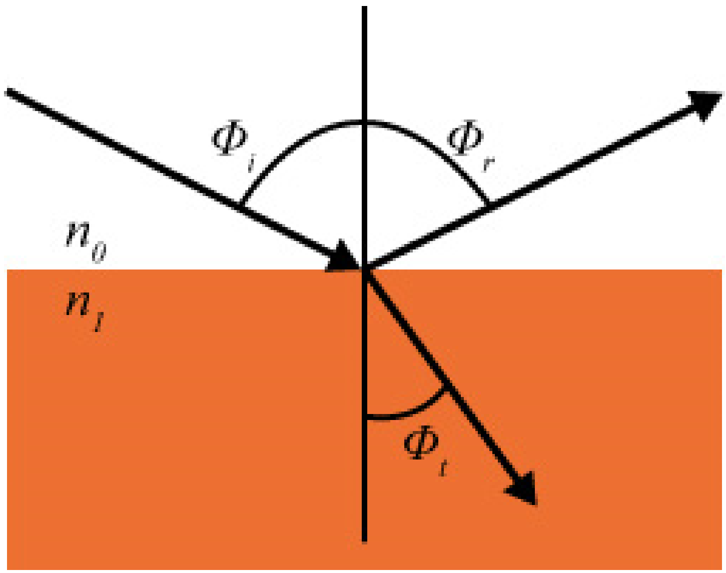

Light reflects and refracts according to Snell's law.

$$r_s = \left(\frac{E_{0r}}{E_{0i}}\right)_s = \frac{n_i \cos(\Phi_i) - n_t \cos(\Phi_t)}{n_i \cos(\Phi_i) + n_t \cos(\Phi_t)}$$

$$r_p = \left(\frac{E_{0r}}{E_{0i}}\right)_p = \frac{n_t \cos(\Phi_i) - n_i \cos(\Phi_t)}{n_i \cos(\Phi_t) + n_t \cos(\Phi_i)}$$

$$t_s = \left(\frac{E_{0t}}{E_{0i}}\right)_s = \frac{2 n_i \cos(\Phi_i)}{n_i \cos(\Phi_i) + n_t \cos(\Phi_t)}$$

$$t_p = \left(\frac{E_{0t}}{E_{0i}}\right)_p = \frac{2 n_i \cos(\Phi_i)}{n_i \cos(\Phi_t) + n_t \cos(\Phi_i)}$$

Hogyan lesz ebből ellipszis?

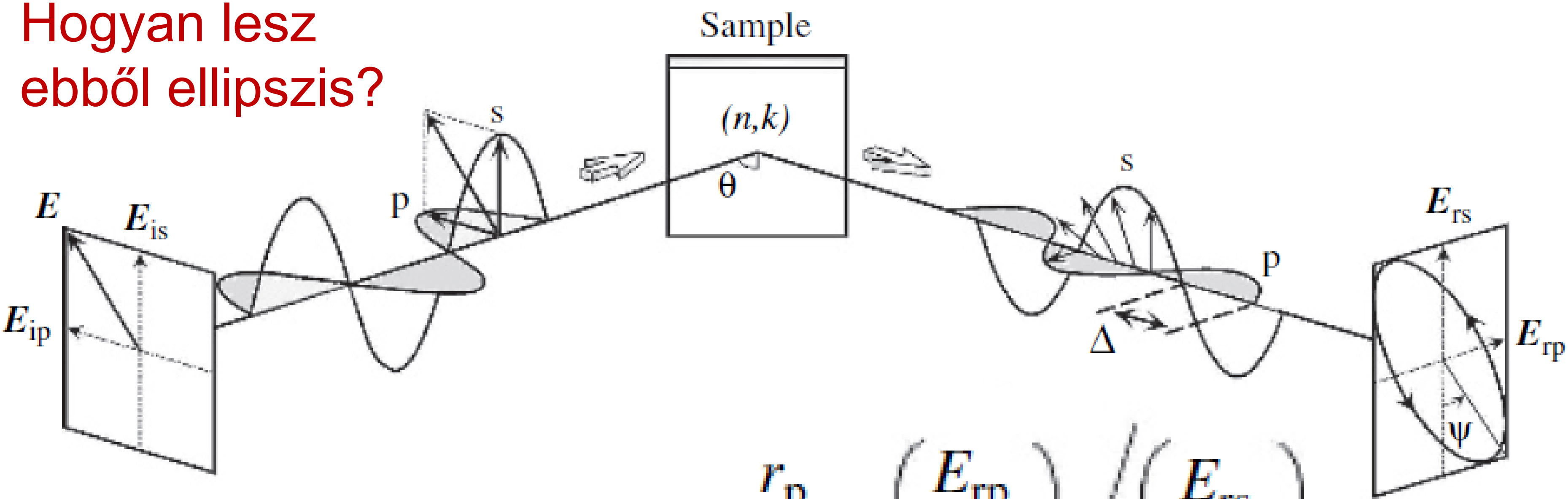

$$\rho \equiv \tan\psi \exp(i\Delta) \equiv \frac{r_p}{r_s} \equiv \left(\frac{E_{rp}}{E_{ip}}\right) \Big/ \left(\frac{E_{rs}}{E_{is}}\right)$$

ρ: komplex reflexiós együttható

Ψ,Δ: ellipszometriai szögek

r_p: reflexiós együttható a beesési sikkal párhuzamos polarizációra

r_s: reflexiós együttható a beesési síkra merőleges polarizációra

“Beépített” referencianyaláb: nem érzékeny a rezgésekre, a háttérre

Parameters measured by ellipsometry directly

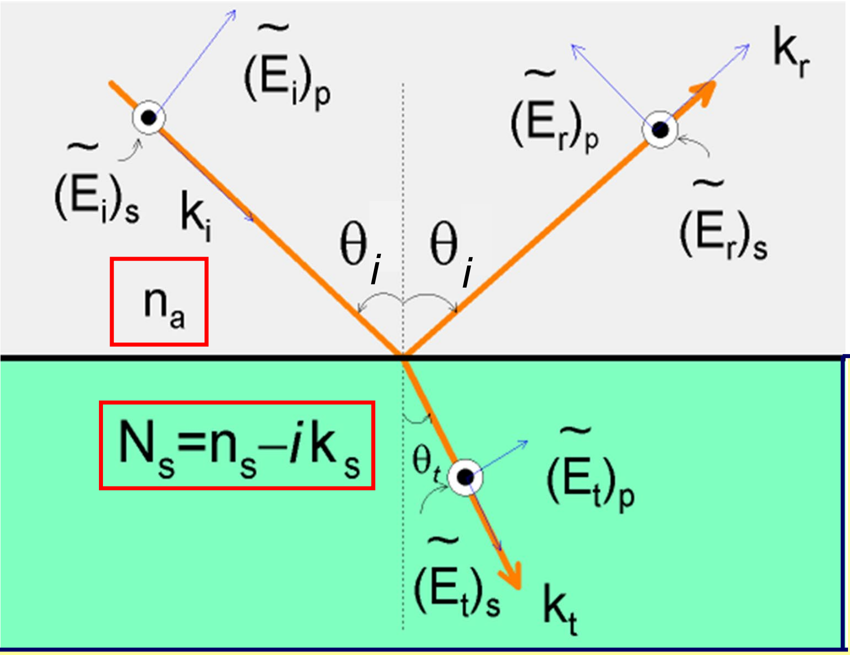

Determination of the Dielectric Function of an Ideal Isotropic Reflecting Solid

Requires: Known angle of incidence
Known index of refraction of ambient
"Perfect" interface between two media

$$\rho \equiv \tan\psi e^{i\Delta} \equiv \frac{r_p}{r_s} = \frac{\left(\dfrac{N_s \cos\theta_i - n_a \cos\theta_t}{N_s \cos\theta_i + n_a \cos\theta_t}\right)}{\left(\dfrac{n_a \cos\theta_i - N_s \cos\theta_t}{n_a \cos\theta_i + N_s \cos\theta_t}\right)}$$

$$n_a \sin\theta_i = N_s \sin\theta_t$$

From Fresnel equations
θ_i : angle of incidence
θ_t : angle of transmission

Inversion gives:

$$N_s = n_s - i\,k_s = n_a \sin\theta_i \left\{1 + \tan^2\theta_i \left(\frac{1-\tan\psi e^{i\Delta}}{1+\tan\psi e^{i\Delta}}\right)^2\right\}^{1/2}$$

(n_s, k_s) can be determined from (ψ, Δ) if θ_i is known.

Dielectric function definition: $\varepsilon_s = N_s^2$

$$\varepsilon_{1s} = n_s^2 - k_s^2 \qquad \varepsilon_{2s} = 2 n_s k_s$$

A measurement of r_p / r_s or (ψ, Δ) by ellipsometry wavelength point by point provides the dielectric function ε_s

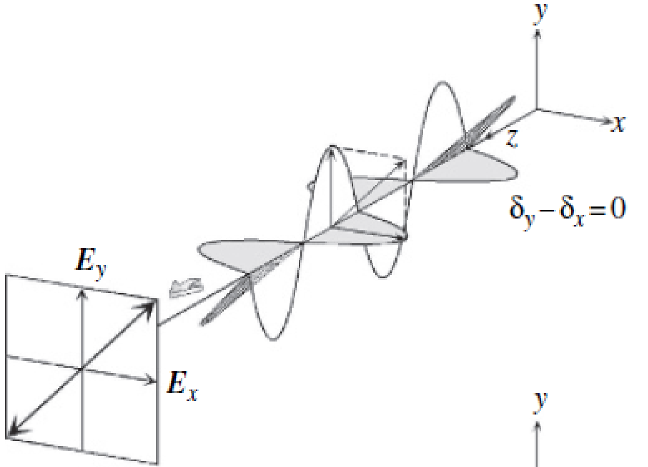

(a) Linear polarization

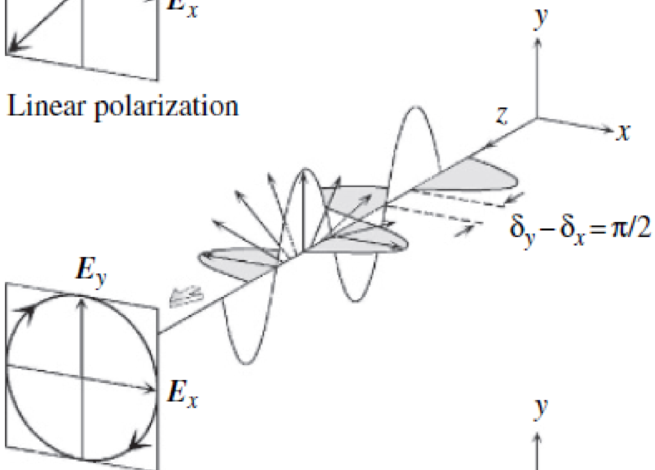

(b) Right-circular polarization

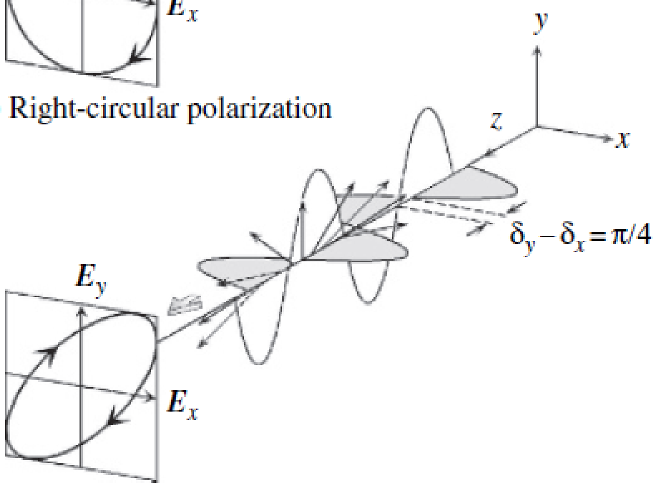

(c) Elliptical polarization

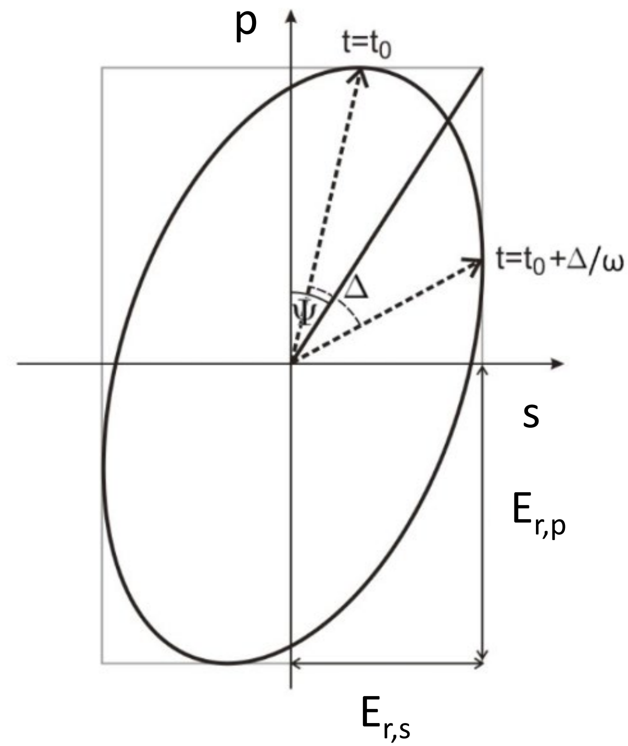

$$\overline{\rho} = \frac{\overline{\chi}_r}{\overline{\chi}_i} = \frac{|\overline{\chi}_r|}{|\overline{\chi}_i|} e^{i(\delta_r - \delta_i)} = \tan\Psi e^{i\Delta}$$

$$\frac{\overline{\chi}_r}{\overline{\chi}_i} = \frac{\frac{\overline{E}_{r,p}}{\overline{E}_{r,s}}}{\frac{\overline{E}_{i,p}}{\overline{E}_{i,s}}} = \frac{\frac{\overline{E}_{r,p}}{\overline{E}_{i,p}}}{\frac{\overline{E}_{r,s}}{\overline{E}_{i,s}}} = \frac{\overline{r}_p}{\overline{r}_s}$$

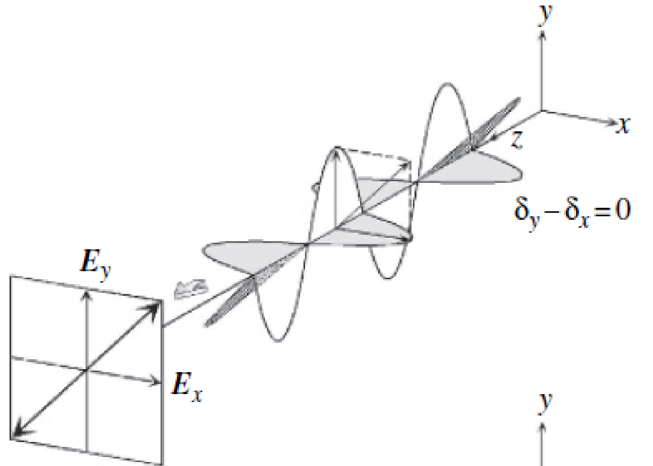

(a) Linear polarization

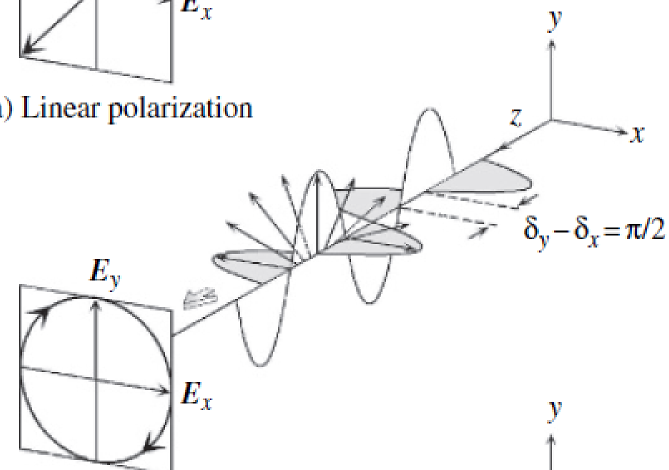

(b) Right-circular polarization

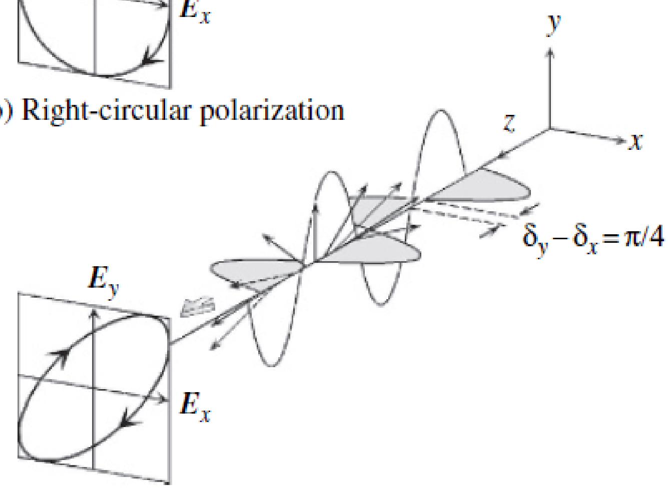

(c) Elliptical polarization

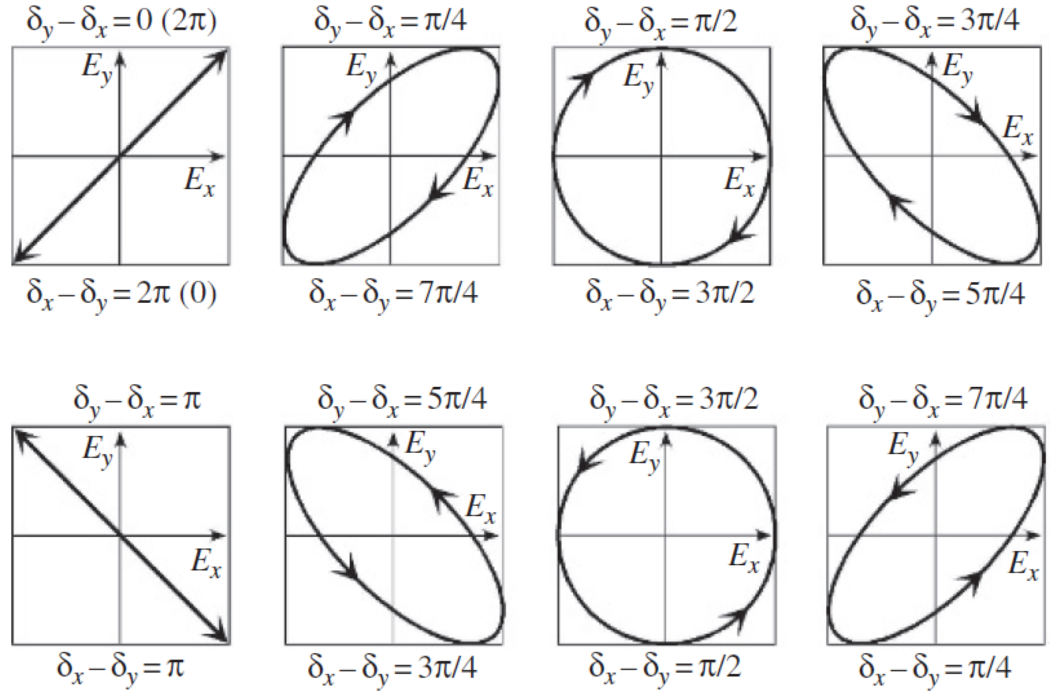

Forgó analizátoros ellipszométer működési elve

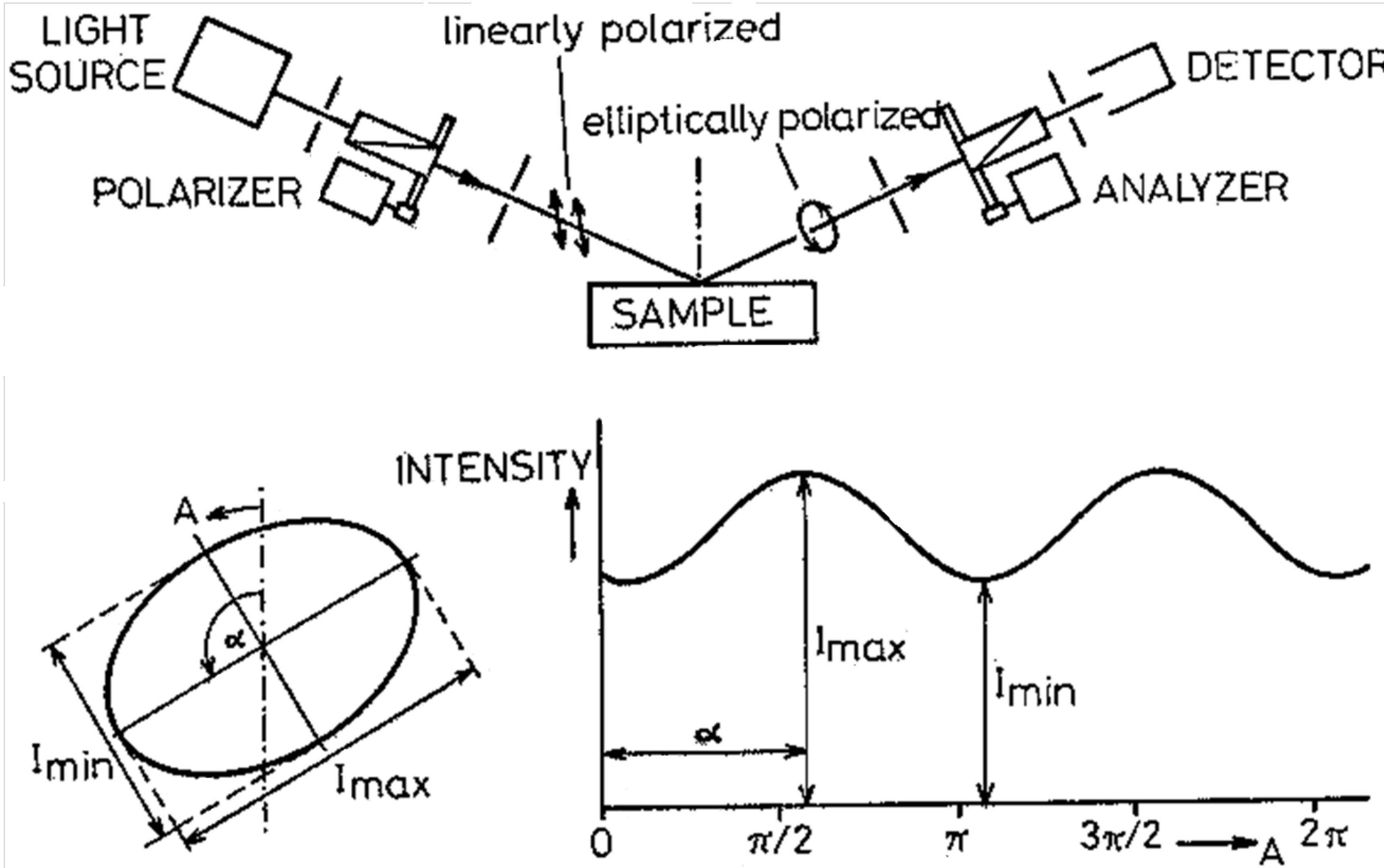

(a) Rotating-analyzer ellipsometry (PSA_R)

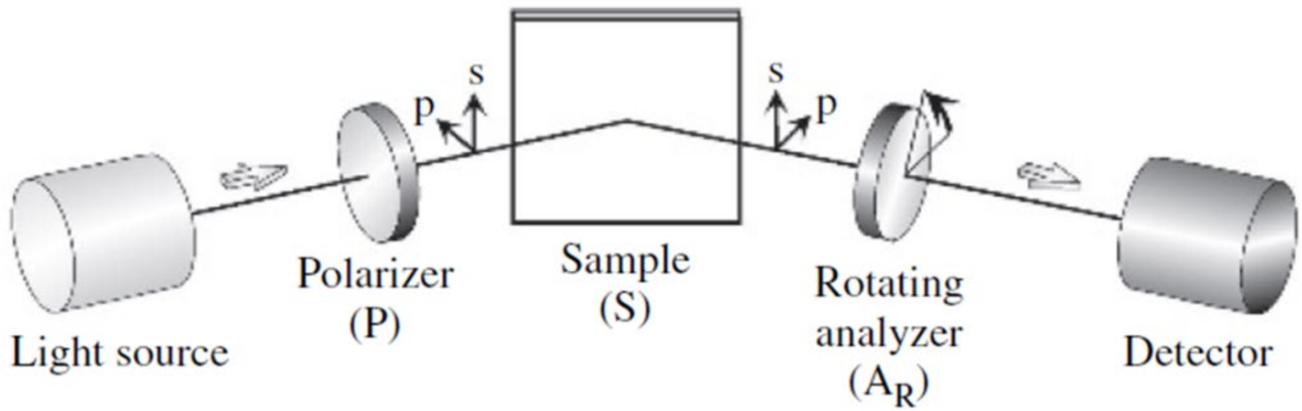

$$\begin{bmatrix} E_A \\ 0 \end{bmatrix} = \begin{bmatrix} 1 & 0 \\ 0 & 0 \end{bmatrix} \begin{bmatrix} \cos A & \sin A \\ -\sin A & \cos A \end{bmatrix} \begin{bmatrix} \sin\psi \exp(i\Delta) & 0 \\ 0 & \cos\psi \end{bmatrix} \times \begin{bmatrix} \cos P & -\sin P \\ \sin P & \cos P \end{bmatrix} \begin{bmatrix} 1 & 0 \\ 0 & 0 \end{bmatrix} \begin{bmatrix} 1 \\ 0 \end{bmatrix}$$

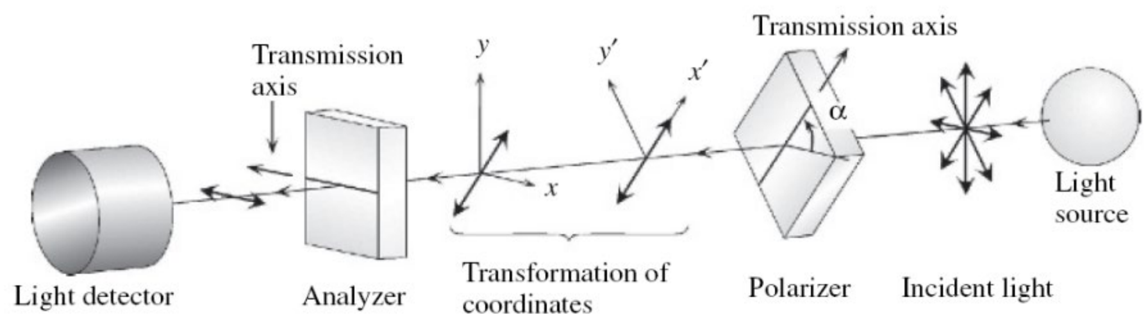

$$\begin{bmatrix} E_x \\ 0 \end{bmatrix} \quad \begin{bmatrix} 1 & 0 \\ 0 & 0 \end{bmatrix} \quad \begin{bmatrix} \cos\alpha & -\sin\alpha \\ \sin\alpha & \cos\alpha \end{bmatrix} \quad \begin{bmatrix} 1 & 0 \\ 0 & 0 \end{bmatrix} \quad \begin{bmatrix} E_P \\ 0 \end{bmatrix}$$

$$\begin{bmatrix} E_A \\ 0 \end{bmatrix} = \begin{bmatrix} 1 & 0 \\ 0 & 0 \end{bmatrix} \begin{bmatrix} \cos A & \sin A \\ -\sin A & \cos A \end{bmatrix} \begin{bmatrix} \sin\psi \exp(i\Delta) & 0 \\ 0 & \cos\psi \end{bmatrix}$$

$$\times \begin{bmatrix} \cos P & -\sin P \\ \sin P & \cos P \end{bmatrix} \begin{bmatrix} 1 & 0 \\ 0 & 0 \end{bmatrix} \begin{bmatrix} 1 \\ 0 \end{bmatrix}$$

P = 45°

⇩

$$\begin{bmatrix} E_A \\ 0 \end{bmatrix} = \begin{bmatrix} 1 & 0 \\ 0 & 0 \end{bmatrix} \begin{bmatrix} \cos A & \sin A \\ -\sin A & \cos A \end{bmatrix} \begin{bmatrix} \sin\psi \exp(i\Delta) \\ \cos\psi \end{bmatrix}$$

$$E_A = \cos A \sin\psi \exp(i\Delta) + \sin A \cos\psi$$

$$\begin{aligned} I &= |E_A|^2 \\ &= I_0 (1 - \cos 2\psi \cos 2A + \sin 2\psi \cos\Delta \sin 2A) \\ &= I_0 (1 + \alpha \cos 2A + \beta \sin 2A) \end{aligned}$$

$$\alpha = \frac{\cos 2P - \cos 2\psi}{1 - \cos 2P \cos 2\psi} \qquad \beta = \frac{\sin 2\psi \cos \Delta \sin 2P}{1 - \cos 2P \cos 2\psi}$$

$$\tan \psi = \sqrt{\frac{1+\alpha}{1-\alpha}}\,|\tan P| \qquad \cos \Delta = \frac{\beta}{\sqrt{1-\alpha^2}}$$

No sign obtained

Only the shape counts
Independent of intensity

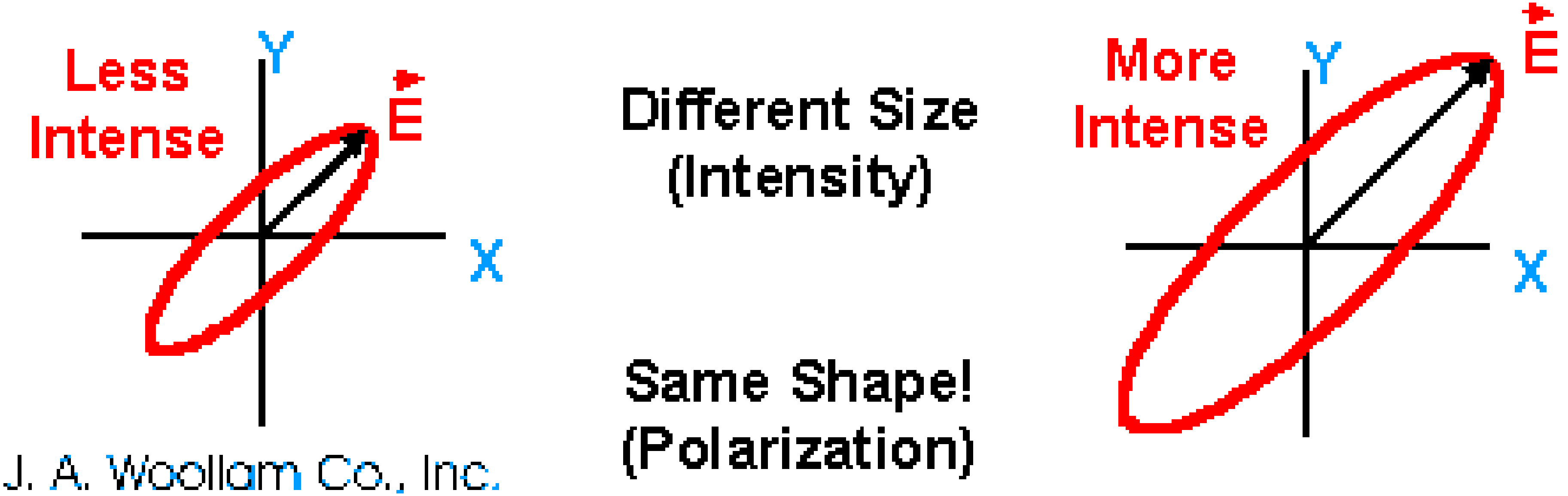

What can be measured

$$\rho = \tan(\psi)e^{i\Delta} = \frac{\tilde{R}_p}{\tilde{R}_s}$$

What Ellipsometry Measures:

Psi (Ψ)
Delta (Δ)

What we are Interested in:

- Film Thickness
- Refractive Index
- Surface Roughness
- Interfacial Regions
- Composition
- Crystallinity
- Anisotropy
- Uniformity

Desired information must be extracted Through a model-based analysis using equations to describe interaction of light and materials

J. A. Woollam Co., Inc.

Absorption

$$I = I_o e^{-\alpha z}$$

$$\alpha = \frac{4\pi k}{\lambda}$$

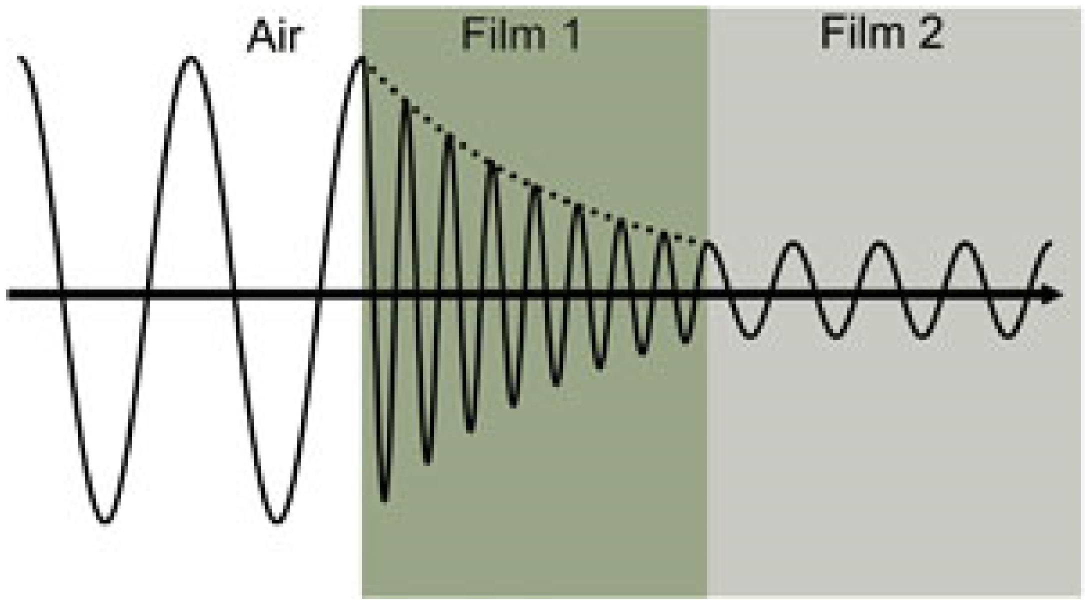

Wave travels from air into absorbing Film 1 and then transparent Film 2. The phase velocity and wavelength change in each material depending on index of refraction (Film 1: n=4, Film 2: n=2).

Optical penetration depth

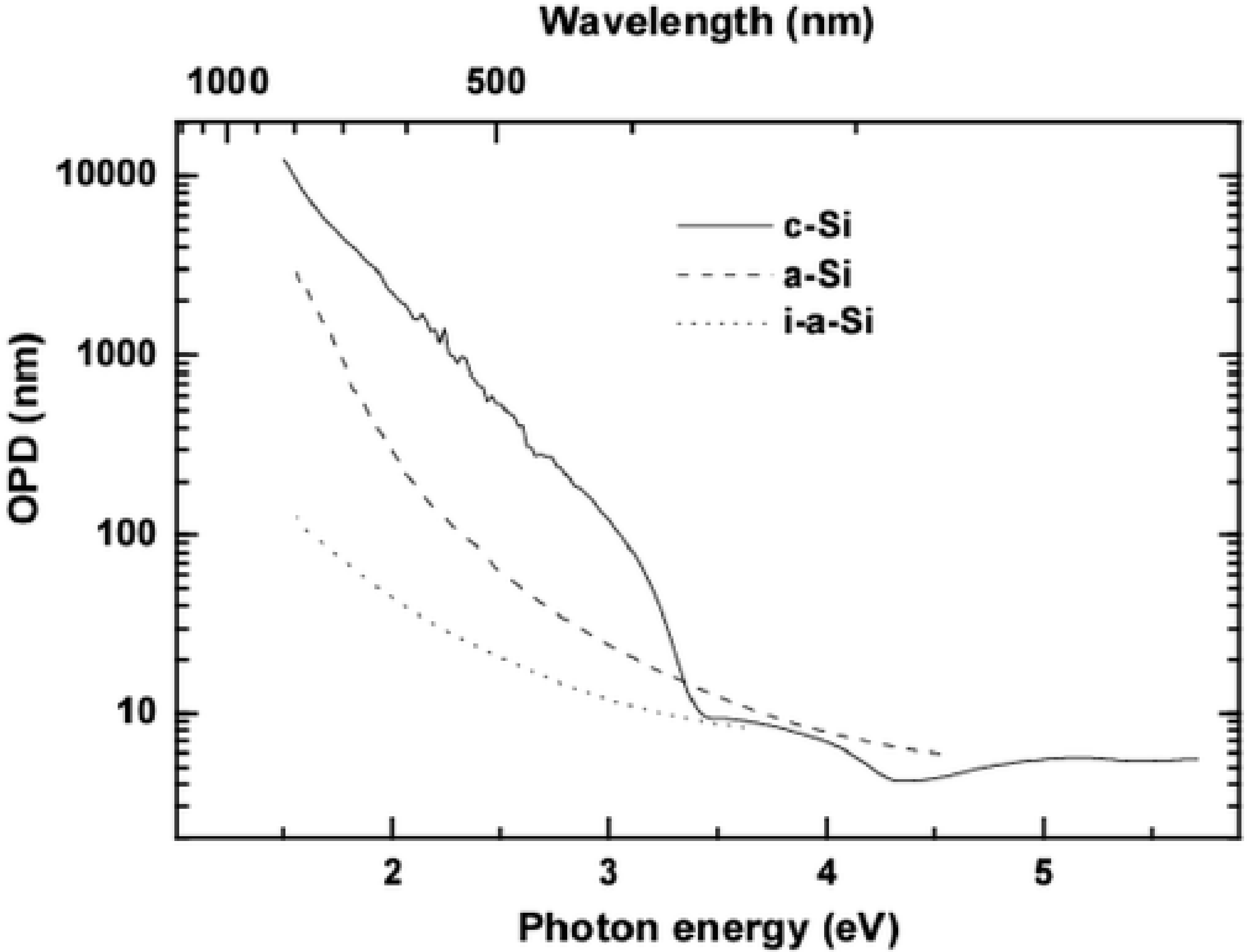

Fresnel coefficients

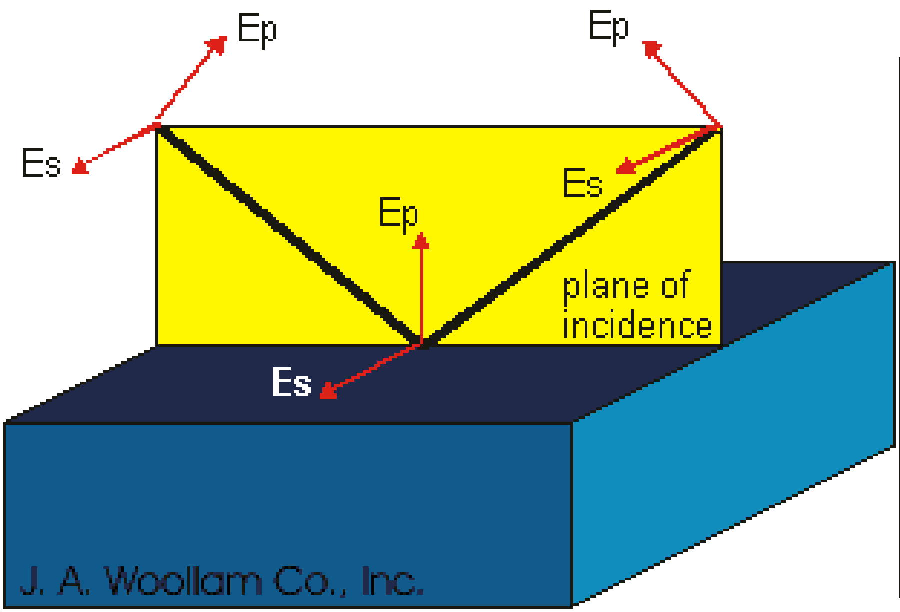

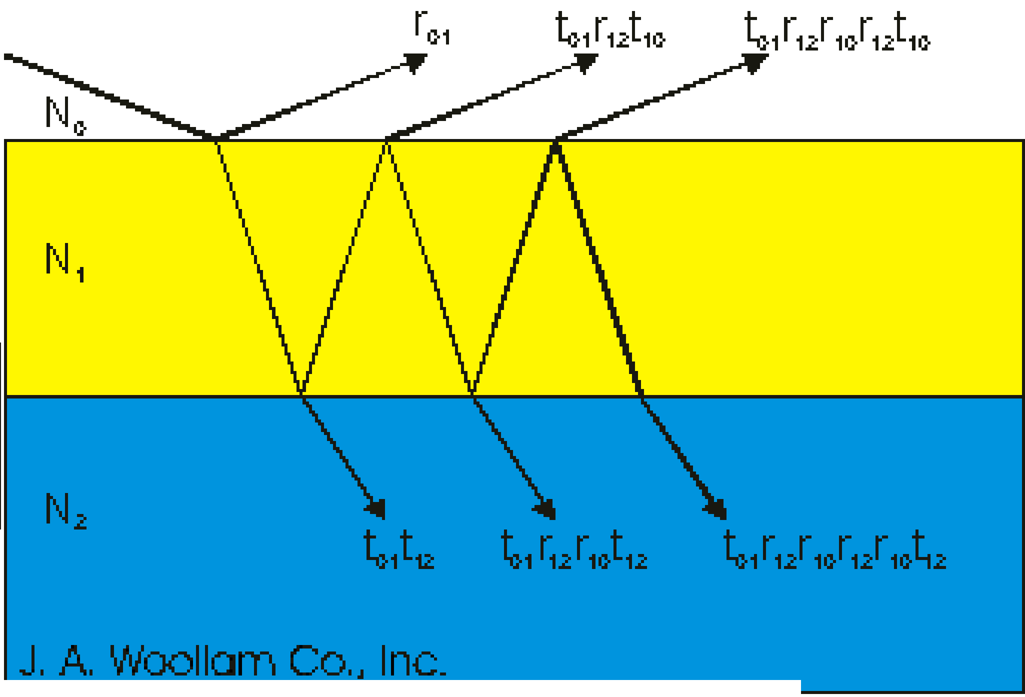

$$r_{tot} = r_{01} + t_{01} r_{12} t_{10} \mathrm{e}^{-2i\beta} + t_{01} r_{12}^{\;2} r_{10} t_{10} \mathrm{e}^{-4i\beta} + \ldots$$

$$r_p = \frac{-(n_2/n_1)\cos\theta + \sqrt{1-[(n_1/n_2)\sin\theta]^2}}{(n_2/n_1)\cos\theta + \sqrt{1-[(n_1/n_2)\sin\theta]^2}}$$

$$\beta = 2\pi\left(\frac{d_1}{\lambda}\right) n_1 \cos\theta_1$$

$$r_s = \frac{\cos\theta - (n_2/n_1)\sqrt{1-[(n_1/n_2)\sin\theta]^2}}{\cos\theta + (n_2/n_1)\sqrt{1-[(n_1/n_2)\sin\theta]^2}}$$

$$\rho = \tan(\psi) e^{i\Delta} = \frac{\tilde{R}_p}{\tilde{R}_s}$$

ELLIPSOMETRY

Petrik Péter
MFA Laboratory of Ellipsometry
(ellipsometry.hu, petrik.ellipsometry.hu)
Institute for Technical Physics and Materials Science

- Polarized light
- Hardver
- Modeling and evaluations
- Applications

Challenges in Real Time Polarization Spectroscopy

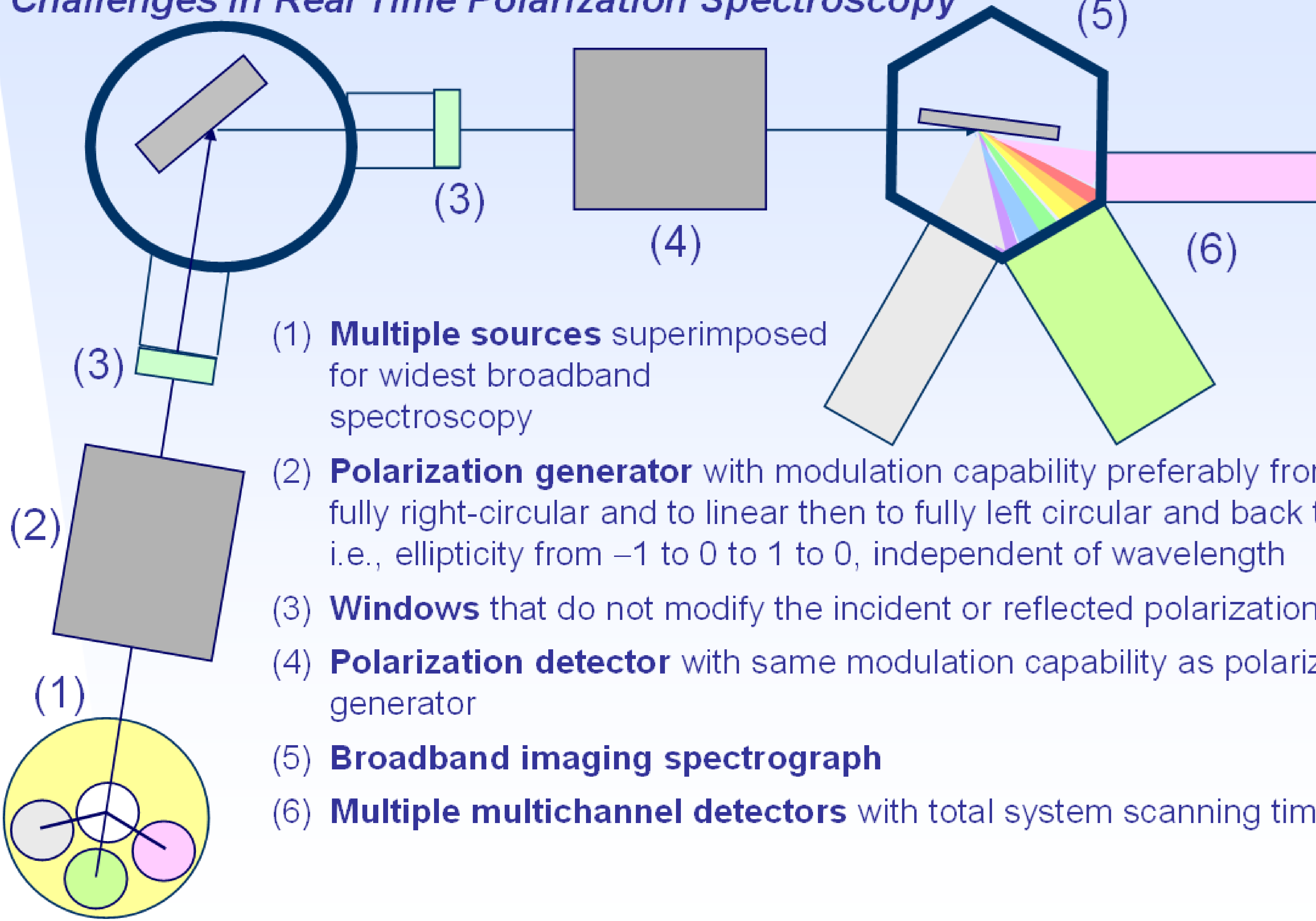

(1) **Multiple sources** superimposed for widest broadband spectroscopy

(2) **Polarization generator** with modulation capability preferably fro fully right-circular and to linear then to fully left circular and back t i.e., ellipticity from –1 to 0 to 1 to 0, independent of wavelength

(3) **Windows** that do not modify the incident or reflected polarization

(4) **Polarization detector** with same modulation capability as polariz generator

(5) **Broadband imaging spectrograph**

(6) **Multiple multichannel detectors** with total system scanning tim

Null ellipsometry

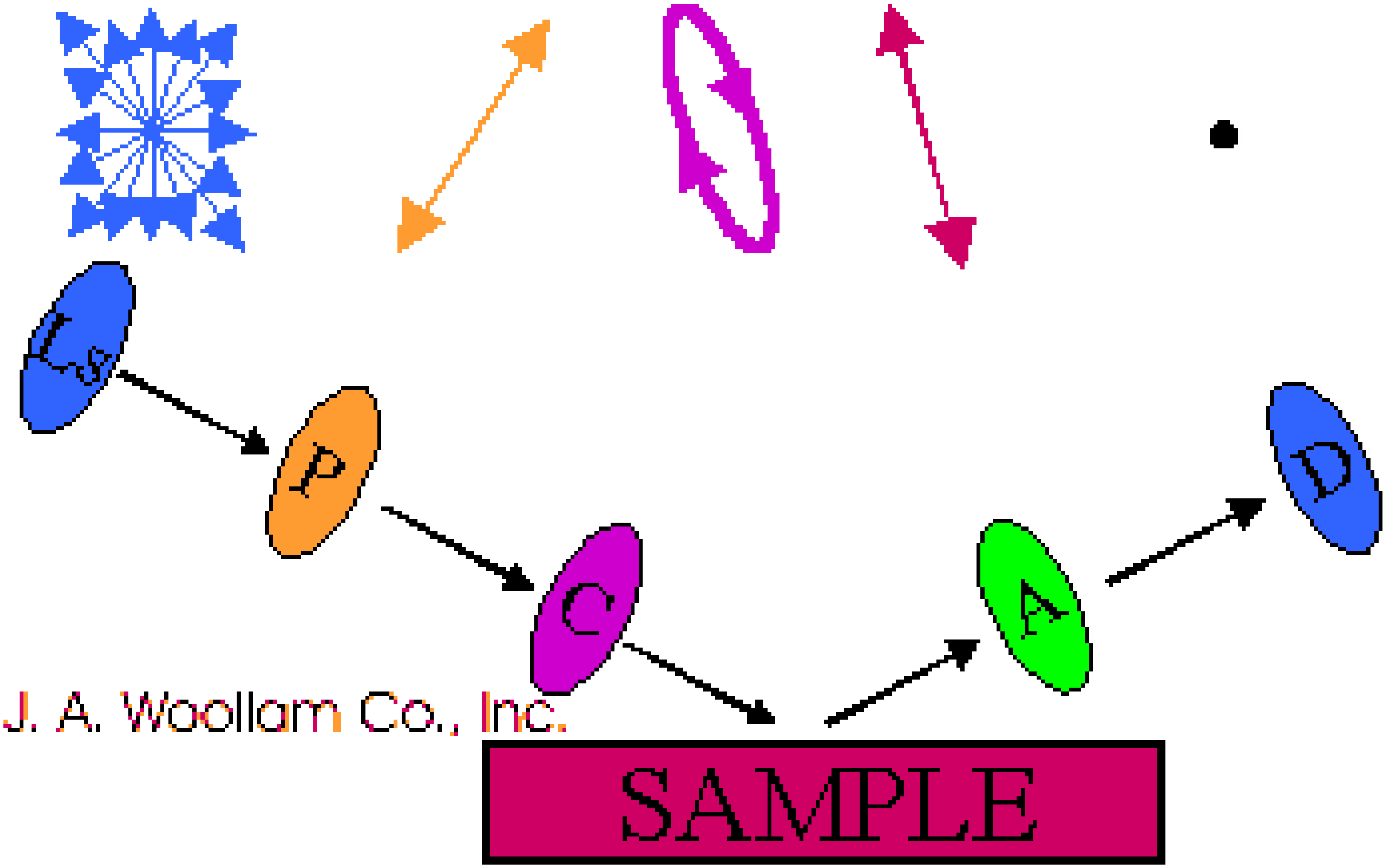

J. A. Woollam Co., Inc.

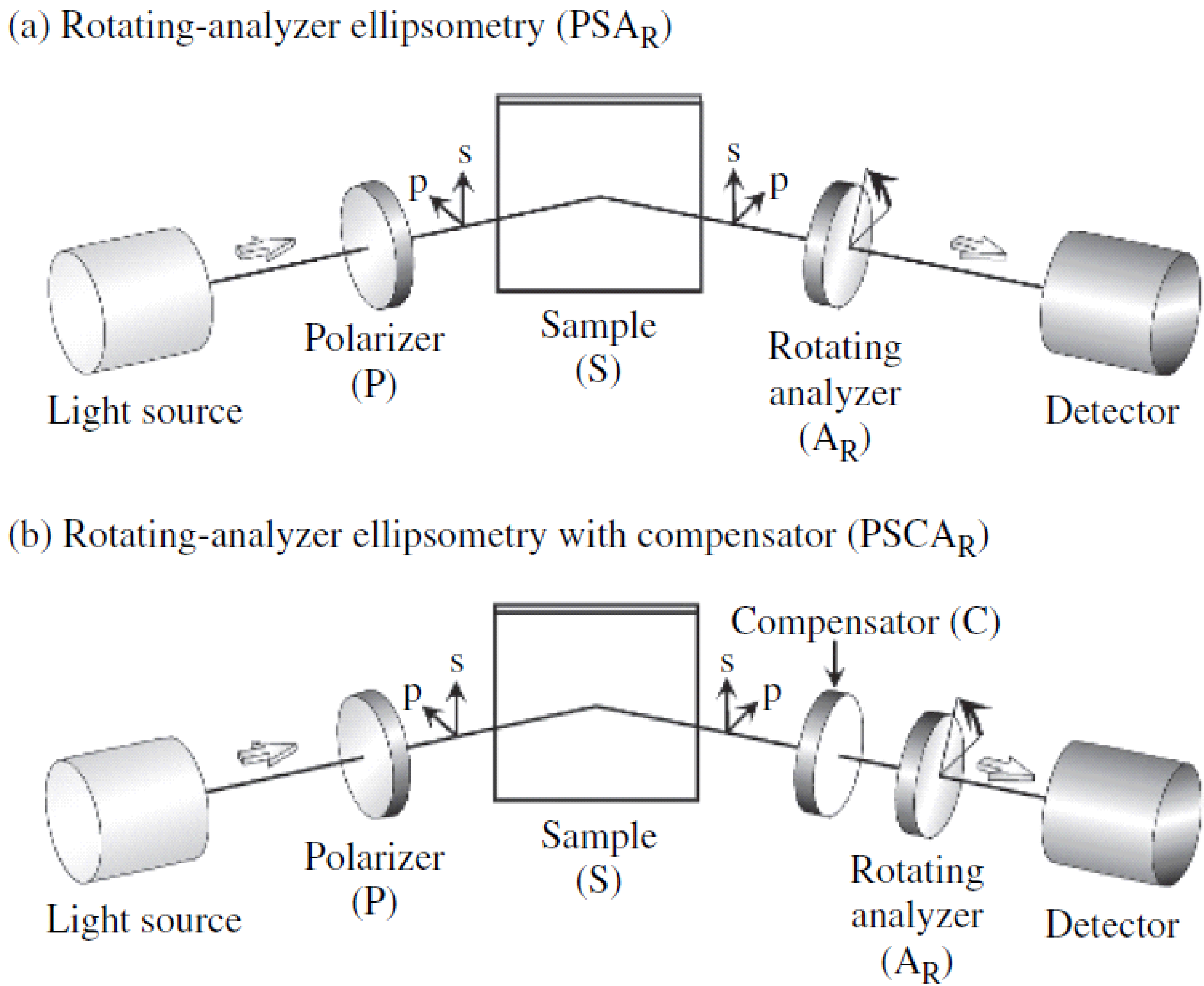
(a) Rotating-analyzer ellipsometry (PSA_R)
s
p
s
p
Light source
Polarizer
(P)
Sample
(S)
Rotating
analyzer
(A_R)
Detector
(b) Rotating-analyzer ellipsometry with compensator ($PSCA_R$)
Compensator (C)
s
p
s
p
Light source
Polarizer
(P)
Sample
(S)
Rotating
analyzer
(A_R)
Detector

(c) Rotating-compensator ellipsometry (PSC_RA)

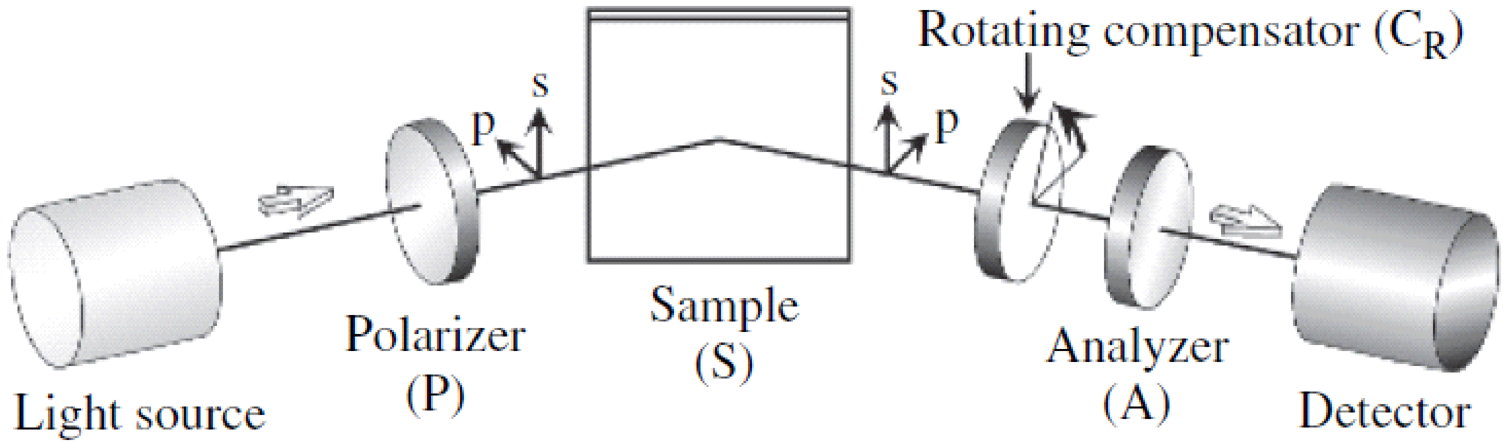

(d) Phase-modulation ellipsometry (PSMA)

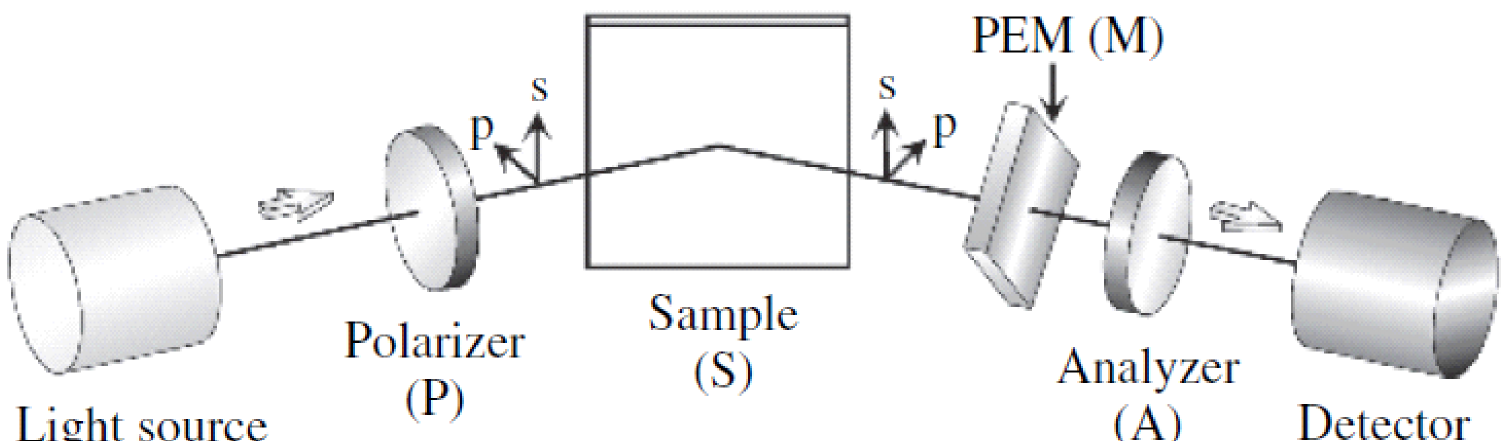

Types of ellipsometry

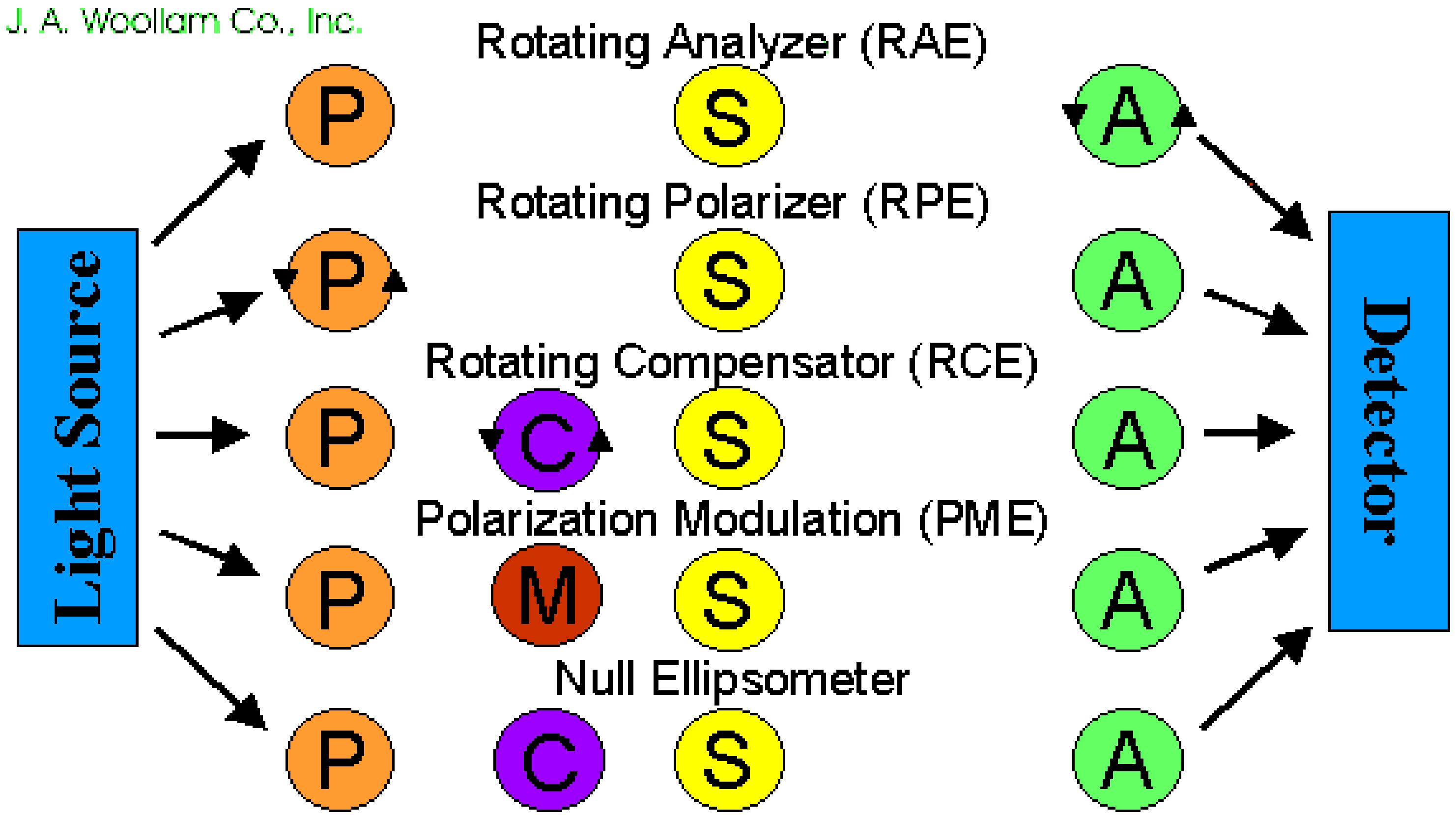

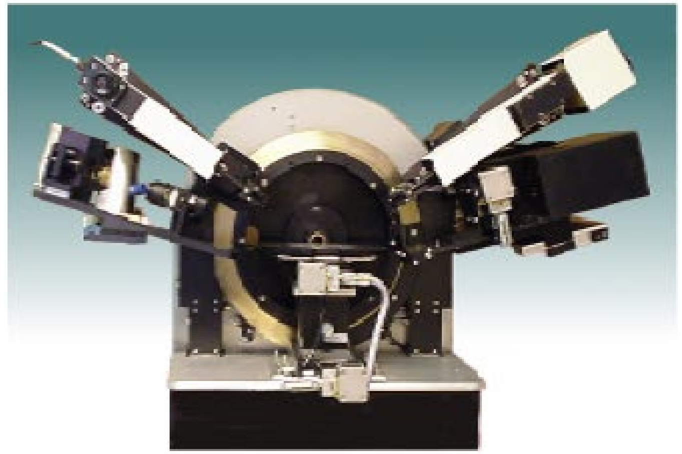

Optical solutions
for your research

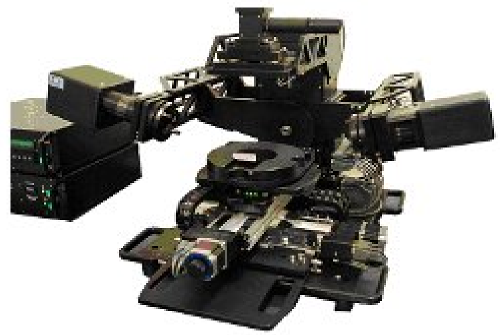

Woollam M2000DI

Forgókompenzátoros spektroszkópiai ellipszométer a 190-1700 nm hullámhossztartományban automatikus goniométerrel és mintamozgató asztallal. Fókuszálás minimálisan 0.15 mm-es folton. A mérési idő pontonként néhány másodperc.

SOPRA ES4G

Dupla-monokromátoros forgó-polarizátoros spektroszkópiai ellipszométer a 250-850 nm hullámhossztartományban. A foltméret kb. 1 mm. Különösen alkalmas nagy hullámhosszfelbontású precíziós mérésekre, ahol a sebesség nem annyira fontos követelmény.

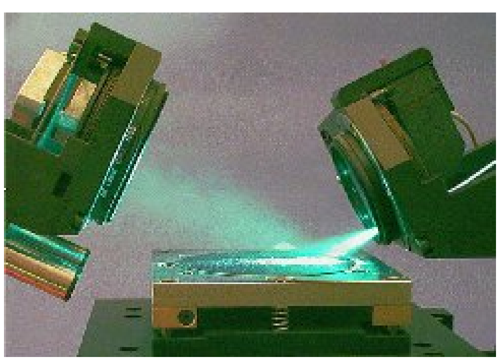

Divergens nyalábú térképező ellipszométer

Saját fejlesztésű térképező ellipszométer, amely számos hardver-változatban elkészült, többek között cluster-kamrára szerelve.

Measurement of sample in a Liquid Cell or gase cell

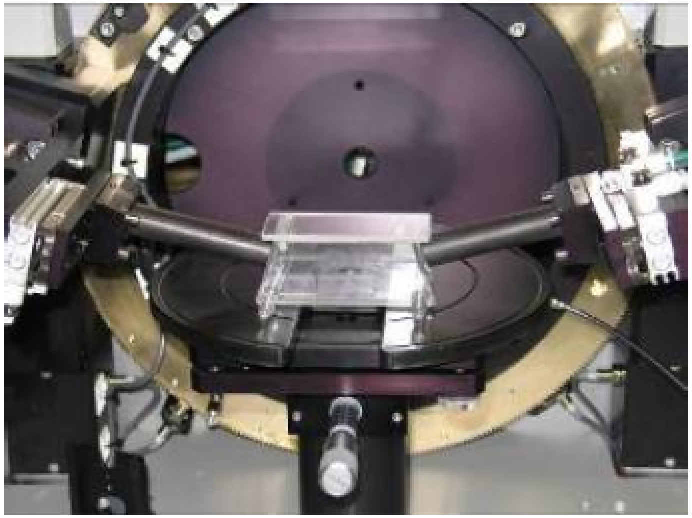

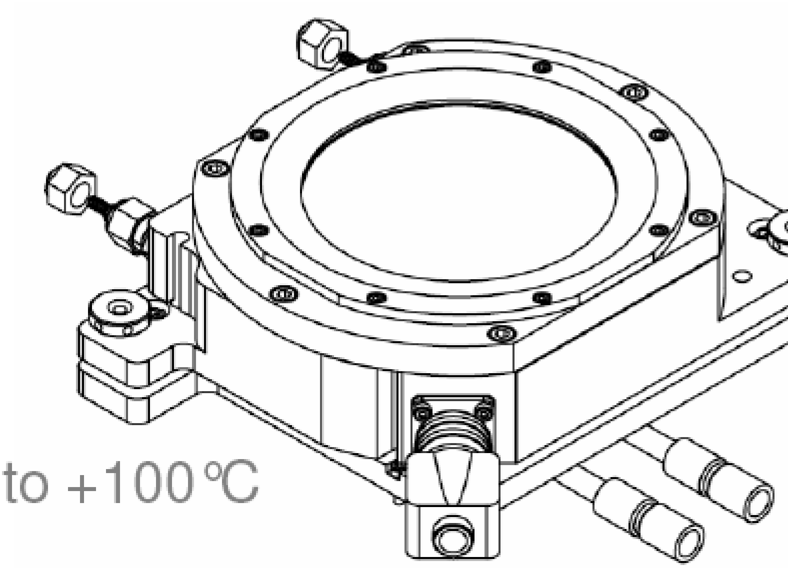

-10℃ to +100℃

timised for absorbant liquid Or UV measurement

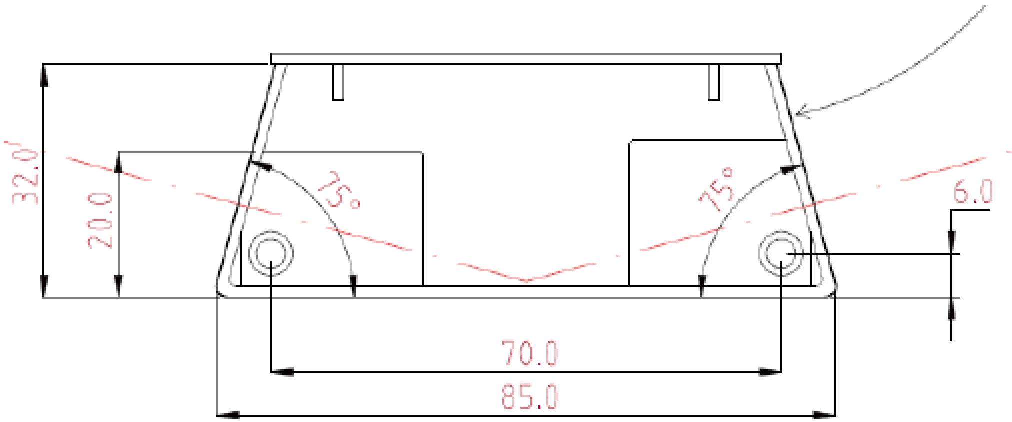

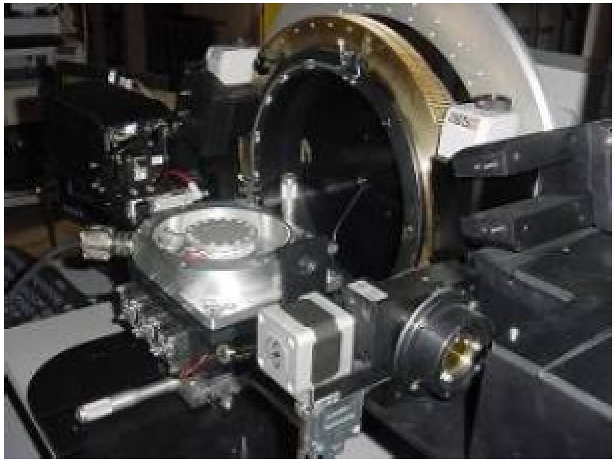

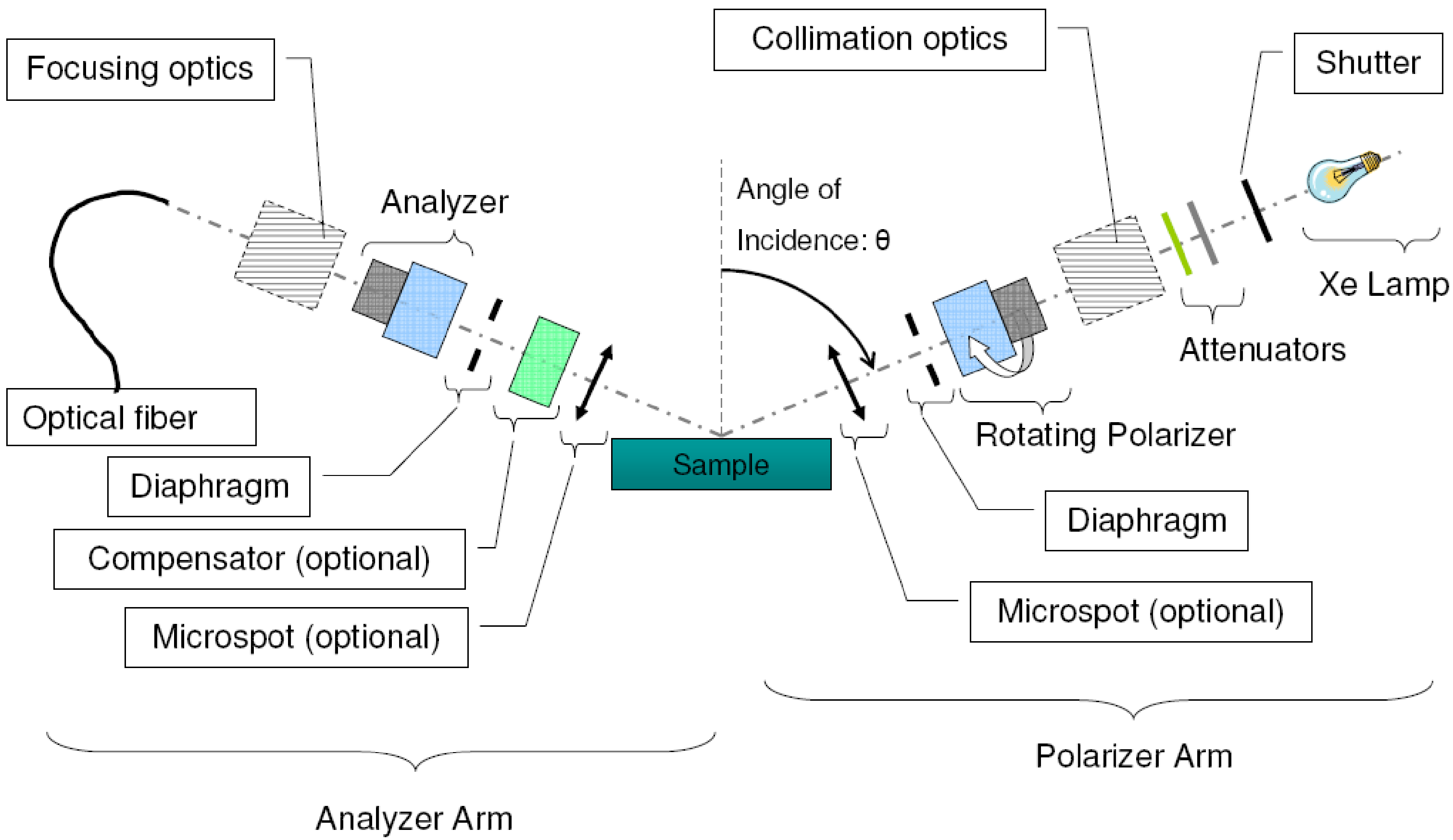
Focusing optics
Collimation optics
Shutter
Analyzer
Angle of
Incidence: θ
Xe Lamp
Attenuators
Optical fiber
Rotating Polarizer
Sample
Diaphragm
Diaphragm
Compensator (optional)
Microspot (optional)
Microspot (optional)
Polarizer Arm
Analyzer Arm

High resolution Mode: Spectrometer based

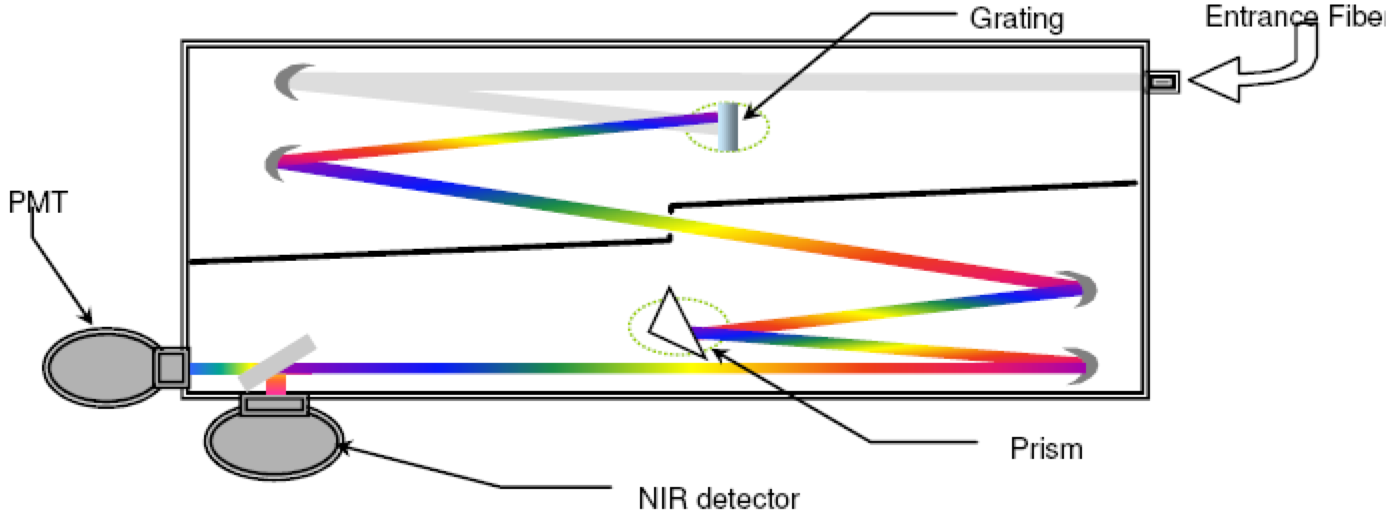

Fast Measurement Mode: Spectrograph based

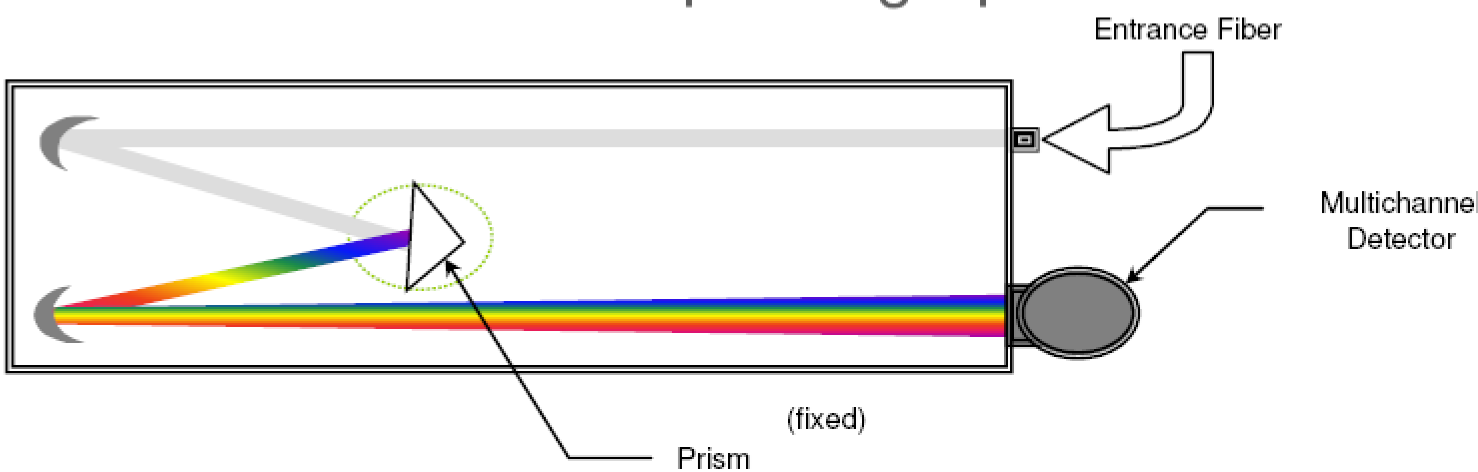

Role of focusing

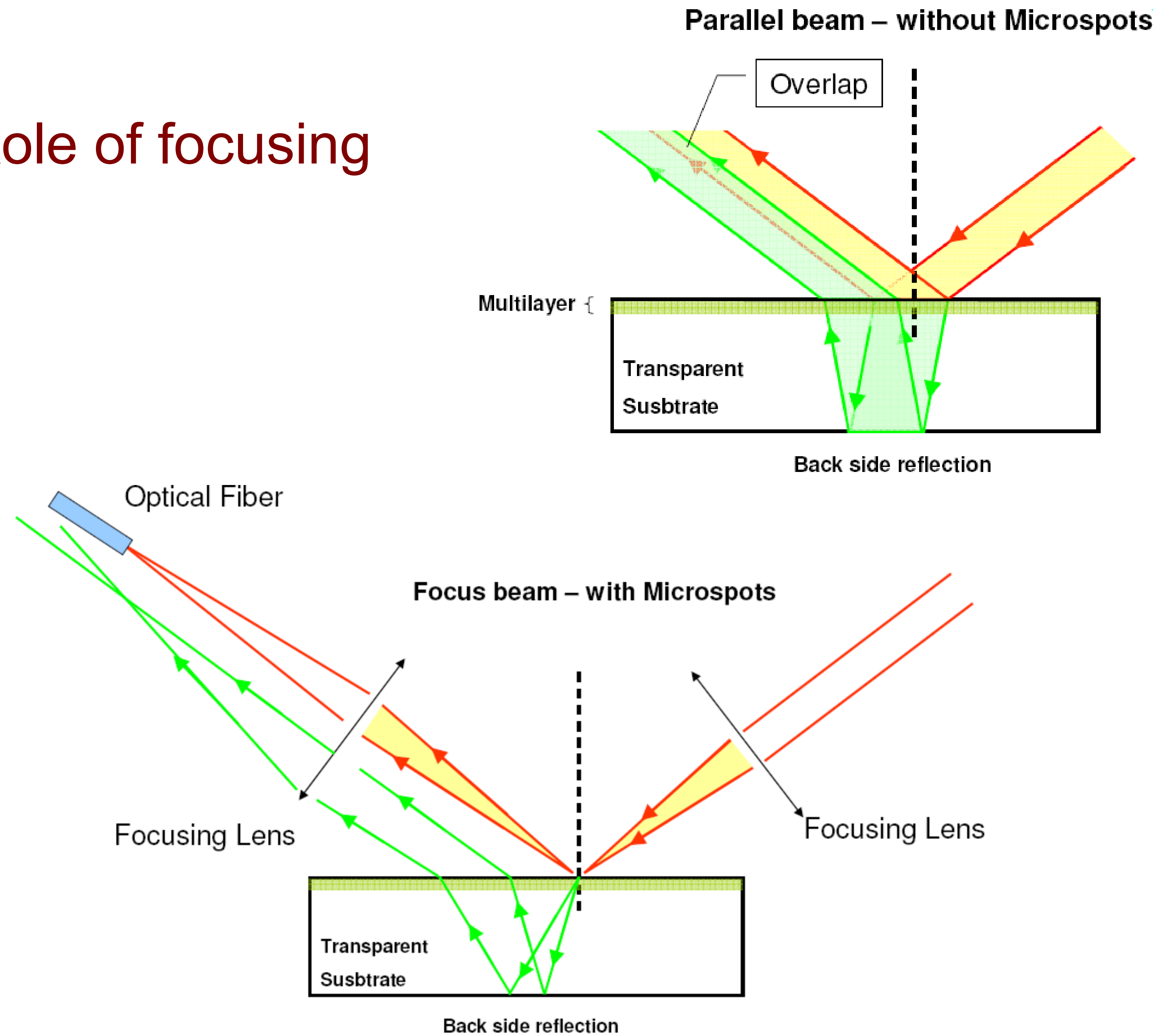

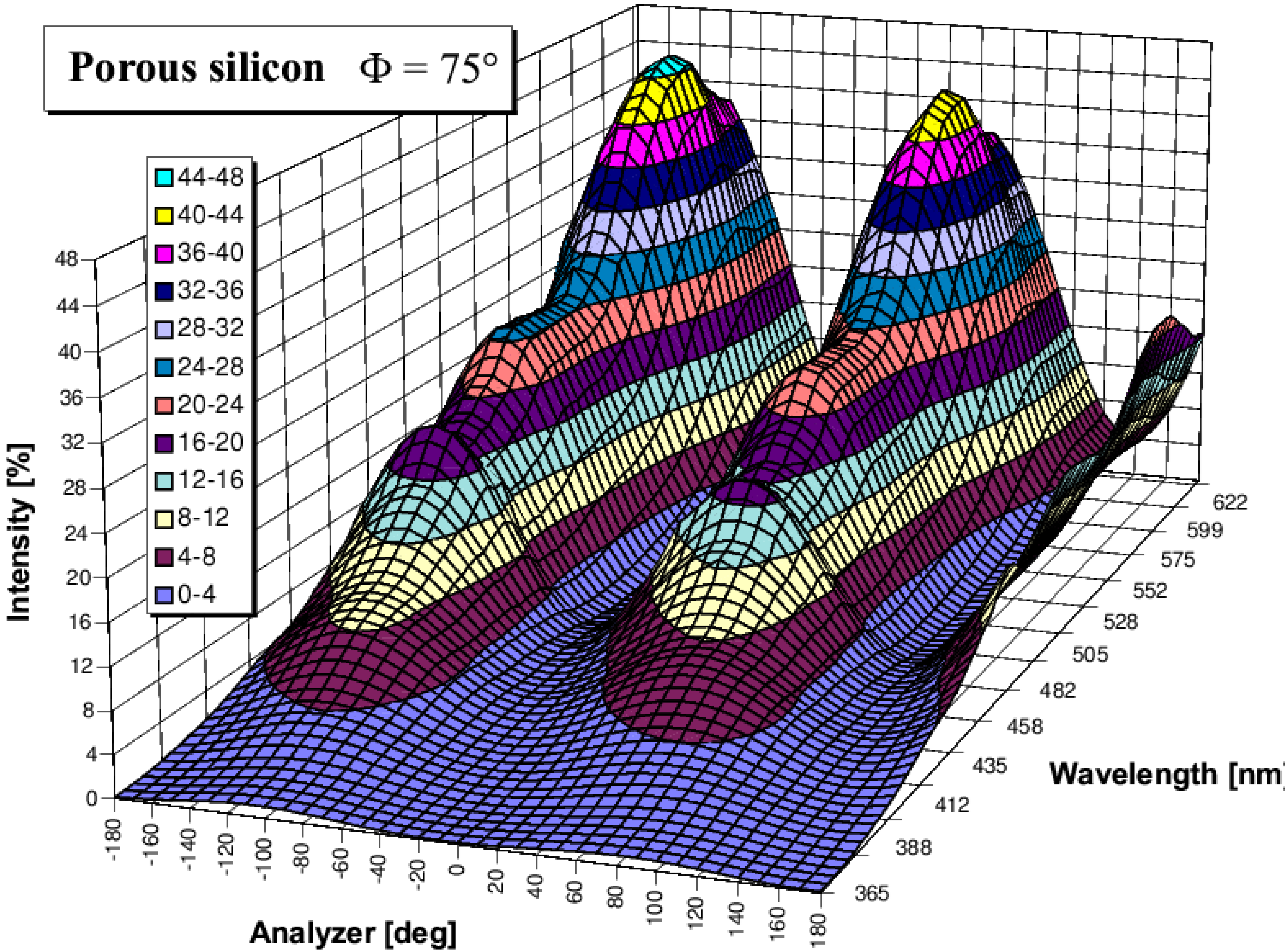

Porous silicon Φ = 75°
44-48
40-44
36-40
32-36
28-32
24-28
20-24
16-20
12-16
8-12
4-8
0-4
Intensity [%]
48
44
40
36
32
28
24
20
16
12
8
4
0
Analyzer [deg]
-180
-160
-140
-120
-100
-80
-60
-40
-20
0
20
40
60
80
100
120
140
160
180
Wavelength [nm]
622
599
575
552
528
505
482
458
435
412
388
365

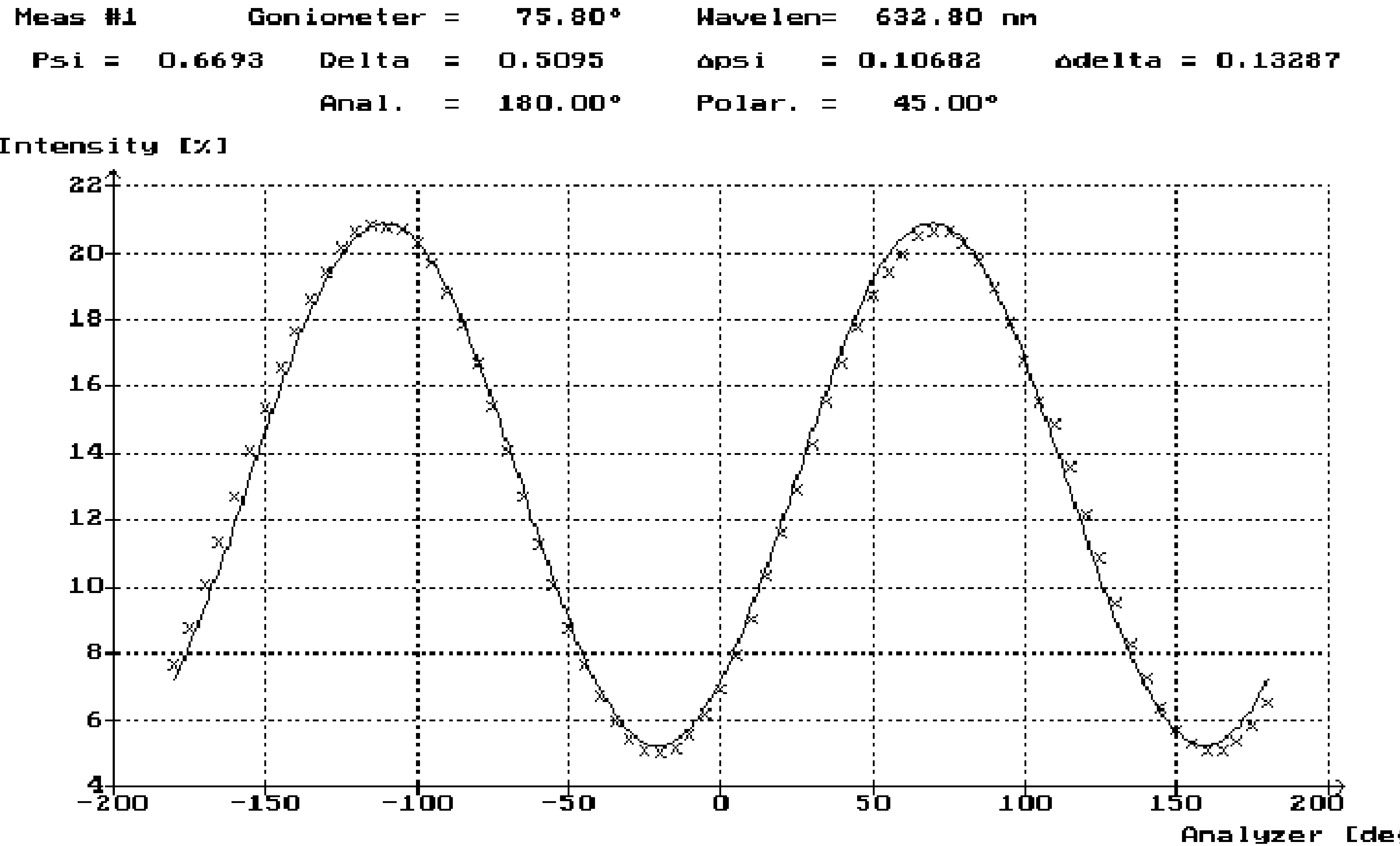

Meas #1
Goniometer = 75.80°
Wavelen= 632.80 nm
Psi = 0.6693
Delta = 0.5095
Δpsi = 0.10682
Δdelta = 0.13287
Anal. = 180.00°
Polar. = 45.00°
Intensity [%]
22
20
18
16
14
12
10
8
6
4
-200
-150
-100
-50
0
50
100
150
200
Analyzer [de

ELLIPSOMETRY

Petrik Péter
MFA Laboratory of Ellipsometry
(ellipsometry.hu, petrik.ellipsometry.hu)
Institute for Technical Physics and Materials Science

- Polarized light
- Hardver
- Modeling and evaluations
- Applications

Measurement and evaluation

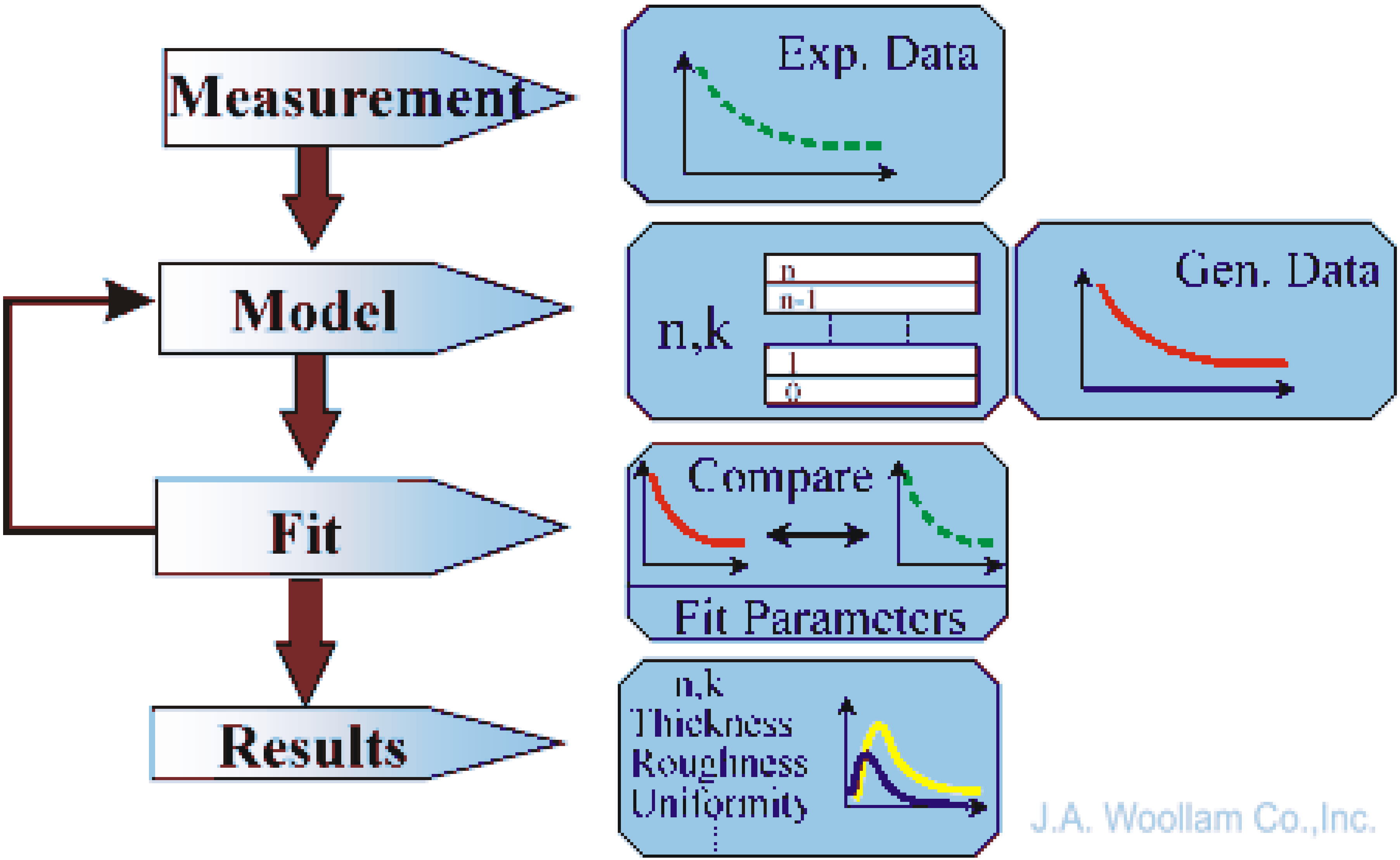

Interference

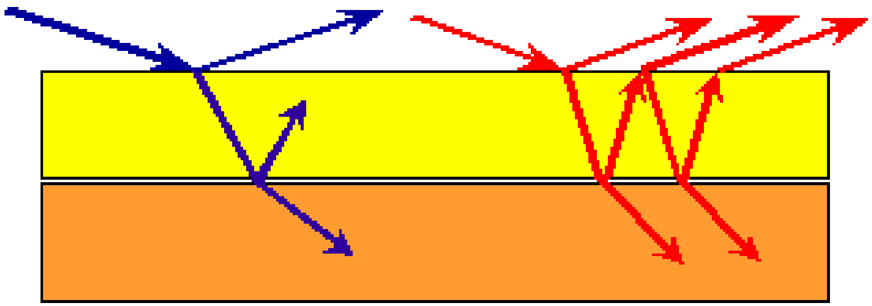

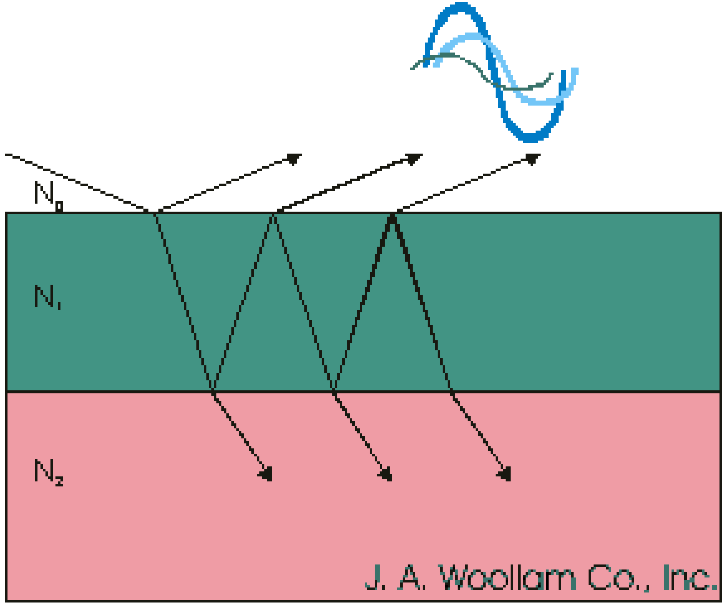

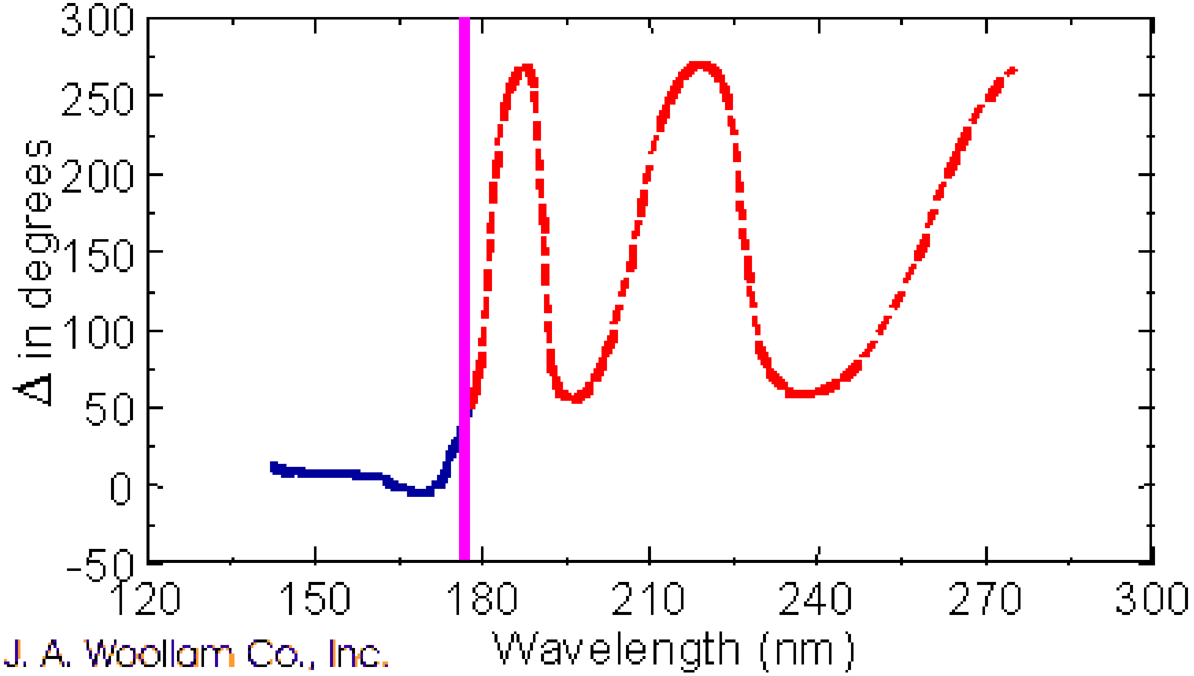

Interference

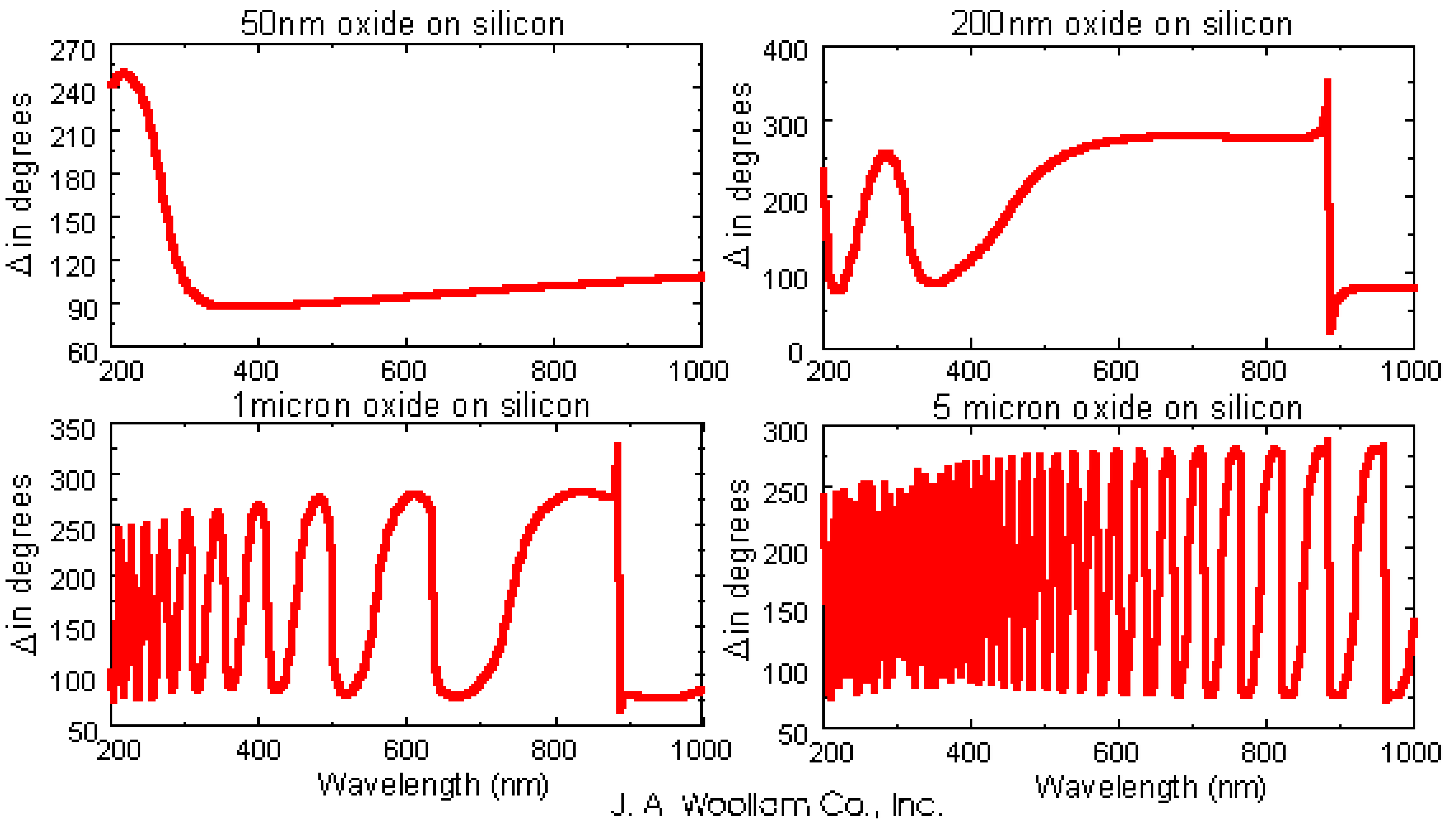

Evaluation

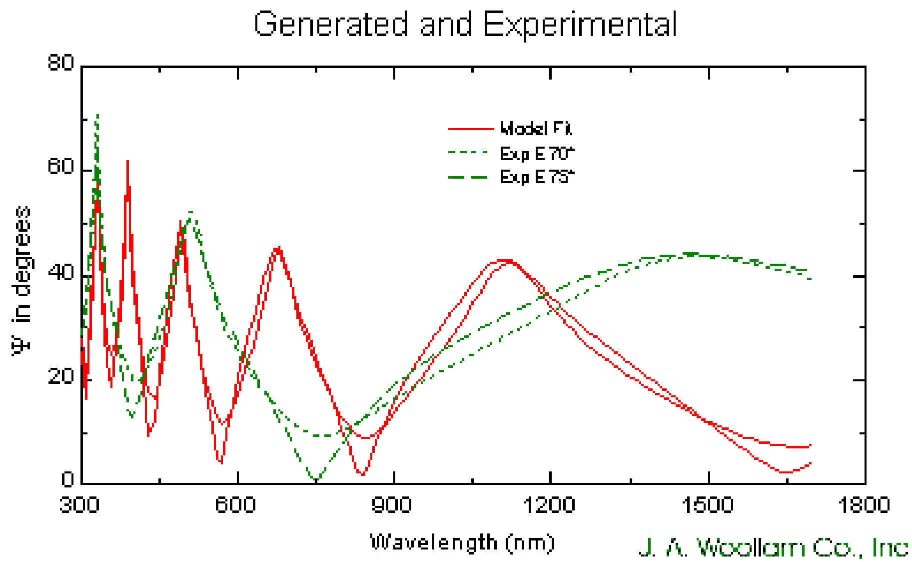

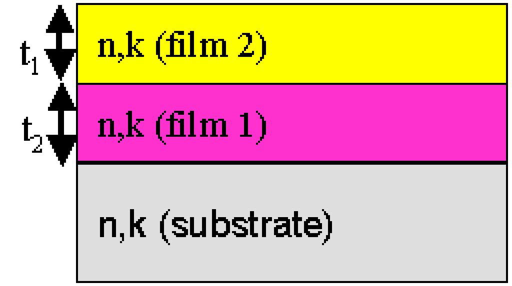

2	amorphous si	500 Å
1	sio2	1000 Å
0	si	1 mm

$$MSE = \frac{1}{2N-M}\sum_{i=1}^{N}\left[\left(\frac{\Psi_i^{mod}-\Psi_i^{exp}}{\sigma_{\Psi,i}^{exp}}\right)^2+\left(\frac{\Delta_i^{mod}-\Delta_i^{exp}}{\sigma_{\Delta,i}^{exp}}\right)^2\right]=\frac{1}{2N-M}\chi^2$$

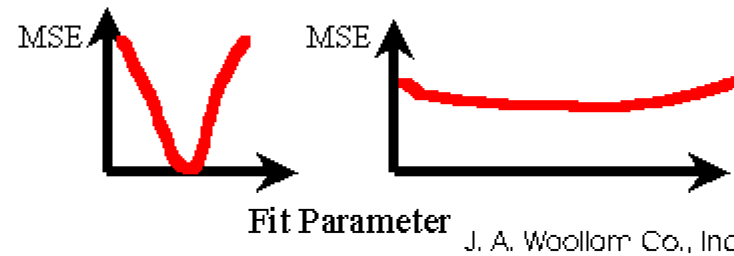

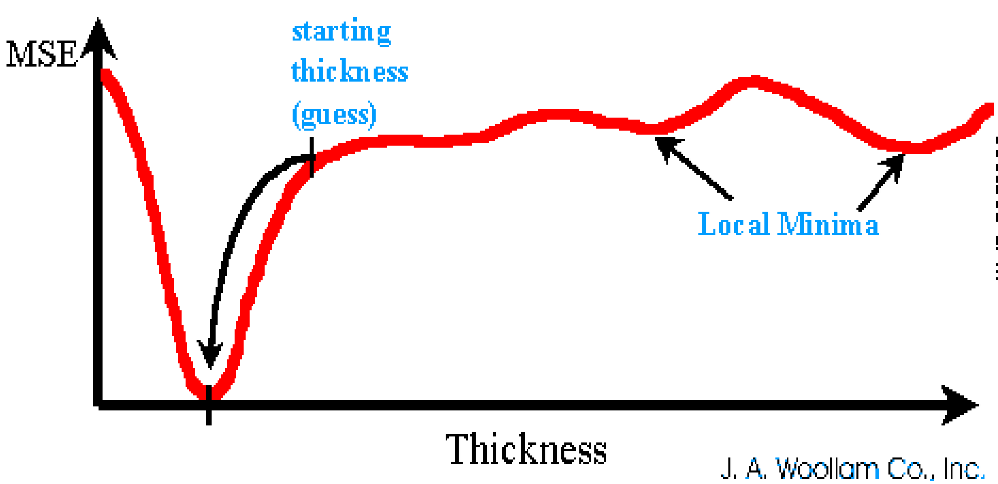

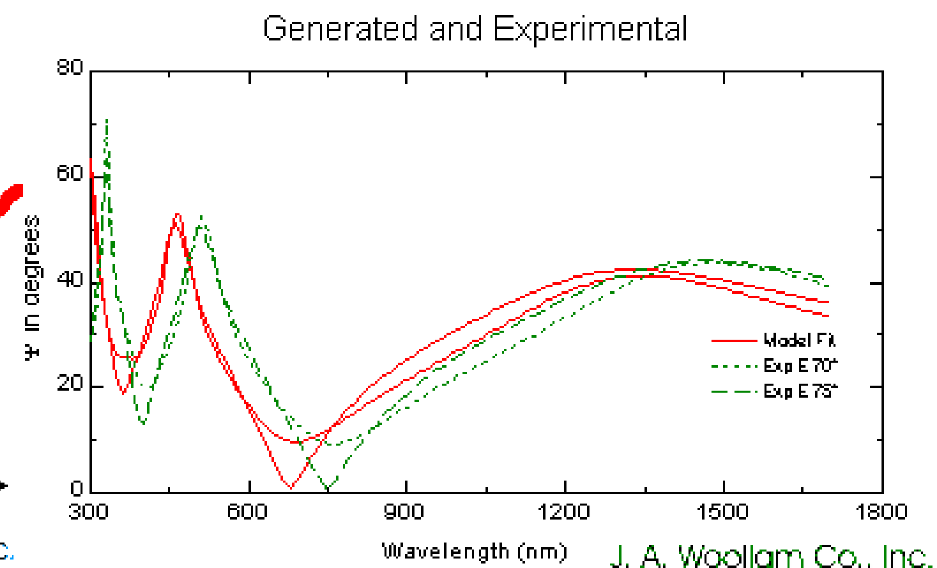

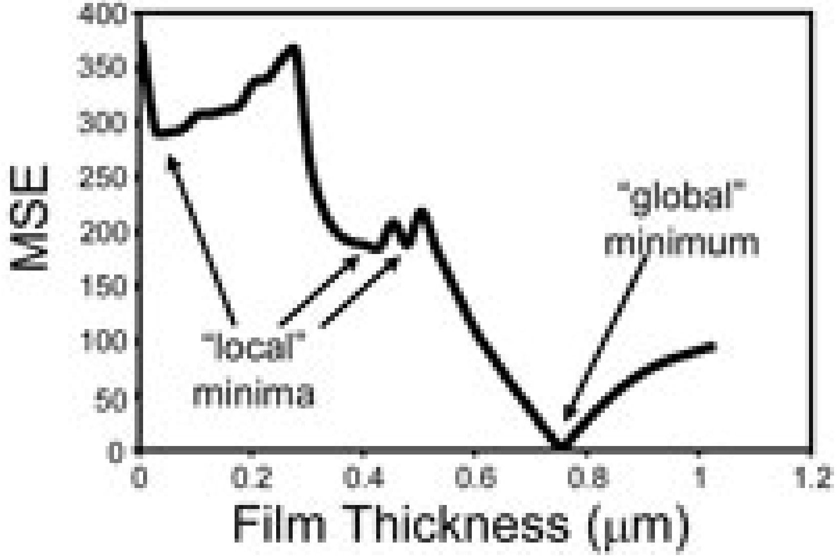

MSE
Film Thickness (μm)
"local"
minima
"global"
minimum

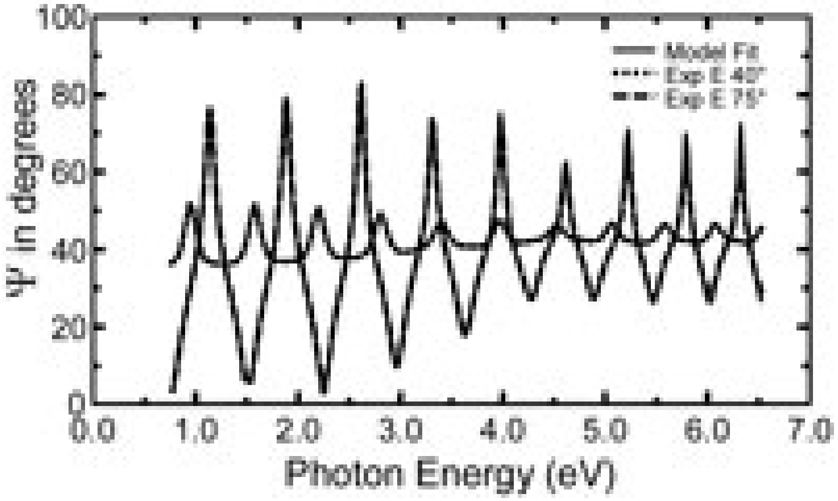

Ψ in degrees
Photon Energy (eV)
Model Fit
Exp E 40°
Exp E 75°

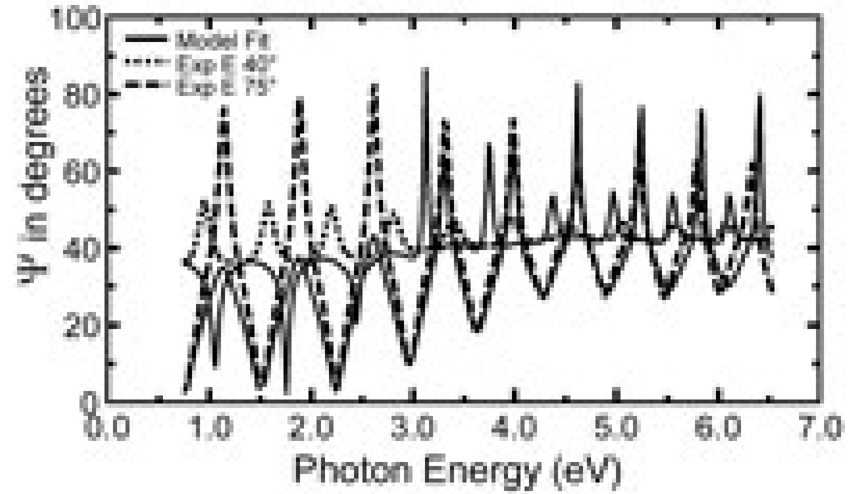

Ψ in degrees
Photon Energy (eV)
Model Fit
Exp E 40°
Exp E 75°

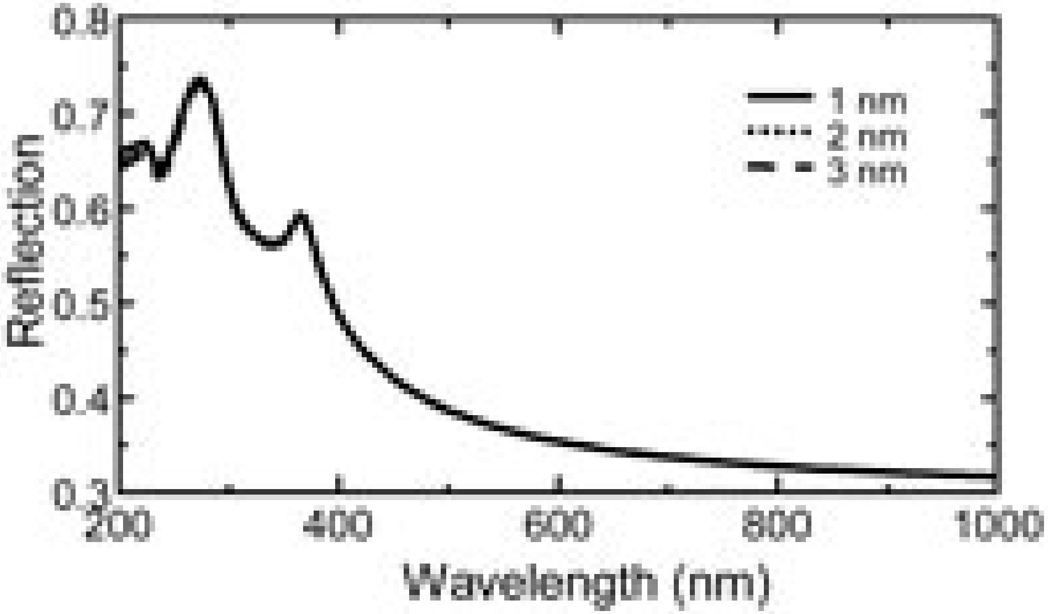

Reflection
0.8
0.7
0.6
0.5
0.4
0.3
200
400
600
800
1000
Wavelength (nm)
1 nm
2 nm
3 nm

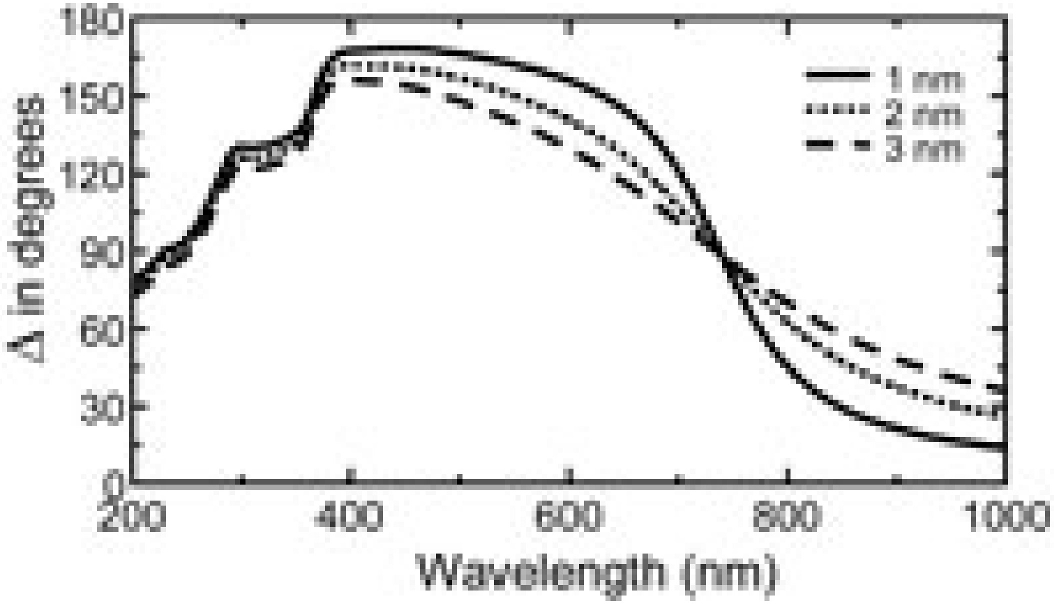

Δ in degrees
180
150
120
90
60
30
0
200
400
600
800
1000
Wavelength (nm)
1 nm
2 nm
3 nm

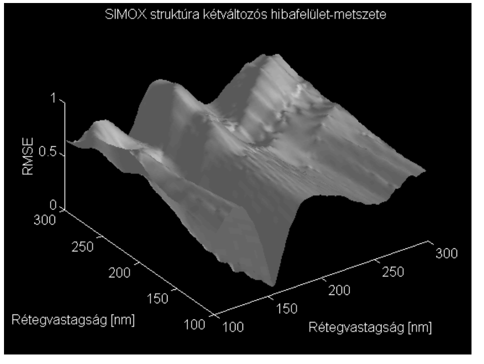
SIMOX struktúra kétváltozós hibafelület-metszete
1
RMSE
0.5
0
300
250
200
150
100
Rétegvastagság [nm]
100
150
200
250
300
Rétegvastagság [nm]

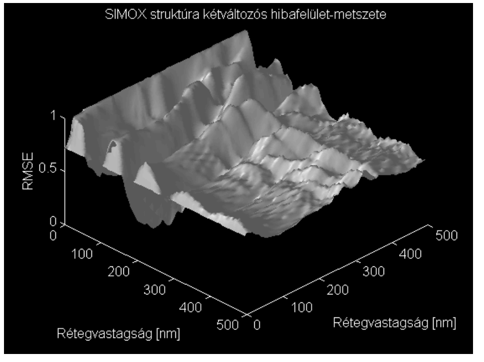
SIMOX struktúra kétváltozós hibafelület-metszete
RMSE
1
0.5
0
0
100
200
300
400
500
Rétegvastagság [nm]
0
100
200
300
400
500
Rétegvastagság [nm]

Typical Accuracy

Straight-through measurement of empty beam:
(Met by 95% of the measured wavelengths with ten second averaging time.)

$\Psi = 45° \pm 0.075°$ $\tan(\Psi) = 1 \pm 0.0013$

$\Delta = 0° \pm 0.05$ $\cos(\Delta) = 1 \pm 0.0000015$

Note: *When looking at ellipsometric specifications, it is easy to erroneously compare Δ to cos (Δ) and Ψ to tan(Ψ). We provide both numbers for your convenience. The Woollam Company IR-VASE is orders of magnitude better than the competition when measuring Δ near 0° and 180°. This is a benefit of our patented rotating compensator technology.*

As witnessed in the representative data shown below, the accuracy for most wavelengths is much better than specified.

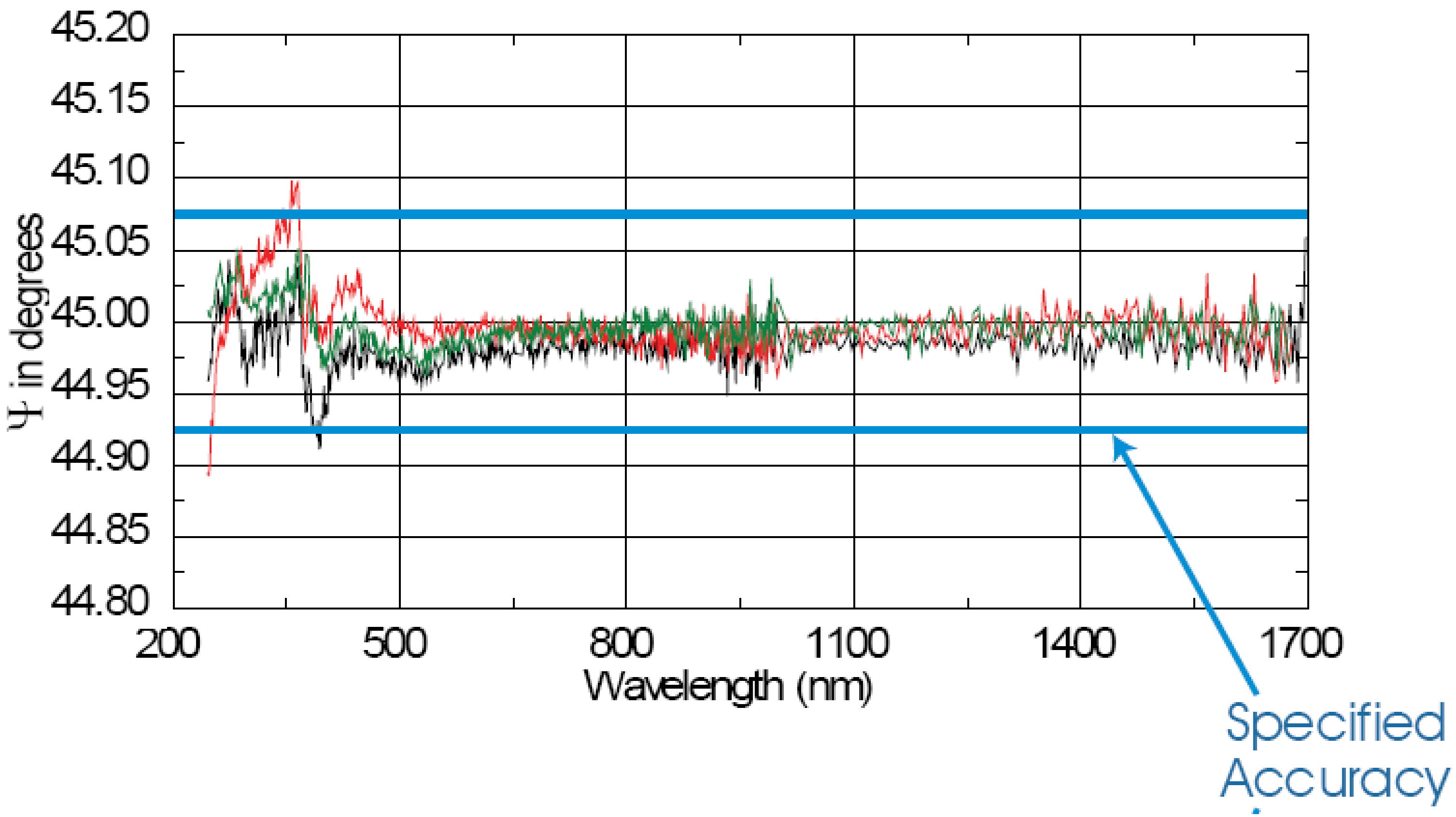

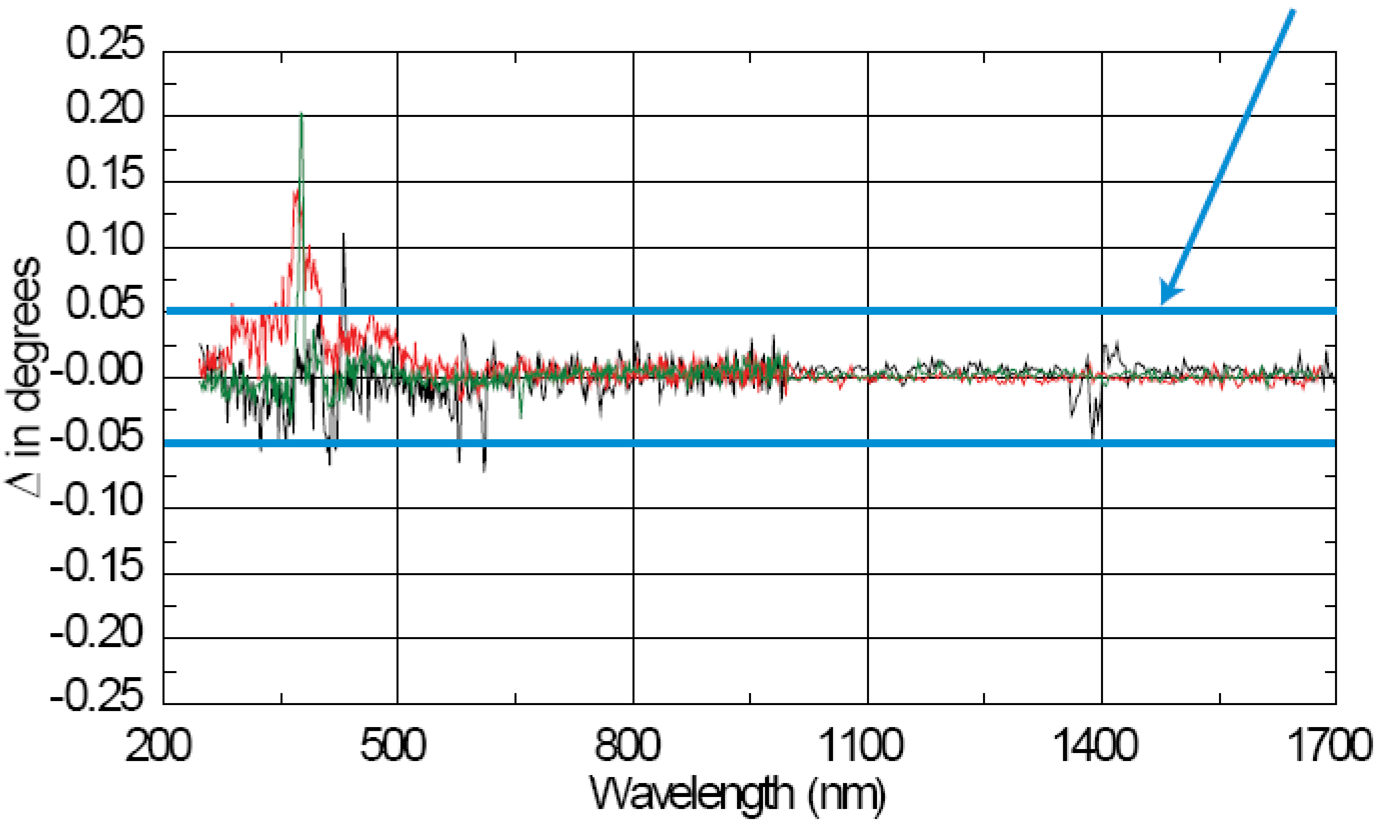

0.25
0.20
0.15
0.10
0.05
-0.00
-0.05
-0.10
-0.15
-0.20
-0.25
Δ in degrees
200
500
800
1100
1400
1700
Wavelength (nm)

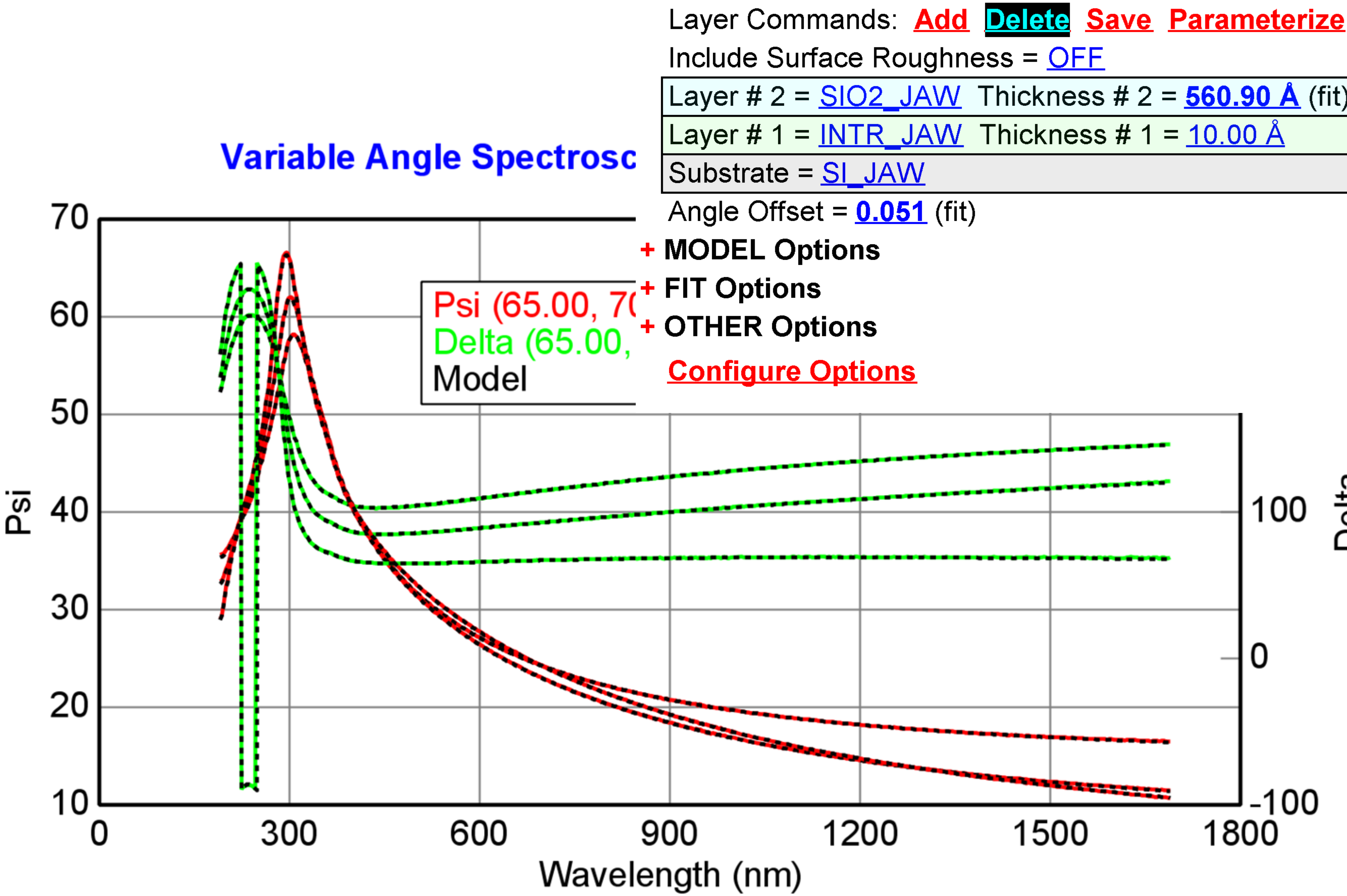

Layer Commands: Add Delete Save Parameterize
Include Surface Roughness = OFF
Layer # 2 = SIO2_JAW Thickness # 2 = 560.90 Å (fit)
Layer # 1 = INTR_JAW Thickness # 1 = 10.00 Å
Substrate = SI_JAW
Angle Offset = 0.051 (fit)
+ MODEL Options
+ FIT Options
+ OTHER Options
Configure Options
Variable Angle Spectrosc
Psi (65.00, 7(
Delta (65.00,
Model
Psi
Delta
Wavelength (nm)
70
60
50
40
30
20
10
0
300
600
900
1200
1500
1800
100
0
-100

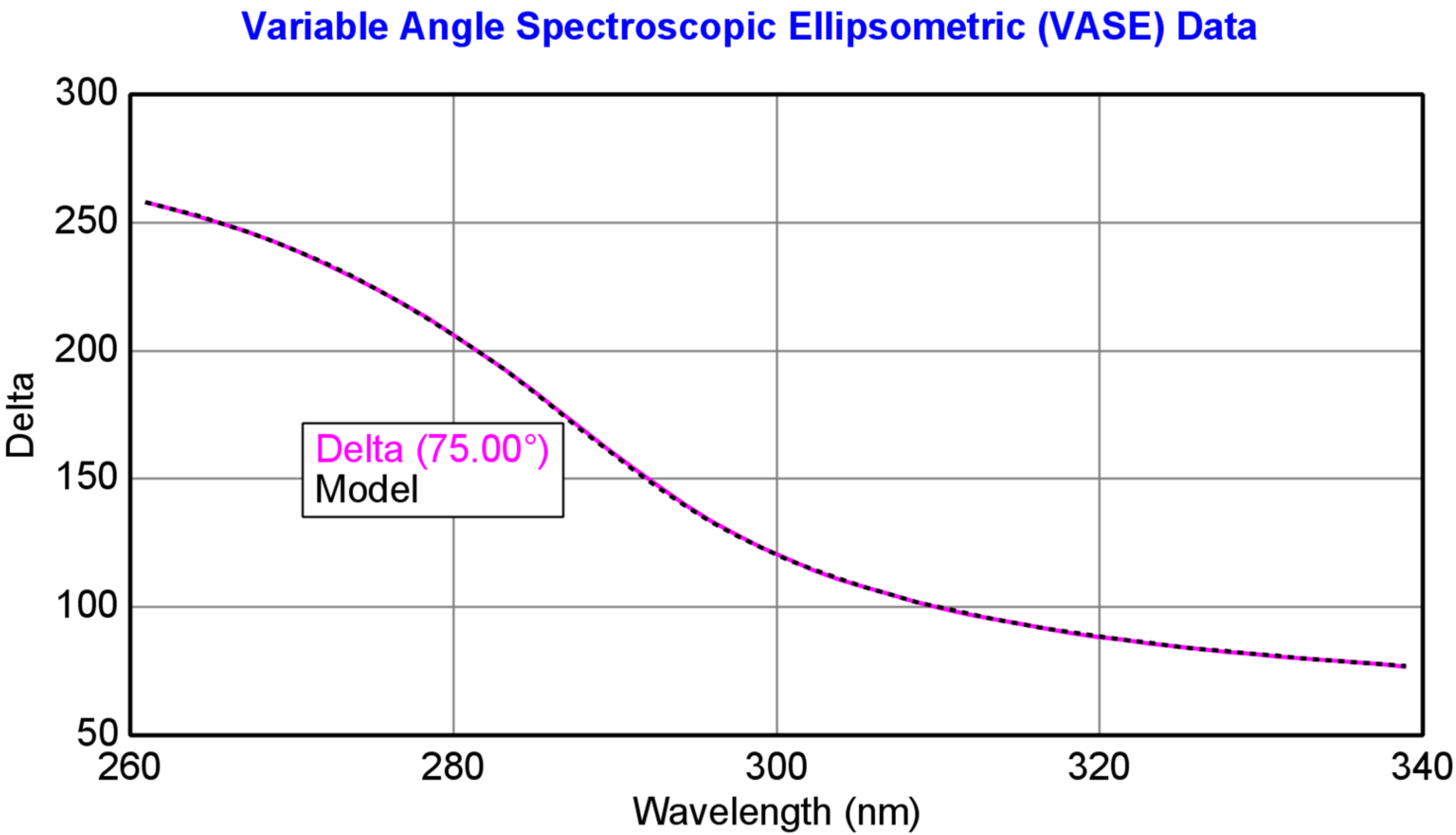

Variable Angle Spectroscopic Ellipsometric (VASE) Data
300
250
200
150
100
50
Delta
Delta (75.00°)
Model
260
280
300
320
340
Wavelength (nm)

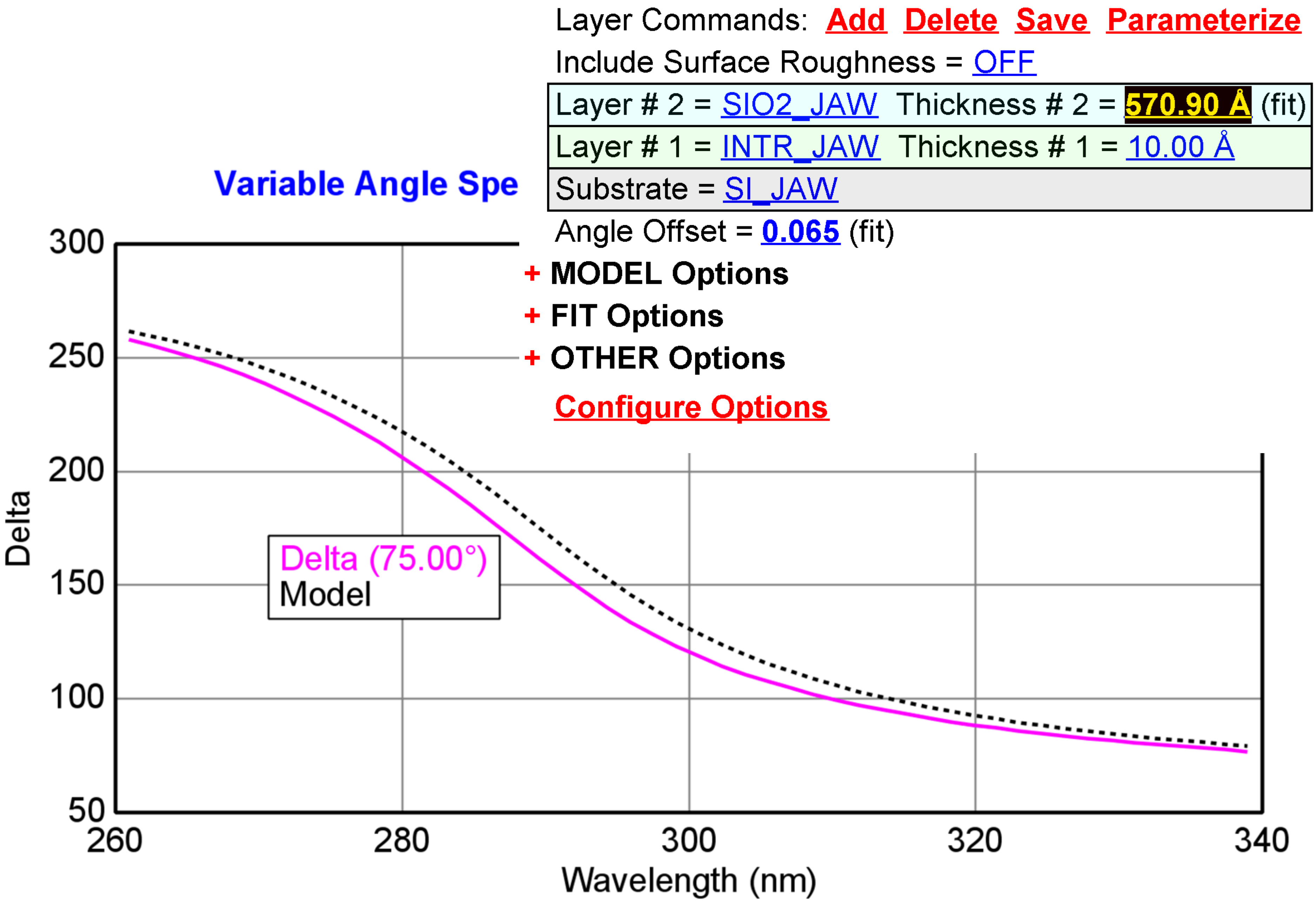
Layer Commands: Add Delete Save Parameterize
Include Surface Roughness = OFF
Layer # 2 = SIO2_JAW Thickness # 2 = 570.90 Å (fit)
Layer # 1 = INTR_JAW Thickness # 1 = 10.00 Å
Substrate = SI_JAW
Angle Offset = 0.065 (fit)
+ MODEL Options
+ FIT Options
+ OTHER Options
Configure Options
Variable Angle Spe
Delta
300
250
200
150
100
50
260
280
300
320
340
Wavelength (nm)
Delta (75.00°)
Model

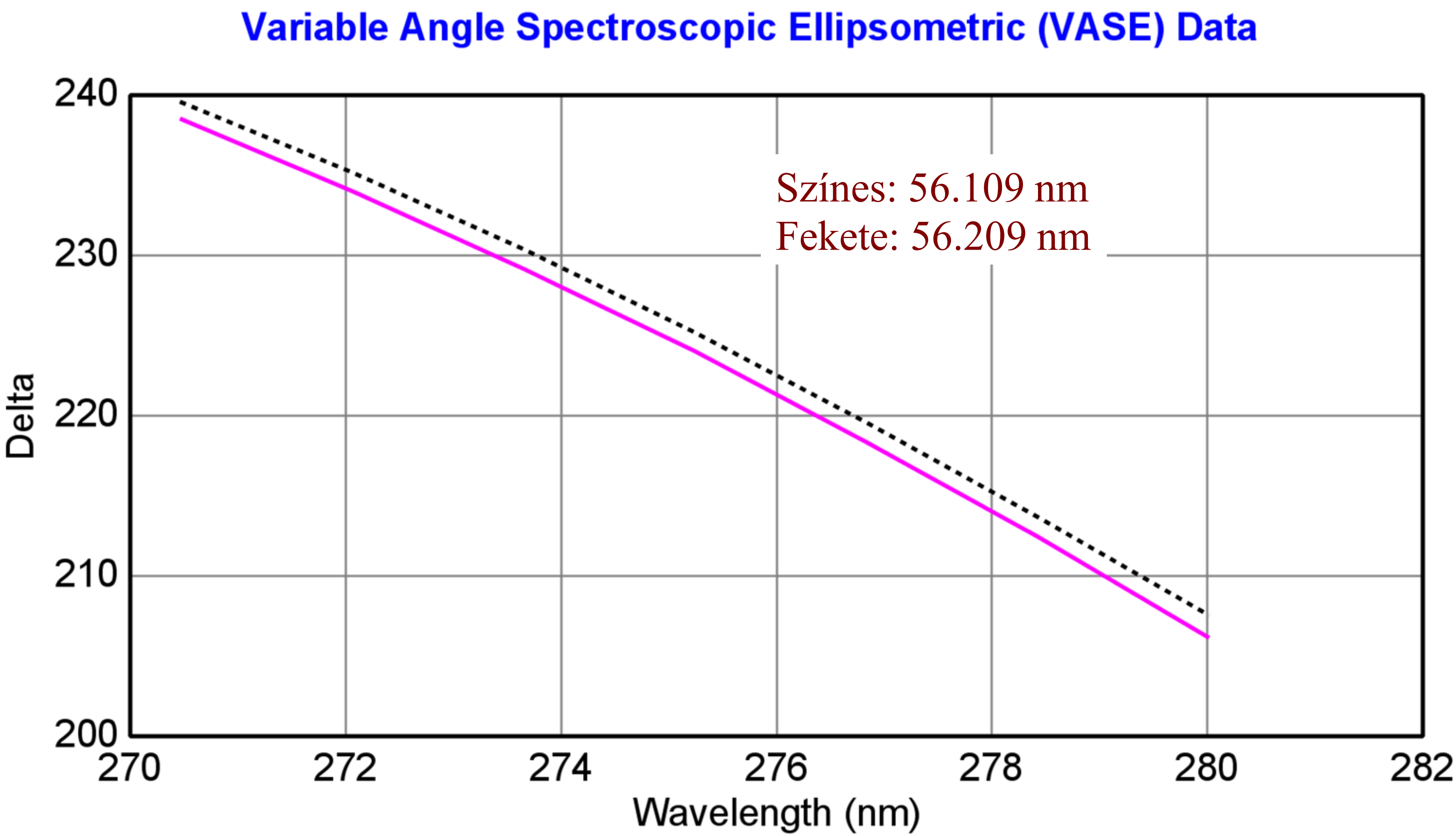
Variable Angle Spectroscopic Ellipsometric (VASE) Data
Színes: 56.109 nm
Fekete: 56.209 nm
Delta
240
230
220
210
200
270
272
274
276
278
280
282
Wavelength (nm)

ELLIPSOMETRY

Petrik Péter
MFA Laboratory of Ellipsometry
(ellipsometry.hu, petrik.ellipsometry.hu)
Institute for Technical Physics and Materials Science

- Polarized light
- Hardver
- Modeling and evaluations
- Applications

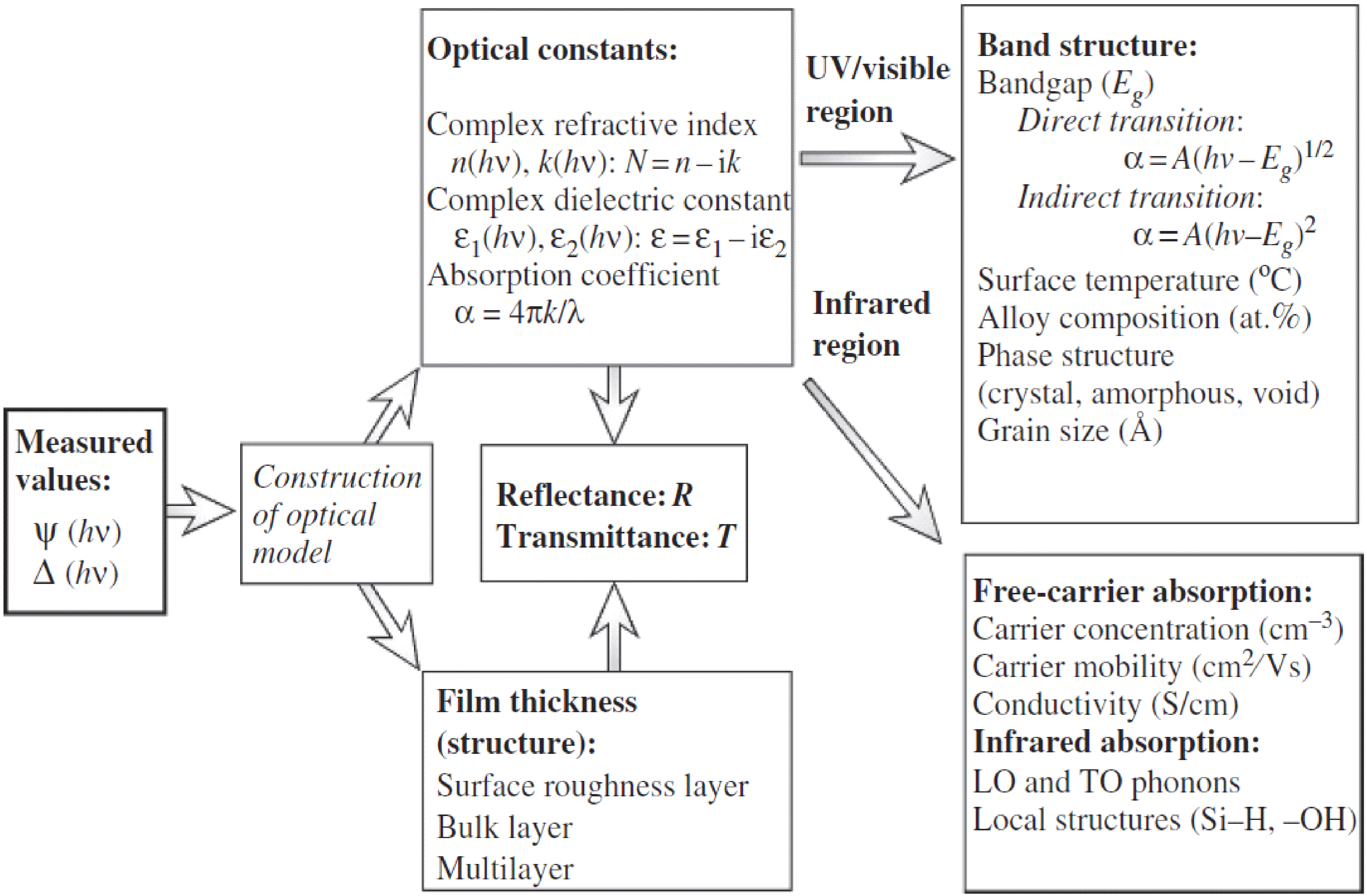
Measured values:
ψ (hν)
Δ (hν)
Construction of optical model
Optical constants:
Complex refractive index
n(hν), k(hν): N = n – ik
Complex dielectric constant
ε1(hν), ε2(hν): ε = ε1 – iε2
Absorption coefficient
α = 4πk/λ
Reflectance: R
Transmittance: T
Film thickness (structure):
Surface roughness layer
Bulk layer
Multilayer
UV/visible region
Infrared region
Band structure:
Bandgap (Eg)
Direct transition:
α = A(hν – Eg)^1/2
Indirect transition:
α = A(hν–Eg)^2
Surface temperature (°C)
Alloy composition (at.%)
Phase structure
(crystal, amorphous, void)
Grain size (Å)
Free-carrier absorption:
Carrier concentration (cm^–3)
Carrier mobility (cm^2/Vs)
Conductivity (S/cm)
Infrared absorption:
LO and TO phonons
Local structures (Si–H, –OH)

Aim: to investigate interface processes using thin film characterization methods

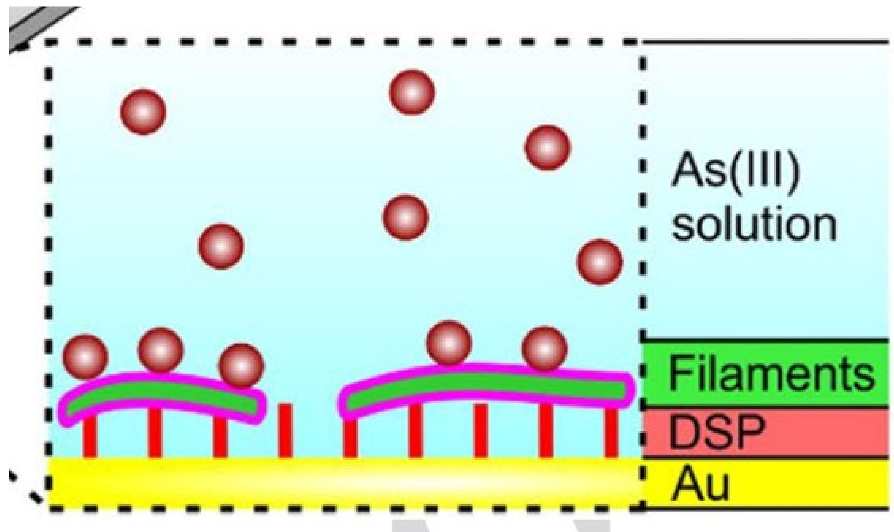

Why ellipsometry?

Measuring by particles

(+scanning probe, electrical, etc.)

	Detected		
Incident	Foton	e^-, e^+	n^0, p^+, Ion
Foton	Ellipsometry	XPS	
	Reflectometry		
	Raman		
	GI-XRD		
	XRD		
	SHG		
e^-, e^+	Positron annihilation	AES	
	EDS	TEM, SEM	
n^0, p^+, Ion	GD-OES		SIMS
	PIXE		RBS
			ND
			GD-MS

Measuring by particles

(+scanning probe, electrical, etc.)

	Detected		
Incident	Foton	e^-, e^+	n^0, p^+, Ion
Foton	Ellipsometry Reflectometry Raman GI-XRD XRD SHG	XPS	
e^-, e^+	Positron annihilation EDS	AES TEM, SEM	
n^0, p^+, Ion	GD-OES PIXE		SIMS RBS ND GD-MS

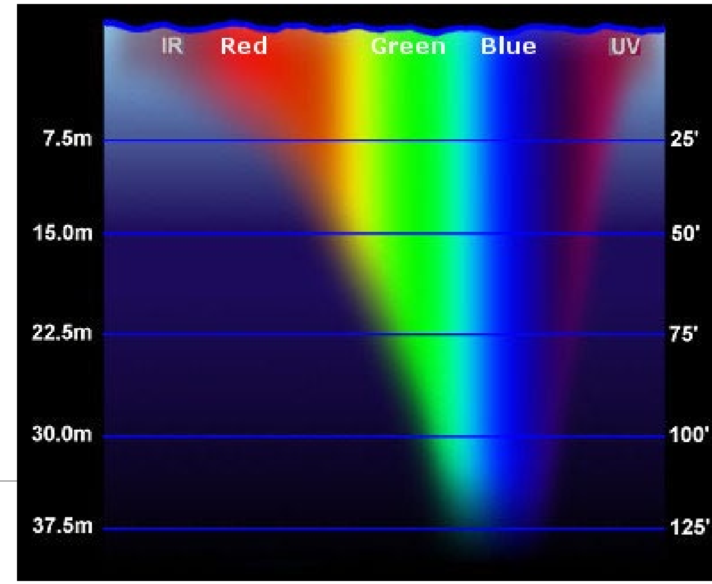

Methods for thin film characterization and depth profiling

Technique	Analysis Mode	Lateral Resolution (nm)	Depth Resolution (nm)	Duration (min)	Availability	Detection Limits (at.%)	Quantification of Results
SIMS	DP	5×10^3	4	45	Good	10^{-7}–10^{-3}	Standard
SNMS	DP	10^6	1	120	Medium	0.05	Standard
GD-OES	DP	10^6	3–100	5	Good	10^{-5}–10^{-3}	Standard
GD-MS	DP	10^7	10	10	Medium	10^{-7}–10^{-5}	Standard
AES	DP	10^5	10	45	Good	0.3	Standard
XPS	DP	10^5	1–10	120	Good	0.1	Standard-free
Raman depth-profiling	DP	10^5	100	50	Medium	1	Standard
RBS	Surf	10^7	10	10	Rare	1	Standard-free
ERDA	Surf	10^7	10	30	Rare	10^{-4}	Standard-free
GIXRD	Surf	10^6	100	420	Good	1	Difficult
AXES	Surf	10^5	10–80	420	Rare	1	Standard
Ellipsometry	Surf	10^3	1	10^{-2}	Good	0.2–2	Difficult
TEM-EDX	CS	5	Specimen thickness	30	Good-medium	0.5	Standard
SEM-EDX	CS	150	Few 100	20	Good	0.5	Standard
SEM-WDX	CS	150	Few 100	60	Good	3	Standard
Scanning Auger	CS	10	1	137	Good	3	Standard
TOF-SIMS	CS	100	1	2	Medium	10^{-6}	Standard
Raman mapping	CS	400	100	120	Medium	1	Standard

Abou-Ras D, Caballero R, Fischer C H, Kaufmann C A, Lauermann I, Mainz R, Mönig H, Schöpke A, Stephan C, Streeck C, Schorr S, Eicke A, Döbeli M, Gade B, Hinrichs J, Nunney T, Dijkstra H, Hoffmann V, Klemm D, Efimova V, Bergmaier A, Dollinger G, Wirth T, Unger W, Rockett A A, Perez-Rodriguez A, Alvarez-Garcia J, Izquierdo-Roca V, Schmid T, Choi P P, Müller M, Bertram F, Christen J, Khatri H, Collins R W, Marsillac S and Kötschau I, 2011 Microsc. Microanal. 17 (2011) 728.

Methods for thin film characterization

Technique	Analysis Mode	Lateral Resolution (nm)	Depth Resolution (nm)	Duration (min)	Availability	Detection Limits (at.%)	Quantification of Results
SIMS	DP	5×10^3	4	45	Good	10^{-7}–10^{-3}	Standard
SNMS	DP	10^6	1	120	Medium	0.05	Standard
GD-OES	DP	10^6	3–100	5	Good	10^{-5}–10^{-3}	Standard
GD-MS	DP	10^7	10	10	Medium	10^{-7}–10^{-5}	Standard
AES	DP	10^5	10	45	Good	0.3	Standard
XPS	DP	10^5	1–10	120	Good	0.1	Standard-free
Raman depth-profiling	DP	10^5	100	[illegible]	Medium	1	Standard
RBS	Surf	10^7	10	[illegible]	[illegible]	1	Standard-free
ERDA	Surf	10^7	10	[illegible]	[illegible]	10^{-4}	Standard-free
GIXRD	Surf	10^6	100	420	Good	1	Difficult
AXES	Surf	10^5	10–80	420	Rare	1	Standard
Ellipsometry	Surf	10^3	1	10^{-2}	Good	0.2–2	Difficult
TEM-EDX	CS	5	Specimen thickness	30	Good-medium	0.5	Standard
SEM-EDX	CS	150	Few 100	20	Good	0.5	Standard
SEM-WDX	CS	150	Few 100	60	Good	3	Standard
Scanning Auger	CS	10	1	137	Good	3	Standard
TOF-SIMS	CS	100	1	2	Medium	10^{-6}	Standard
Raman mapping	CS	400	100	120	Medium	1	Standard

Quick

Abou-Ras D, Caballero R, Fischer C H, Kaufmann C A, Lauermann I, Mainz R, Mönig H, Schöpke A, Stephan C, Streeck C, Schorr S, Eicke A, Döbeli M, Gade B, Hinrichs J, Nunney T, Dijkstra H, Hoffmann V, Klemm D, Efimova V, Bergmaier A, Dollinger G, Wirth T, Unger W, Rockett A A, Perez-Rodriguez A, Alvarez-Garcia J, Izquierdo-Roca V, Schmid T, Choi P P, Müller M, Bertram F, Christen J, Khatri H, Collins R W, Marsillac S and Kötschau I, 2011 Microsc. Microanal. 17 (2011) 728.

Point-by-point mapping of large surfaces

MEASUREMENT TIME

Area: 30 cm x 30 cm
Resolution: 1 cm

6 s / point

1.5 h

Department of Physics & Astronomy and Center for Photovoltaics Innovation and Commercialization, The University of Toledo

L. R. Dahal , Z. Huang , C. Salupo , N. J. Podraza , S. Marsillac , R. W. Collins, „MAPPING AMORPHOUS SILICON p-TYPE LAYERS IN ROLL-TO-ROLL DEPOSITION: TOWARD SPATIALLY RESOLVED PECVD PHASE DIAGRAMS, IEEE Photovoltaics Specialists Conference 6185876 (2011) 182.

Divergent source mapping of large surfaces

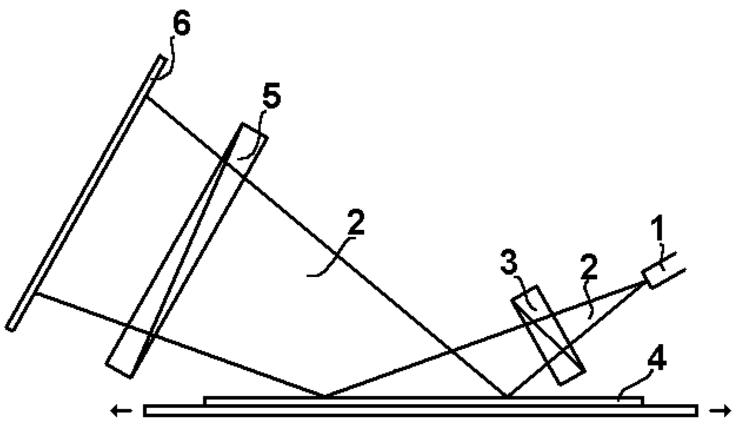

G. Juhasz, Z. Horvath, C. Major, P. Petrik, O. Polgar, M. Fried, "Non-collimated beam ellipsometry," physica status solidi c 5 (2008) 1081-1084.

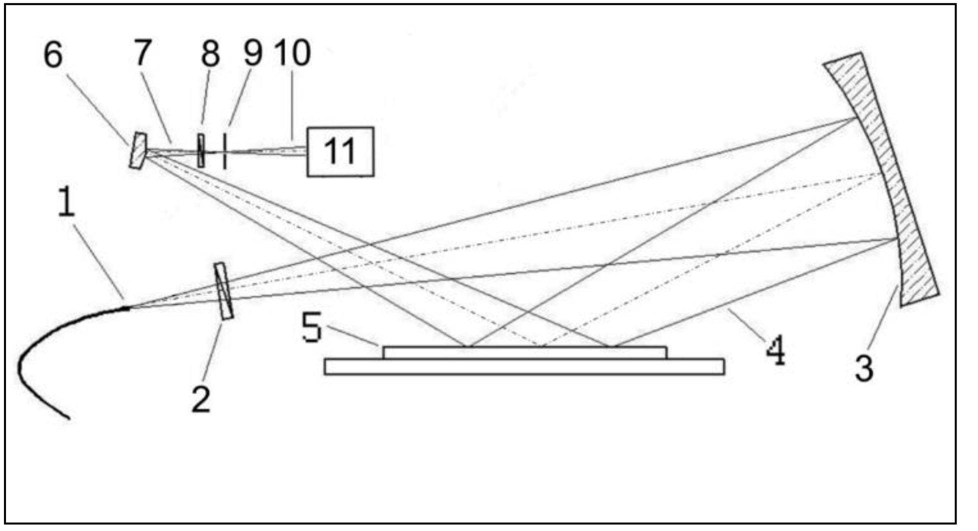

M. Fried, G. Juhász, C. Major, P. Petrik, O. Polgár, Z. Horváth, A. Nutsch, "Expanded beam (macro-imaging) ellipsometry", Thin Solid Films 519 (2011) 2730.

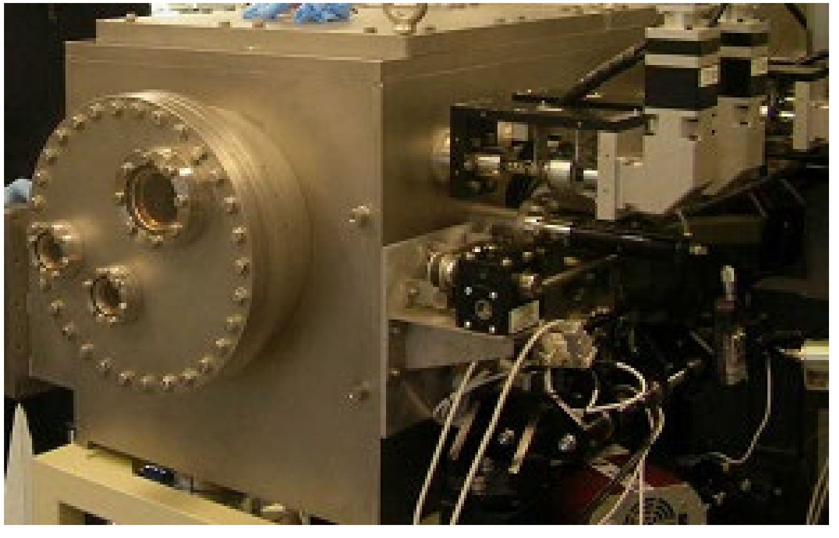

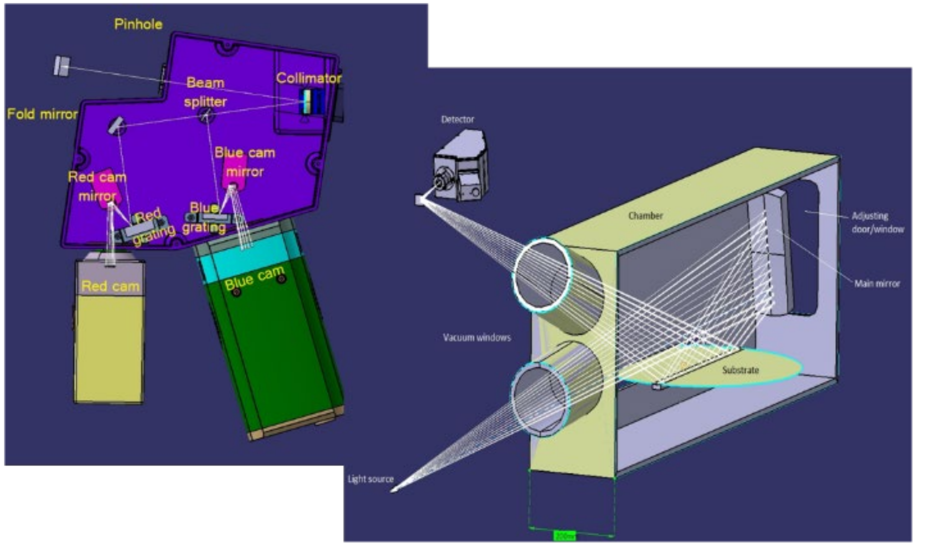

Psi-map of (nominally 110 nm) SiO_2 /Si wafer

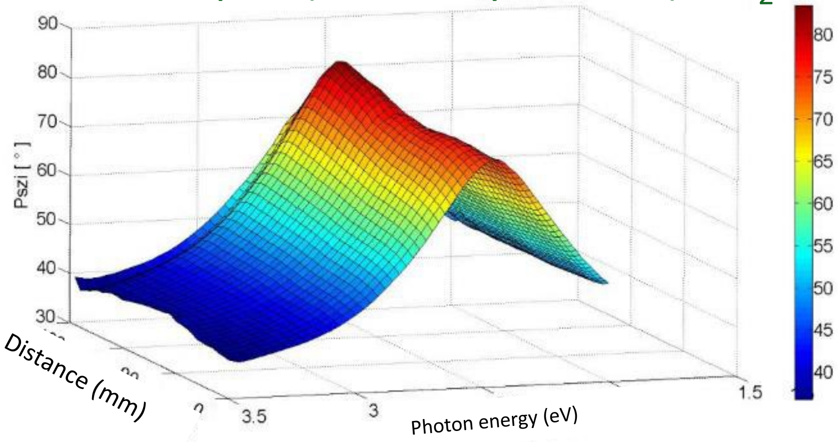

Spectroscopic mapping

Area: 30 cm x 30 cm
Resolution: 1 cm

1 min

Map by moving the sample

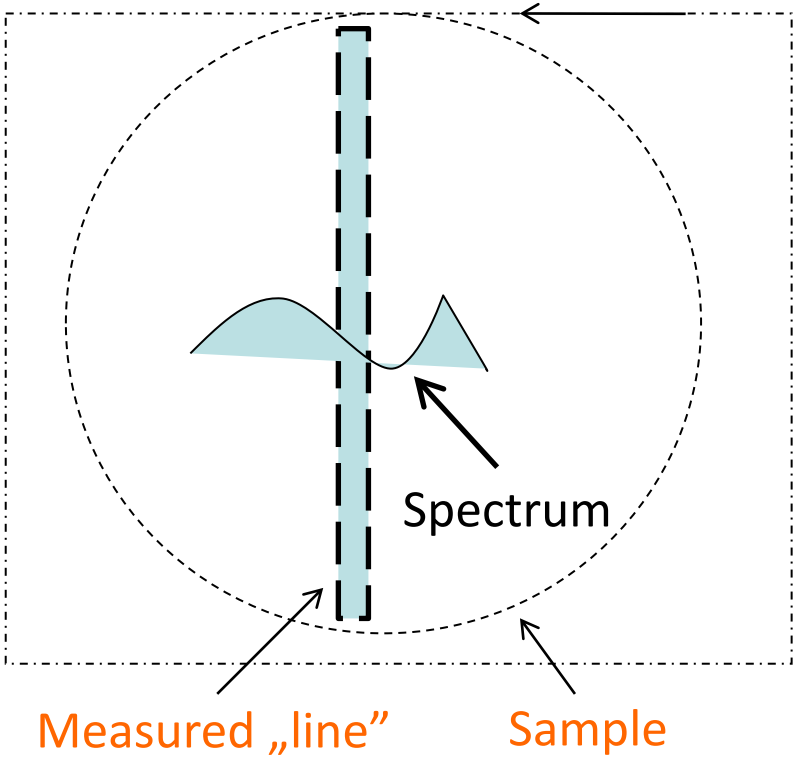

5/10 mm periodic SiO_2 pattern

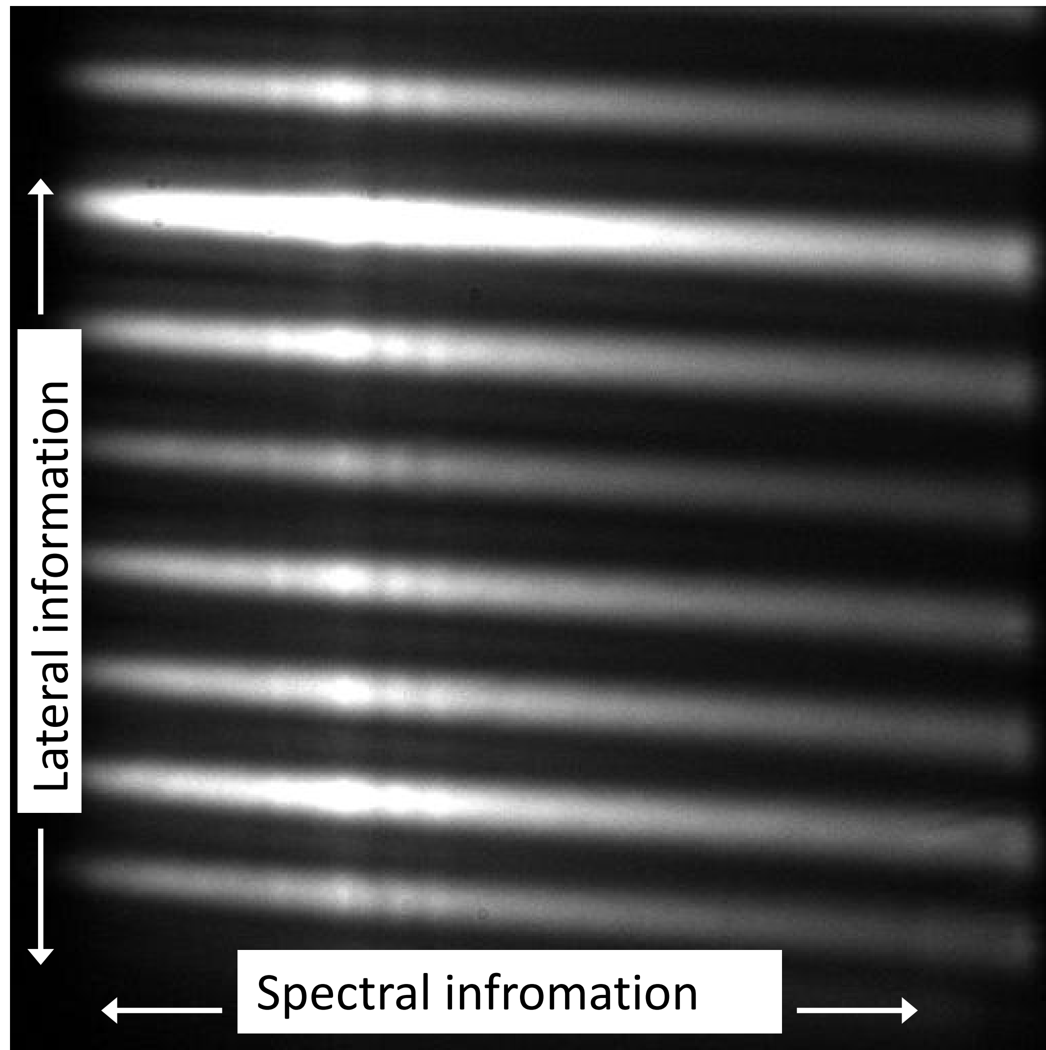

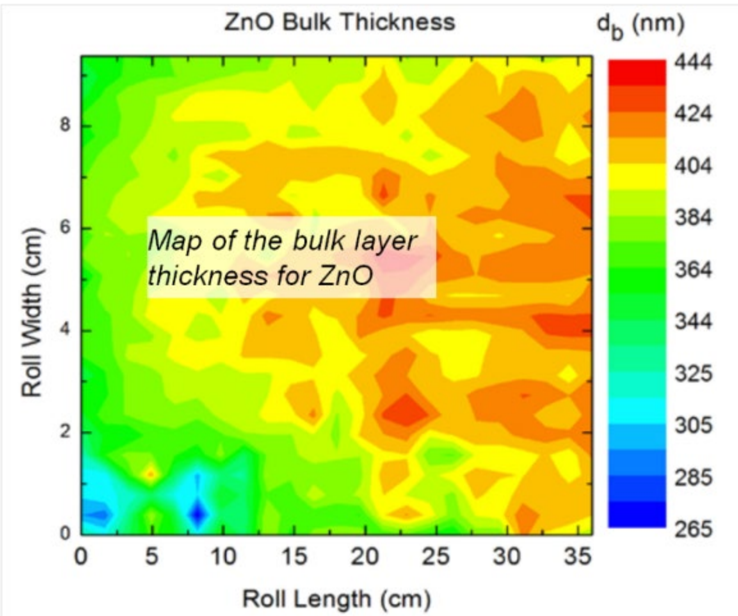
ZnO Bulk Thickness
d_b (nm)
444
424
404
384
364
344
325
305
285
265
Map of the bulk layer thickness for ZnO
Roll Width (cm)
Roll Length (cm)
0
2
4
6
8
0 5 10 15 20 25 30 35

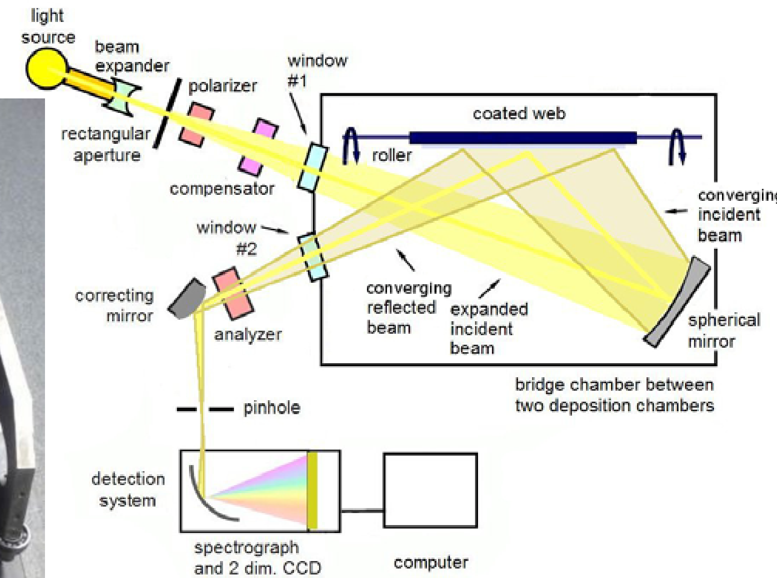
light source
beam expander
rectangular aperture
polarizer
compensator
window #1
window #2
coated web
roller
converging incident beam
converging reflected beam
expanded incident beam
spherical mirror
correcting mirror
analyzer
pinhole
bridge chamber between two deposition chambers
detection system
spectrograph and 2 dim. CCD
computer

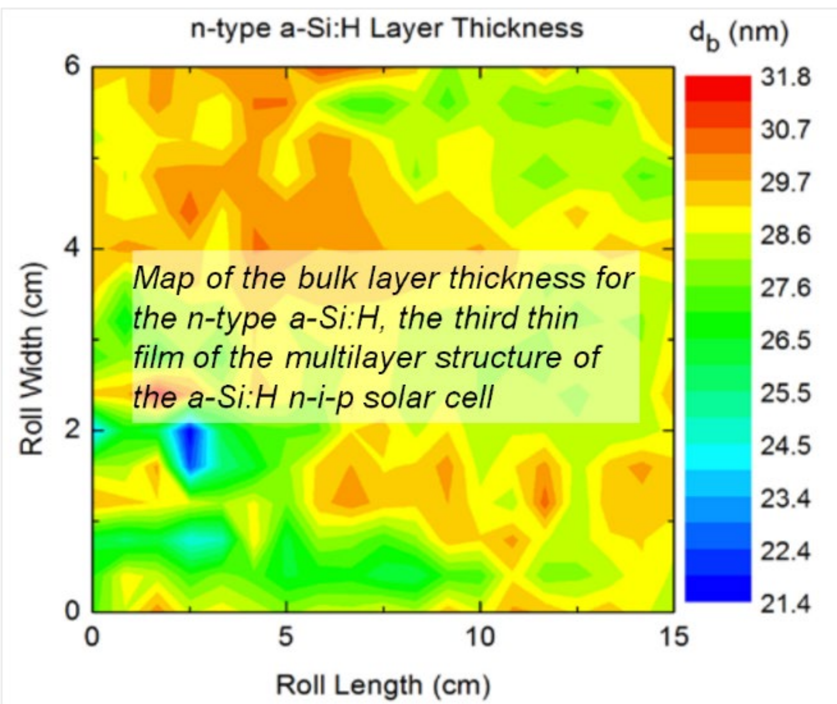
n-type a-Si:H Layer Thickness
d_b (nm)
31.8
30.7
29.7
28.6
27.6
26.5
25.5
24.5
23.4
22.4
21.4
Map of the bulk layer thickness for the n-type a-Si:H, the third thin film of the multilayer structure of the a-Si:H n-i-p solar cell
Roll Width (cm)
Roll Length (cm)
0
2
4
6
0 5 10 15

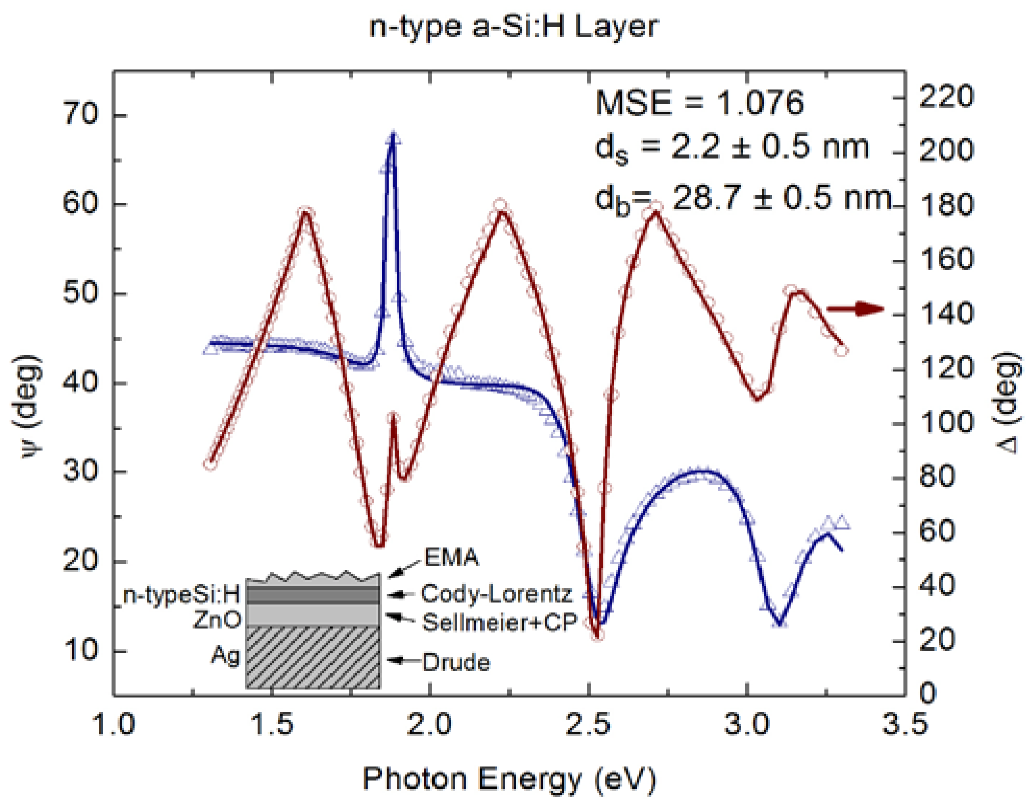
n-type a-Si:H Layer
MSE = 1.076
d_s = 2.2 ± 0.5 nm
d_b = 28.7 ± 0.5 nm
ψ (deg)
Δ (deg)
Photon Energy (eV)
10 20 30 40 50 60 70
0 20 40 60 80 100 120 140 160 180 200 220
1.0 1.5 2.0 2.5 3.0 3.5
n-typeSi:H
ZnO
Ag
EMA
Cody-Lorentz
Sellmeier+CP
Drude

3 prototypes of expanded beam mapping spectroscopic ellipsometer

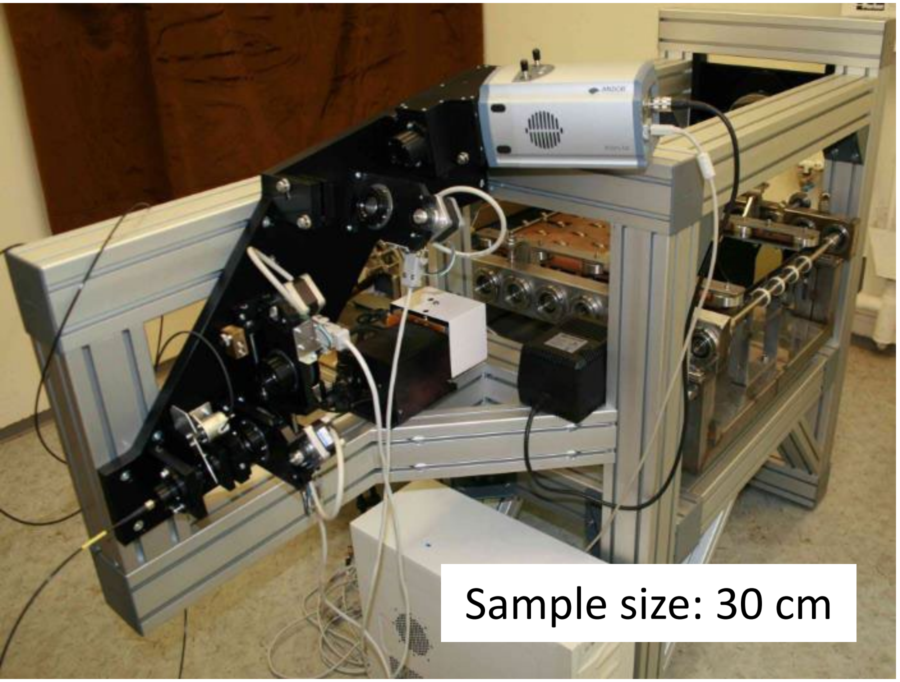

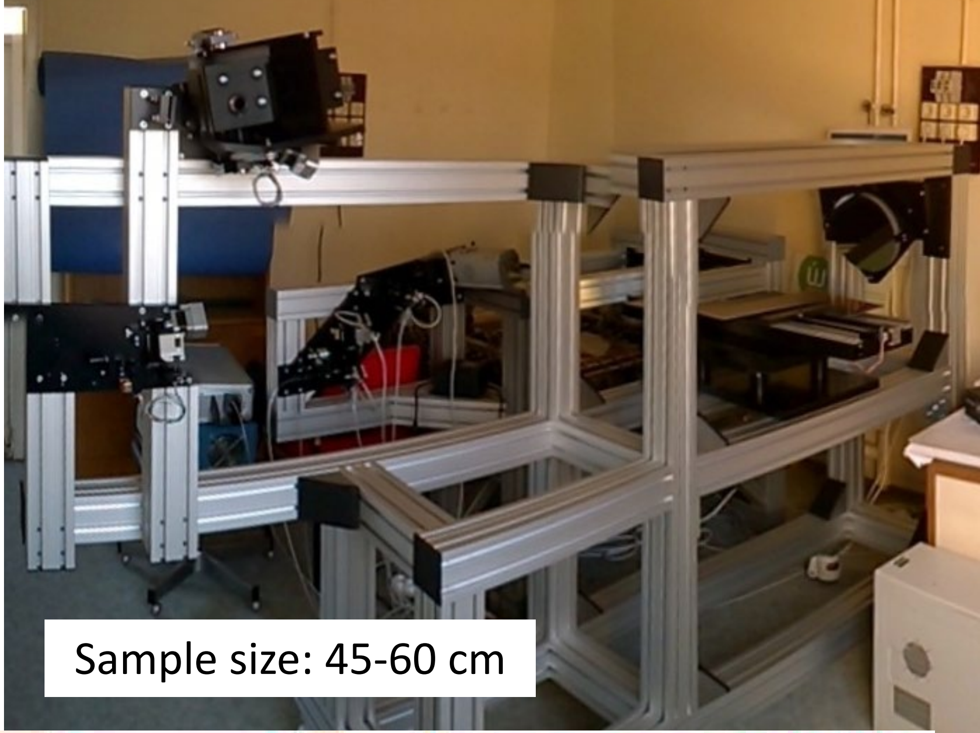

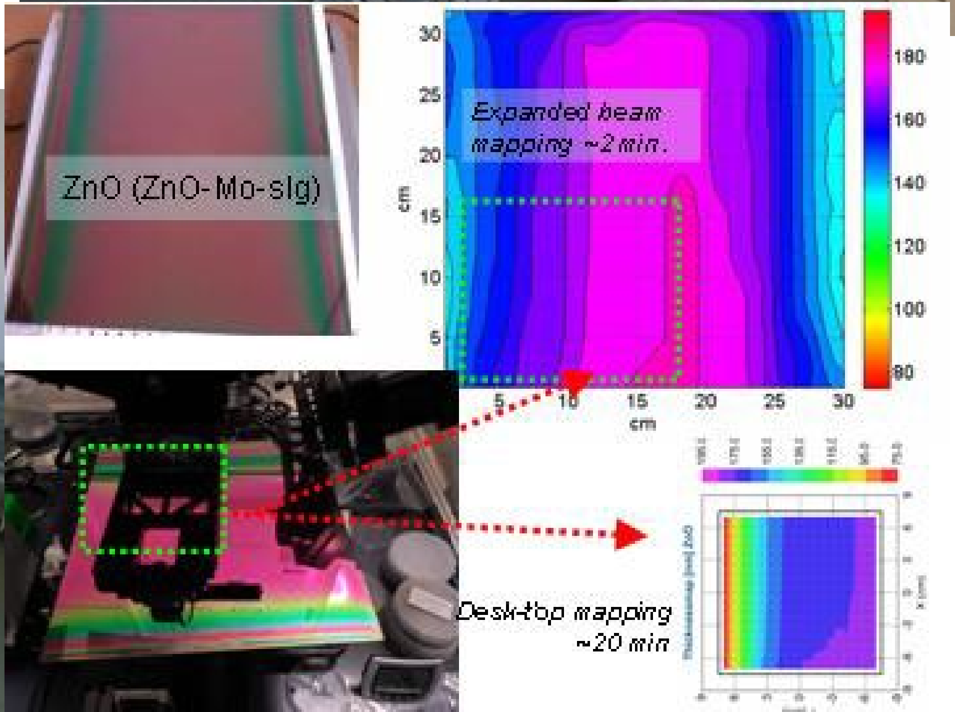

Methods for thin film characterization

Technique	Analysis Mode	Lateral Resolution (nm)	Depth Resolution (nm)	Duration (min)	Availability	Detection Limits (at.%)	Quantification of Results
SIMS	DP	5×10^3	4	45	Good	10^{-7}–10^{-3}	Standard
SNMS	DP	10^6	1	120	Medium	0.05	Standard
GD-OES	DP	10^6	3–100	5	Good	10^{-5}–10^{-3}	Standard
GD-MS	DP	10^7	10	10	Medium	10^{-7}–10^{-5}	Standard
AES	DP	10^5	10	45	Good	0.3	Standard
XPS	DP	10^5	1–10	120	Good	0.1	Standard-free
Raman	[illegible]	[illegible]	100	50	Medium	1	Standard
RBS	[illegible]	[illegible]	10	10	Rare	1	Standard-free
ERDA	[illegible]	[illegible]	10	30	Rare	10^{-4}	Standard-free
GIXRD	Surf	10^6	100	420	Good	1	Difficult
AXES	Surf	10^5	10–80	420	Rare	1	Standard
Ellipsometry	Surf	10^3	1	10^{-2}	Good	0.2–2	Difficult
TEM-EDX	CS	5	Specimen thickness	30	Good-medium	0.5	Standard
SEM-EDX	CS	150	Few 100	20	Good	0.5	Standard
SEM-WDX	CS	150	Few 100	60	Good	3	Standard
Scanning Auger	CS	10	1	137	Good	3	Standard
TOF-SIMS	CS	100	1	2	Medium	10^{-6}	Standard
Raman mapping	CS	400	100	120	Medium	1	Standard

Non-destructive

Abou-Ras D, Caballero R, Fischer C H, Kaufmann C A, Lauermann I, Mainz R, Mönig H, Schöpke A, Stephan C, Streeck C, Schorr S, Eicke A, Döbeli M, Gade B, Hinrichs J, Nunney T, Dijkstra H, Hoffmann V, Klemm D, Efimova V, Bergmaier A, Dollinger G, Wirth T, Unger W, Rockett A A, Perez-Rodriguez A, Alvarez-Garcia J, Izquierdo-Roca V, Schmid T, Choi P P, Müller M, Bertram F, Christen J, Khatri H, Collins R W, Marsillac S and Kötschau I, 2011 Microsc. Microanal. 17 (2011) 728.

Combination of grating coupled interferometry with spectroscopic ellipsometry

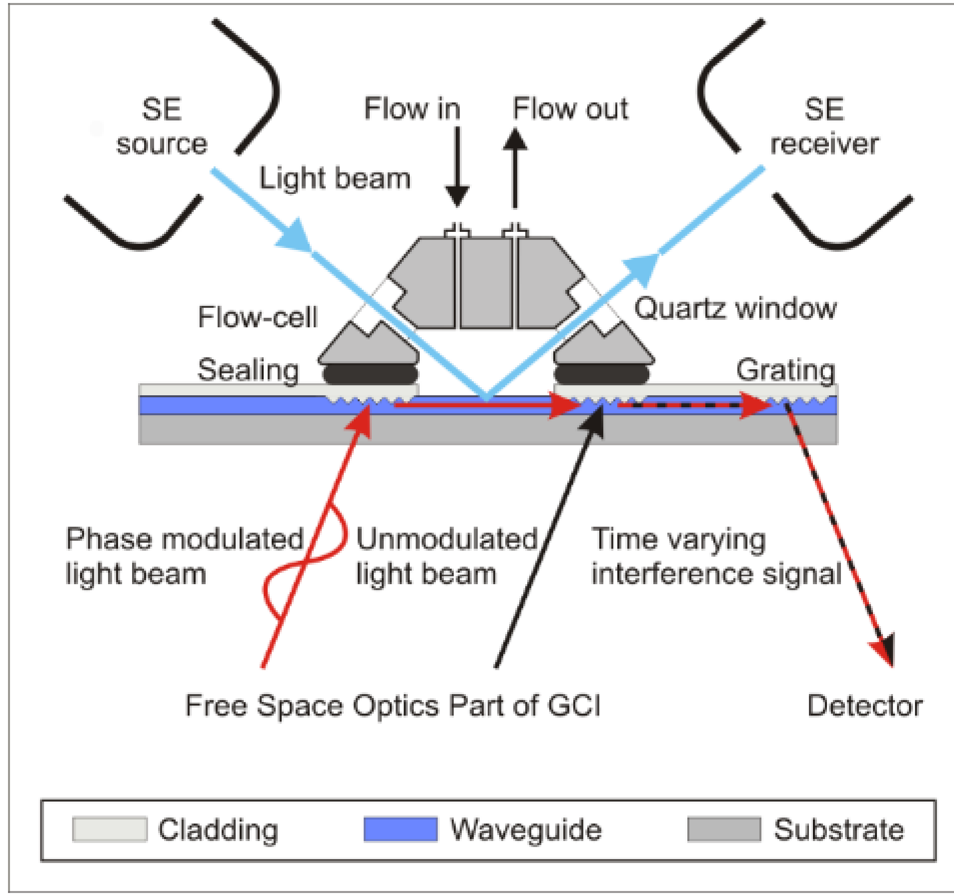

THE INTERFEROMETER:

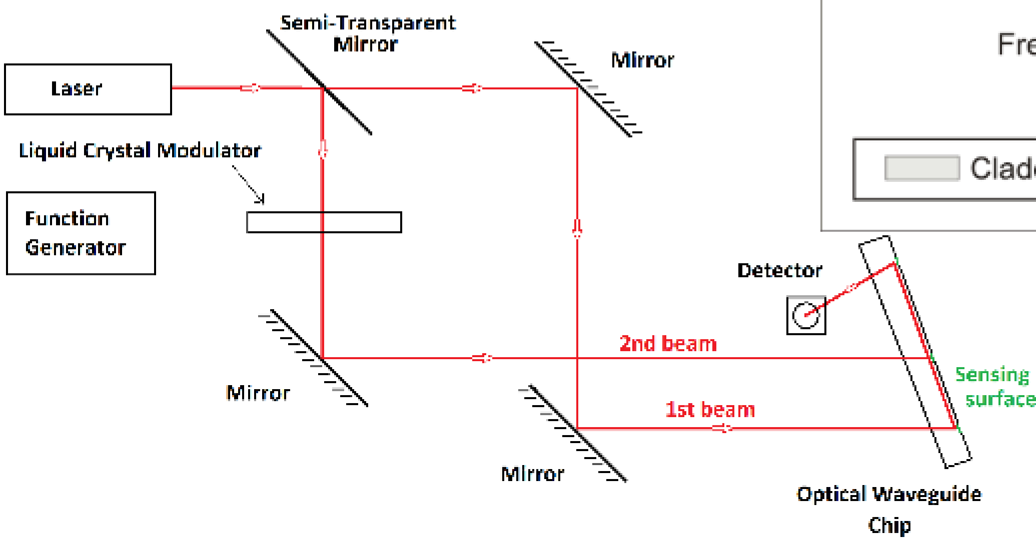

E. Agocs, P. Kozma, J. Nador, B. Kalas, A. Hamori, M. Janosov, S. Kurunczi, B. Fodor, M. Fried, R. Horvath, P. Petrik, “In-situ simultaneous monitoring of layer adsorption in aqueous solutions using grating coupled optical waveguide interferometry combined with spectroscopic ellipsometry“, Appl. Surf. Sci. 421 (2017) 289.

Methods for thin film characterization

Technique	Analysis Mode	Lateral Resolution (nm)	Depth Resolution (nm)	Duration (min)	Availability	Detection Limits (at.%)	Quantification of Results
SIMS	DP	5×10^3	4	45	Good	10^{-7}–10^{-3}	Standard
SNMS	DP	10^6	1	120	Medium	0.05	Standard
GD-OES	DP	10^6	3–100	5	Good	10^{-5}–10^{-3}	Standard
GD-MS	DP	10^7	10	10	Medium	10^{-7}–10^{-5}	Standard
AES	DP	10^5	10	45	Good	0.3	Standard
XPS	DP	10^5	1–10	120	Good	0.1	Standard-free
Raman depth-profiling	DP	[illegible]	[illegible]	[illegible]	Medium	1	Standard
RBS	Surf	[illegible]	[illegible]	[illegible]	Rare	1	Standard-free
ERDA	Surf	[illegible]	[illegible]	[illegible]	Rare	10^{-4}	Standard-free
GIXRD	Surf	10^6	100	420	Good	1	Difficult
AXES	Surf	10^5	10–80	420	Rare	1	Standard
Ellipsometry	Surf	10^3	1	10^{-2}	Good	0.2–2	Difficult
TEM-EDX	CS	5	Specimen thickness	30	Good-medium	0.5	Standard
SEM-EDX	CS	150	Few 100	20	Good	0.5	Standard
SEM-WDX	CS	150	Few 100	60	Good	3	Standard
Scanning Auger	CS	10	1	137	Good	3	Standard
TOF-SIMS	CS	100	1	2	Medium	10^{-6}	Standard
Raman mapping	CS	400	100	120	Medium	1	Standard

Sensitive

Abou-Ras D, Caballero R, Fischer C H, Kaufmann C A, Lauermann I, Mainz R, Mönig H, Schöpke A, Stephan C, Streeck C, Schorr S, Eicke A, Döbeli M, Gade B, Hinrichs J, Nunney T, Dijkstra H, Hoffmann V, Klemm D, Efimova V, Bergmaier A, Dollinger G, Wirth T, Unger W, Rockett A A, Perez-Rodriguez A, Alvarez-Garcia J, Izquierdo-Roca V, Schmid T, Choi P P, Müller M, Bertram F, Christen J, Khatri H, Collins R W, Marsillac S and Kötschau I, 2011 Microsc. Microanal. 17 (2011) 728.

Conventional flow cell

Kretschmann-Raether configuration

Combination of methods

Tuning of the resonance

Mid infrared range

Electrochemical sensing

Combinatory

Summary

Applied Surface Science 257 (2011) 7160–7166

Contents lists available at ScienceDirect

Applied Surface Science

journal homepage: www.elsevier.com/locate/apsusc

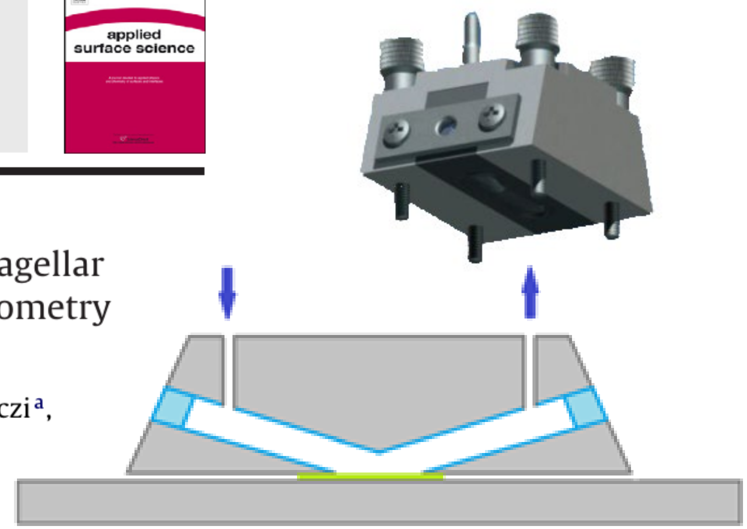

In-depth characterization and computational 3D reconstruction of flagellar filament protein layer structure based on in situ spectroscopic ellipsometry measurements

Peter Kozma[a,b,*], Daniel Kozma[c], Andrea Nemeth[a], Hajnalka Jankovics[b], Sandor Kurunczi[a], Robert Horvath[a], Ferenc Vonderviszt[a,b], Miklos Fried[a], Peter Petrik[a]

[a] Research Institute for Technical Physics and Materials Science (MFA), H-1121, Budapest, Konkoly-Thege út 29-33, Hungary
[b] Department of Nanotechnology, Faculty of Information Technology, University of Pannonia, H-8200, Veszprém, Egyetem u. 10, Hungary
[c] Institute of Enzimology, Hungarian Academy of Sciences, H-1113, Budapest, Karolina út 29, Hungary

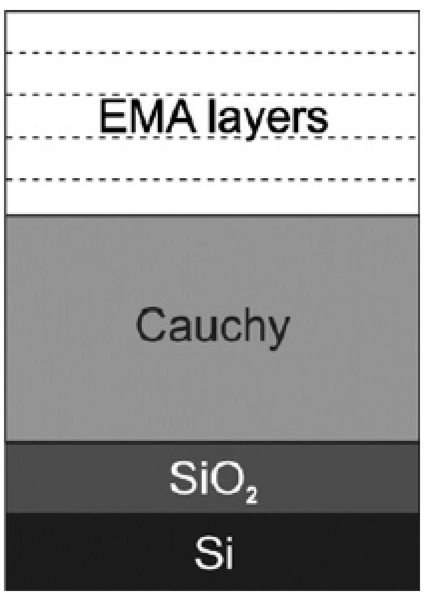

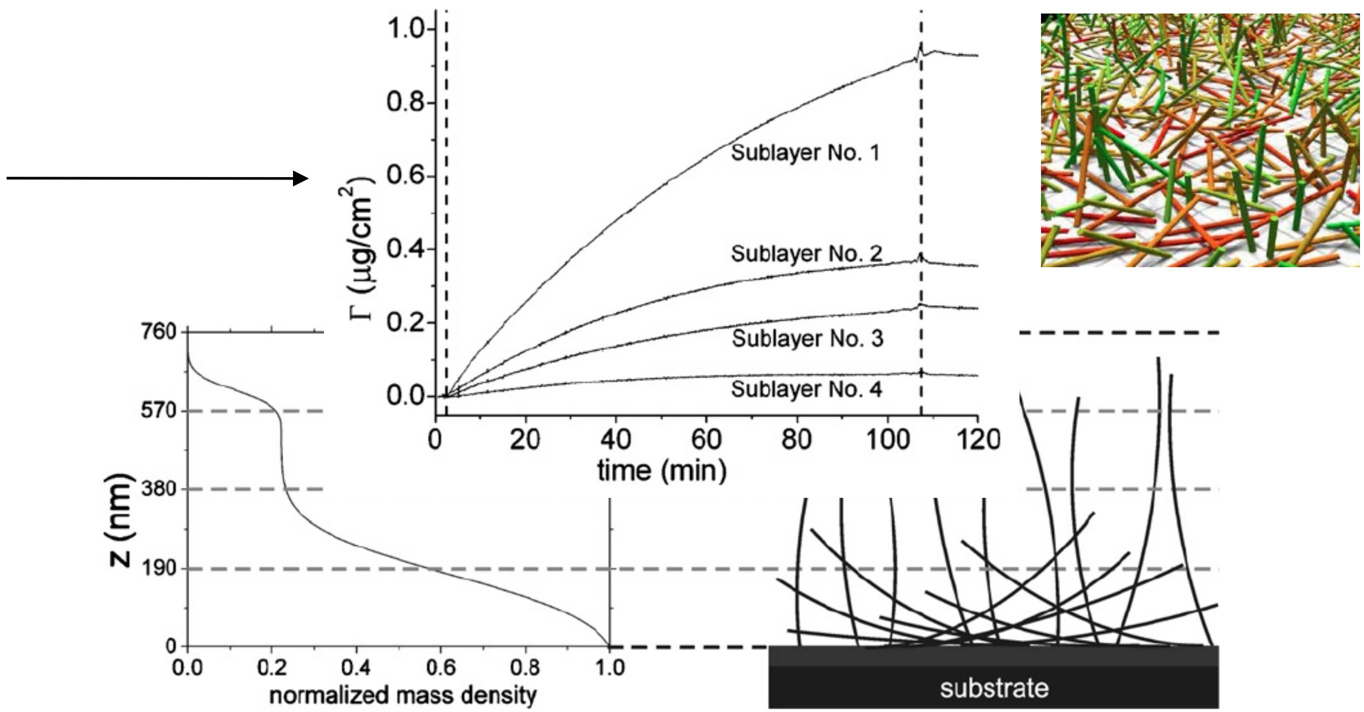

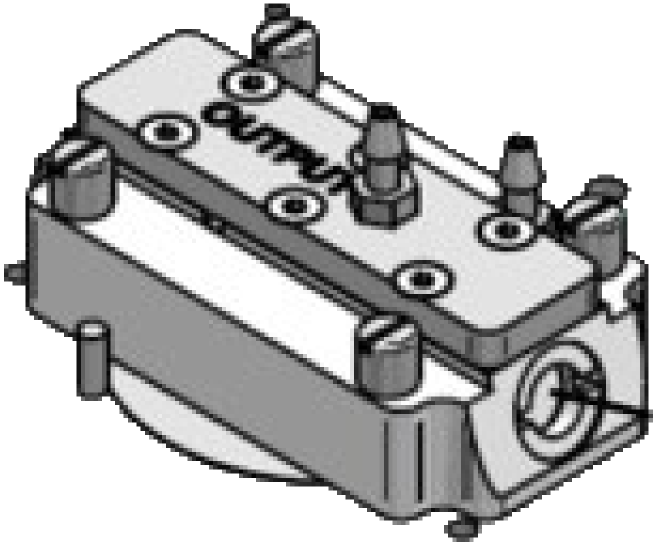

Decrease size,

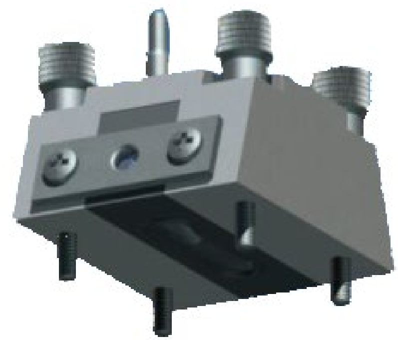

To decrease

- the time to mix,
- the amount of material

A new simple tubular flow cell for use with variable angle spectroscopic ellipsometry: A high throughput in situ protein adsorption study

T.M. Byrne[a], S. Trussler[a], M.A. McArthur[a], L.B. Lohstreter[b], Zhijun Bai[c], M.J. Filiaggi[c,d], J.R. Dahn[a,e,*]

[a] Department of Physics and Atmospheric Science, Dalhousie University, Halifax, NS, Canada B3H 3J5
[b] Medtronic Corporation, Minneapolis, MN, USA
[c] School of Biomedical Engineering, Dalhousie University, Halifax, NS, Canada B3H 3J5
[d] Department of Applied Oral Sciences, Faculty of Dentistry, Halifax, NS, Canada B3H 3J5
[e] Department of Chemistry, Dalhousie University, Halifax, NS, Canada B3H 3J5

Change the angle

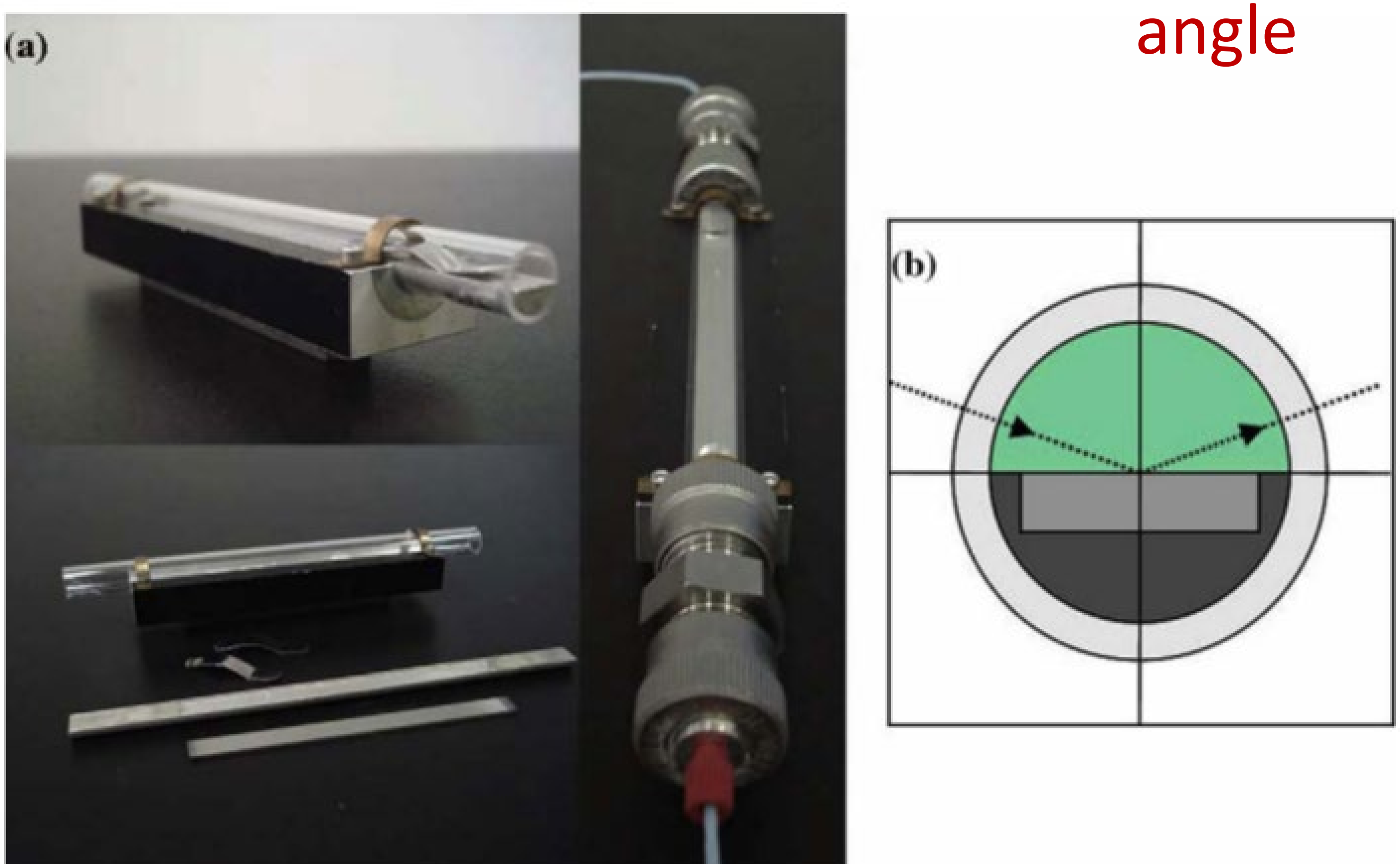

Conventional flow cell

Kretschmann-Raether configuration

Combination of methods

Tuning of the resonance

Mid infrared range

Electrochemical sensing

Combinatory

Summary

Kretschmann configuration

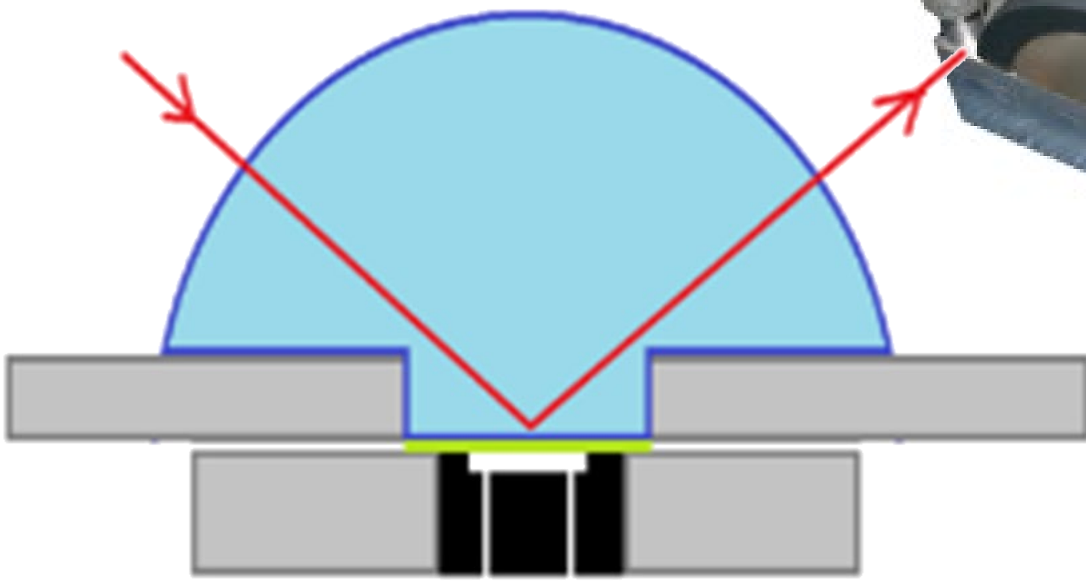

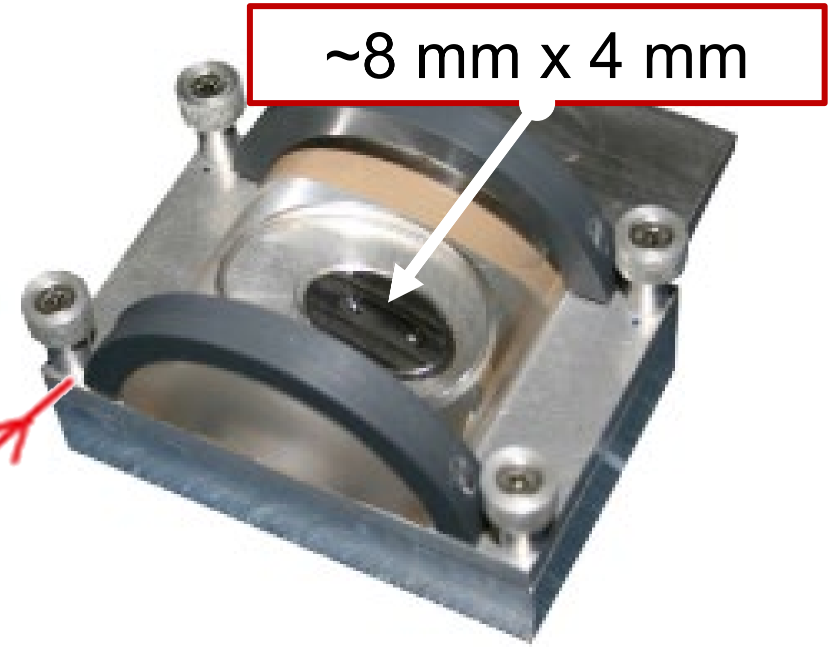

J. Nador, B. Kalas, A. Saftics, E. Agocs, P. Kozma, L. Korosi, I. Szekacs, M. Fried, R. Horvath, P. Petrik, Plasmon-enhanced two-channel in situ Kretschmann ellipsometry of protein adsorption , cellular adhesion and polyelectrolyte deposition on titania nanostructures, Opt Express. 24 (2016) 4812–4823.

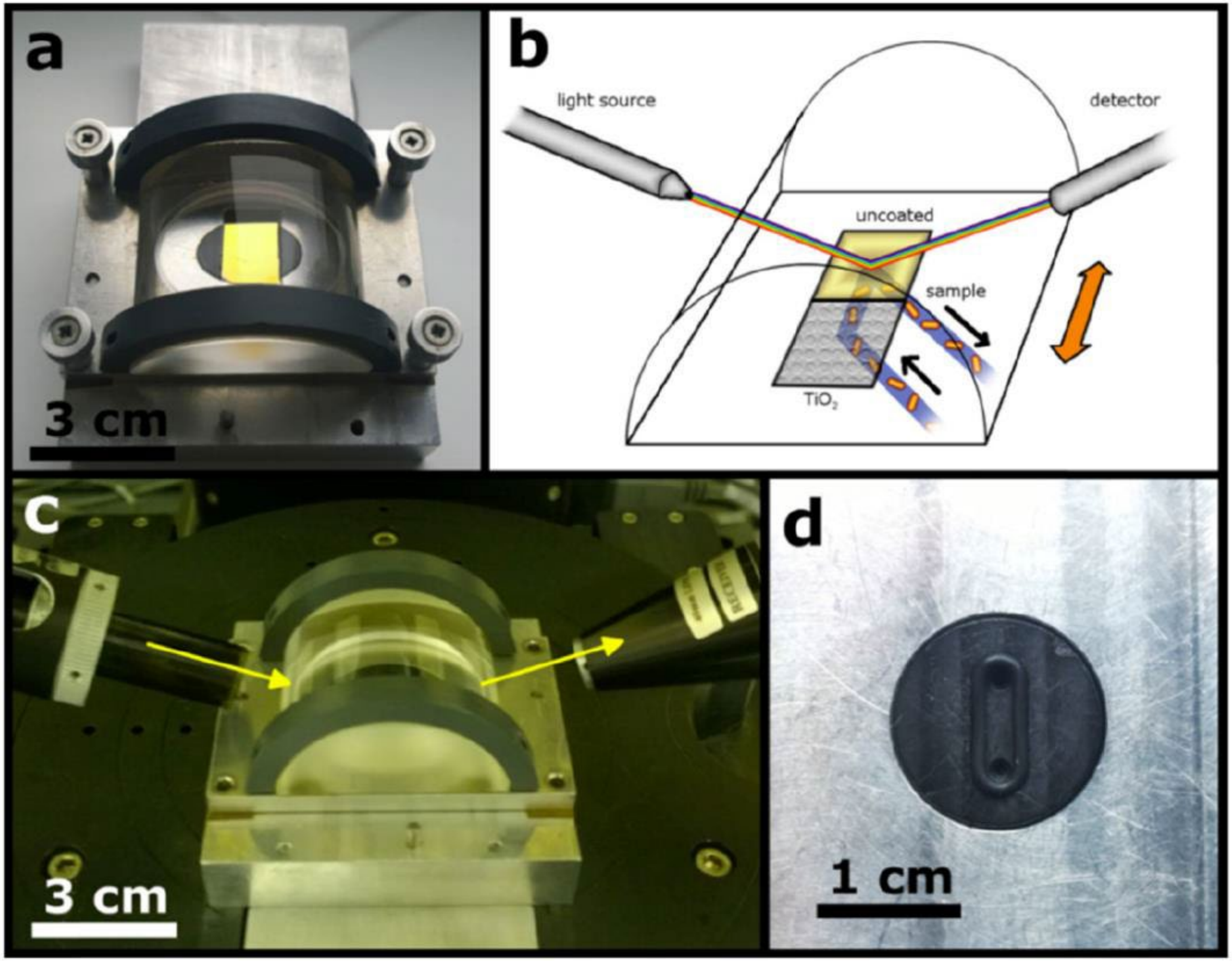

Moving spot (two-channel capabilities)

J. Nador, B. Kalas, A. Saftics, E. Agocs, P. Kozma, L. Korosi, I. Szekacs, M. Fried, R. Horvath, P. Petrik, Plasmon-enhanced two-channel *in situ* Kretschmann ellipsometry of protein adsorption, cellular adhesion and polyelectrolyte deposition on titania nanostructures, Opt. Express. 24 (2016) 4812.

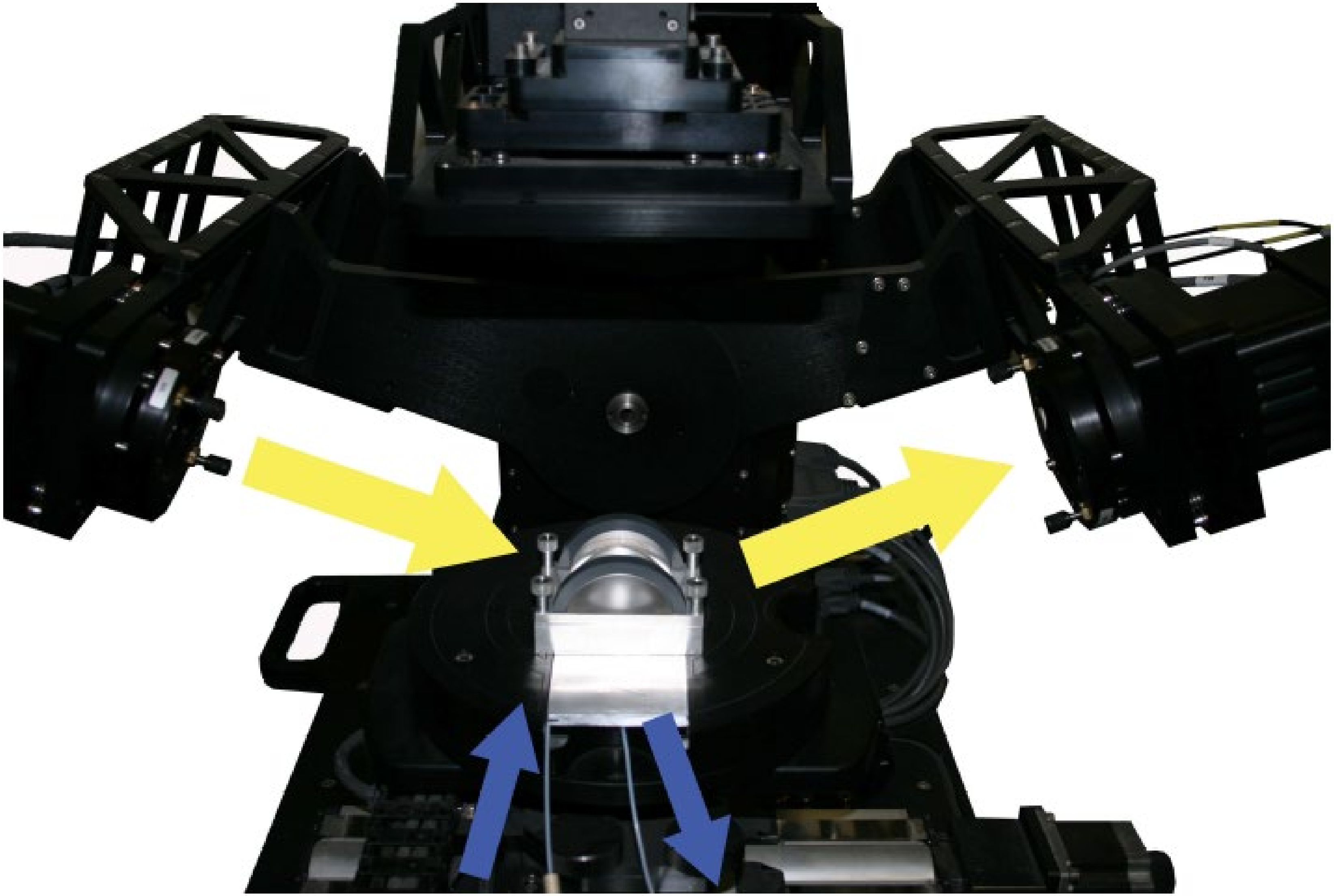

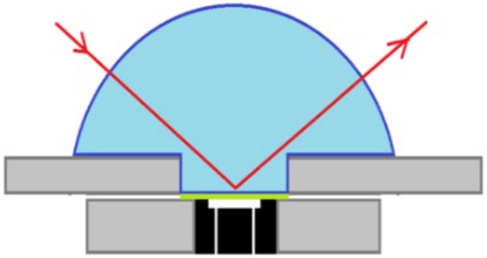

$$\tan \Psi = \text{abs}(r_p/r_s)$$

tan ψ - measured

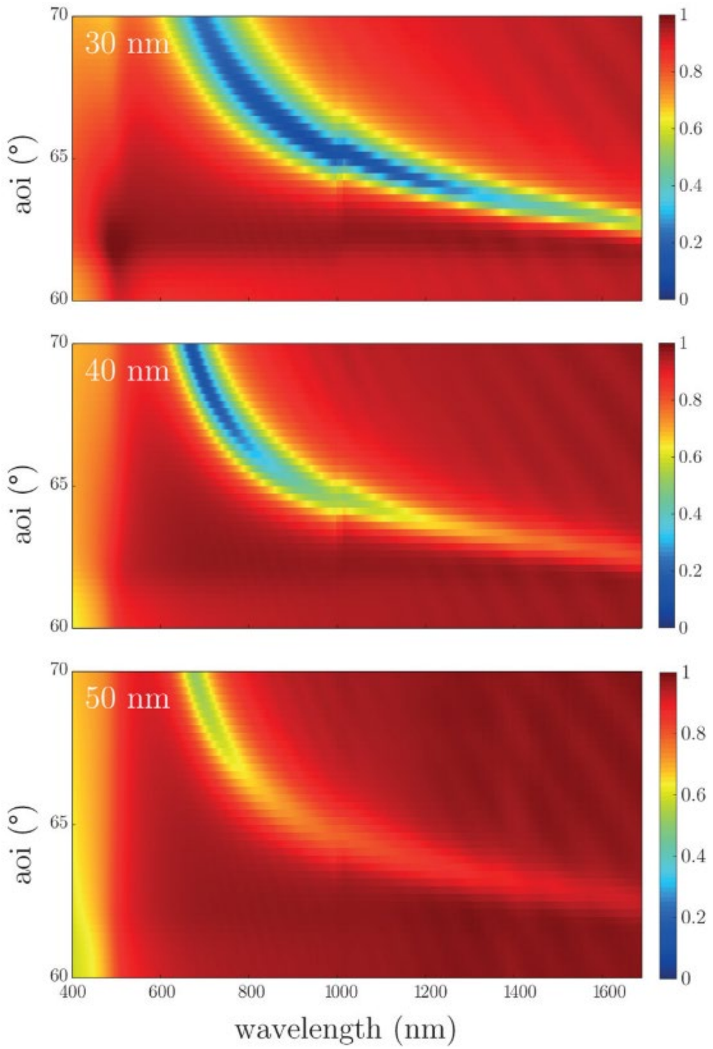

30

40

50

Two-channel fibrinogen adsorption study

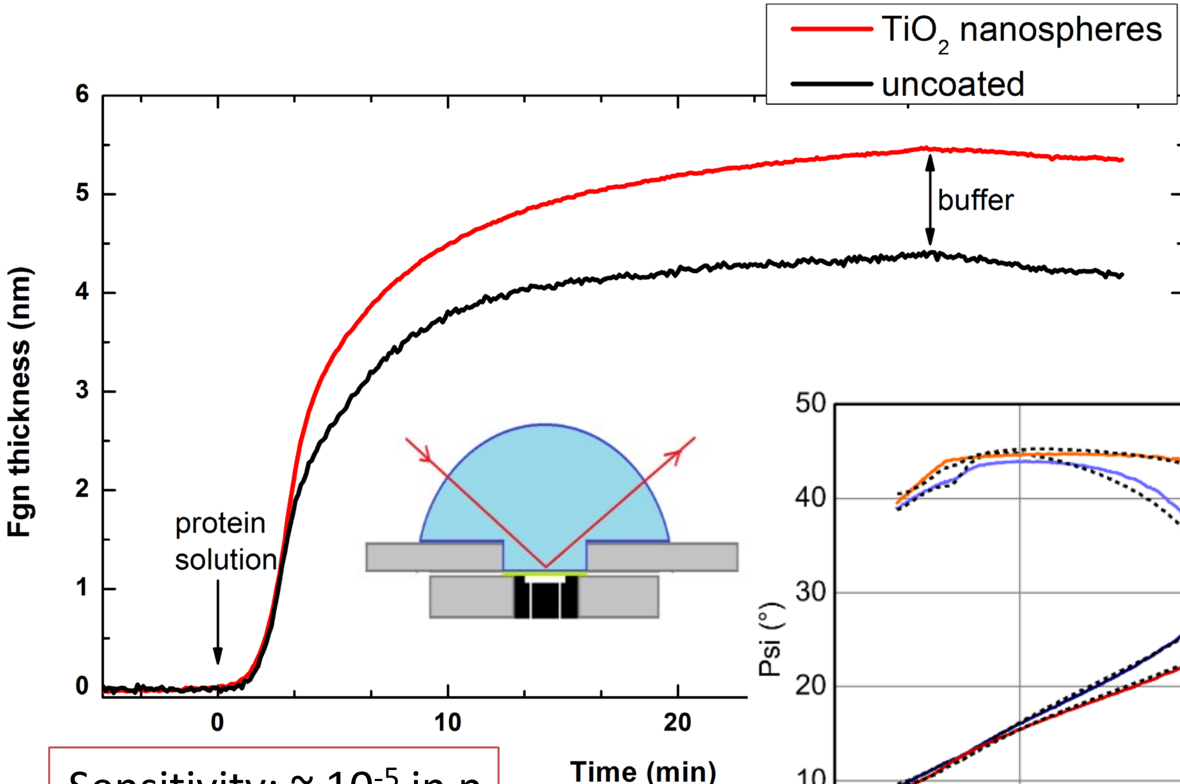

Sensitivity: ~ 10^{-5} in n

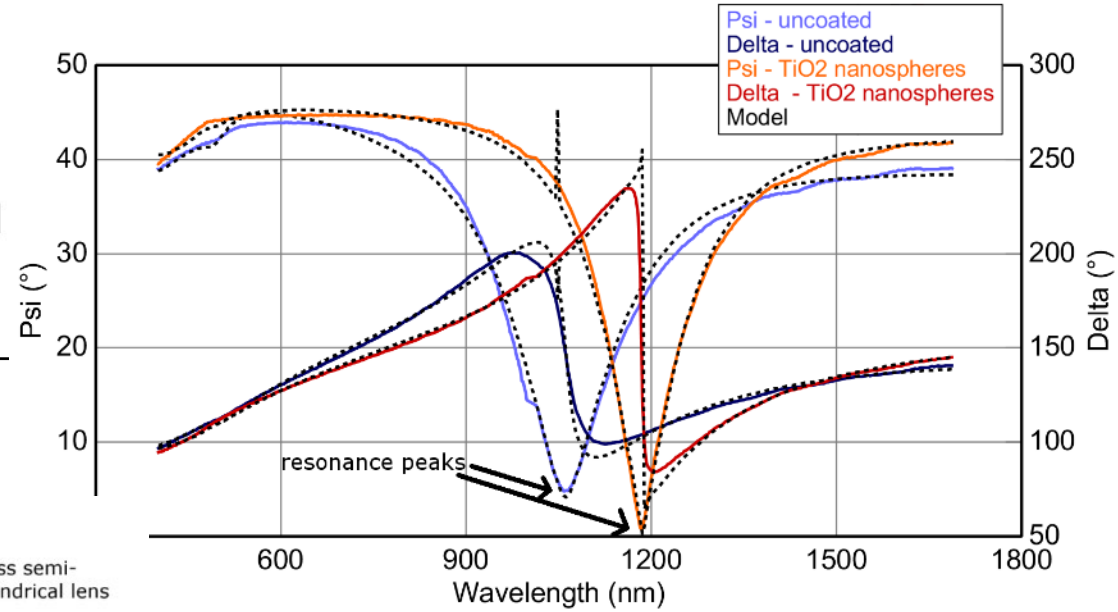

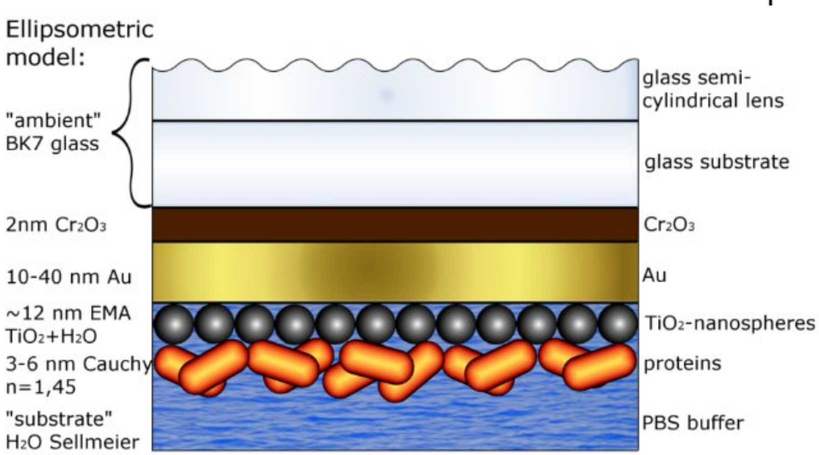

J. Nador, B. Kalas, A. Saftics, E. Agocs, P. Kozma, L. Korosi, I. Szekacs, M. Fried, R. Horvath, P. Petrik, Plasmon-enhanced two-channel in situ Kretschmann ellipsometry of protein adsorption , cellular adhesion and polyelectrolyte deposition on titania nanostructures, Opt Express. 24 (2016) 4812–4823.

Adsorption of flagellar filaments

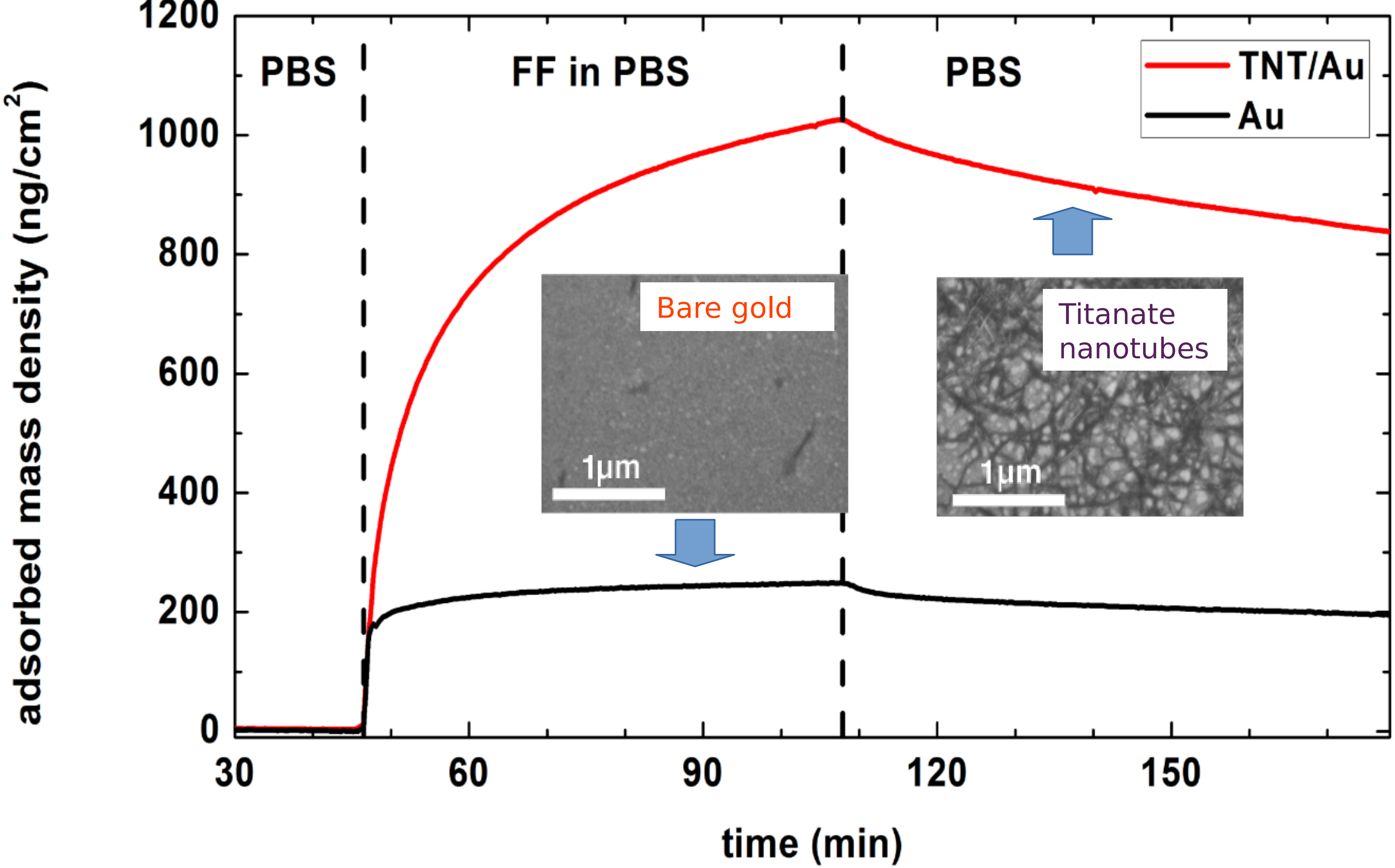

Conventional flow cell

Kretschmann-Raether configuration

Combination of methods

Tuning of the resonance

Mid infrared range

Electrochemical sensing

Combinatory

Summary

Combination of grating coupled interferometry with spectroscopic ellipsometry

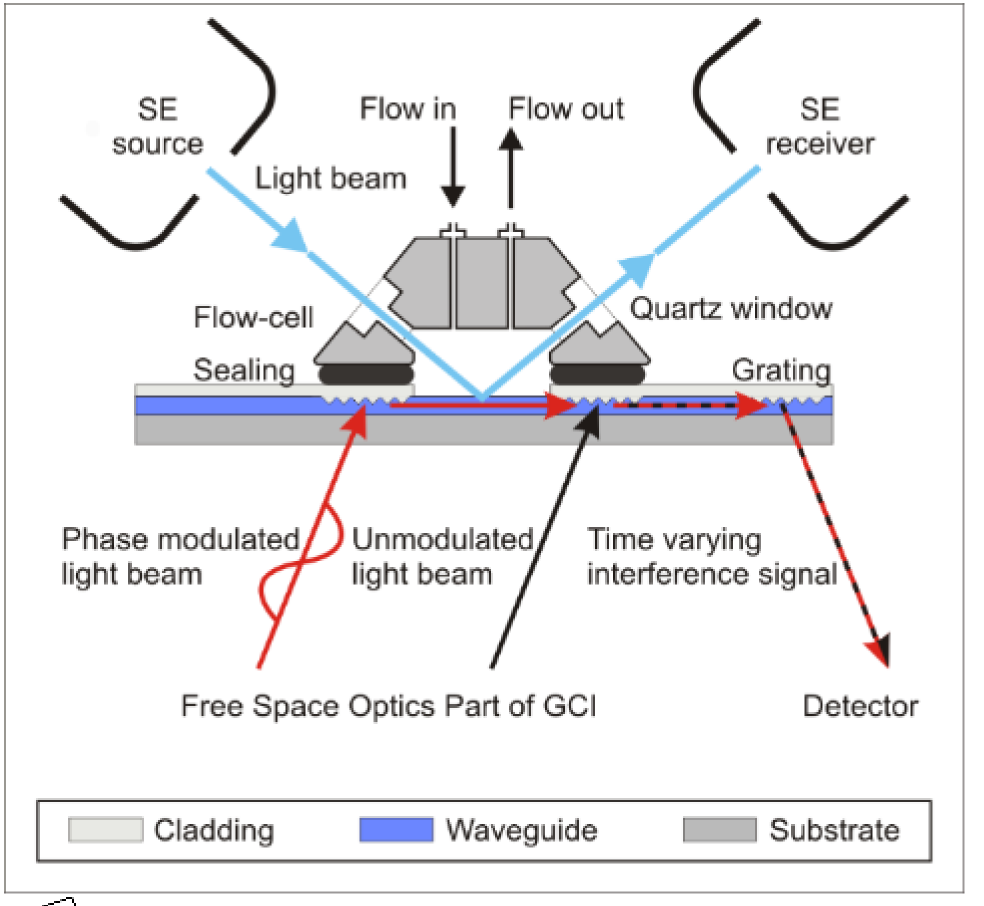

THE INTERFEROMETER:

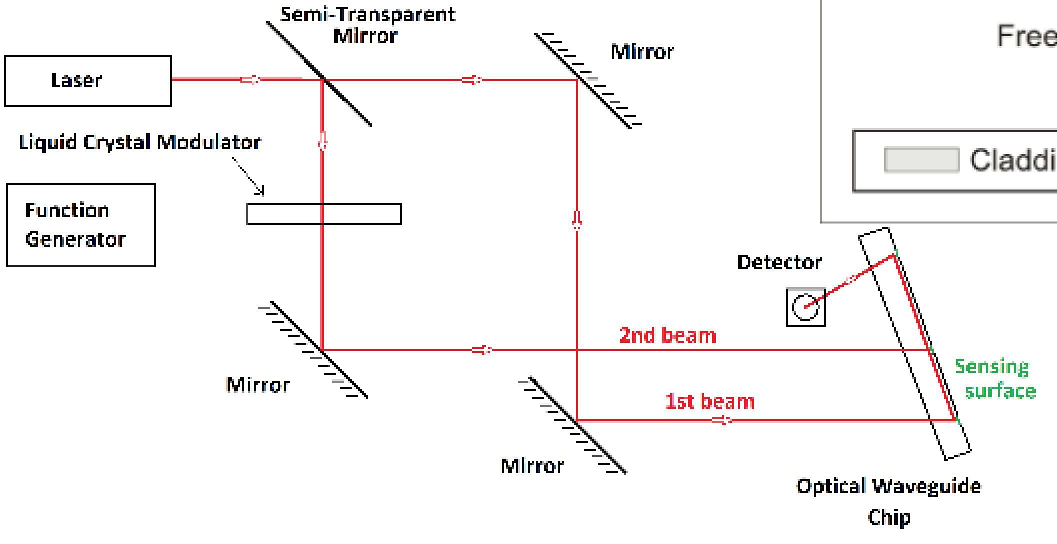

E. Agocs, P. Kozma, J. Nador, B. Kalas, A. Hamori, M. Janosov, S. Kurunczi, B. Fodor, M. Fried, R. Horvath, P. Petrik, "In-situ simultaneous monitoring of layer adsorption in aqueous solutions using grating coupled optical waveguide interferometry combined with spectroscopic ellipsometry", Appl. Surf. Sci. 421 (2017) 289.

GCI + SE on protein deposition

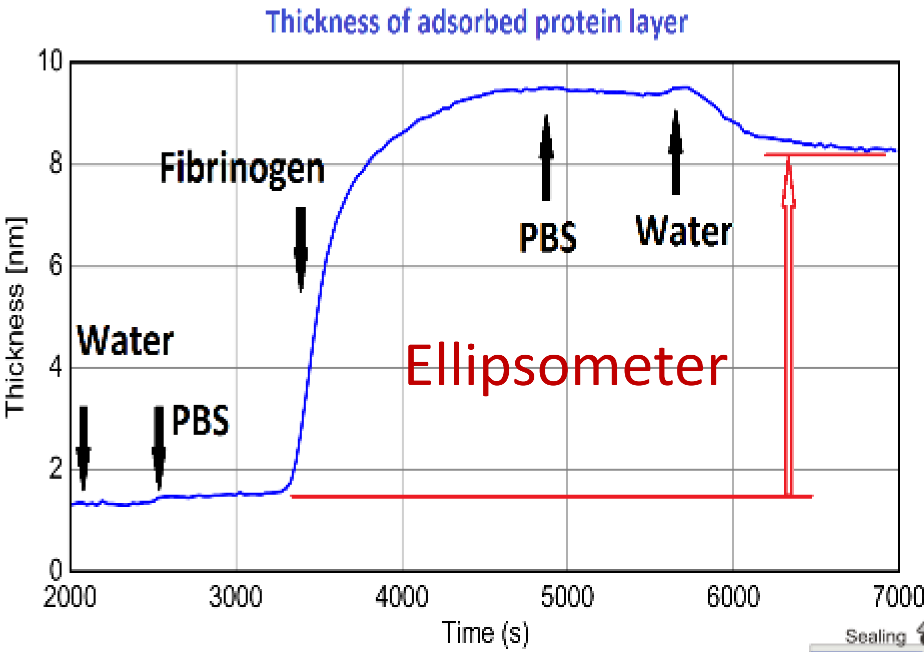

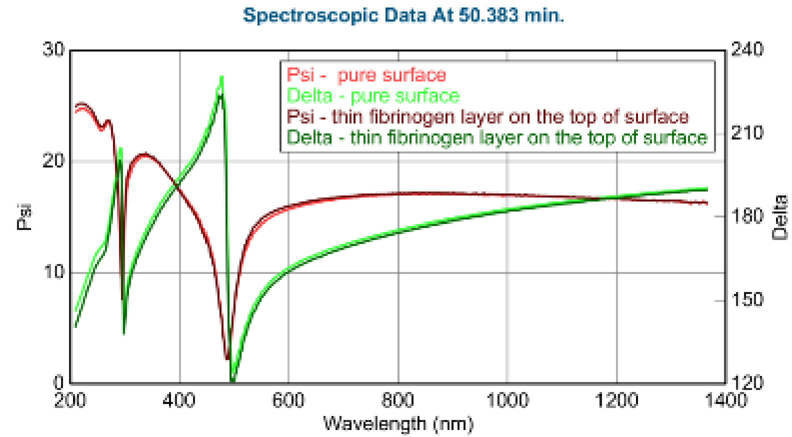

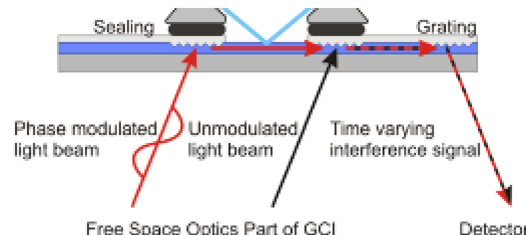

Interferometer

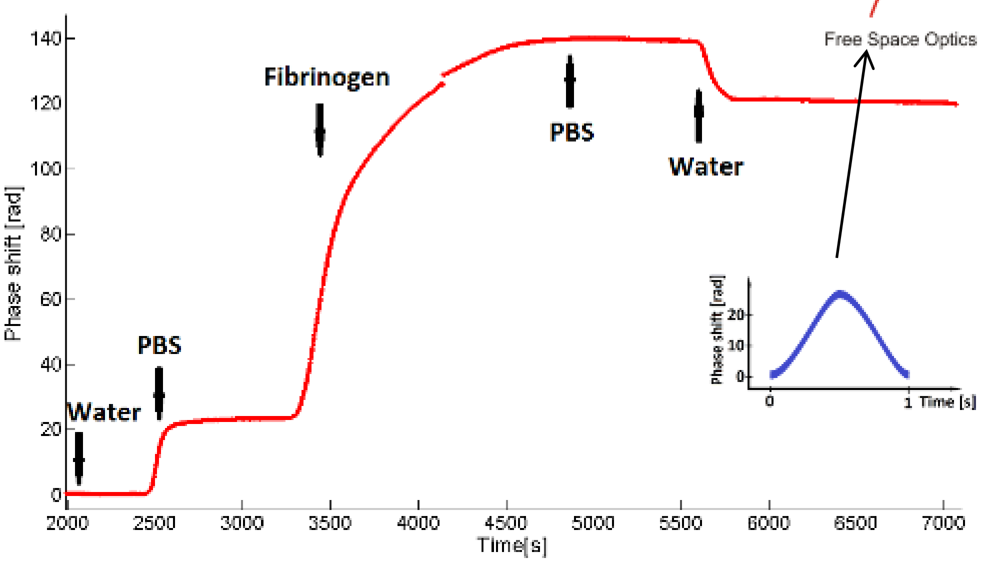

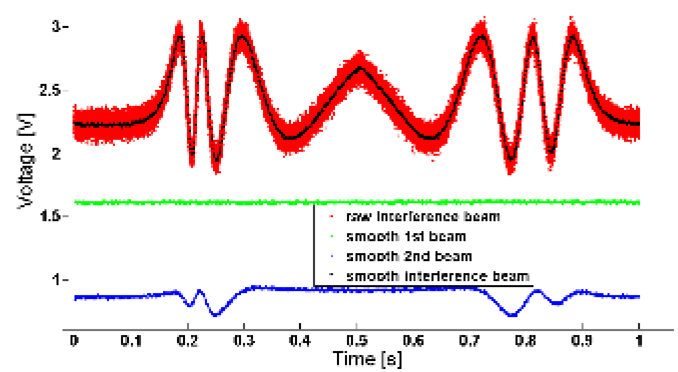

Conventional flow cell

Kretschmann-Raether configuration

Combination of methods

Tuning of the resonance

Mid infrared range

Electrochemical sensing

Combinatory

Summary

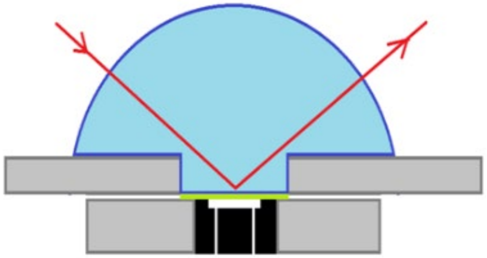

$\tan \Psi = abs(r_p/r_s)$

tan ψ - measured

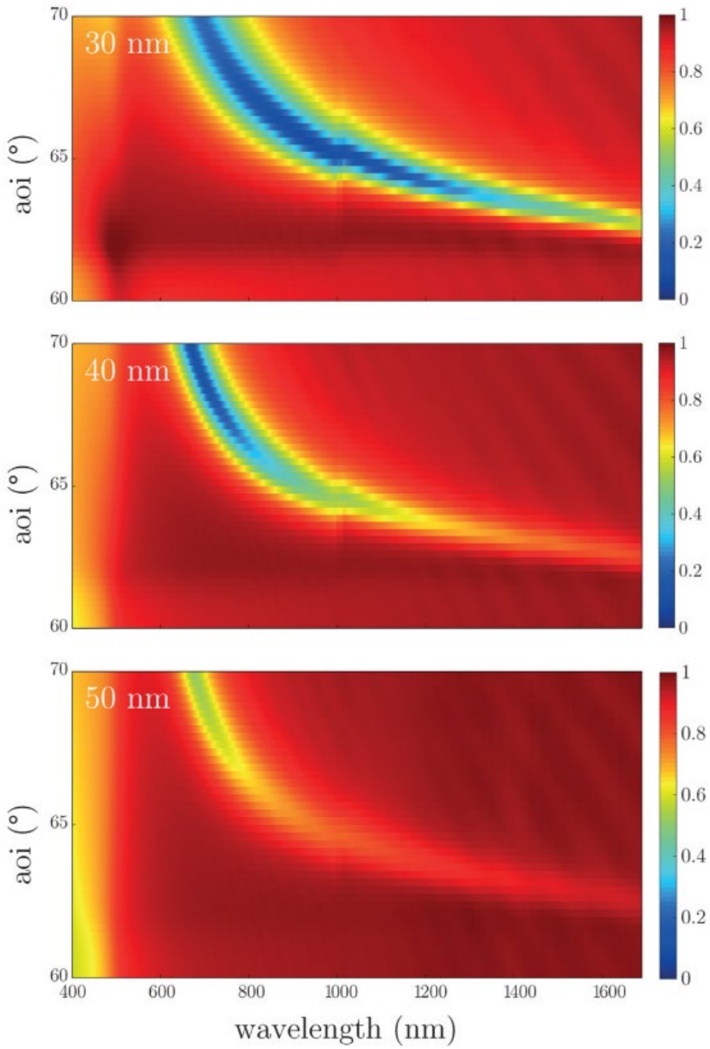

30

40

50

Measured absorbance of fibrinogen

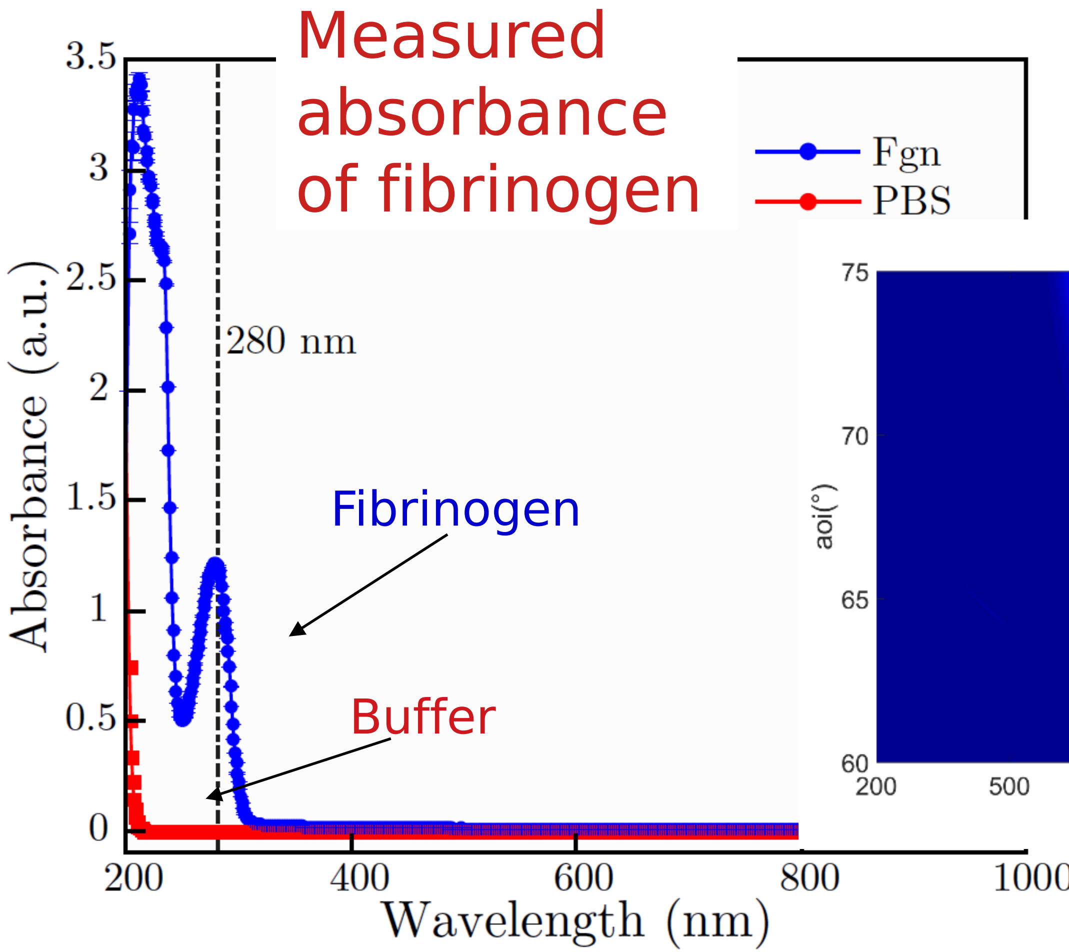

Limitations of gold plasmonics

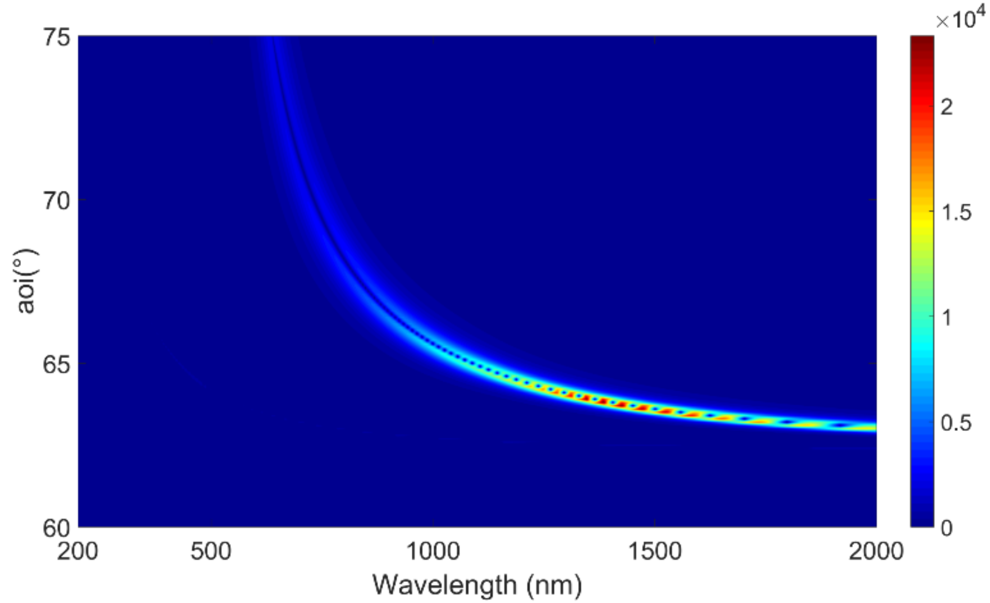

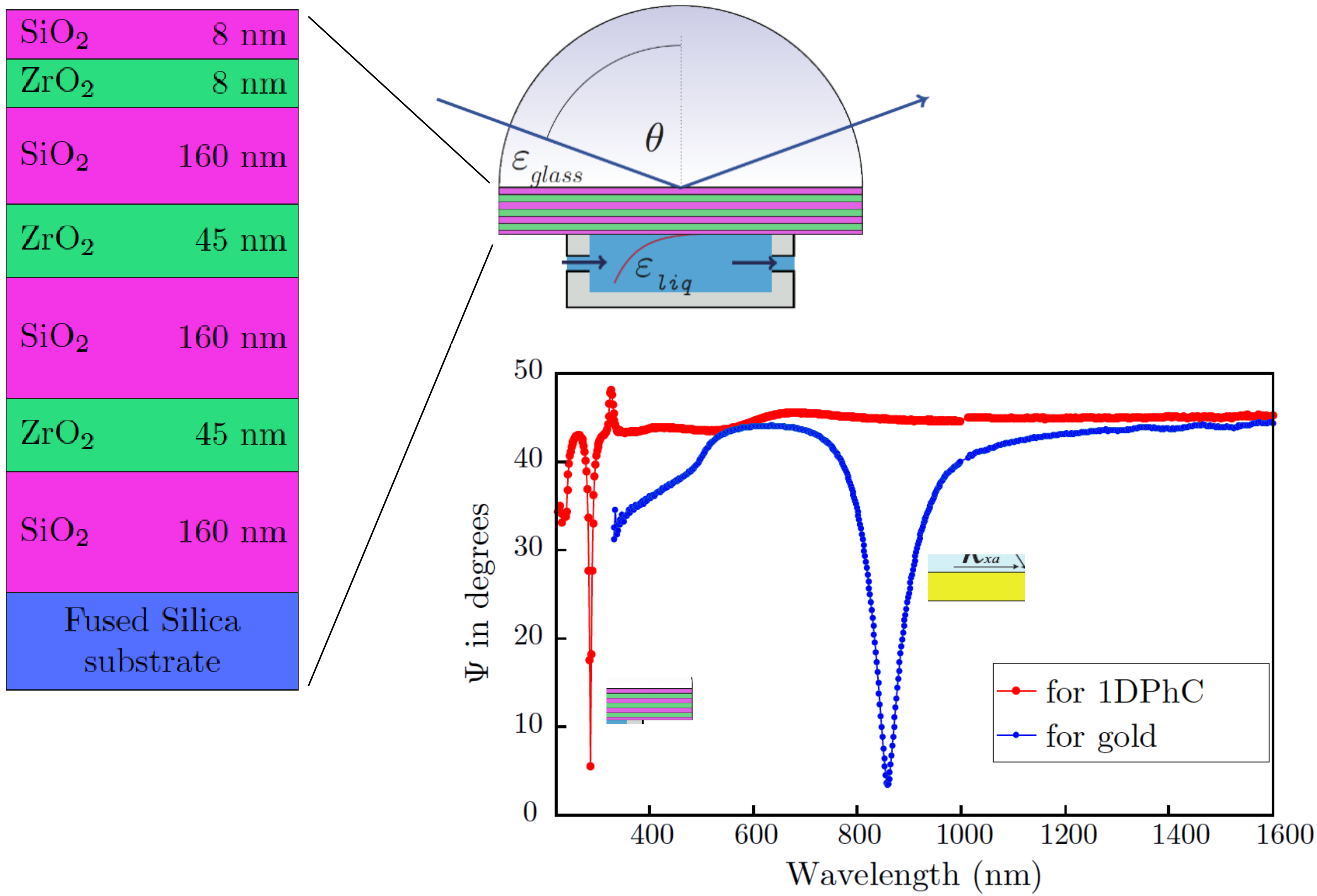

SiO2 8 nm
ZrO2 8 nm
SiO2 160 nm
ZrO2 45 nm
SiO2 160 nm
ZrO2 45 nm
SiO2 160 nm
Fused Silica substrate
θ
ε glass
ε liq
Ψ in degrees
Wavelength (nm)
0
10
20
30
40
50
400
600
800
1000
1200
1400
1600
for 1DPhC
for gold

Sensitivity maps in dψ/dn

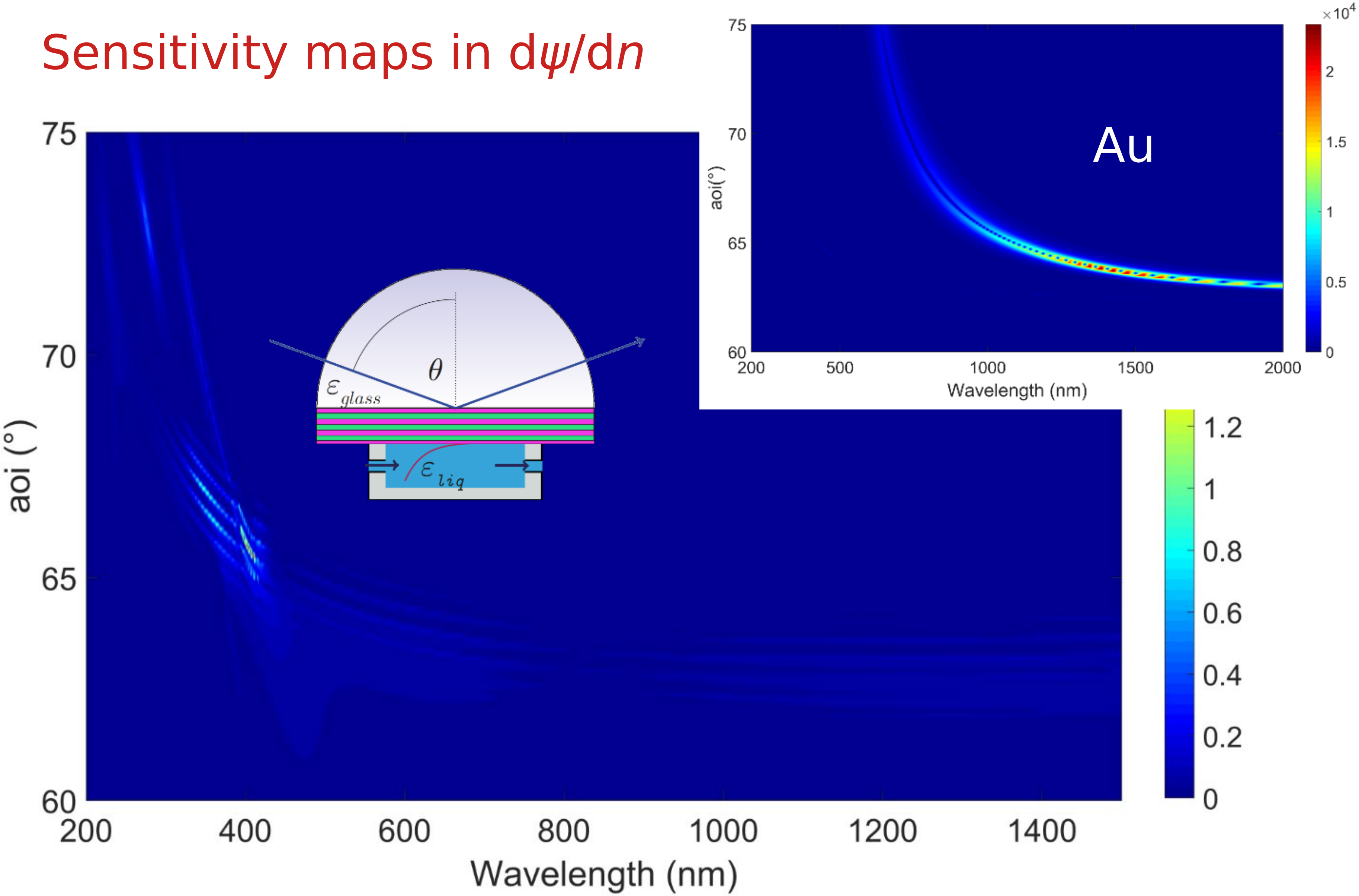

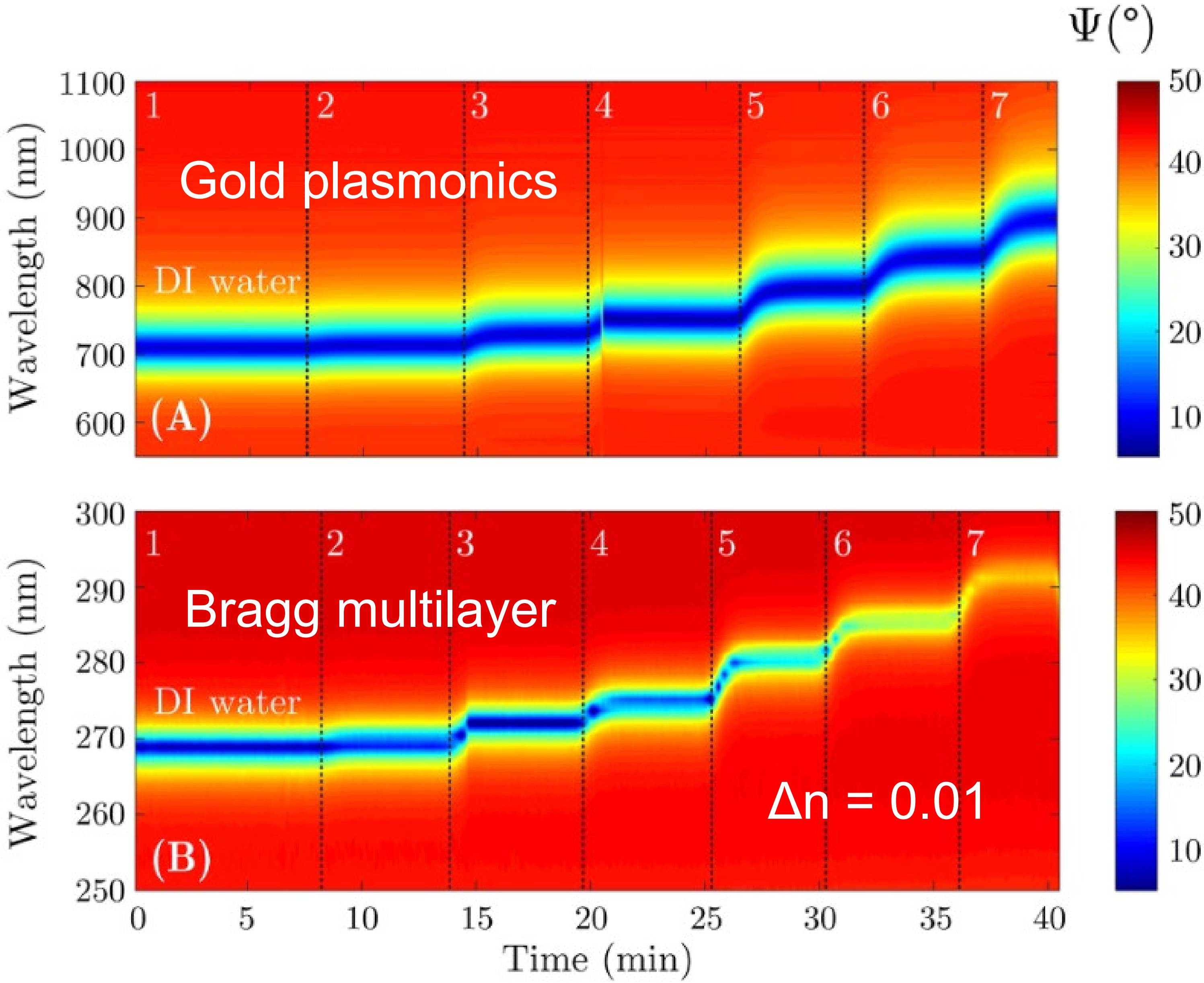
Ψ(°)
Gold plasmonics
DI water
(A)
Wavelength (nm)
Bragg multilayer
DI water
(B)
Δn = 0.01
Wavelength (nm)
Time (min)

Sensitivity maps

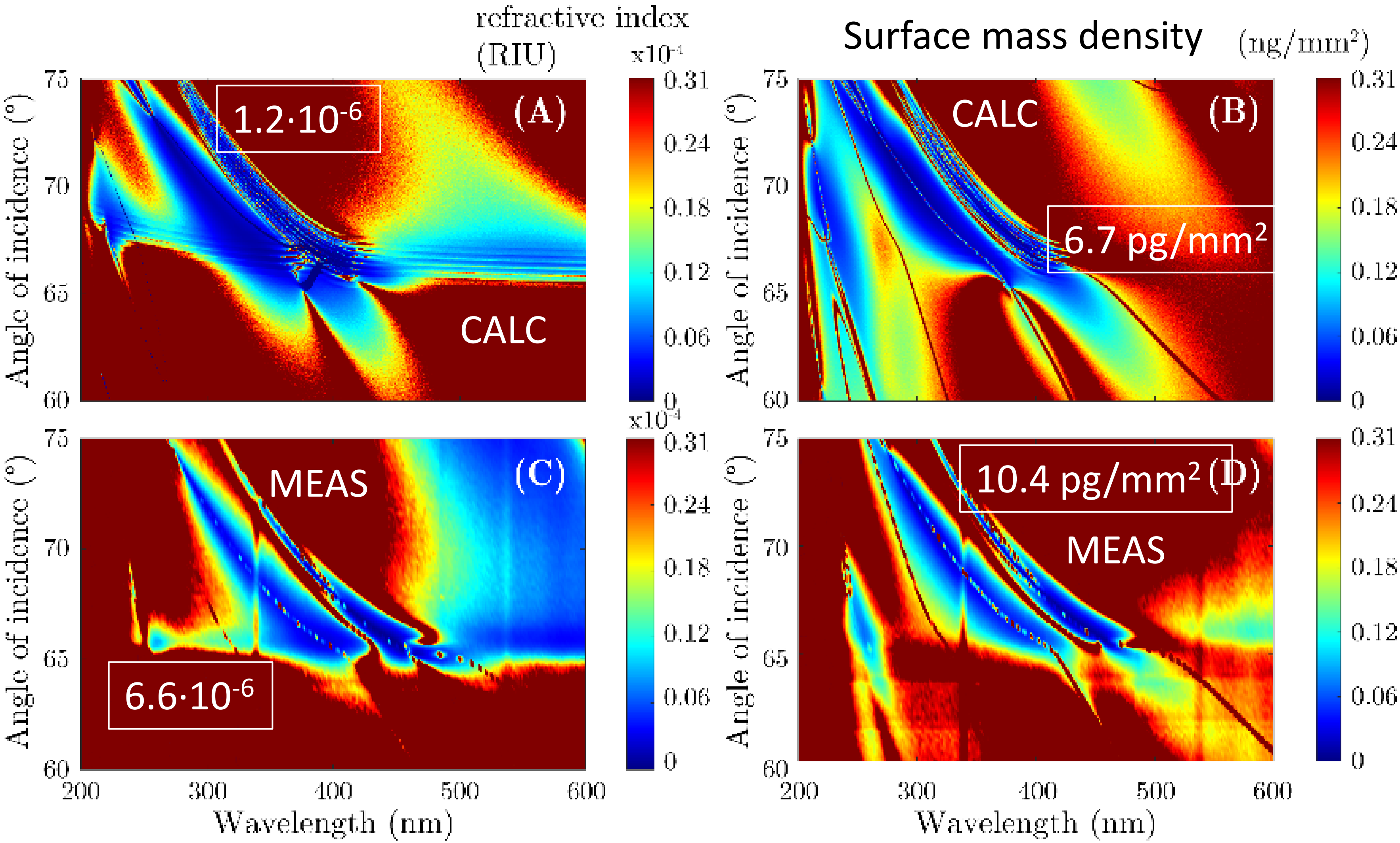

Conventional flow cell

Kretschmann-Raether configuration

Combination of methods

Tuning of the resonance

Mid infrared range

Electrochemical sensing

Combinatory

Summary

Penetration depth of light

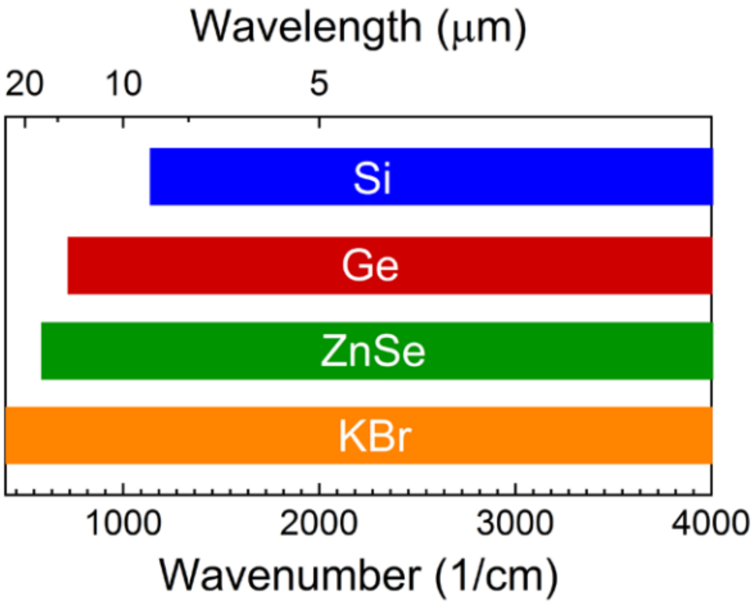

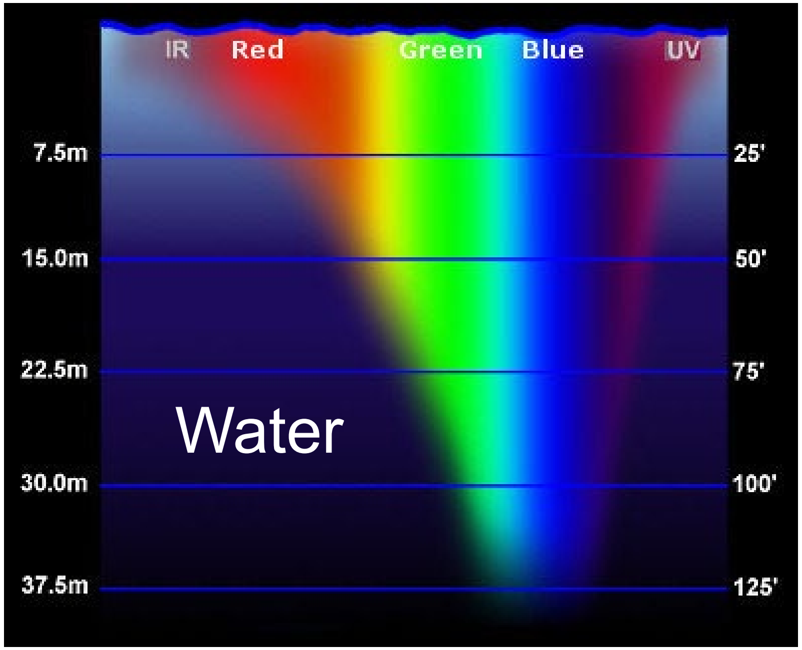

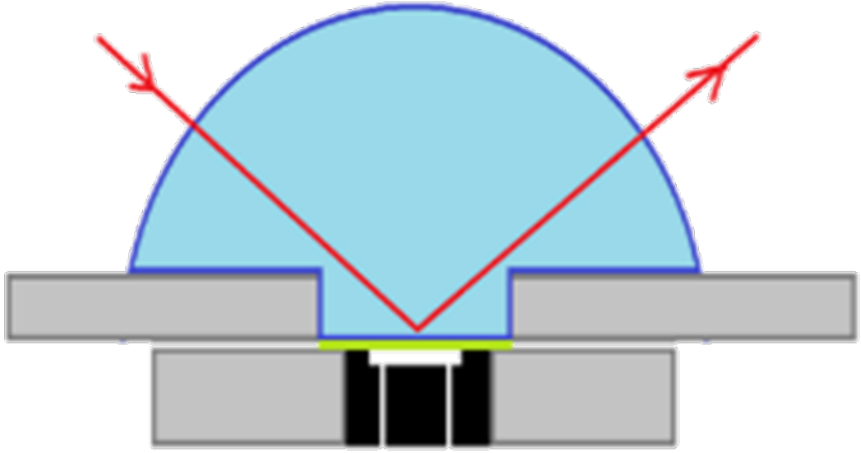

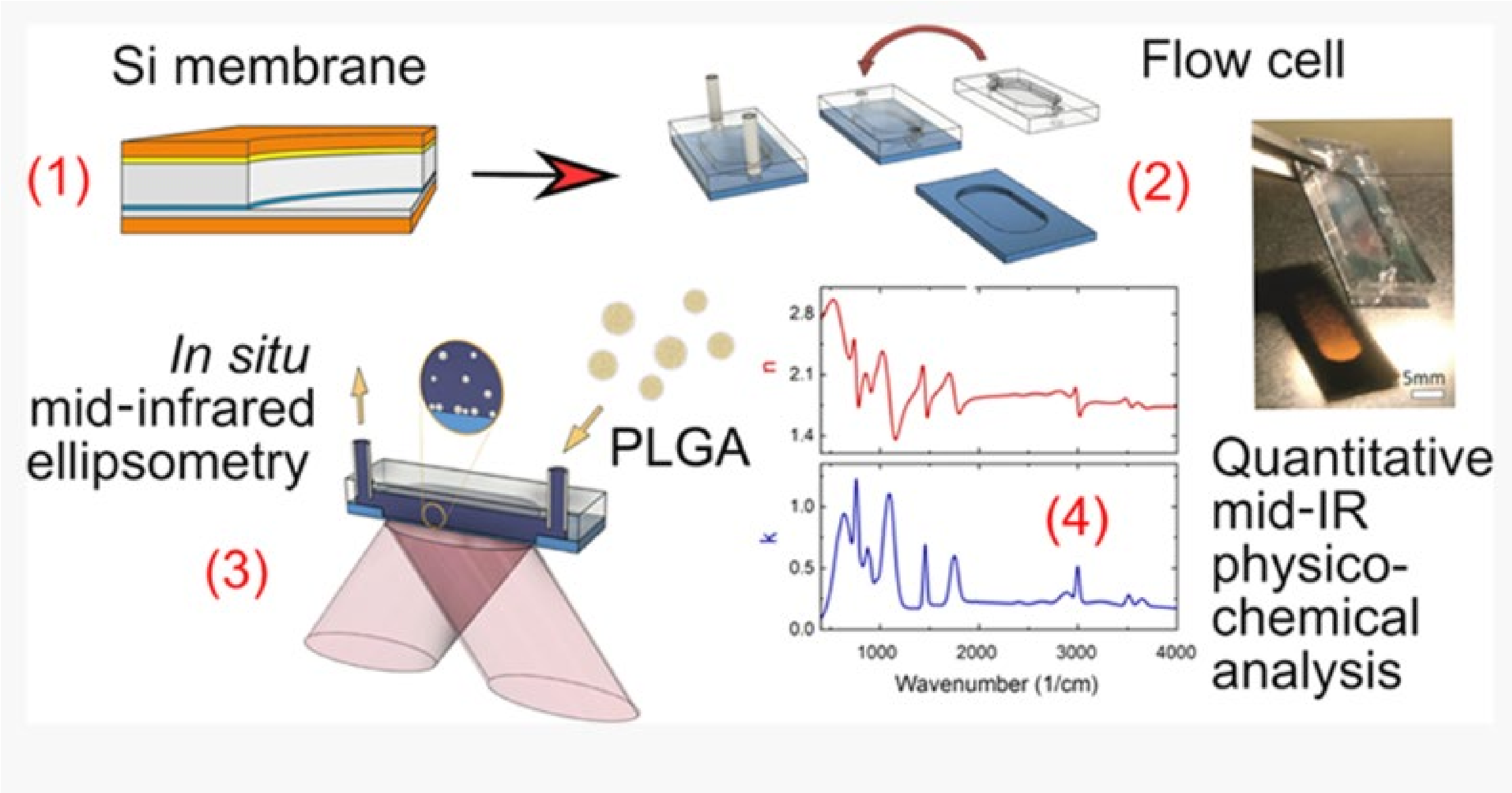

A. Romanenko, B. Kalas, P. Hermann, O. Hakkel, L. Illés, M. Fried, P. Fürjes, G. Gyulai, P. Petrik, Membrane-Based *In Situ* Mid-Infrared Spectroscopic Ellipsometry: A Study on the Membrane Affinity of Polylactide- *co* -glycolide Nanoparticulate Systems, Anal. Chem. 93 (2021) 981–991.

Silicon on insulator (SOI) membrane cell in mid IR

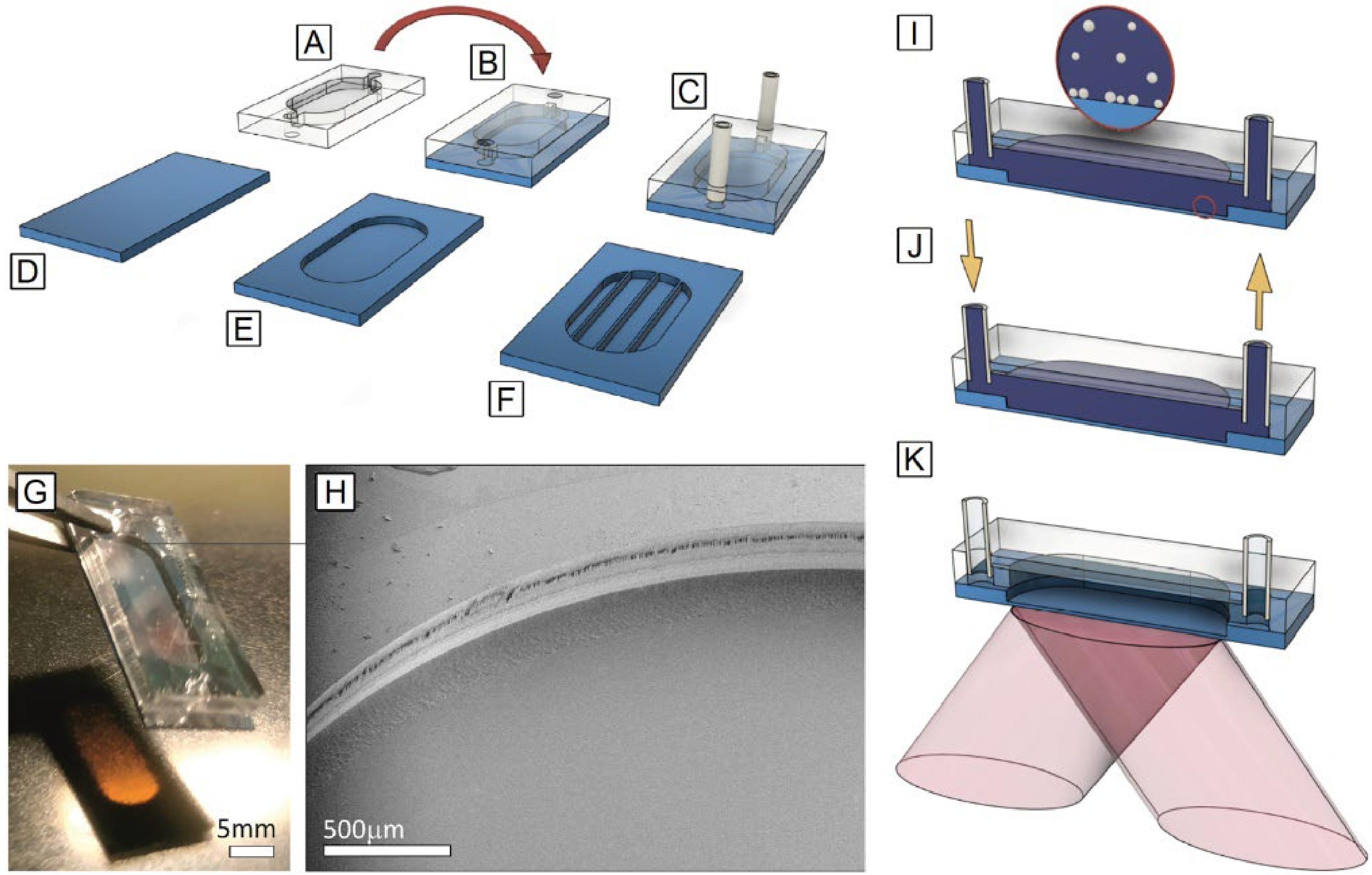

Issues of mechanical stress

20 mm
x 5 mm

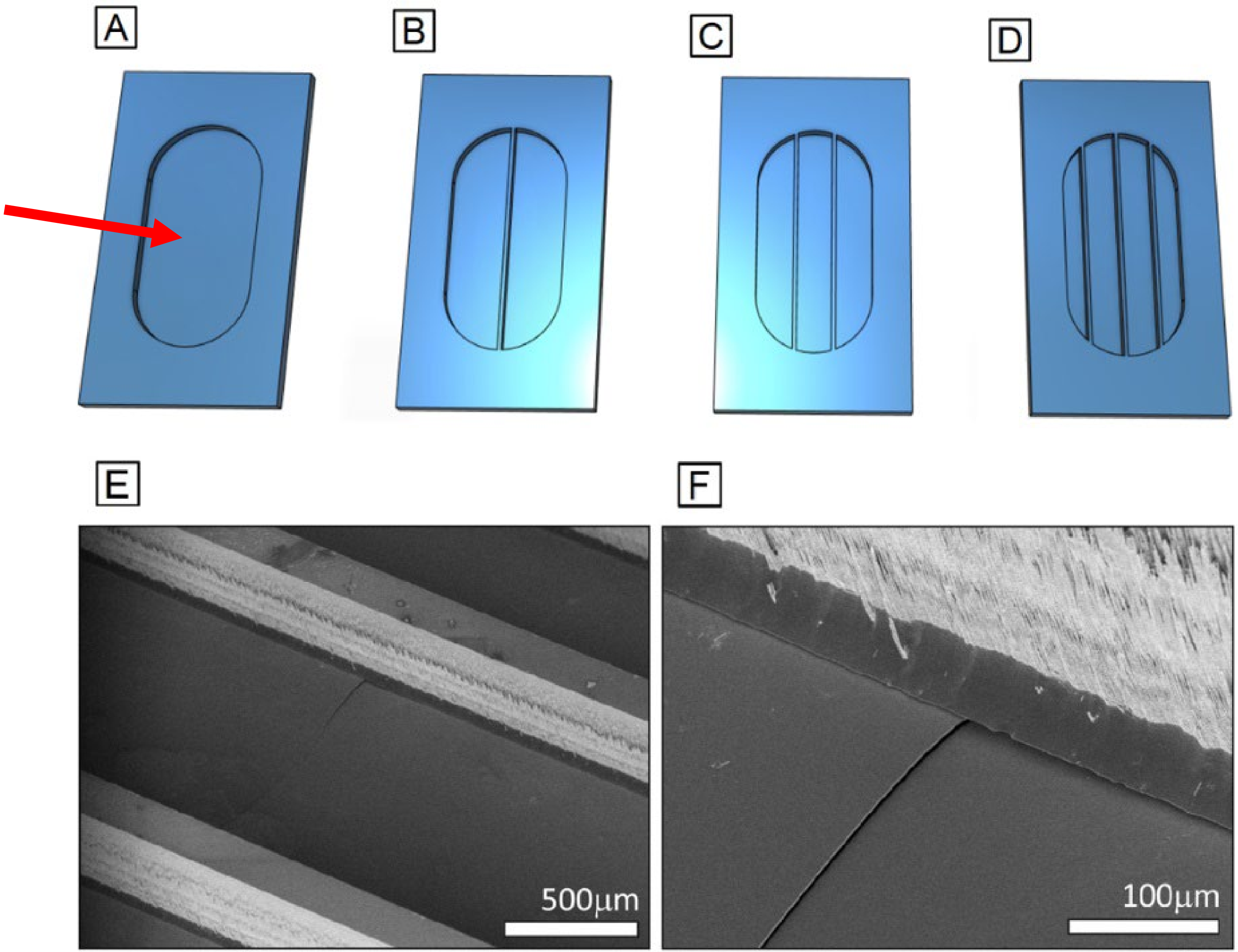

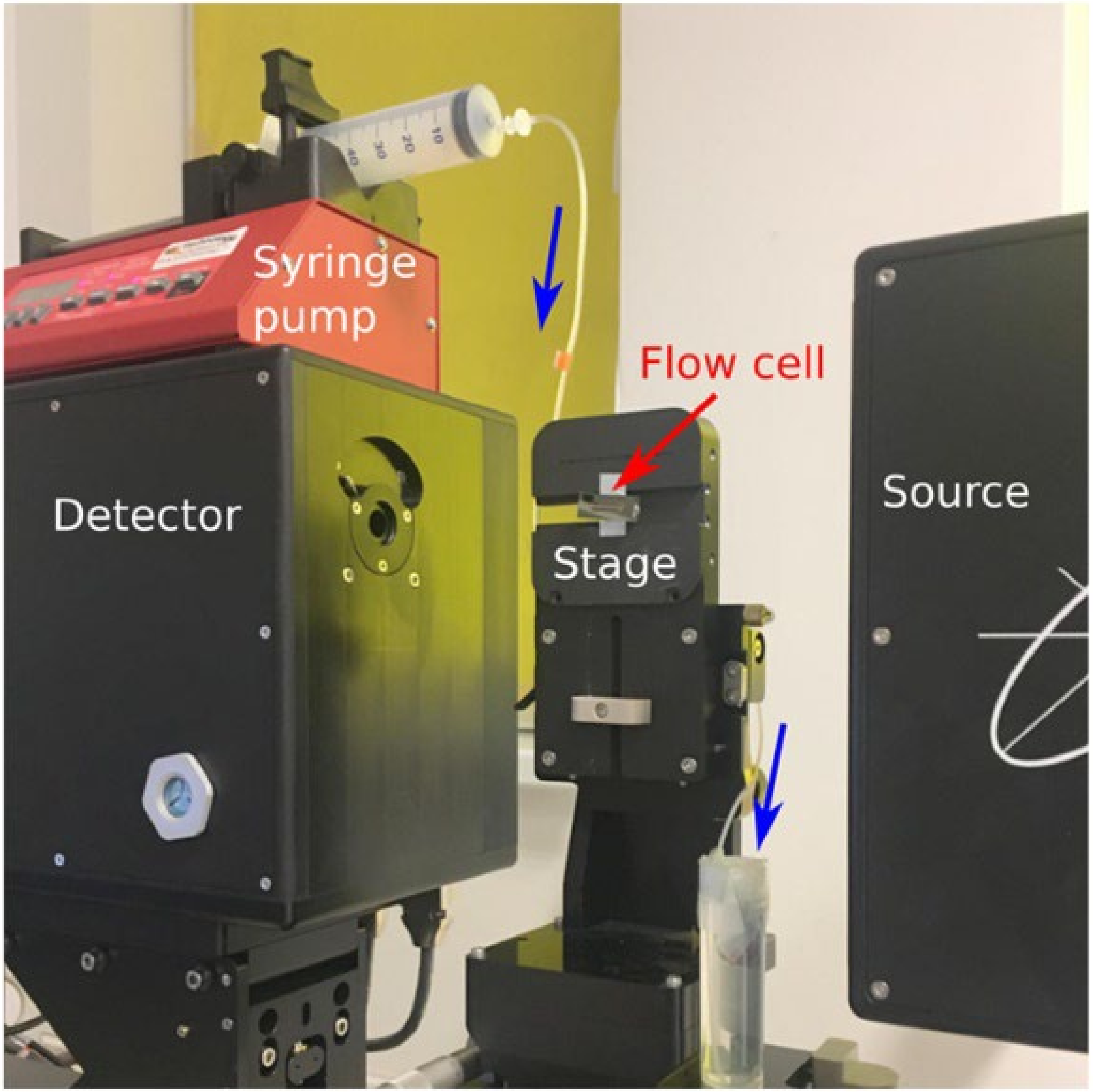

Integration in a commercial mid-IR ellipsometer

Measured and fitted ellipsometry spectra

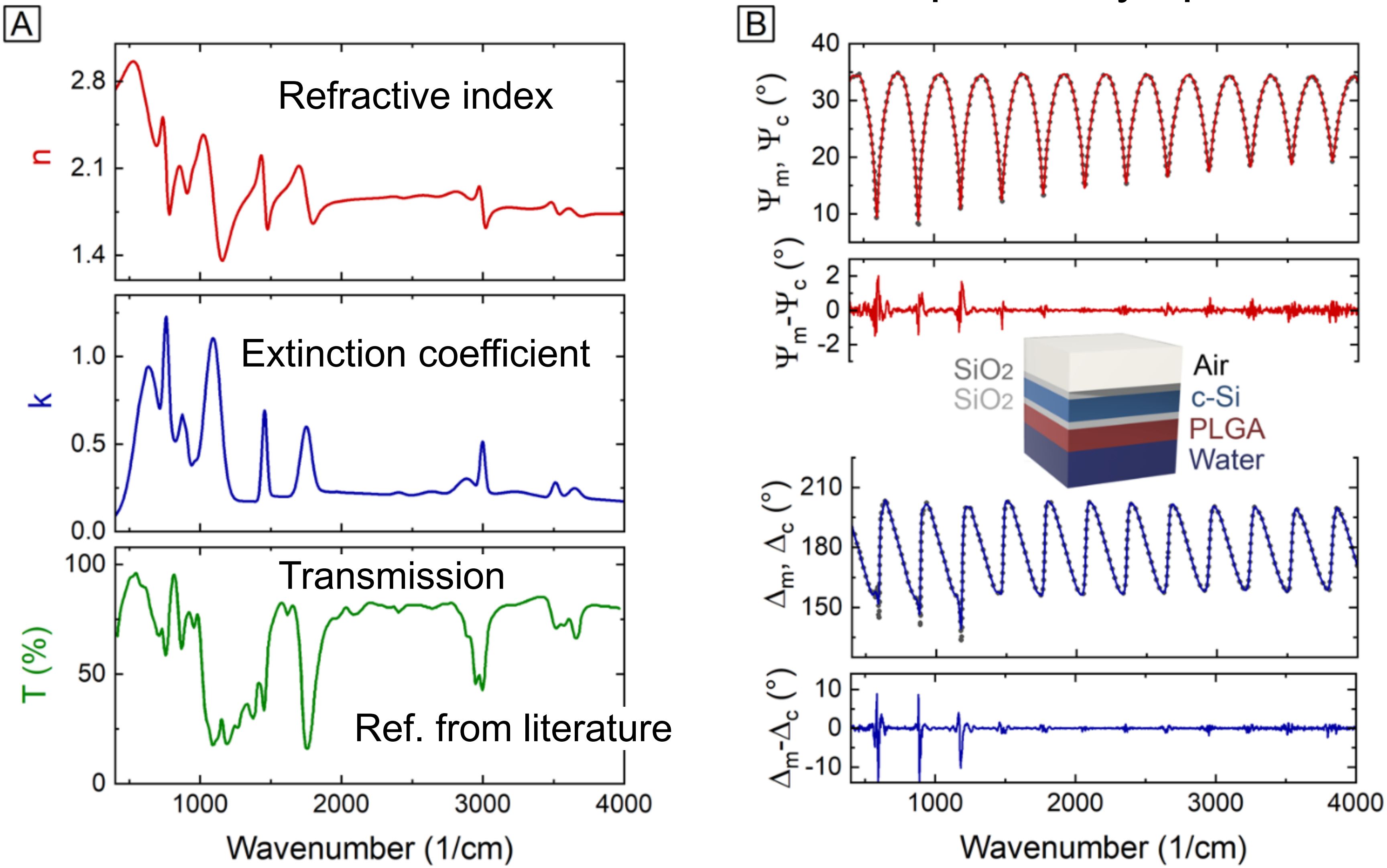

Differences in Ψ (E) and Δ (F) before and after the adsorption of polymer nanoparticles.

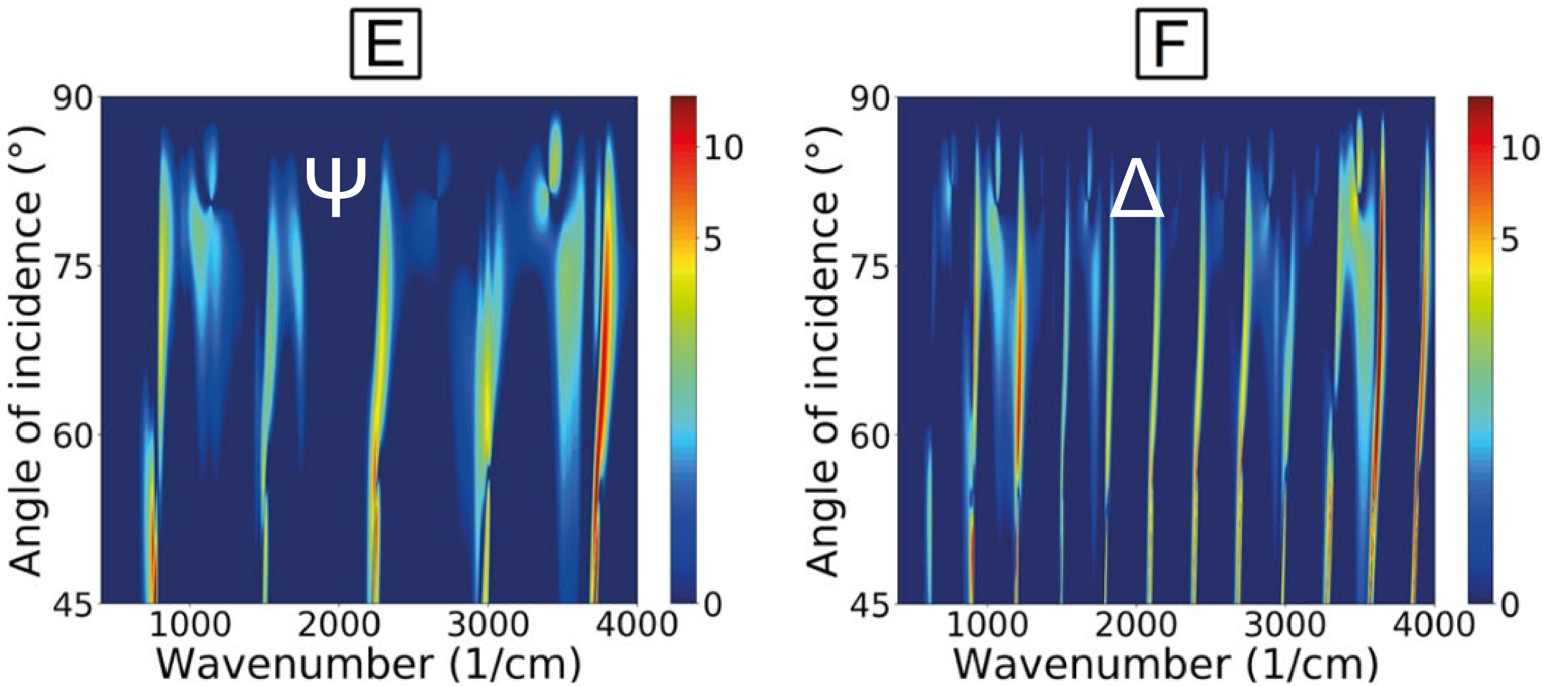

Conventional flow cell

Kretschmann-Raether configuration

Combination of methods

Tuning of the resonance

Mid infrared range

Electrochemical sensing

Combinatory

Summary

Detection of Ni and As in water

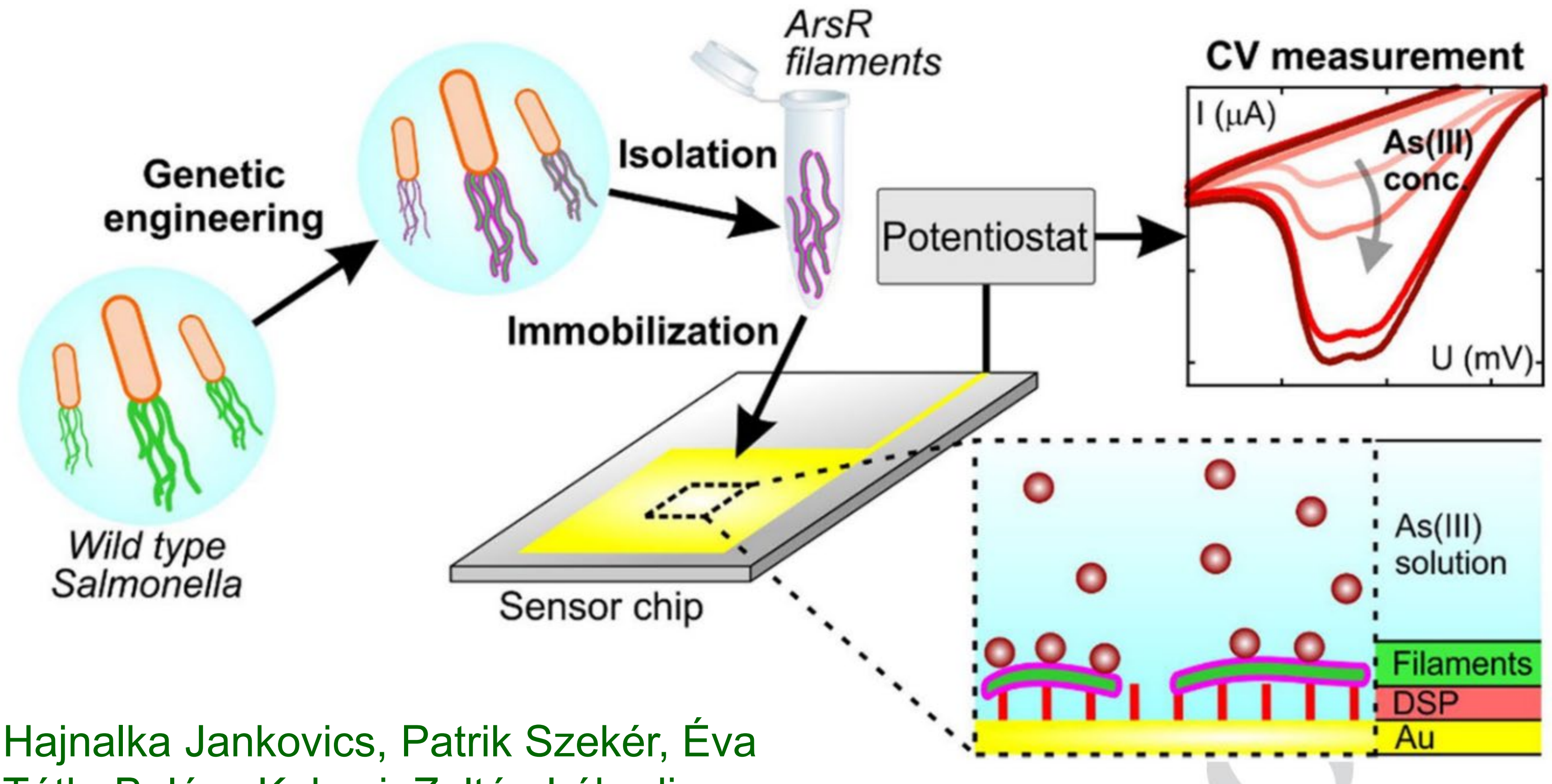

Hajnalka Jankovics, Patrik Szekér, Éva Tóth, Balázs Kakasi, Zoltán Lábadi, András Saftics, Benjamin Kalas, Miklós Fried, Péter Petrik & Ferenc Vonderviszt, „Flagellin-based electrochemical sensing layer for arsenic detection in water”, accepted in Scientific Reports (2021).

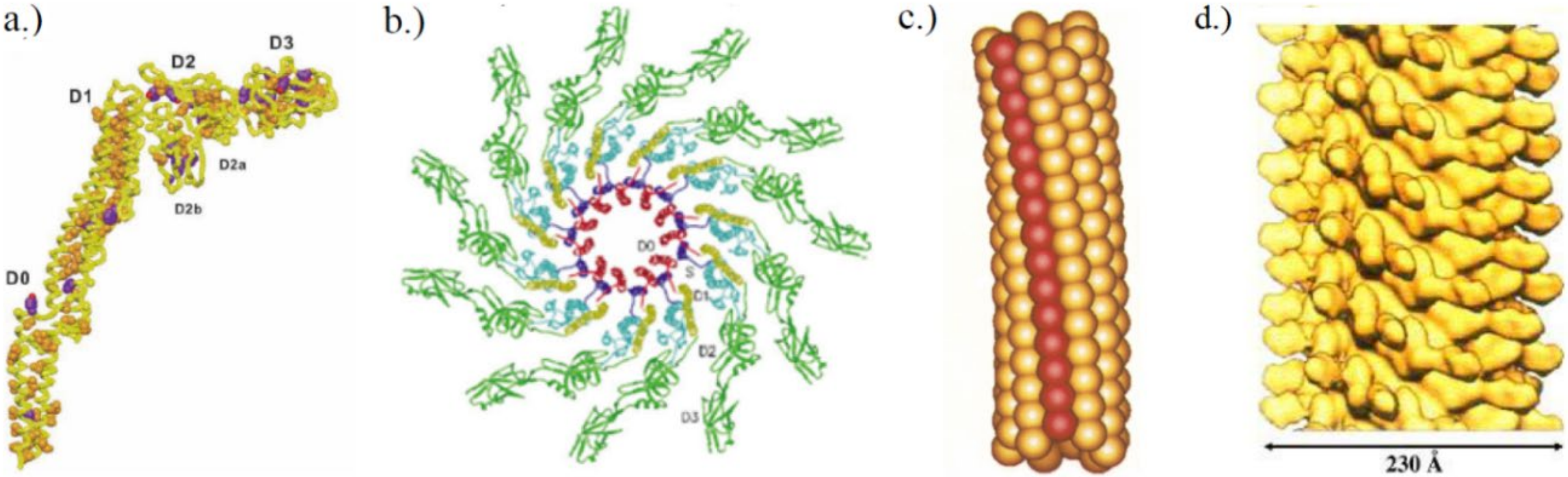
a.)
D3
D2
D1
D2a
D2b
D0
b.)
D0
S
D1
D2
D3
c.)
d.)
230 Å

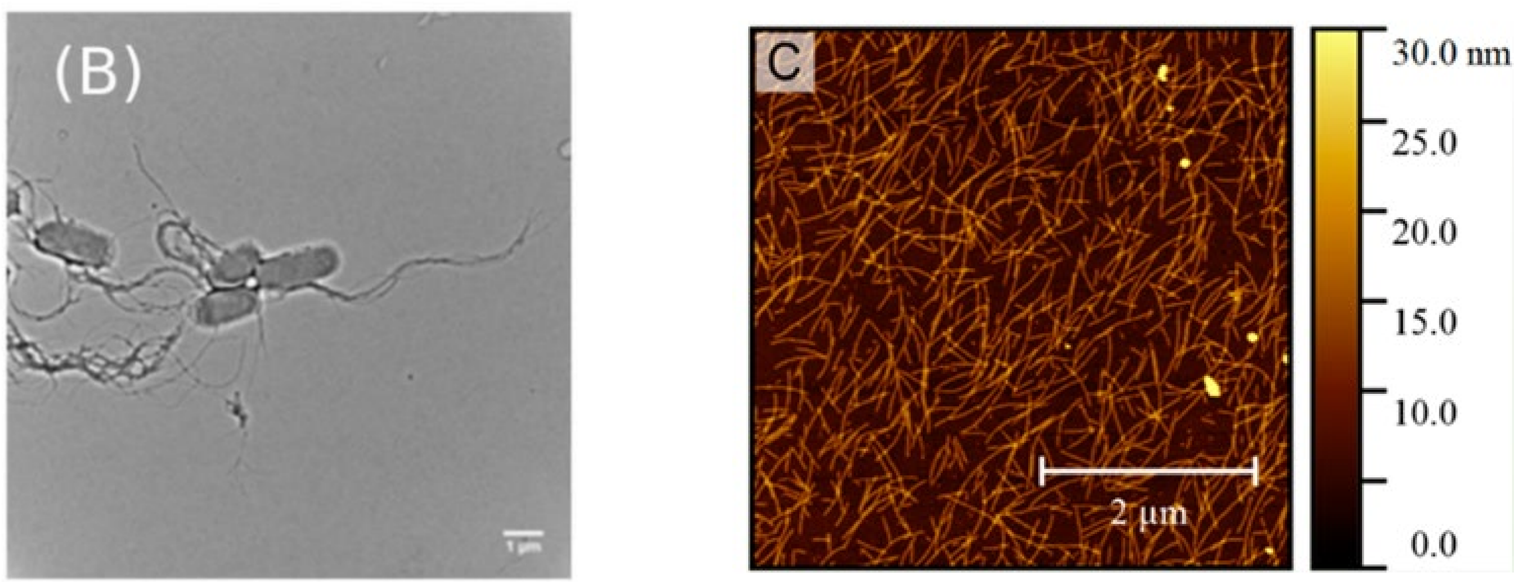
(B)
1 μm
C
2 μm
30.0 nm
25.0
20.0
15.0
10.0
0.0

Cyclic voltammetry

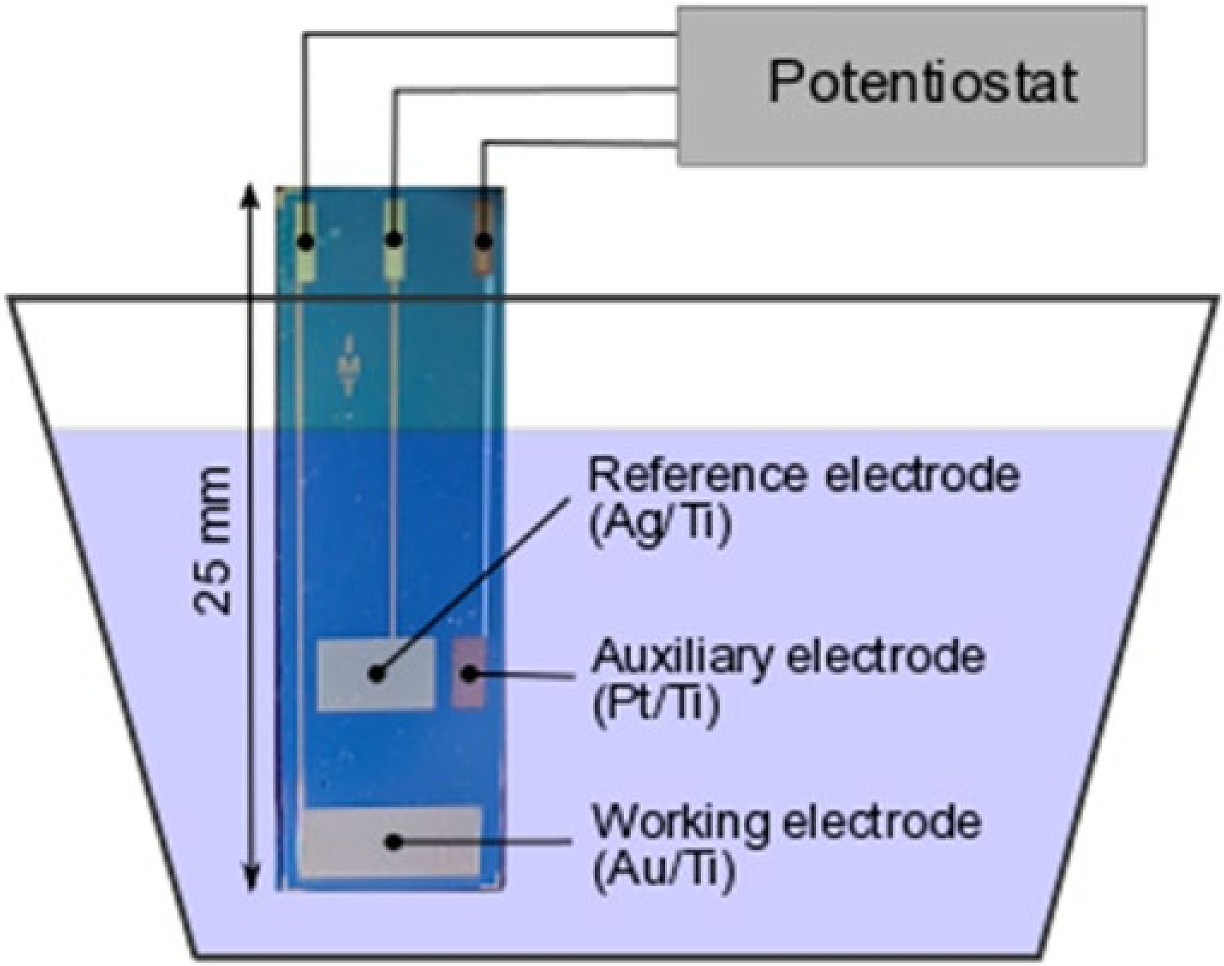

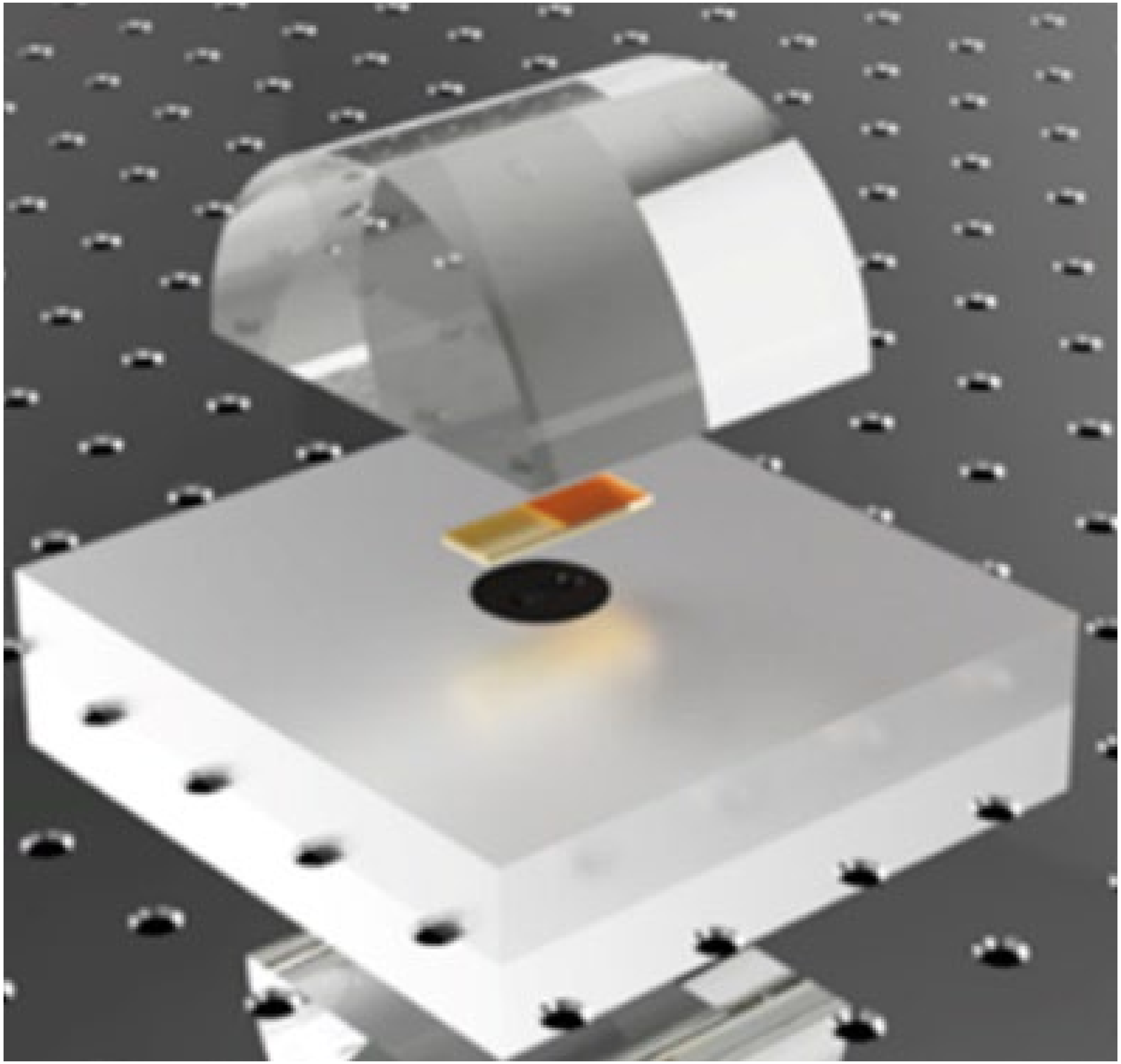

Two-channel Kretschmann ellipsometry

B. Kalas, J. Nador, E. Agocs, A. Saftics, S. Kurunczi, M. Fried, P. Petrik, Protein adsorption monitored by plasmon-enhanced semi-cylindrical Kretschmann ellipsometry, Applied Surface Science. 421 (2017) 585–592

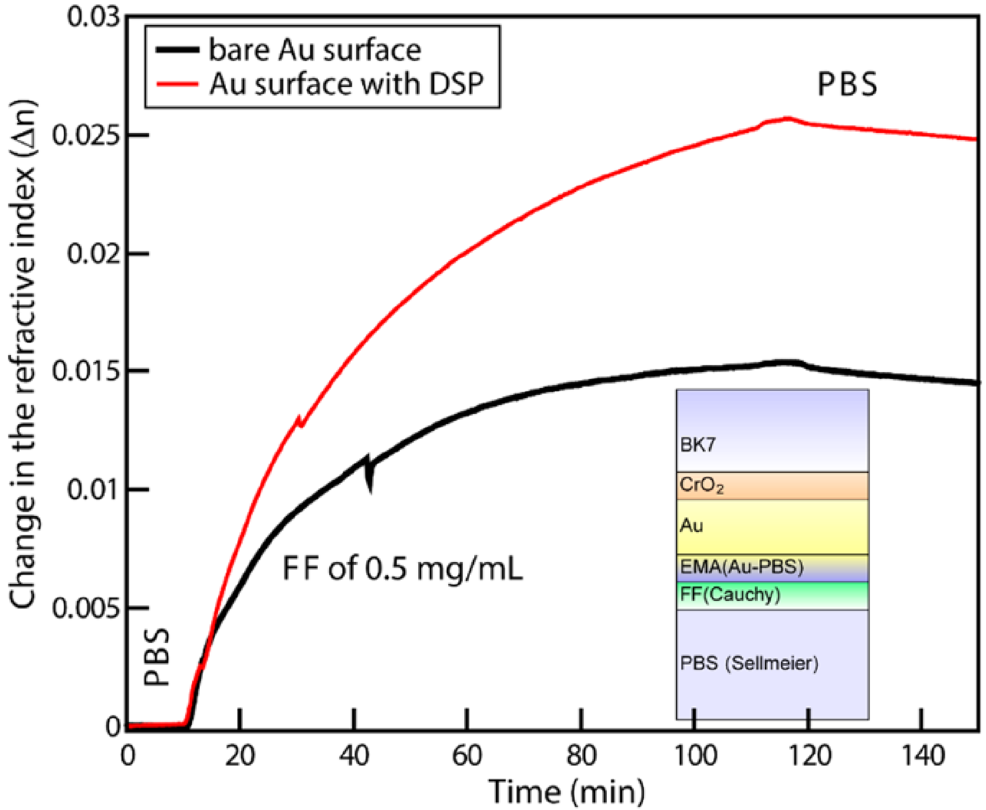
bare Au surface
Au surface with DSP
PBS
PBS
FF of 0.5 mg/mL
Change in the refractive index (Δn)
Time (min)
0.03
0.025
0.02
0.015
0.01
0.005
0
0
20
40
60
80
100
120
140
BK7
CrO2
Au
EMA(Au-PBS)
FF(Cauchy)
PBS (Sellmeier)

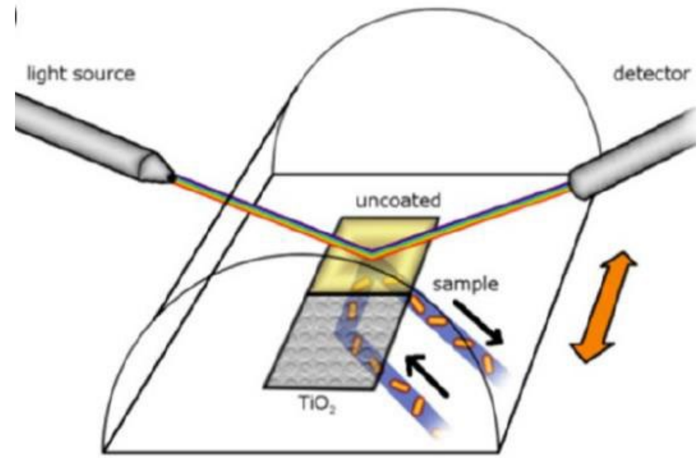
light source
detector
uncoated
sample
TiO2

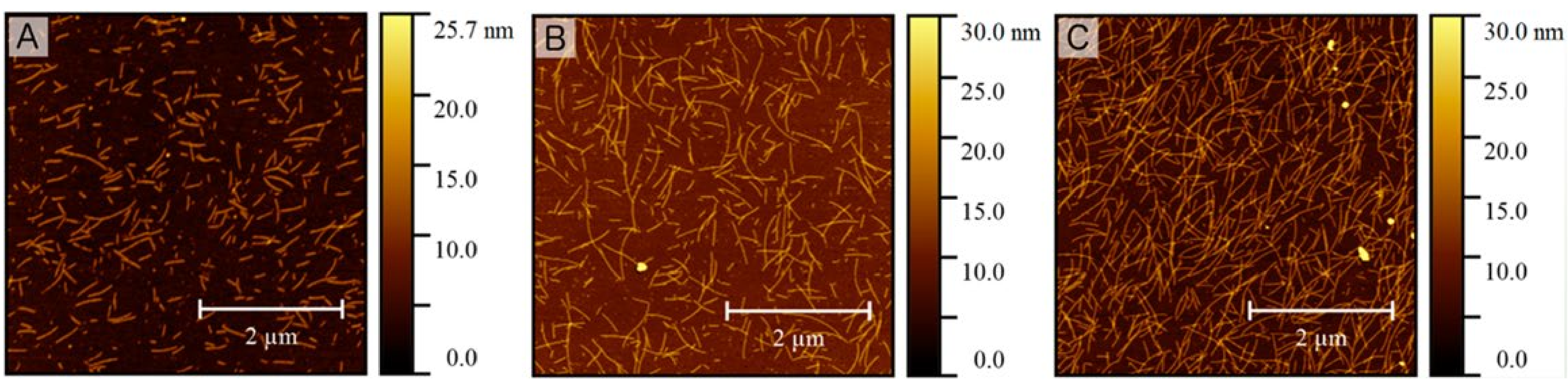
A
2 μm
25.7 nm
20.0
15.0
10.0
0.0
B
2 μm
30.0 nm
25.0
20.0
15.0
10.0
0.0
C
2 μm
30.0 nm
25.0
20.0
15.0
10.0
0.0

Cyclic voltammetry

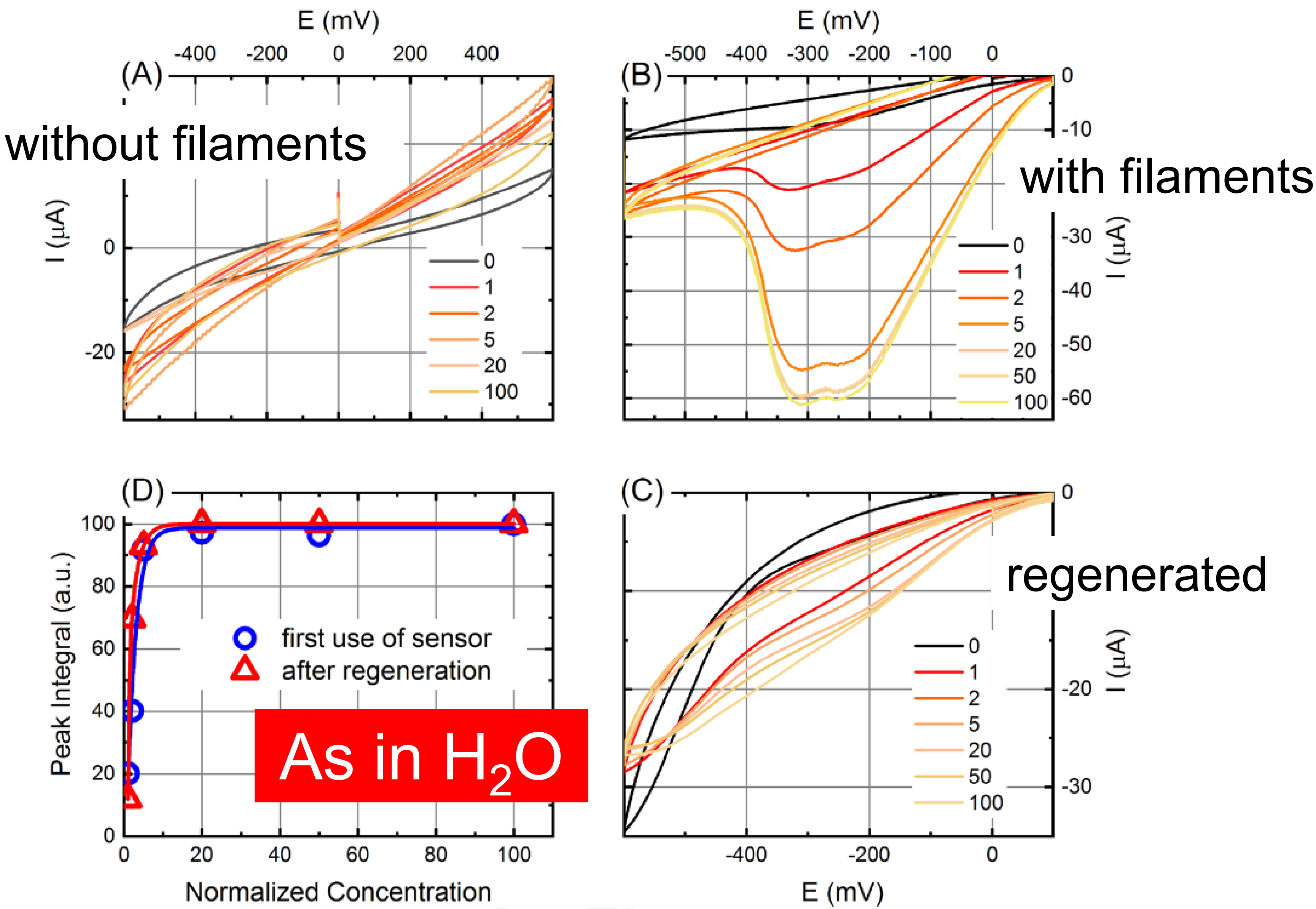

Cyclic voltammetry

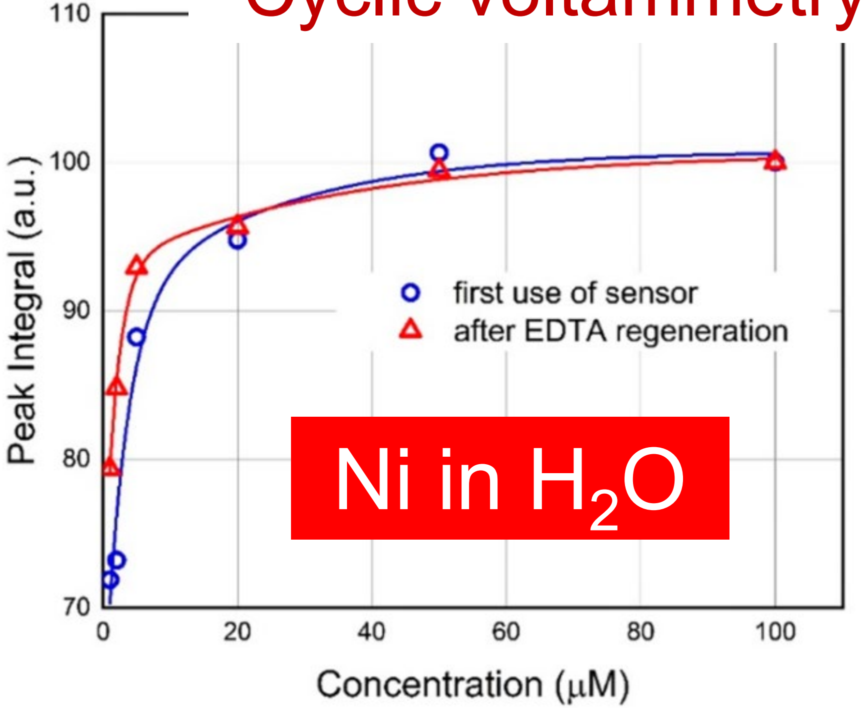

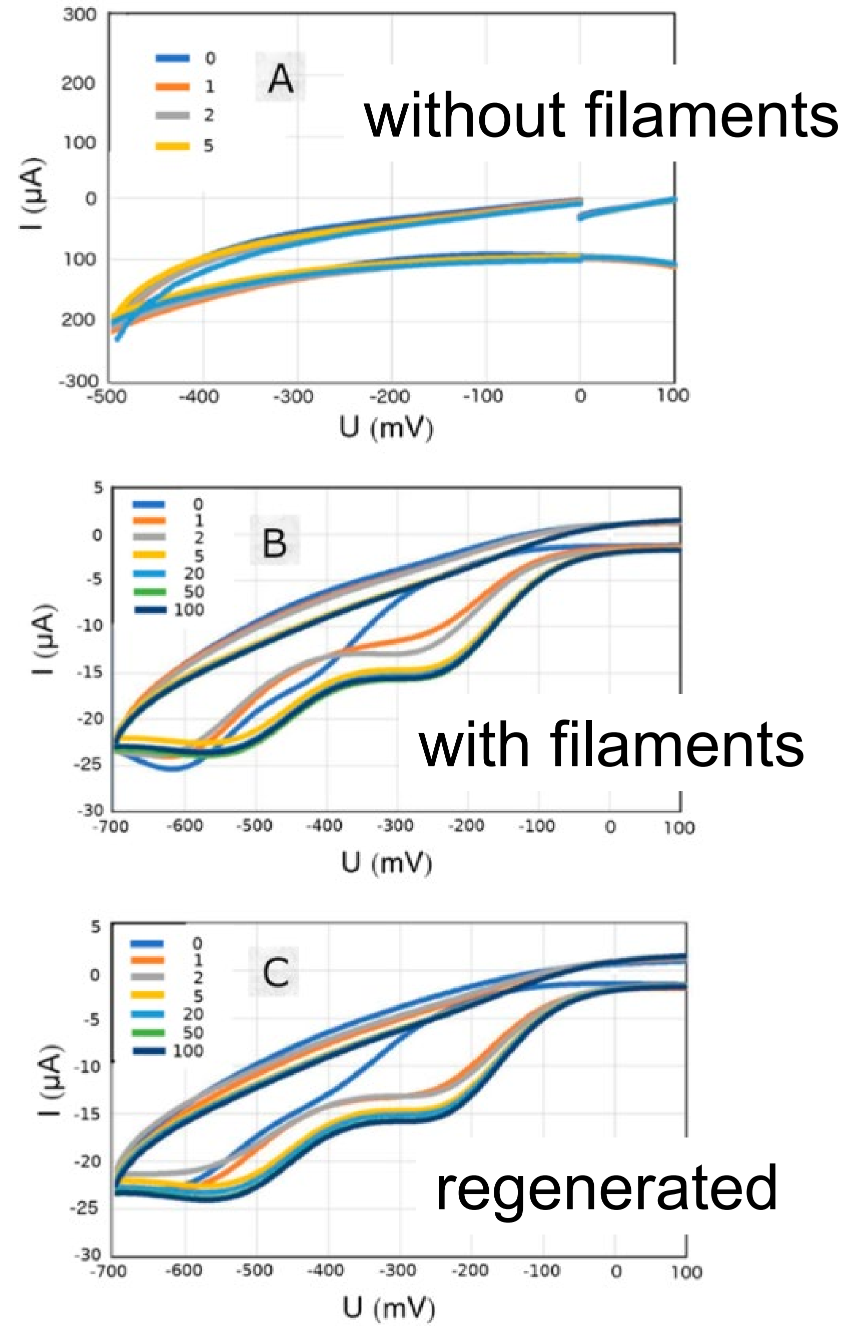

Z. Labadi, B. Kalas, A. Saftics, L. Illes, H. Jankovics, É. Bereczk-Tompa, A. Sebestyén, É. Tóth, B. Kakasi, C. Moldovan, B. Firtat, M. Gartner, M. Gheorghe, F. Vonderviszt, M. Fried, P. Petrik, Sensing Layer for Ni Detection in Water Created by Immobilization of Bioengineered Flagellar Nanotubes on Gold Surfaces, ACS Biomater. Sci. Eng. 6 (2020) 3811–3820.

Conventional flow cell
Kretschmann-Raether configuration
Combination of methods
Tuning of the resonance
Mid infrared range
Electrochemical sensing
Combinatory
Summary

Combinatorial deposition with profile control

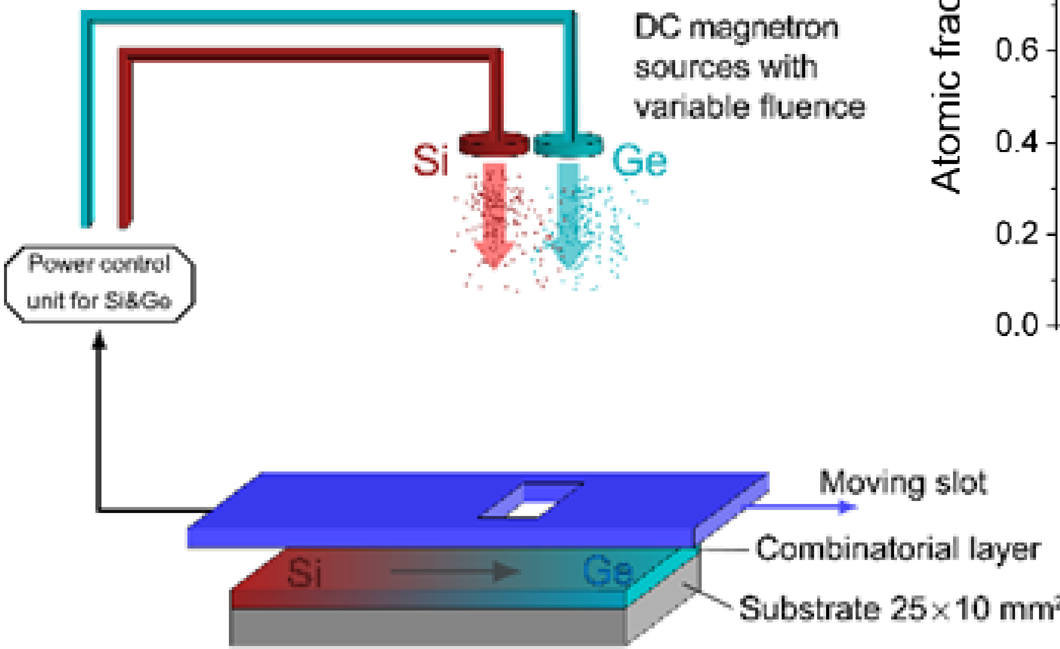

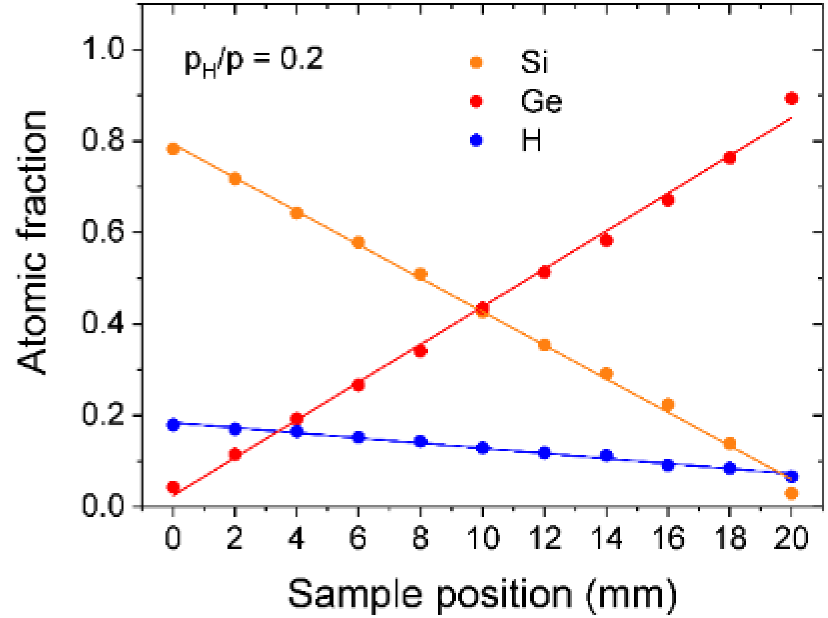

B. Kalas, Z. Zolnai, G. Sáfrán, M. Serényi, E. Agocs, T. Lohner, A. Nemeth, N.Q. Khánh, M. Fried, P. Petrik, Micro-combinatorial sampling of the optical properties of hydrogenated amorphous $Si_{1-x}Ge_x$ for the entire range of compositions towards a database for optoelectronics, Scientific Reports 10 (2020) 19266.

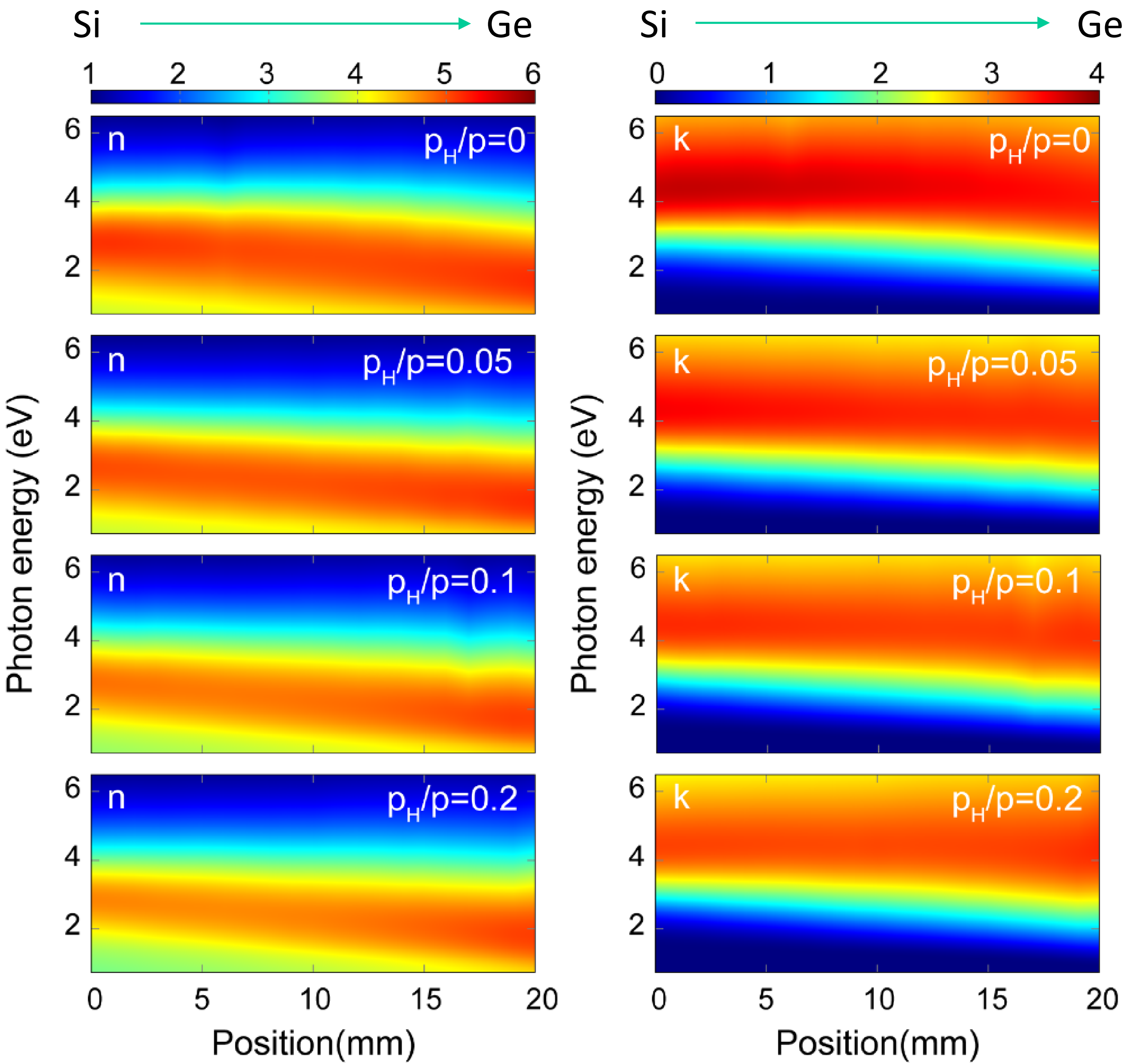

Mapping by spectroscopic ellipsometry

spot size: ~0.2 mm

resolution: ~1%

Dispersion of amorphous SiGe

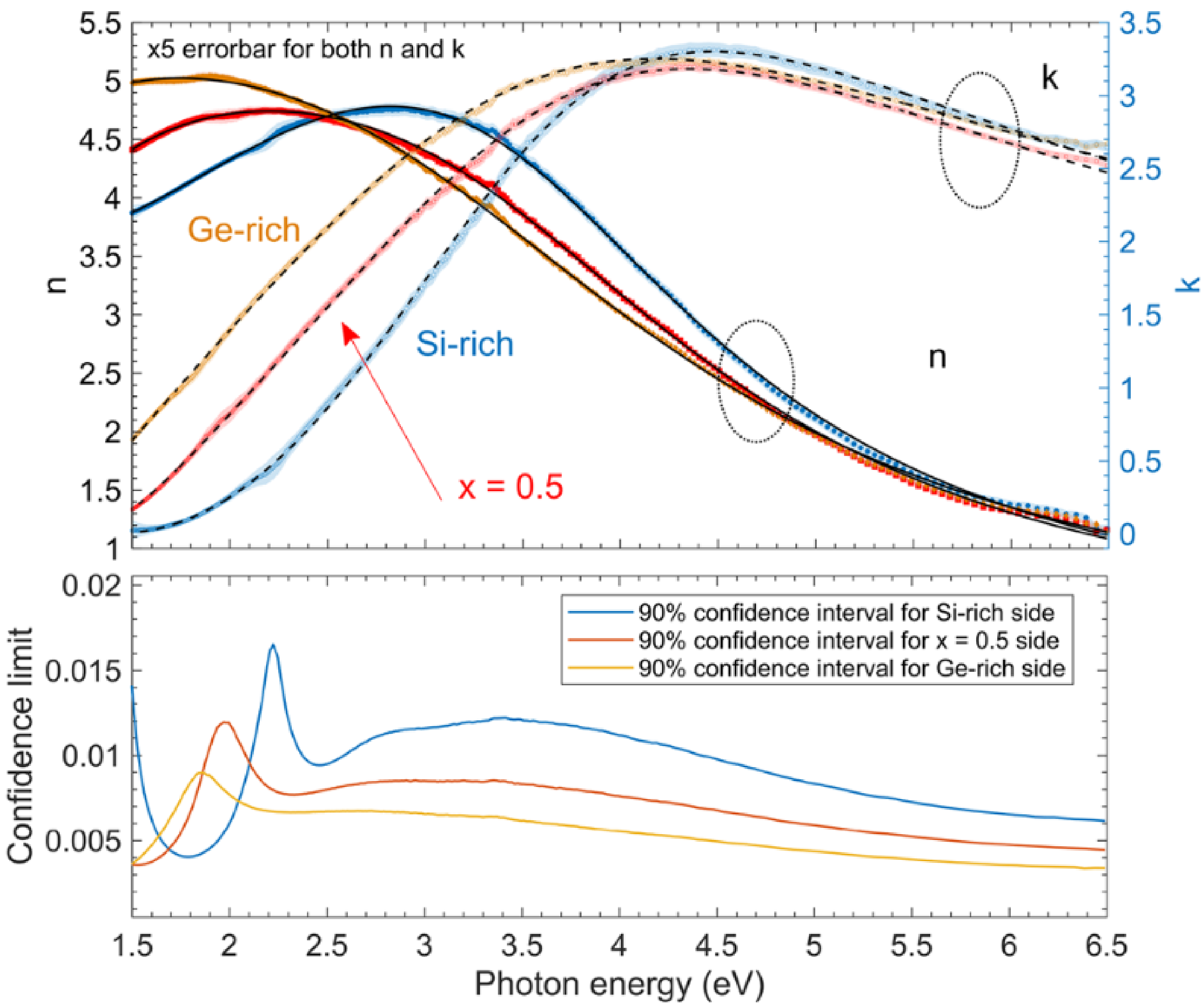

Parameters of the dispersion model

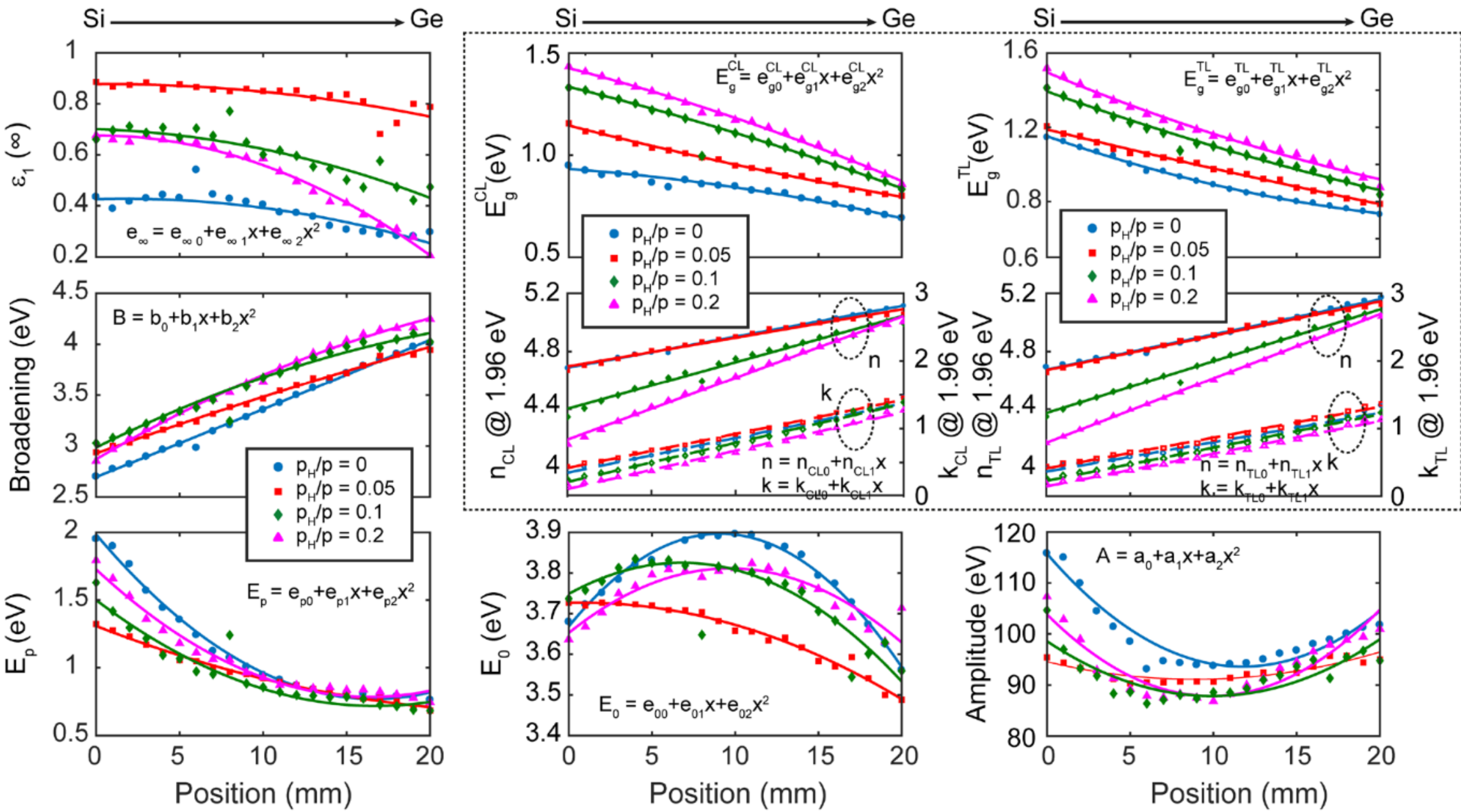

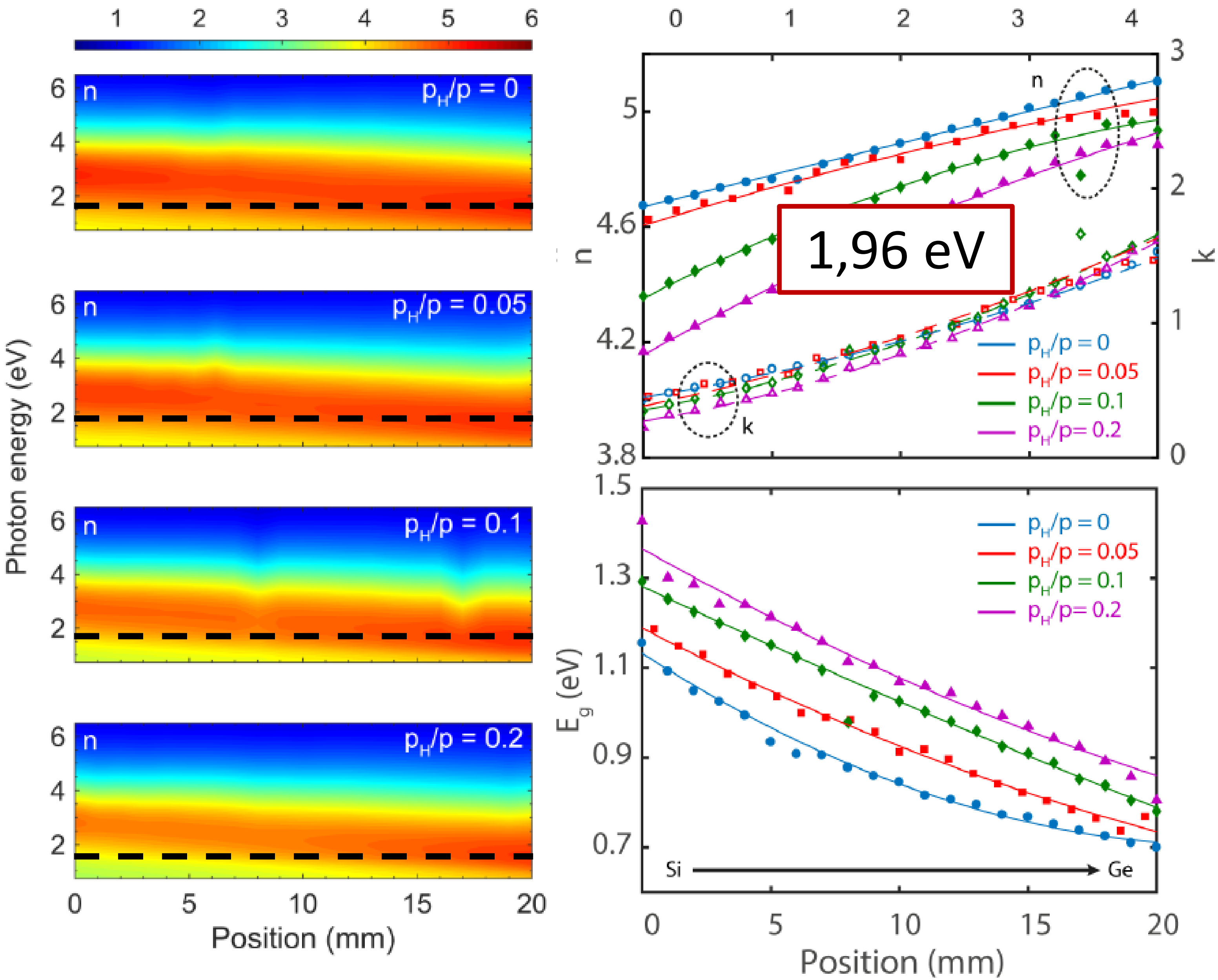
1,96 eV
n
k
$p_H/p = 0$
$p_H/p = 0.05$
$p_H/p = 0.1$
$p_H/p = 0.2$
Photon energy (eV)
Position (mm)
E_g (eV)
Si
Ge

www.ellipsometry.hu

Ellipsometry @ MTA EK MFA

Staff: P. Petrik, M. Fried, T. Lohner, E. Agocs, B. Kalas, A. Romanenko,

Publications, Projects, Equipment, History, Contact, Cooperations, Staff

- Bioellipsometry
- Mapping
- Nanostructures
- Photonic structures
- Photovoltaics
- Modeling
- Optical properties
- Waveguide characterizations
- Books and lectures

- Publications
- Projects
- Equipment
- History
- Contact
- Cooperations
- Staff

Biomaterials and Bioellipsometry

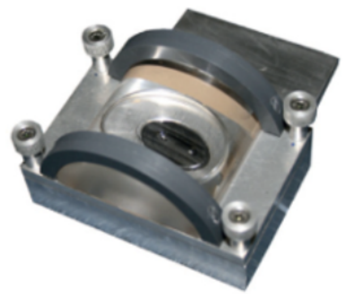

Hemicylindrical plasmon-enhanced Kretschmann ellipsometry

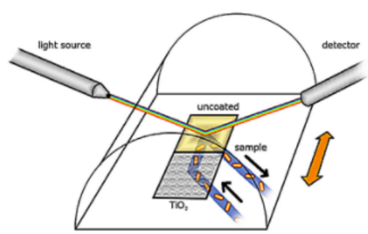

Plasmon-enhanced two-channel, multi-angle *in situ* spectroscopic ellipsometry

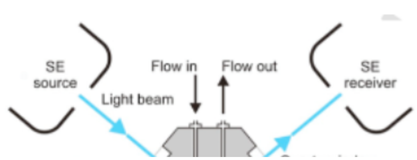

Combination of ellipsometry with waveguide interferometry www.photonics.hu

MFA PHOTONICS LABORATORY

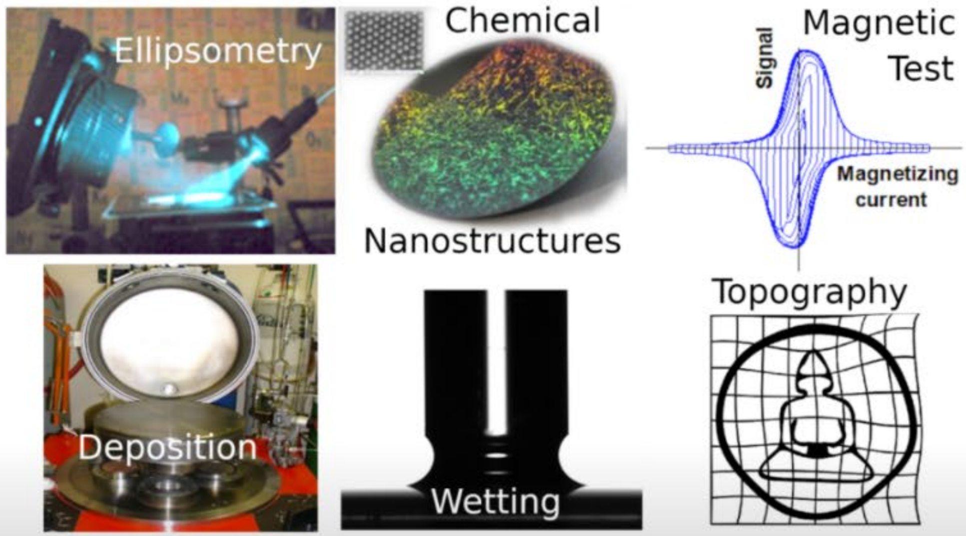

mta EK CENTRE FOR ENERGY RESEARCH

Most important

- What is directly measured by ellipsometry
- What sample properties can be determined
- Some typical applications

•Metrologies for thin film characterizations

Technique	Analysis Mode	Lateral Resolution (nm)	Depth Resolution (nm)	Duration (min)	Availability	Detection Limits (at.%)	Quantification of Results
SIMS	DP	5×10^3	4	45	Good	10^{-7}–10^{-3}	Standard
SNMS	DP	10^6	1	120	Medium	0.05	Standard
GD-OES	DP	10^6	3–100	5	Good	10^{-5}–10^{-3}	Standard
GD-MS	DP	10^7	10	10	Medium	10^{-7}–10^{-5}	Standard
AES	DP	10^5	10	45	Good	0.3	Standard
XPS	DP	10^5	1–10	120	Good	0.1	Standard-free
Raman depth-profiling	DP	10^5	100	50	Medium	1	Standard
RBS	Surf	10^7	10	10	Rare	1	Standard-free
ERDA	Surf	10^7	10	30	Rare	10^{-4}	Standard-free
GIXRD	Surf	10^6	100	420	Good	1	Difficult
AXES	Surf	10^5	10–80	420	Rare	1	Standard
Ellipsometry	Surf	10^6	1	30	Medium	0.2–2	Difficult
TEM-EDX	CS	5	Specimen thickness	30	Good-medium	0.5	Standard
SEM-EDX	CS	150	Few 100	20	Good	0.5	Standard
SEM-WDX	CS	150	Few 100	60	Good	3	Standard
Scanning Auger	CS	10	1	137	Good	3	Standard
TOF-SIMS	CS	100	1	2	Medium	10^{-6}	Standard
Raman mapping	CS	400	100	120	Medium	1	Standard

Abou-Ras D, Caballero R, Fischer C H, Kaufmann C A, Lauermann I, Mainz R, Mönig H, Schöpke A, Stephan C, Streeck C, Schorr S, Eicke A, Döbeli M, Gade B, Hinrichs J, Nunney T, Dijkstra H, Hoffmann V, Klemm D, Efimova V, Bergmaier A, Dollinger G, Wirth T, Unger W, Rockett A A, Perez-Rodriguez A, Alvarez-Garcia J, Izquierdo-Roca V, Schmid T, Choi P P, Müller M, Bertram F, Christen J, Khatri H, Collins R W, Marsillac S and Kötschau I 2011 Microsc. Microanal. doi:10.1017/S1431927611000523 1

Dispersion function

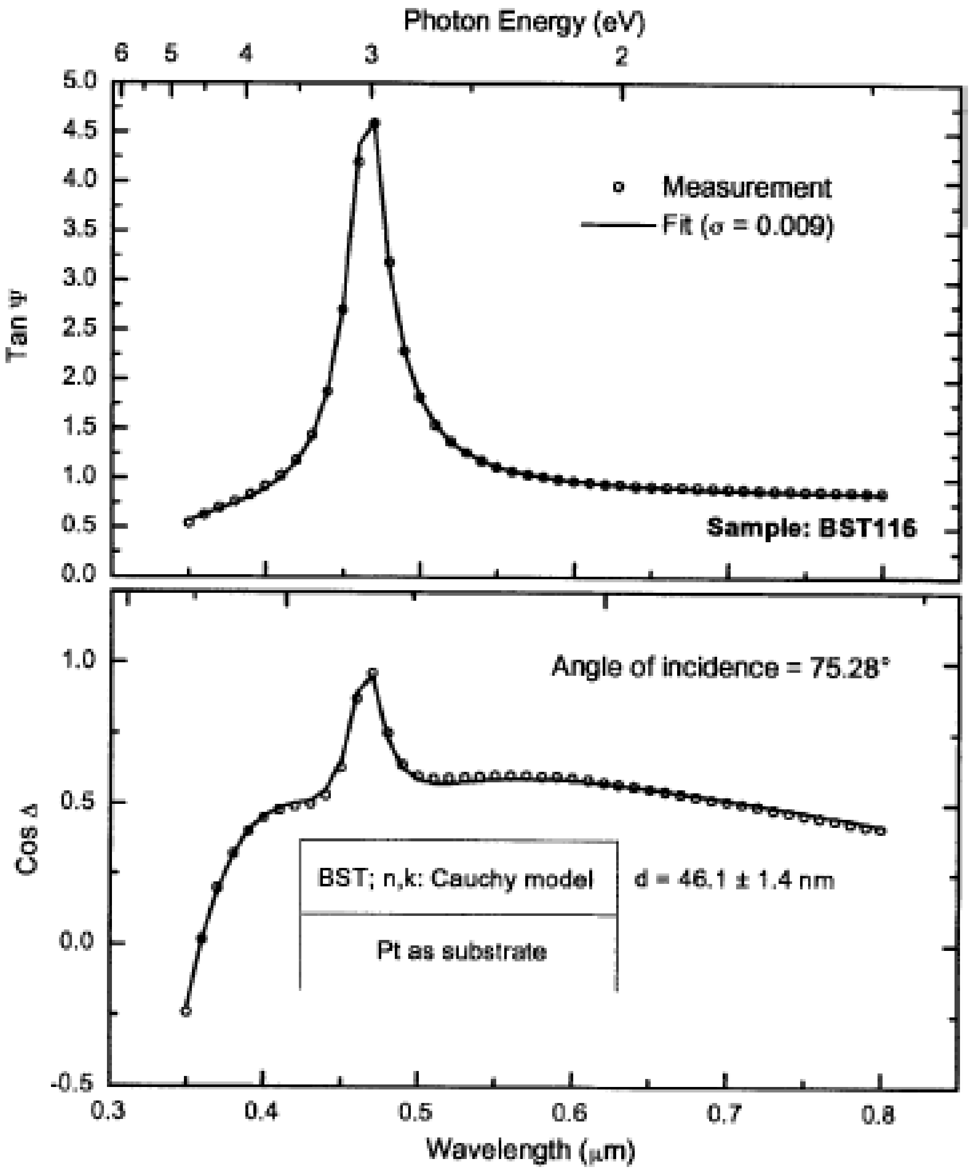

Bárium-stroncium-titanát

$Ba_xSr_{1-x}TiO_3$

Cauchy modellel

$$n = A + \frac{10^6 B}{\lambda^2} + \frac{10^{12} C}{\lambda^4},$$

$$k = D + \frac{10^6 E}{\lambda^2} + \frac{10^{12} F}{\lambda^4},$$

Ion implantation

Damage profiles (c-Si), comparative measurements (SE, RBS, TEM)

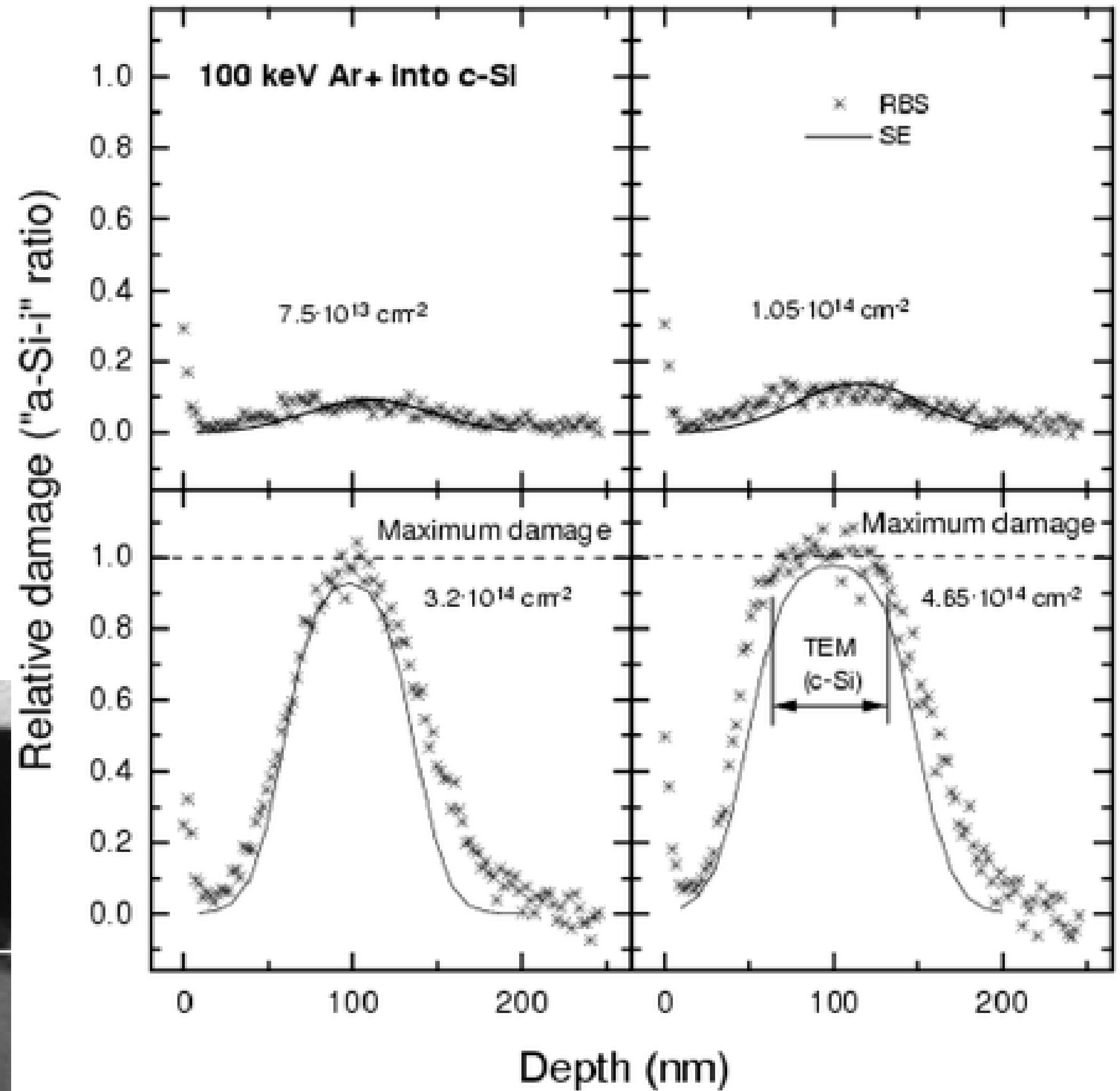

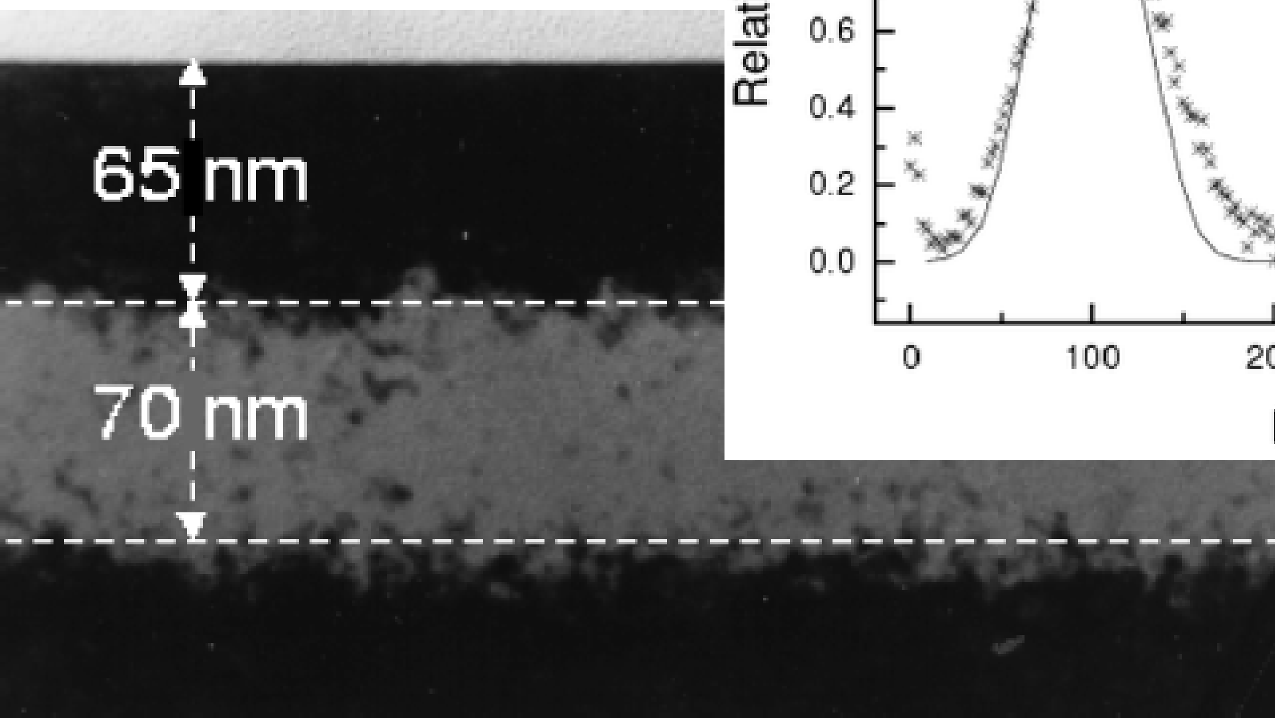

Model 1

Example:
Ion implantation-caused damage.
Determination of the damage profile.
A few fit parameters, equal sub-layer distances

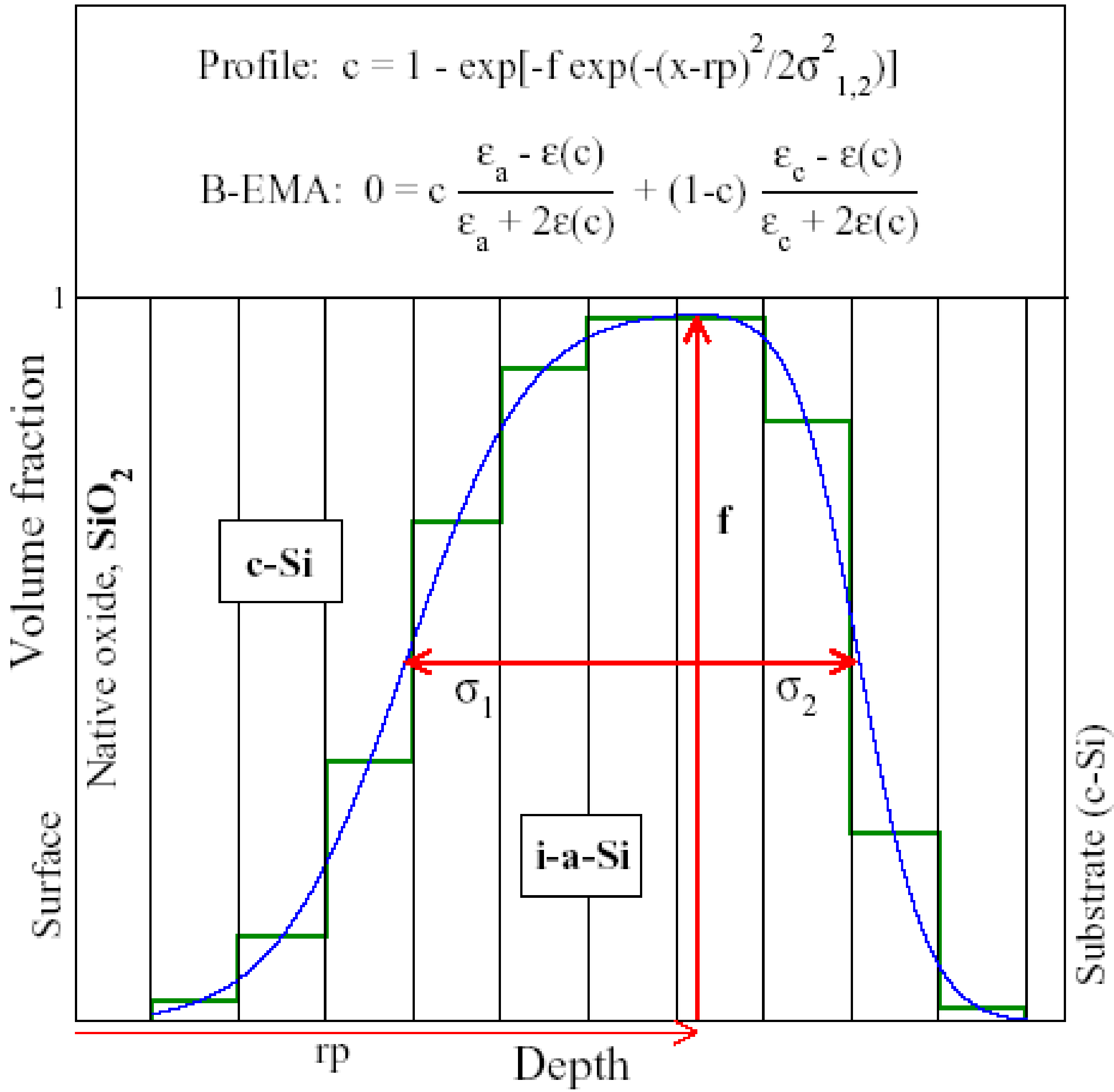

Damage profiles (p-Si), comparative measurements (SE, TEM, RBS not!)

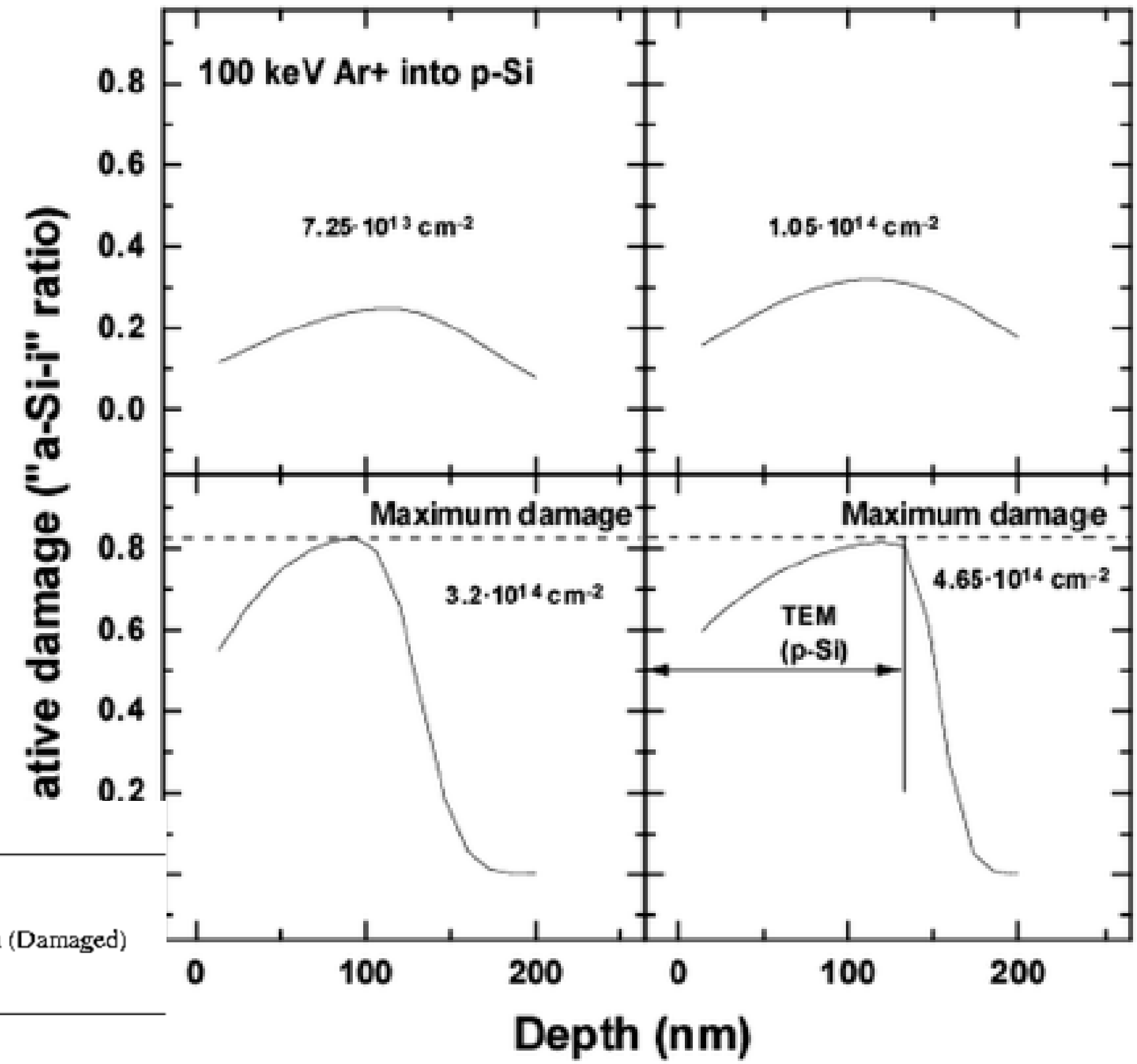

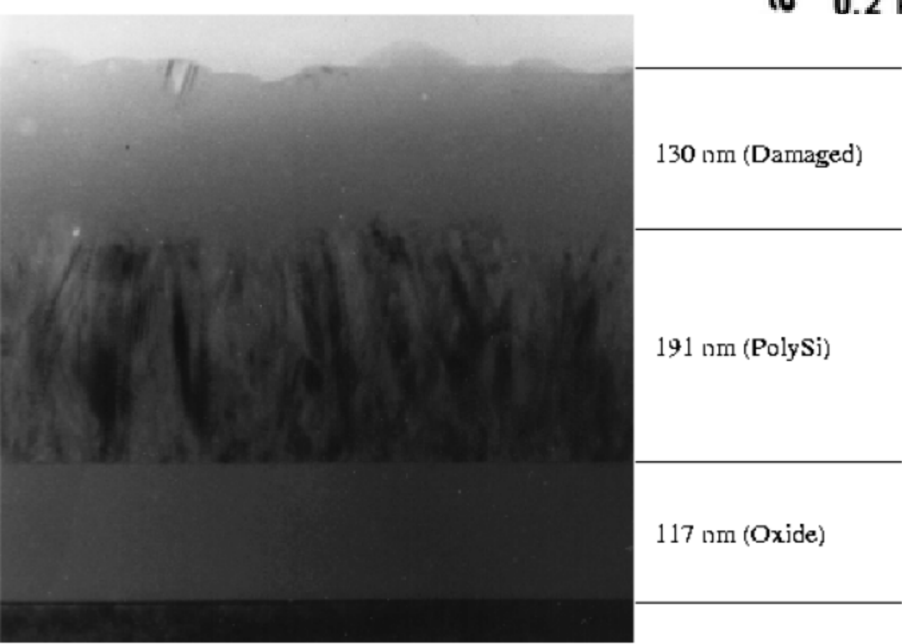

Cavities by high-dose helium implantation

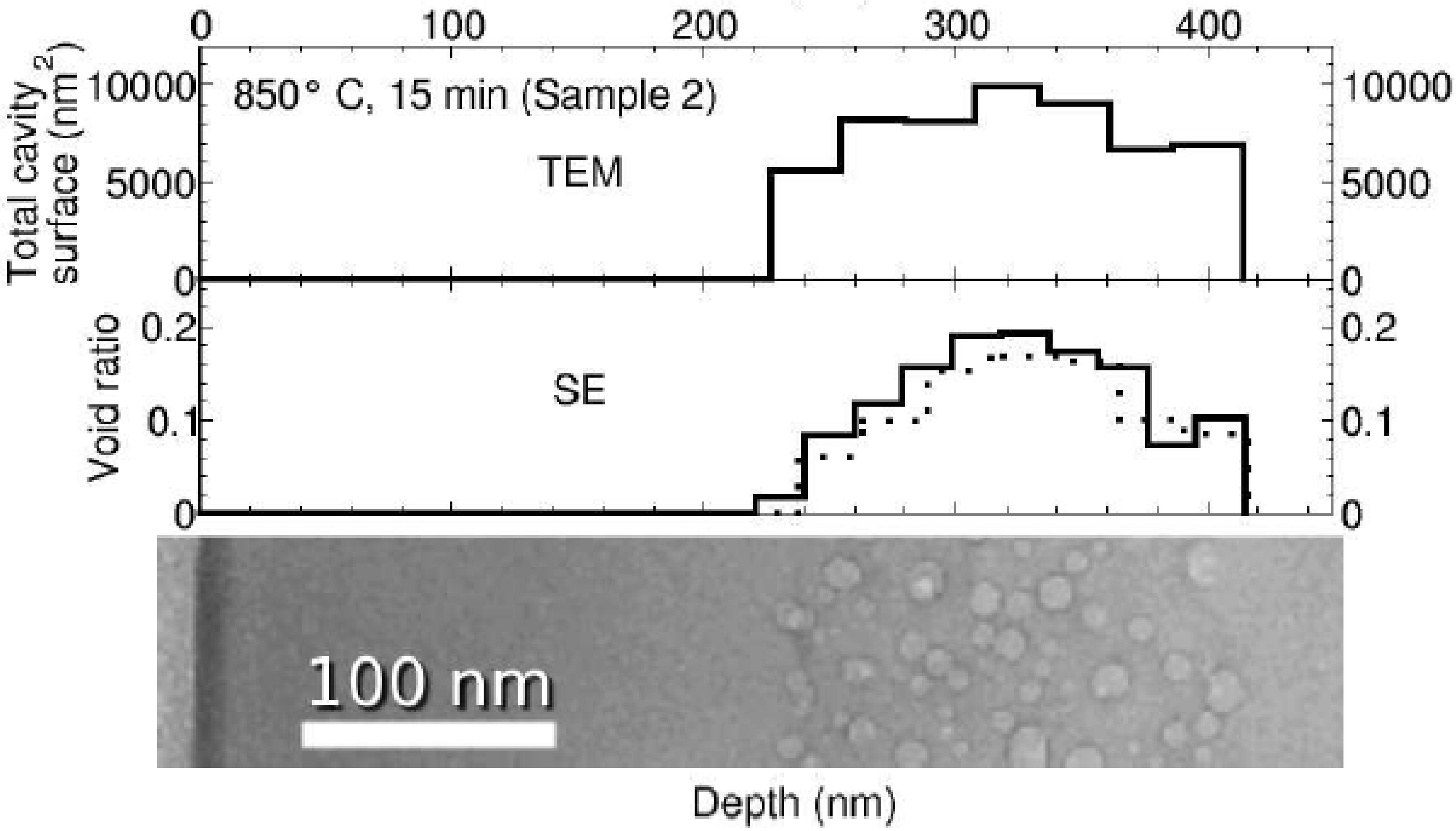

Implantation of 10 keV He into c-Si with a subsequent annealing

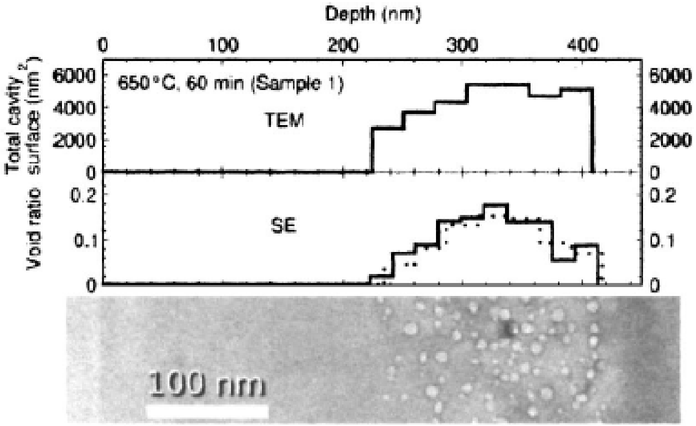

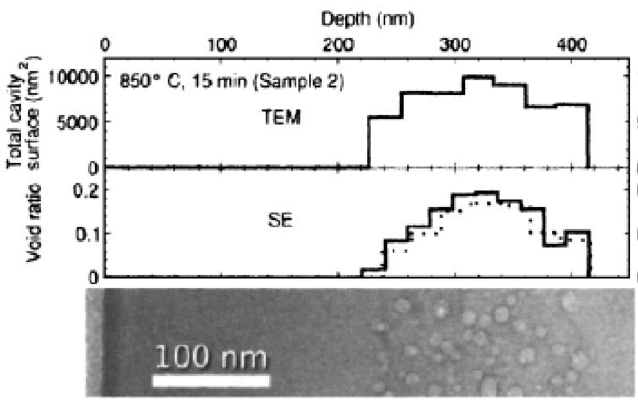

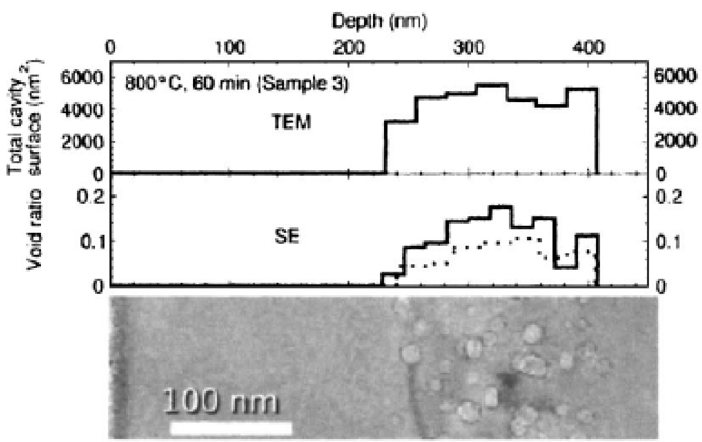

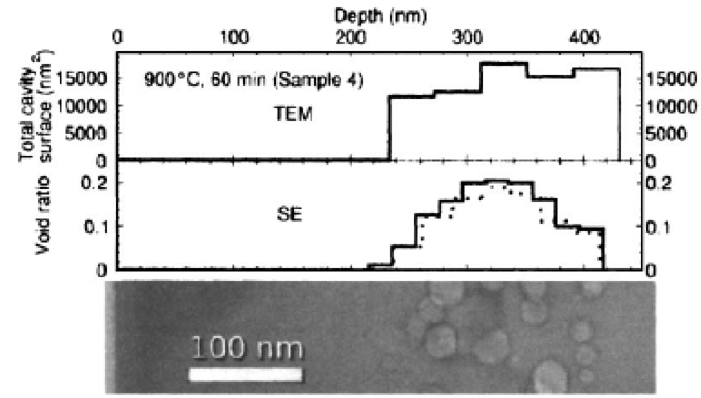

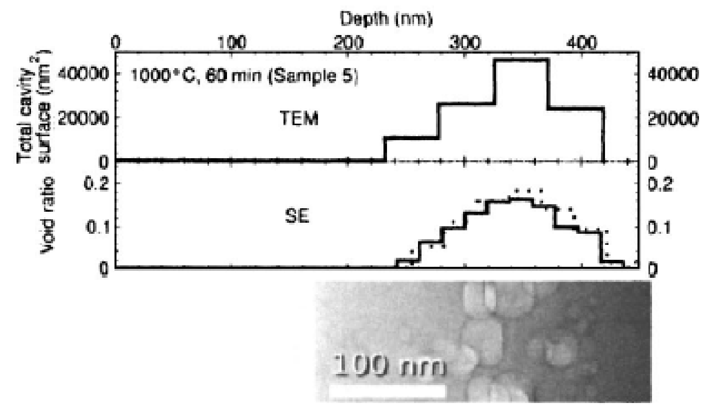

P. Petrik, M. Fried, T. Lohner, O. Polgár, J. Gyulai, F. Cayrel, D. Alquier; Optical models for cavity profiles in high-dose helium-implanted and annealed silicon measured by ellipsometry, J. Appl. Phys. 97 (2005) 1-6.

Polycrystalline silicon

Modeling #1

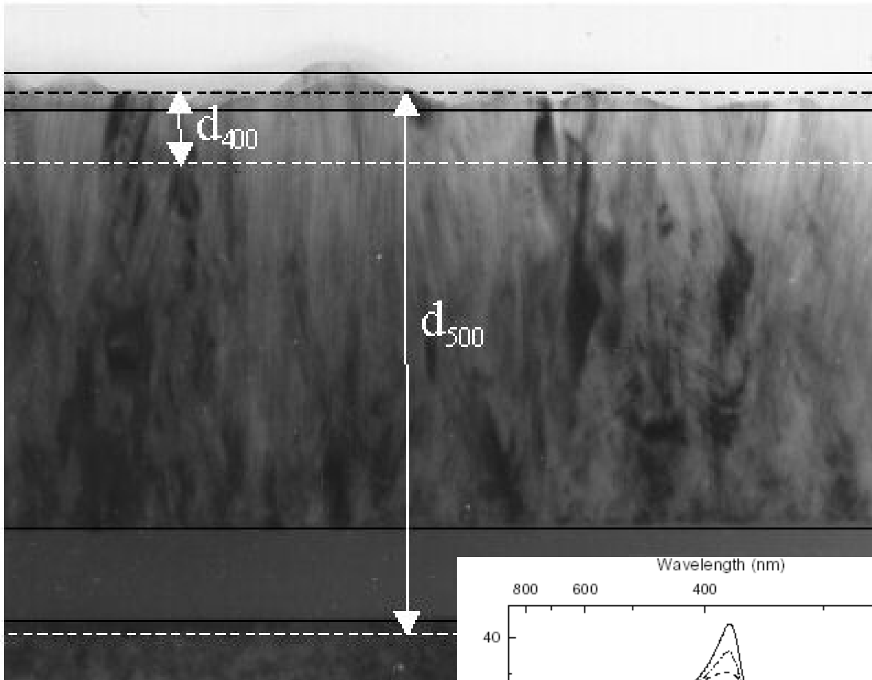

Layer	Model 15	Model 37
Roughness	c-Si + pc-Si + void	c-Si + pc-Si + void
Polysilicon	c-Si + pc-Si + void (regarded as bulk)	c-Si + pc-Si + void
SiO_2		SiO_2

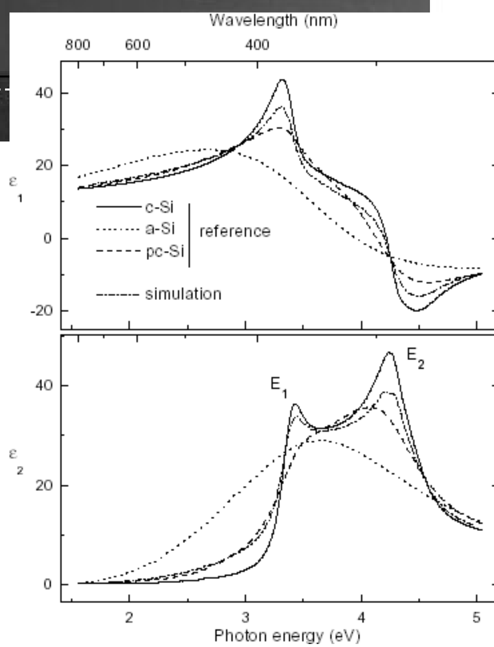

Dielectric functions sensitive to crystal structure

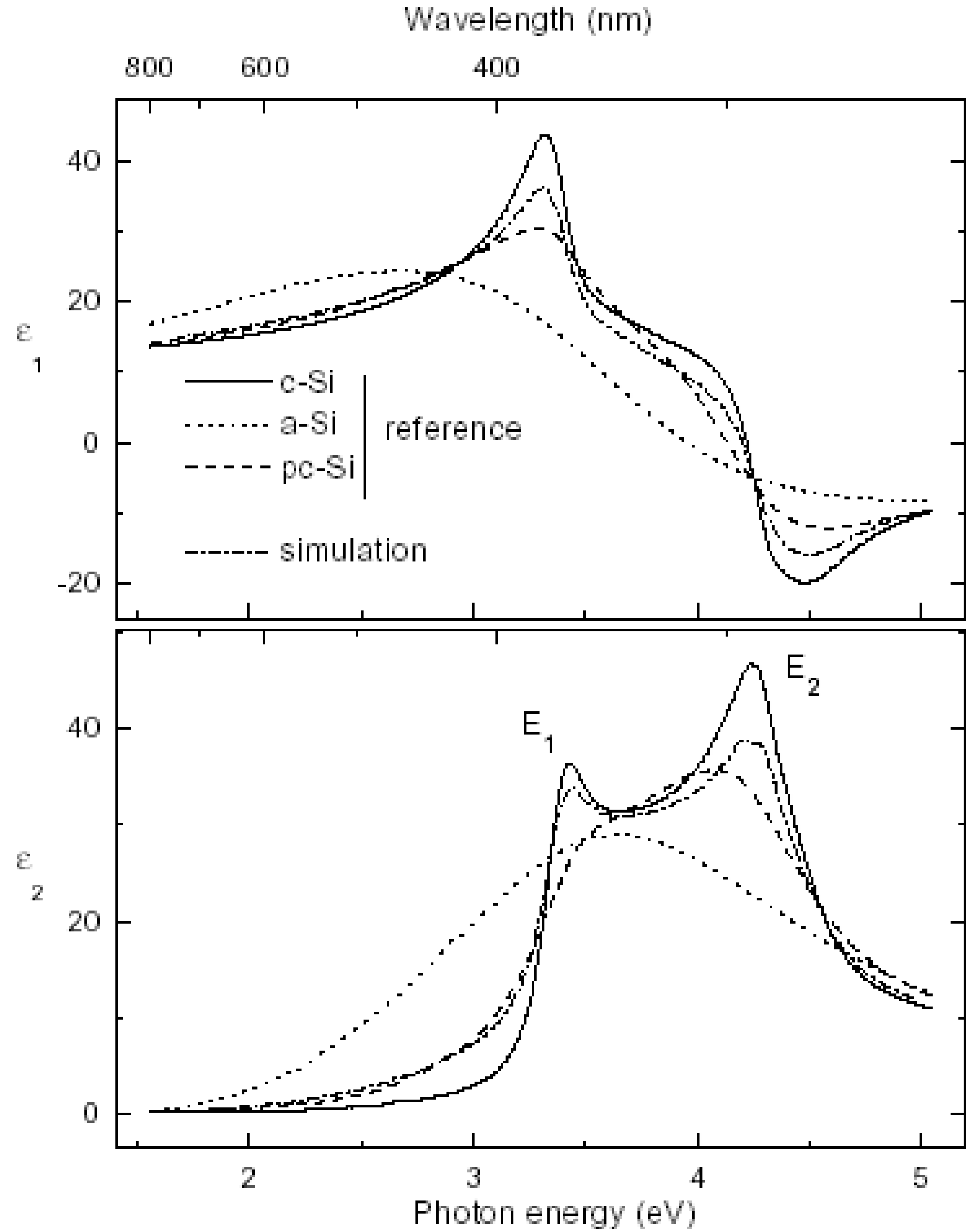

What shows the dielectric function

Optical Properties of Solids: Example Indirect Crystalline Si

After Cohen & Chelikowski, *Handbook on Semiconductors*, edited by W. Paul (North-Holland, Amsterdam, 1982).

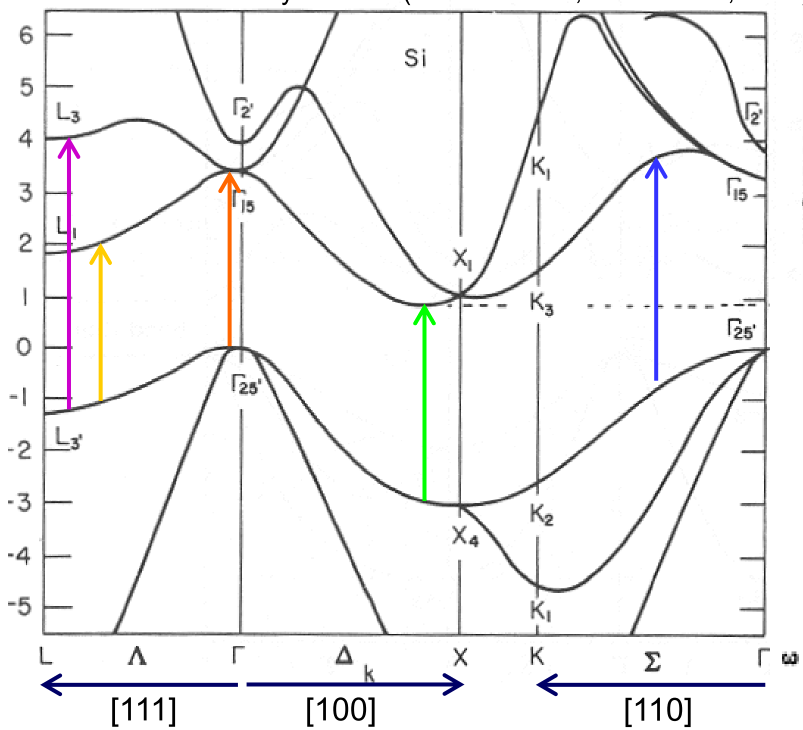

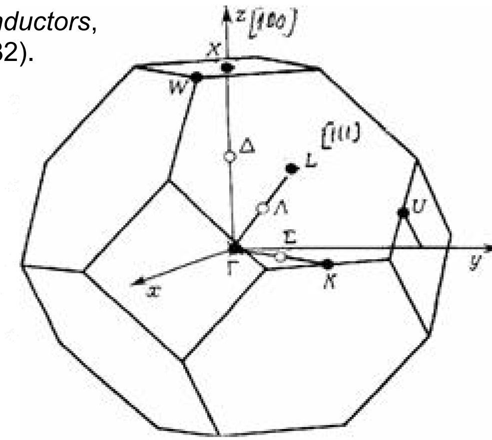

Typical Optical Amplitudes

Indirect: $\varepsilon_2 \sim 10^{-3}$

Direct, non-parallel: $\varepsilon_2 \sim 1$

Direct, parallel: $\varepsilon_2 \sim 10$

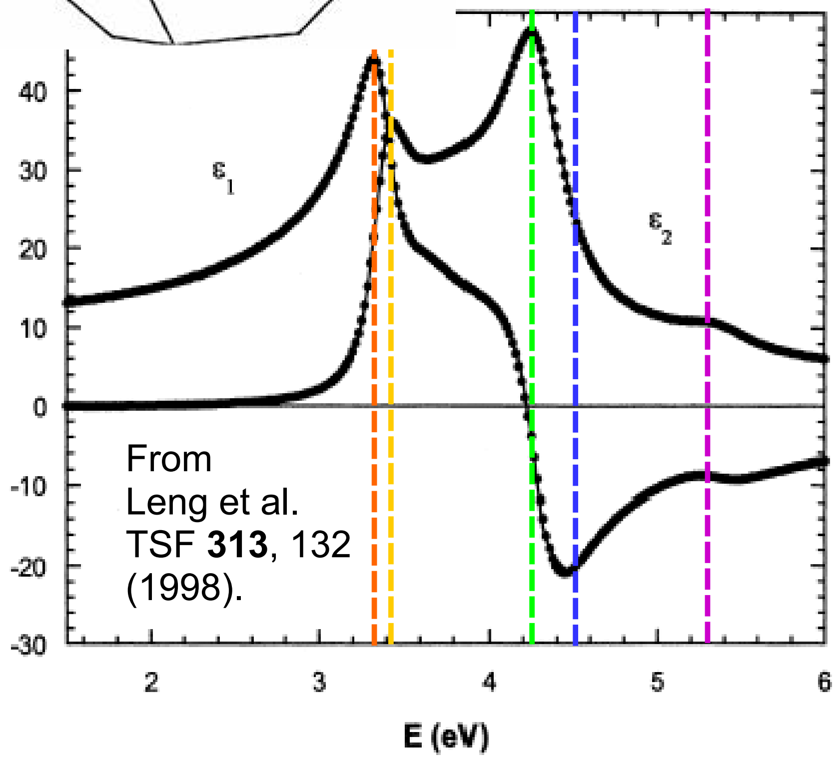

E_0'-E_1 complex:
zone center and toward L <111> directions

$E_2(X)$-$E_2(\Sigma)$ complex:
toward X <100> and toward <110> directions

E_1' :
toward L <111> directions

Optical modeling of polycrystalline silicon and porous silicon

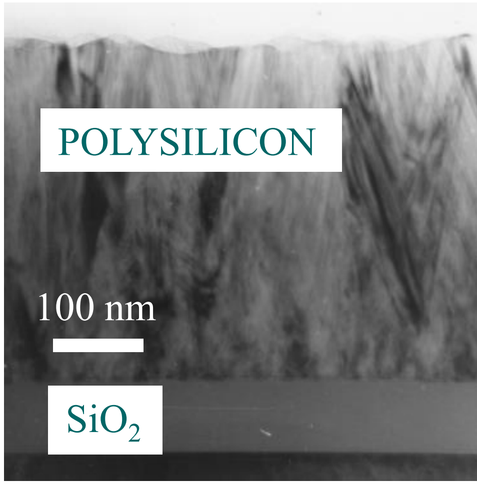

STRUCTURE	MODEL
Roughness	c-Si + a-Si + void
Polysilicon	c-Si + a-Si + void
Buried oxide	SiO_2
Substrate	c-Si

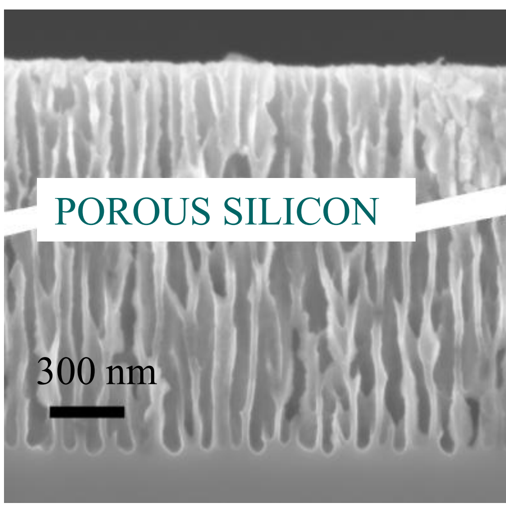

STRUCTURE	MODEL
Roughness	c-Si + void
PorSi layer	c-Si + void
Interface	c-Si + void
Substrate	c-Si

Optical penetration depth in deposited silicon

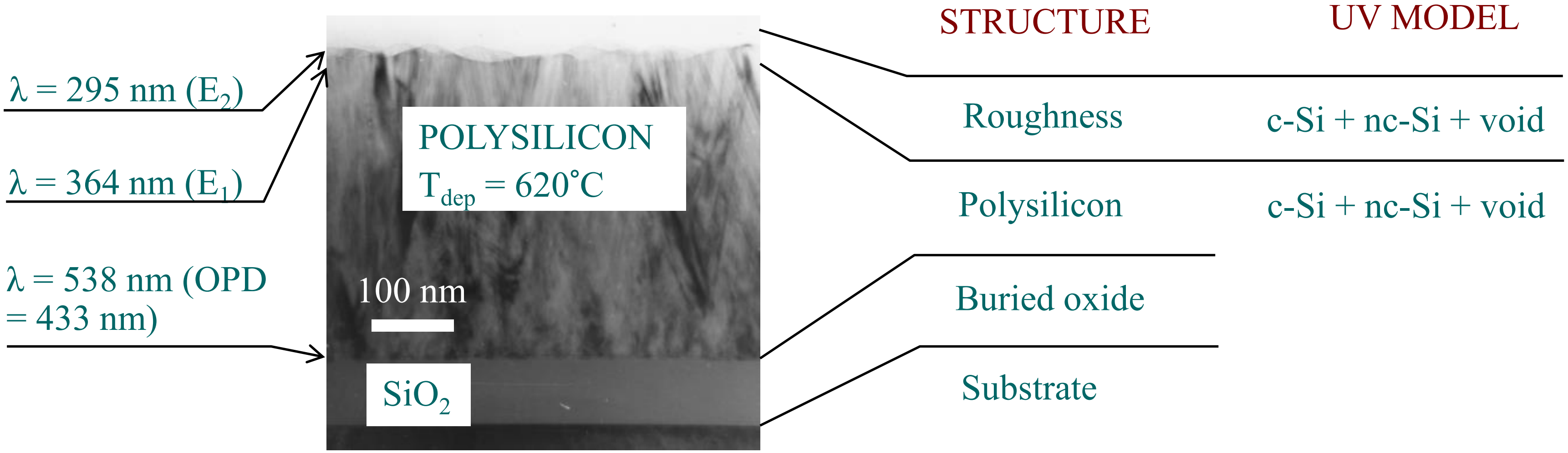

Calculated values of the above structure using best fit composition of (0.2 c-Si + 0.7 nc-Si + 0.1 void):

- E_1 ~ 3.4 eV, 364 nm -> OPD = 13.9 nm
- E_2 ~ 4.2 eV, 295 nm -> OPD = 5.8 nm
- 2.3 eV, 538 nm -> OPD = 433 nm

Microstructural sensitivity at the surface

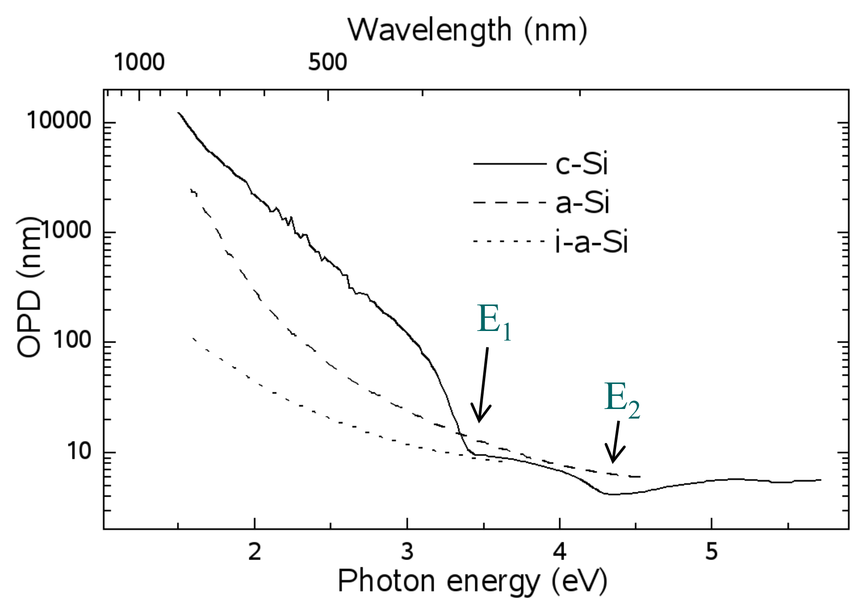

Modeling fine-grained polycrystalline silicon

- Robust model for fine-grained structures (lifetime broadening)

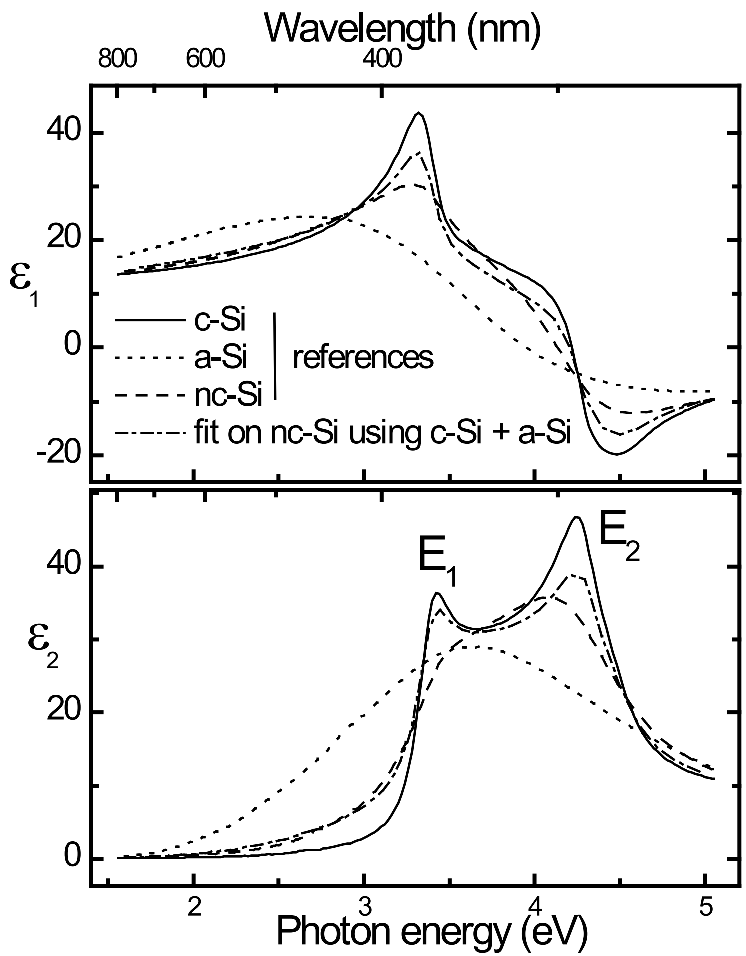

STRUCTURE

Surface roughness
Polysilicon

UV MODEL

Large grains

c-Si + a-Si + void
c-Si + a-Si + void

Small grains

nc-Si + a-Si + void
nc-Si + a-Si + void

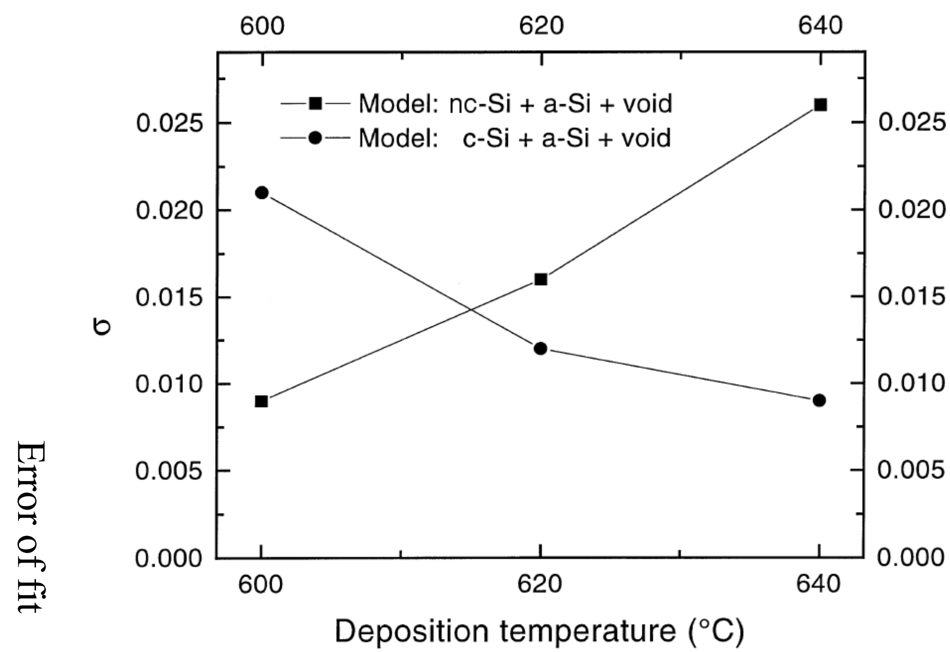

nc-Si from: G. E. Jellison, M. F. Chisholm, and S. M. Gorbatkin, Appl. Phys. Lett. 62, 348 (1993)

P. Petrik, M. Fried, T. Lohner, R. Berger, L. P. Biro, C. Schneider, J. Gyulai, H. Ryssel, Thin Solid Films 313, 259 (1998)

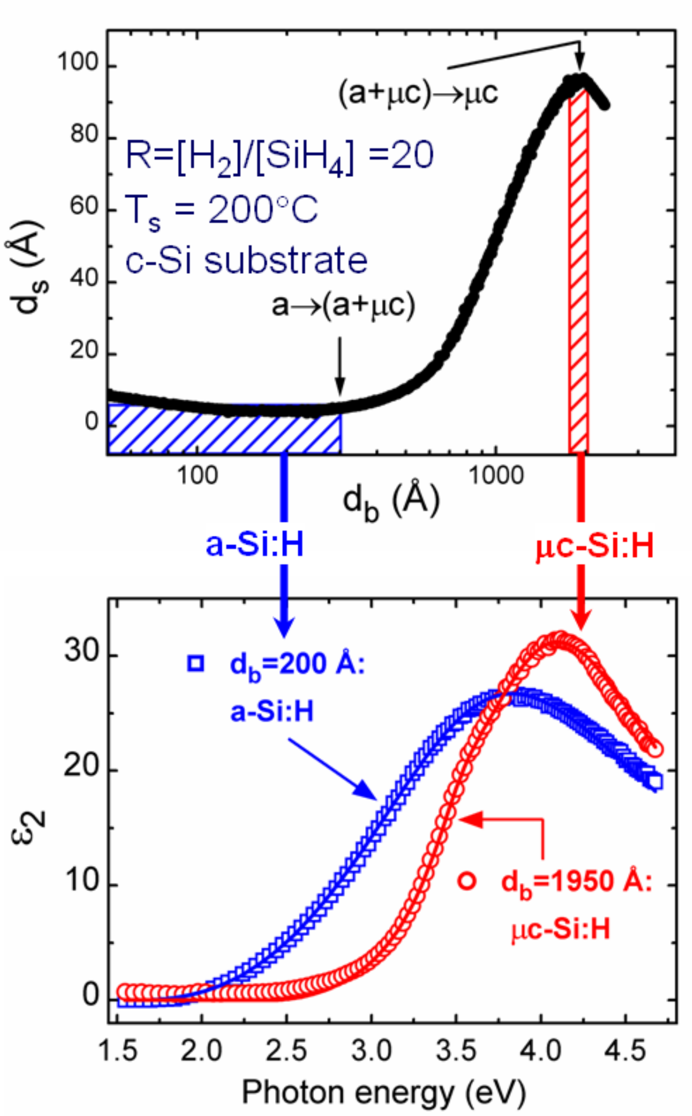

Analysis of the Evolution of Microcrystalline Si:H from Amorphous Silicon under Fixed Growth Conditions

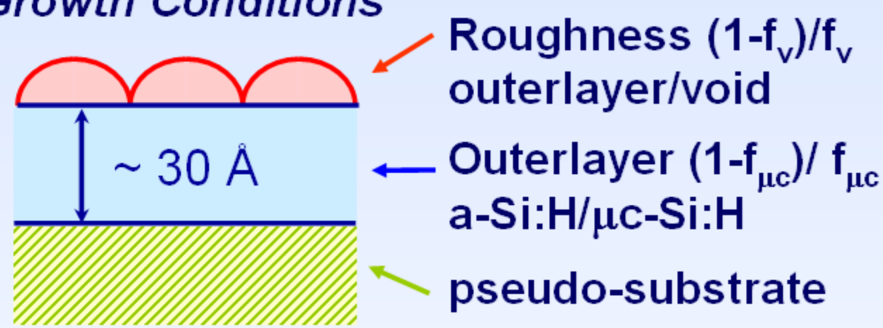

Squares: single-phase **a-Si:H** obtained from RTSE data collected at 200 Å, before the a → (a+μc) transition

Circles: single-phase **μc-Si:H** obtained from RTSE data collected at 1950 Å after the (a+μc) → μc transition

Lines: K.K. consistent analytical models
Ref: A.S. Ferlauto *et al.*,
JNCS **266-269**, 269 (2000).

Surface roughness
AFM vs SE

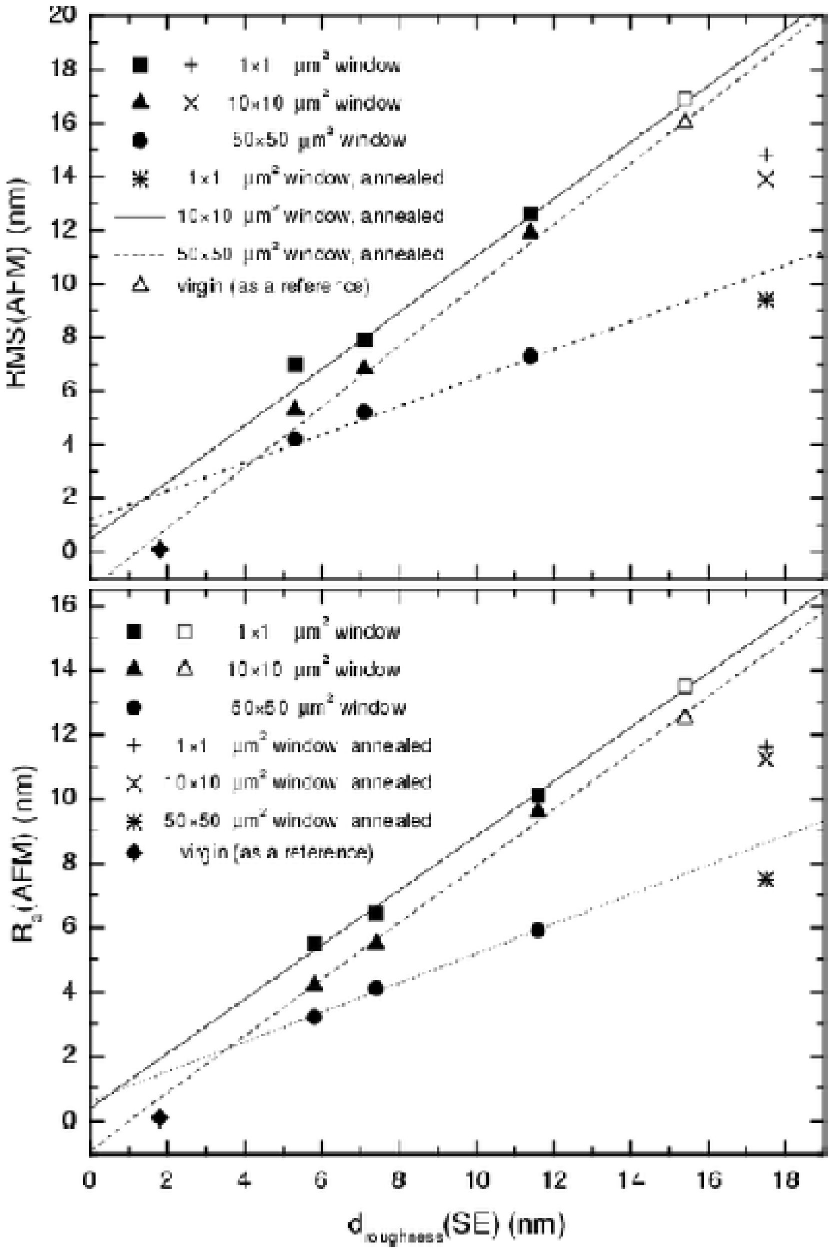

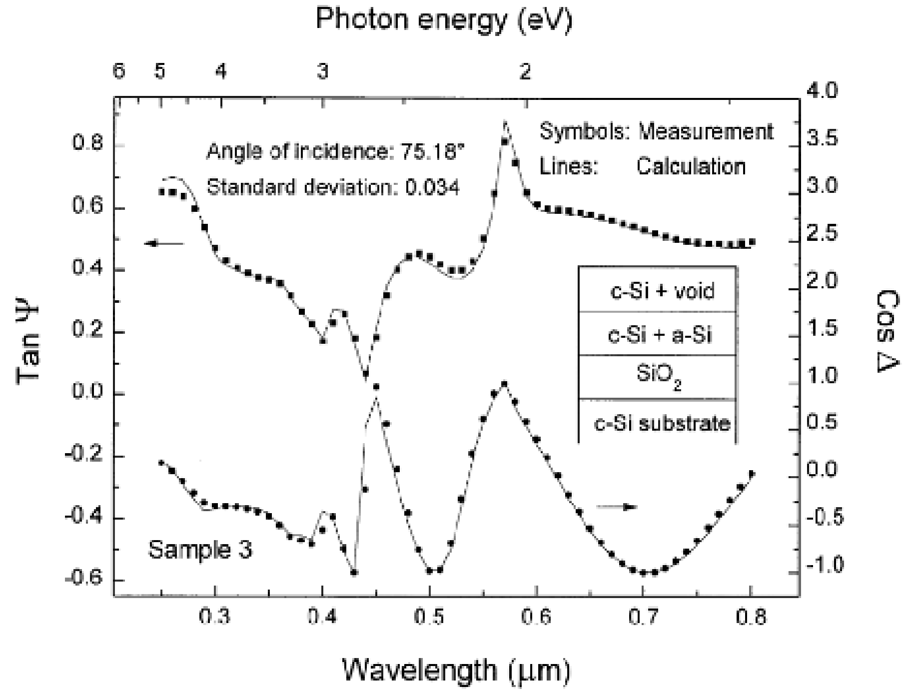

P. Petrik, L. P.Biró, M. Fried, T. Lohner, R. Berger, C. Schneider, J. Gyulai, H. Ryssel; Comparative study of surface roughness measured on polysilicon using SE and AFM; Thin Solid Films v.315 (1998) 186.

In situ ellipsometry

In-situ, real-time

Construction of the heater with active cooling and optics for *in situ* metrology

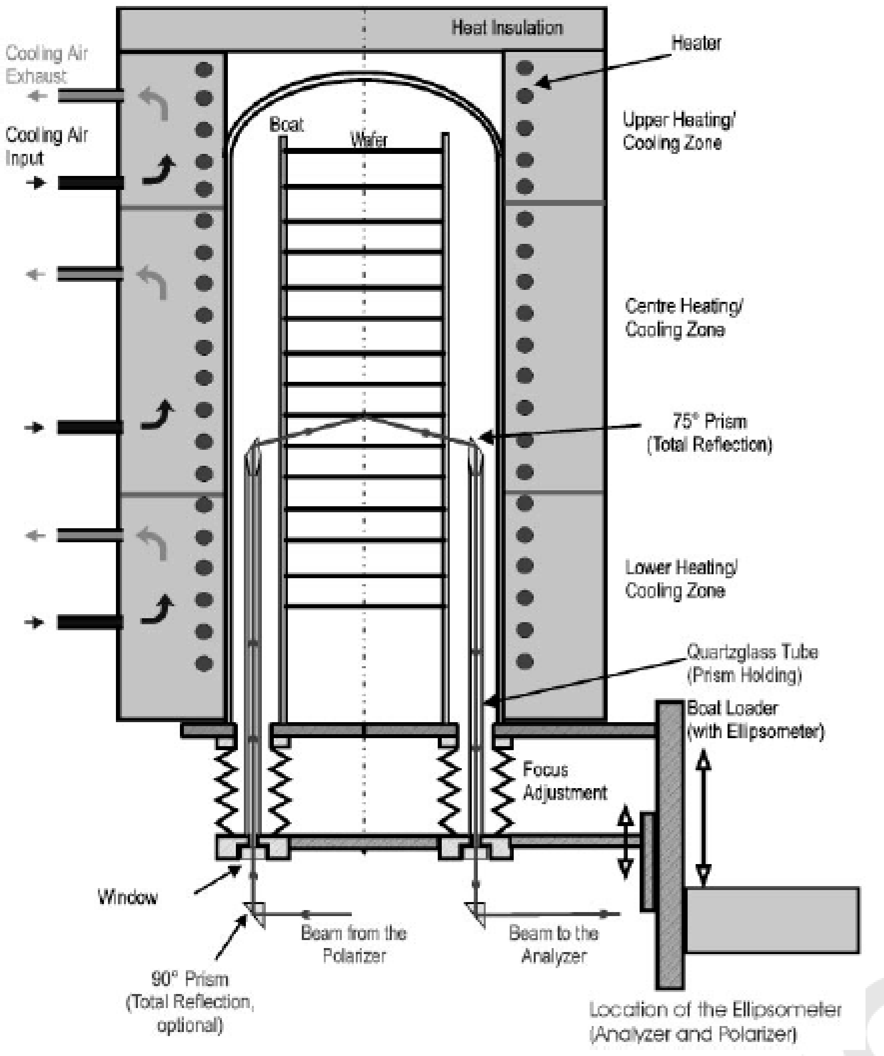

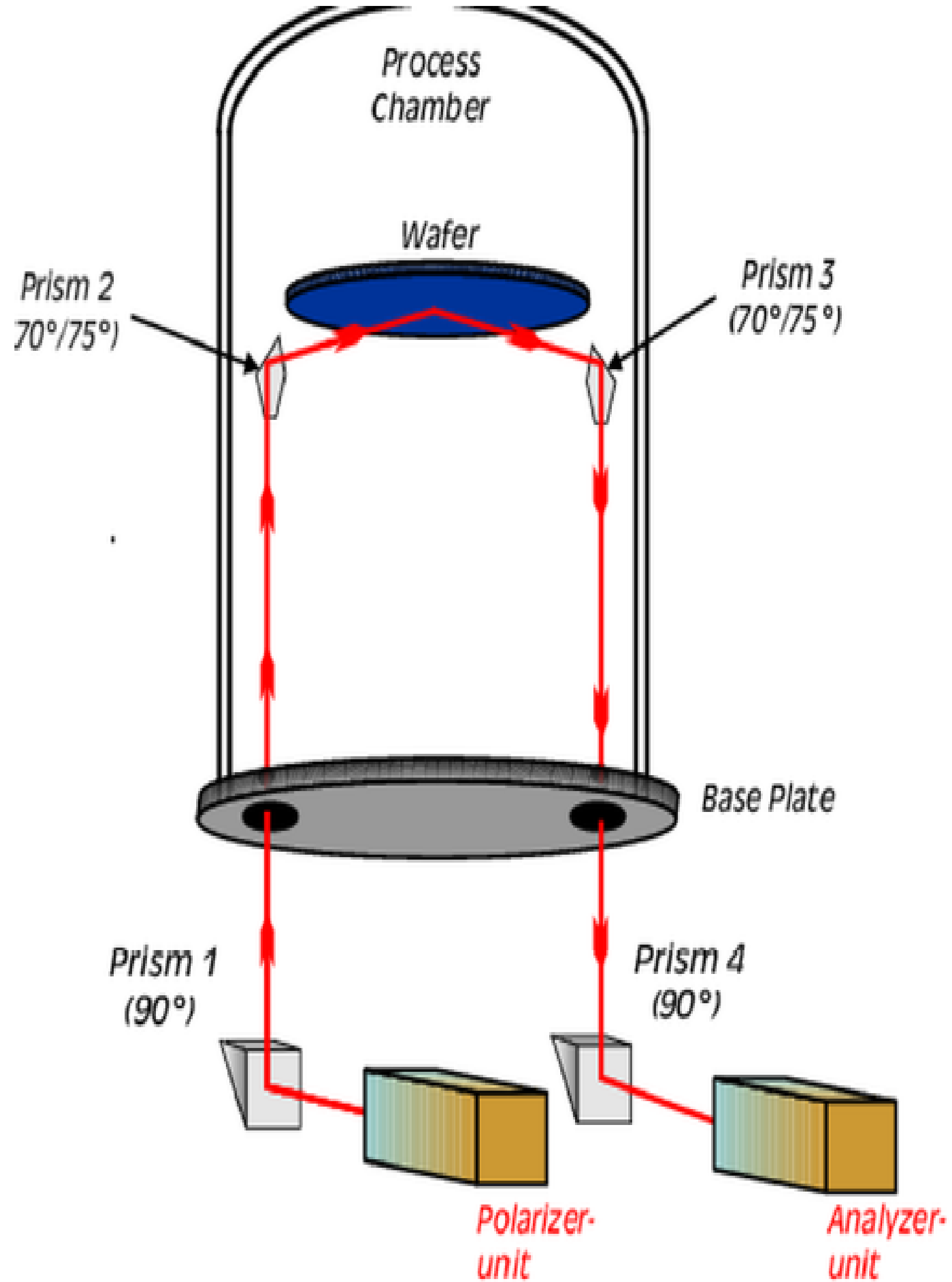

Temperature dependence of the refractive index of silicon

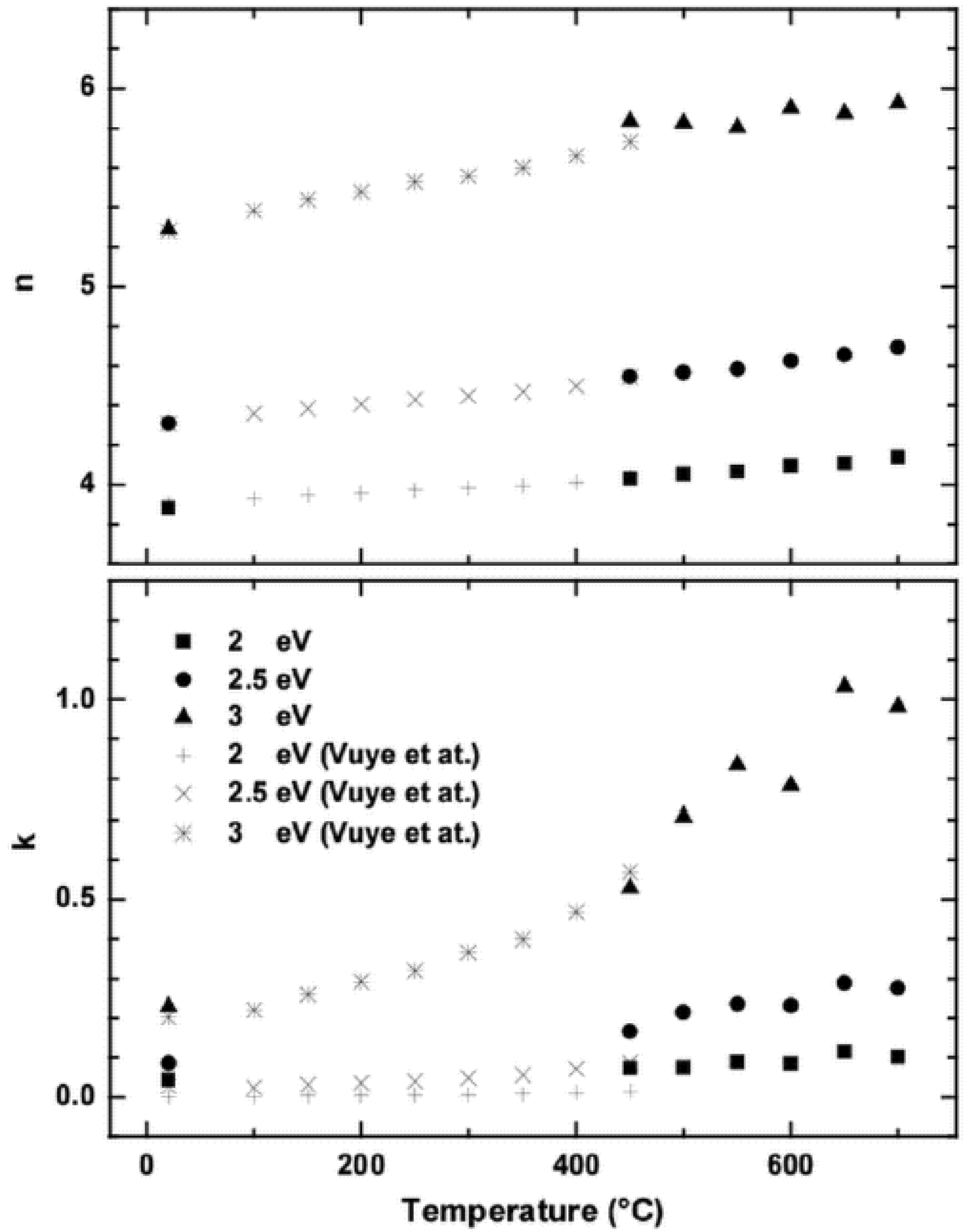

Comparison of two models (fit in a limited range)

Table 5.2. Fitted model parameters as functions of annealing time.

Annealing time (min)	a-Si (%)	pc-Si (%)	Oxide thickness (nm)	σ
0	98.2±1.8	1.8	1.3±0.1	0.003
6	97.4±1.7	2.6	1.2±0.1	0.003
13	96.1±2.1	3.9	1.4±0.2	0.004
20	80.1±2.3	19.9	1.5±0.2	0.004
26	54.5±2.4	45.5	1.8±0.1	0.004
33	29.8±2.4	70.2	1.8±0.1	0.003
39	12.6±2.0	87.4	1.7±0.1	0.003
46	2.4±1.0	97.6	1.6±0.1	0.002
52	0.2±0.2	99.8	1.5±0.1	0.001
59	0.1±0.1	99.9	1.3±0.1	0.001

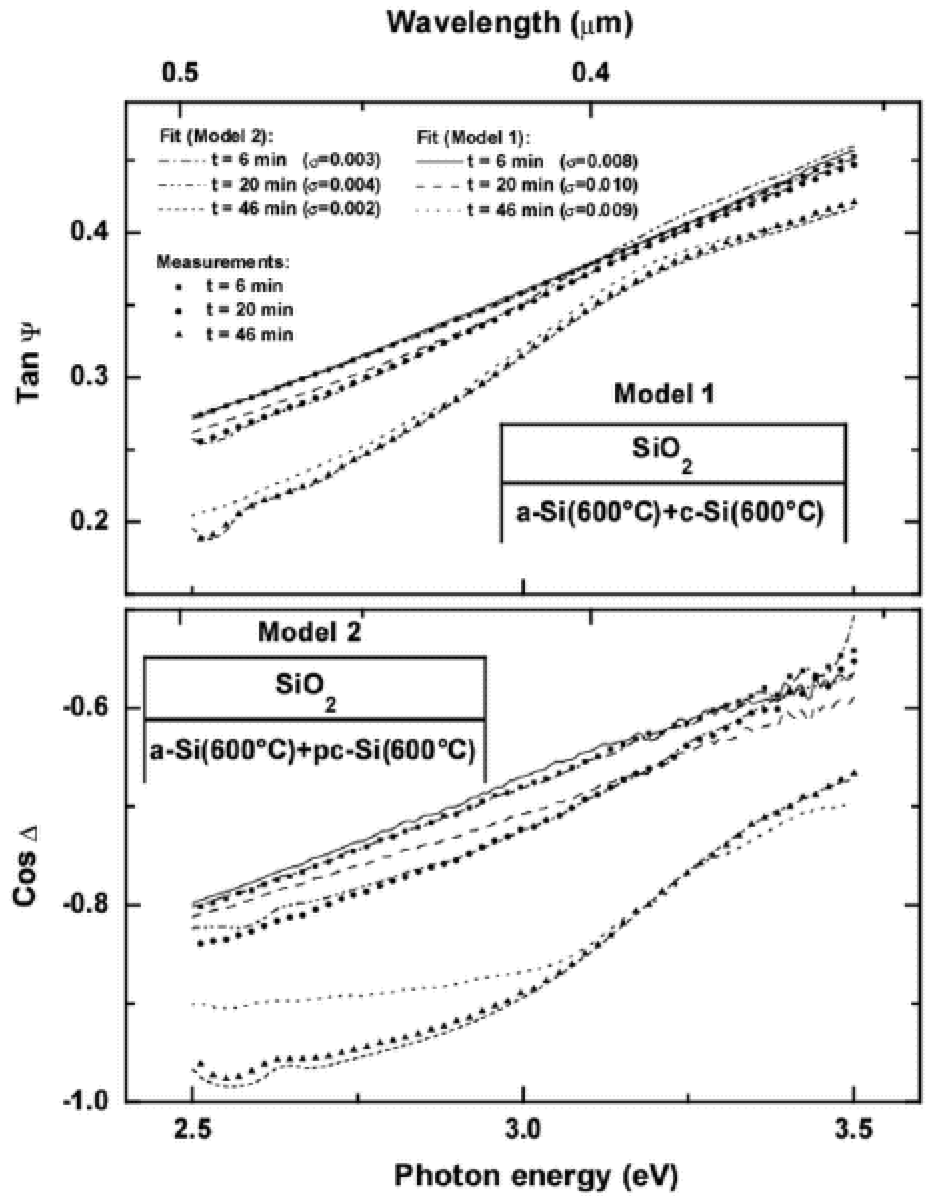

Monitoring of crystallization

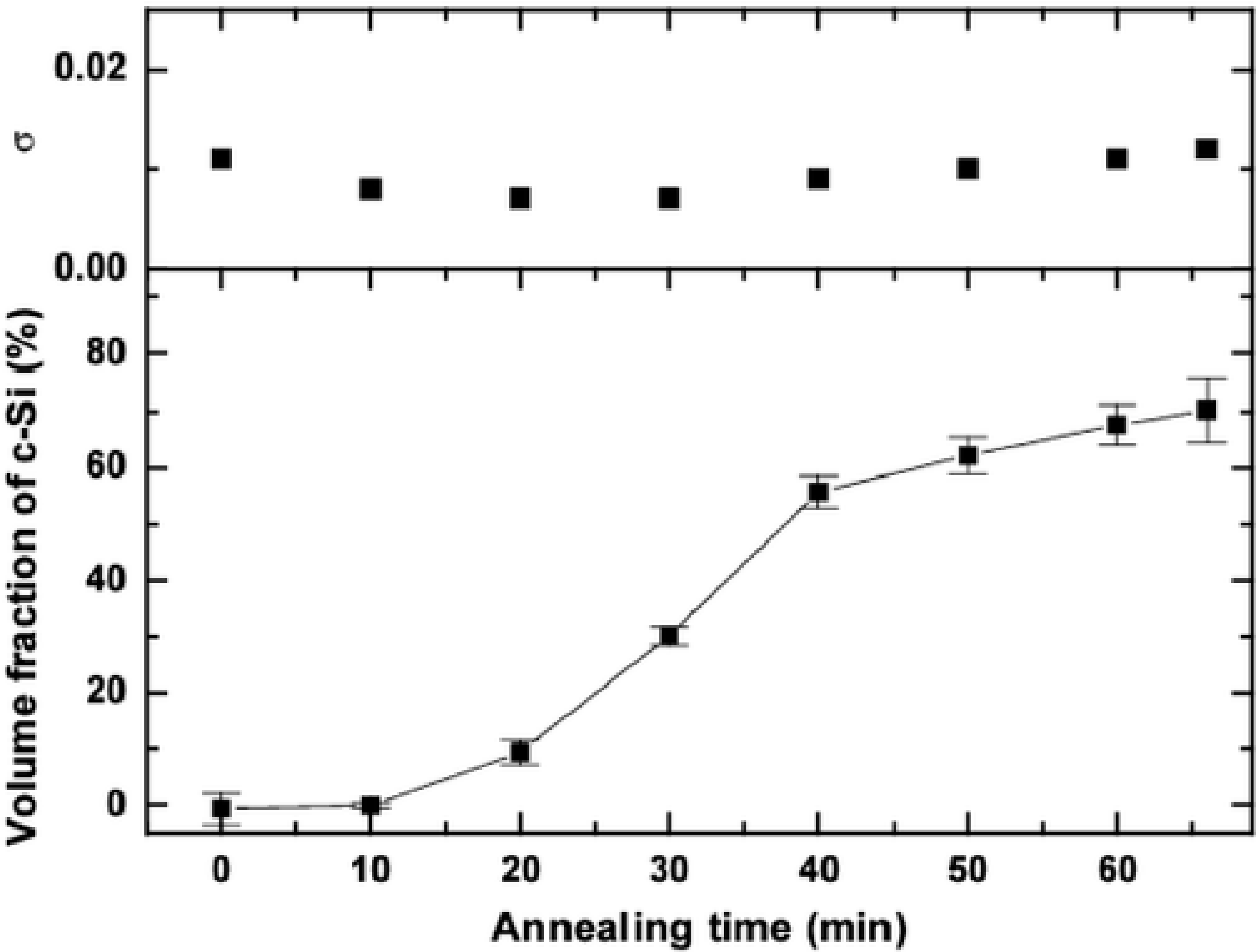

SURFACE ROUGHNESS

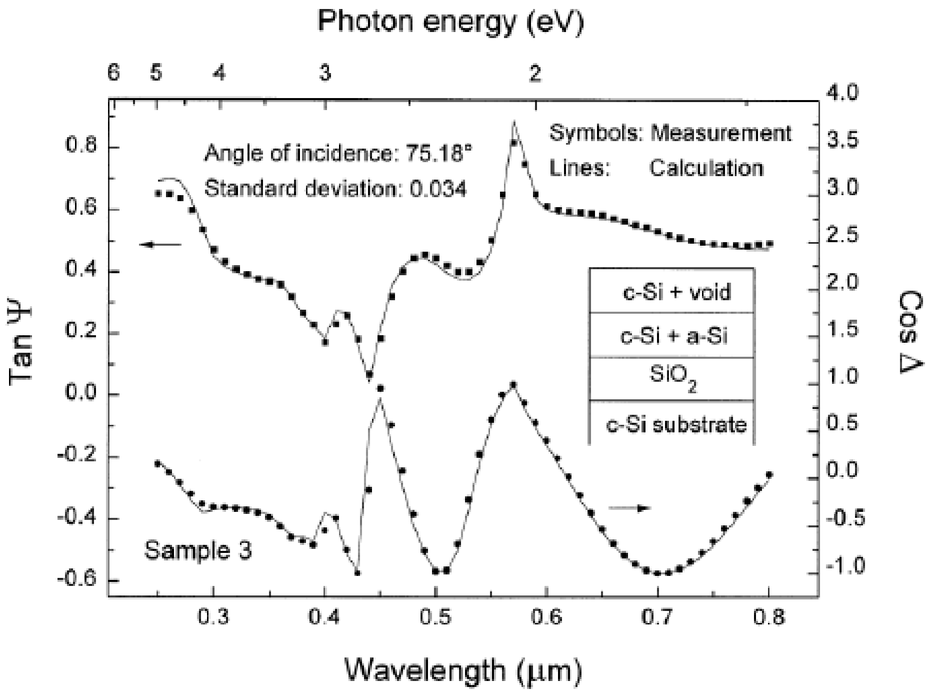

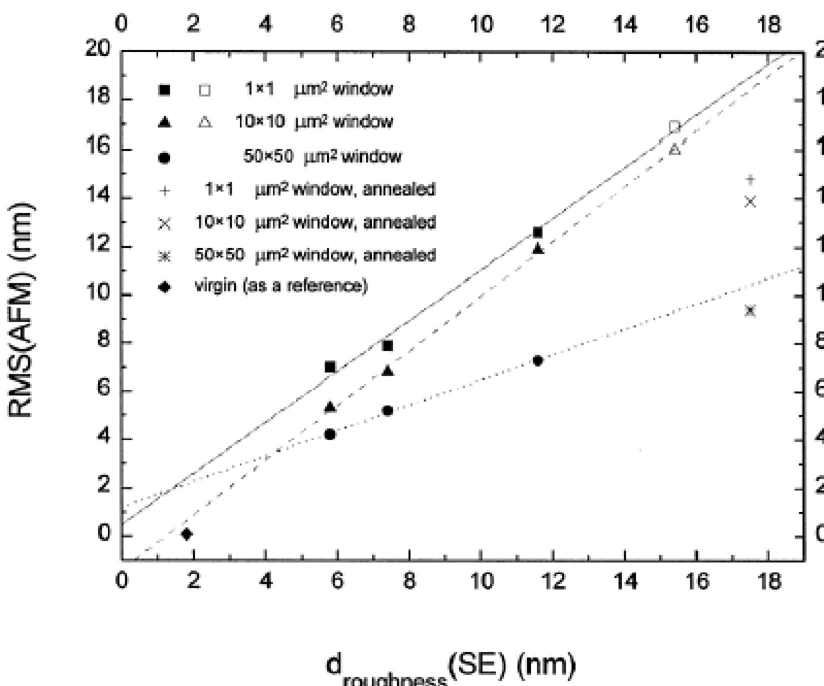

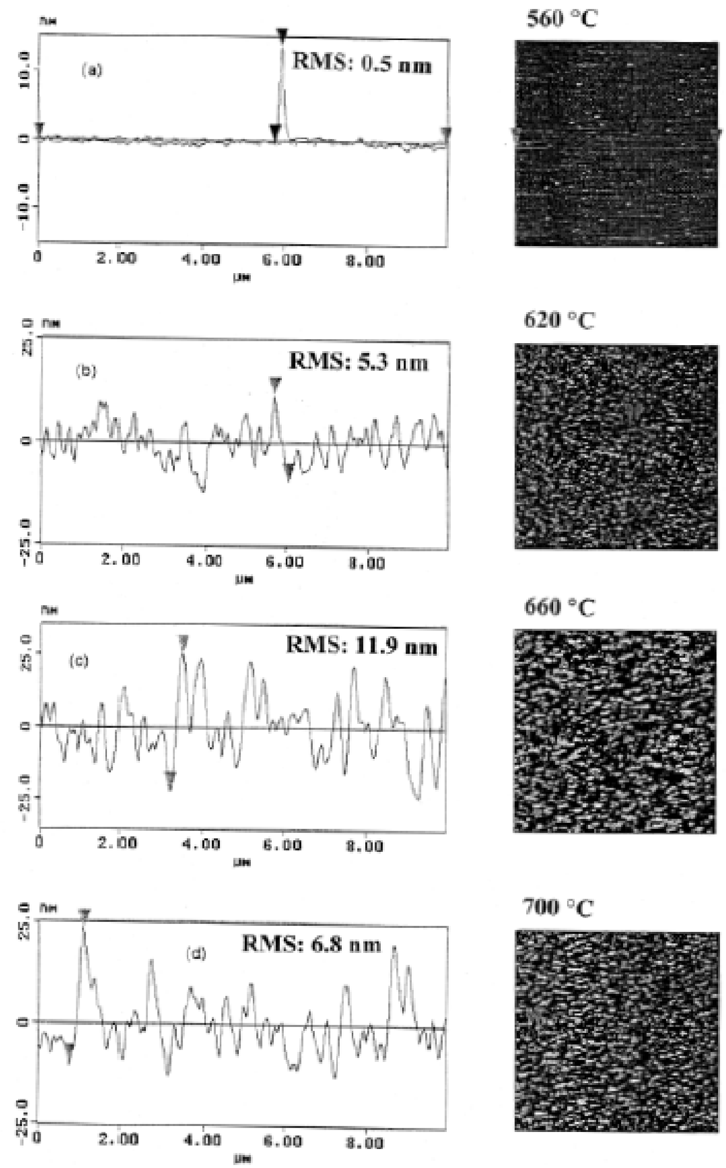

Mapping ellipsometry

Integration of spectroscopic ellipsometry in a vertical furnace

Construction of the heater with active cooling and optics for *in situ* metrology

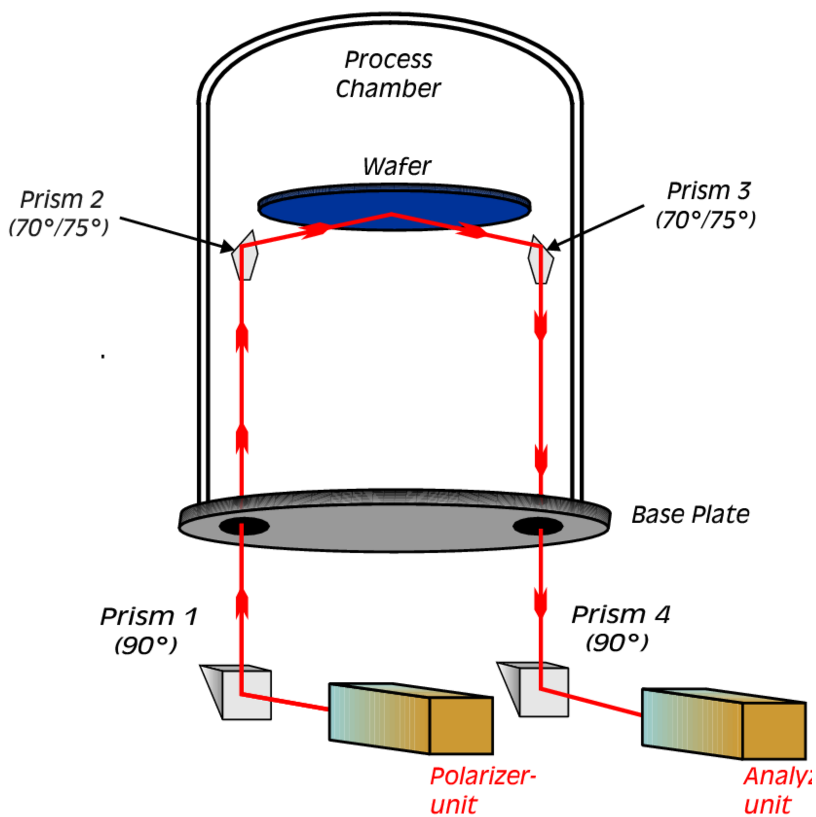

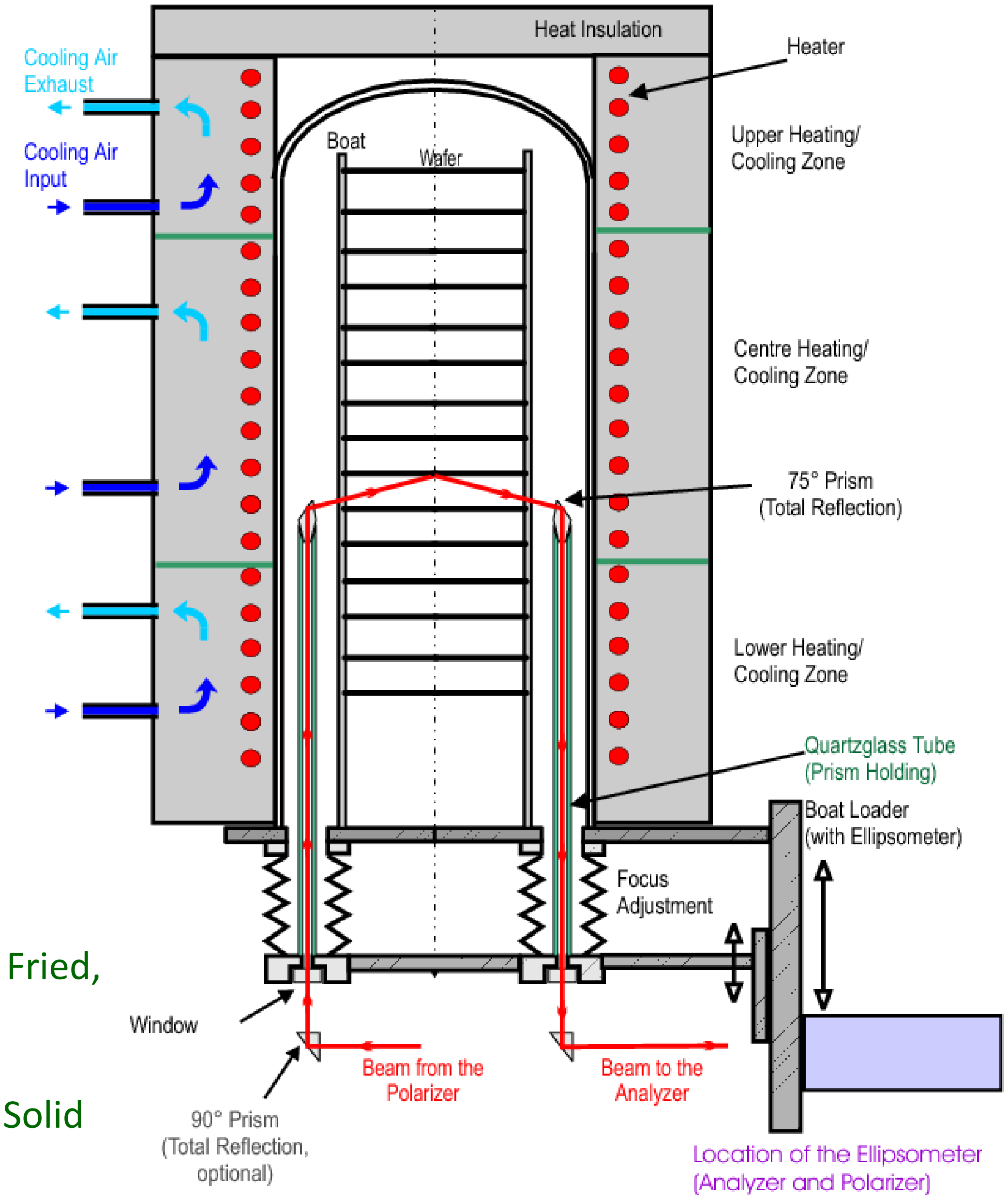

P. Petrik, W. Lehnert, C. Schneider, T. Lohner, M. Fried, J. Gyulai, H. Ryssel, "In situ measurement of the crystallization of amorphous silicon in a vertical furnace using spectroscopic ellipsometry", Thin Solid Films 383 (2001) 235.

Wide-angle ellipsometer first version: (1) point-like-source (2) light-cone (3) polarizer (4) sample, moving stage (5) analizer (6) screen+CCD-camera

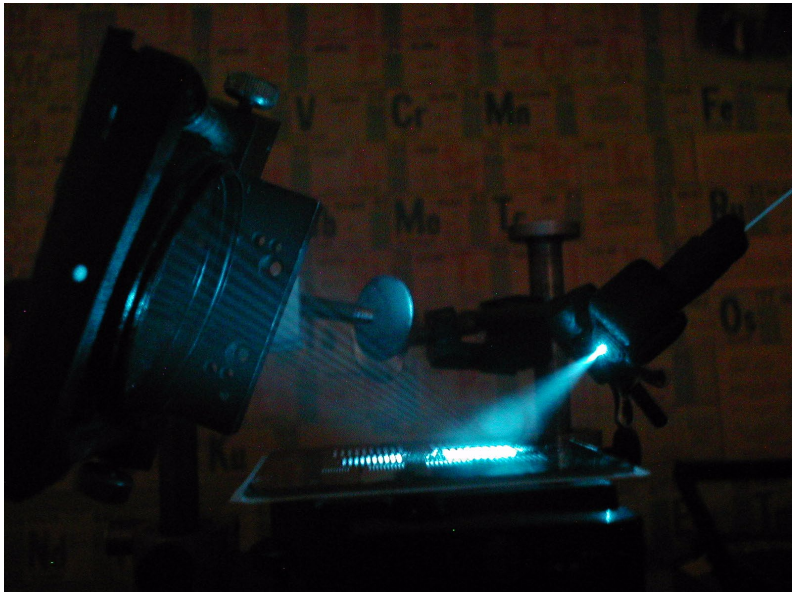

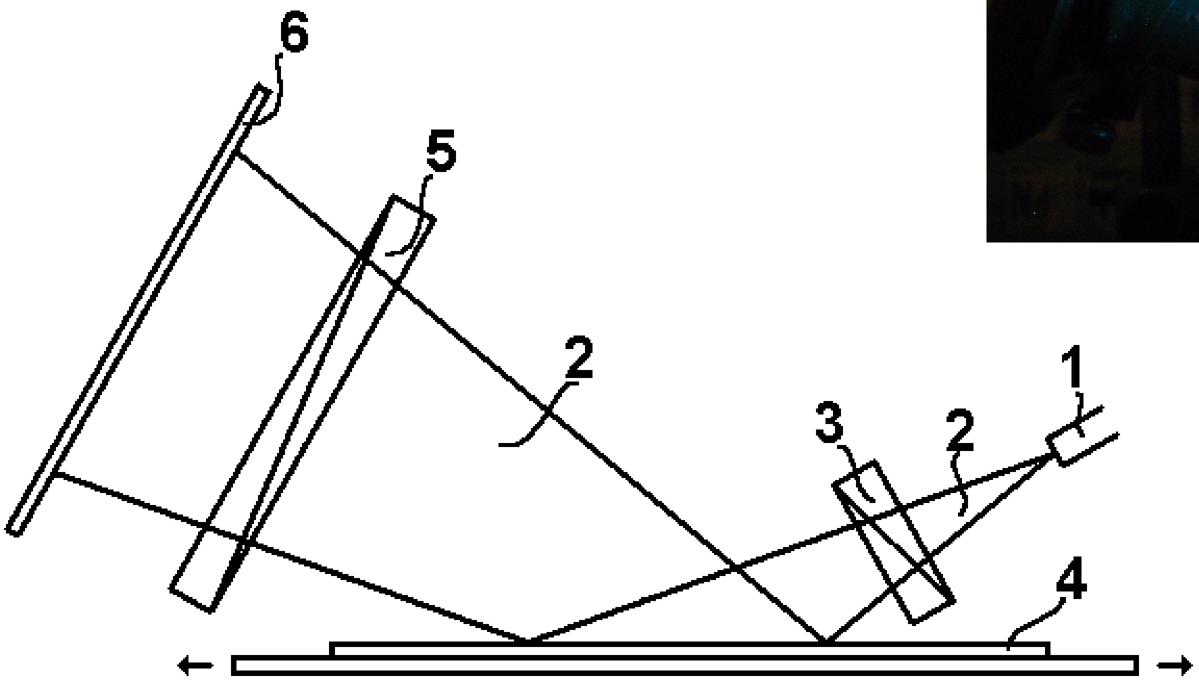

G. Juhasz, Z. Horvath, C. Major, P. Petrik, O. Polgar, M. Fried, "Non-collimated beam ellipsometry," physica status solidi c 5 (2008) 1081-1084.

“Traditional” ellipsometer (1 point)

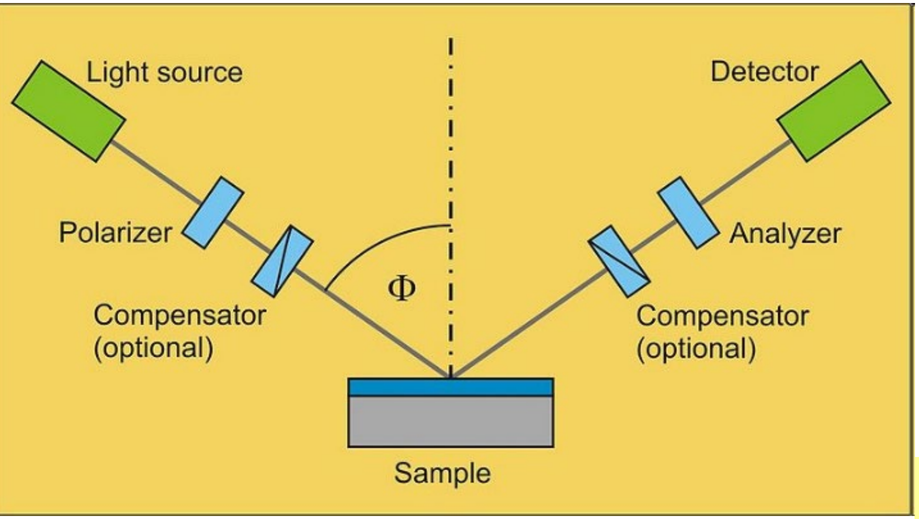

wide-angle ellipsometer ver.1

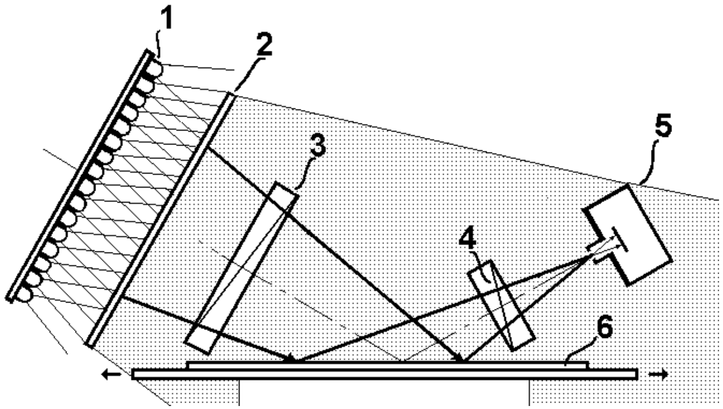

(1) Light-source (LED-panel) (2) diffusor (3) film-polarizer
(4) analyzer (6) sample (5) detector (pin-hole+CCD-detector)

“Imaging” or microscope ellipsometer

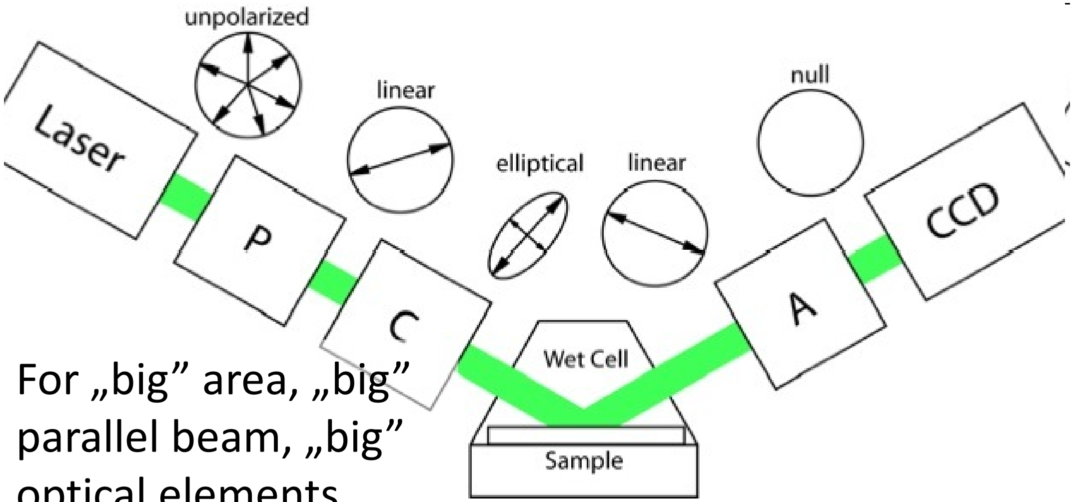

For „big” area, „big” parallel beam, „big” optical elements

„Macroscope”

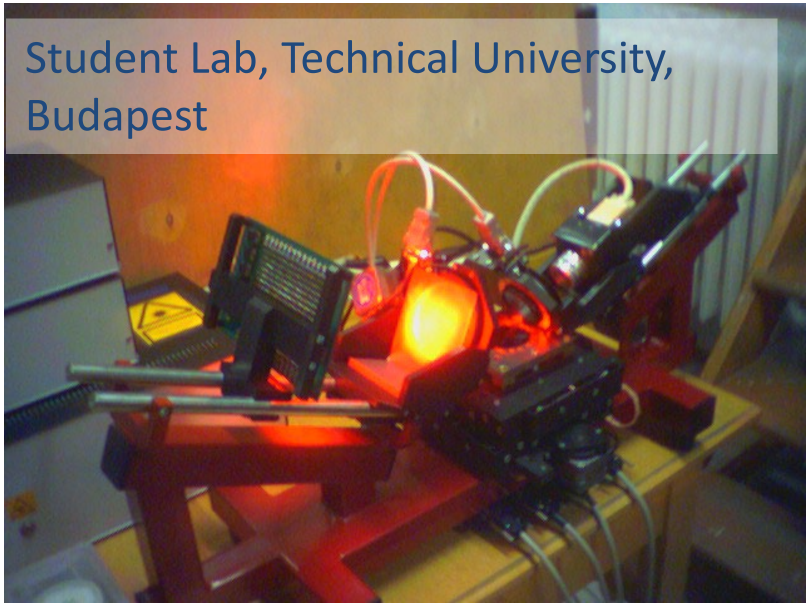

- Student Lab, Technical University, Budapest

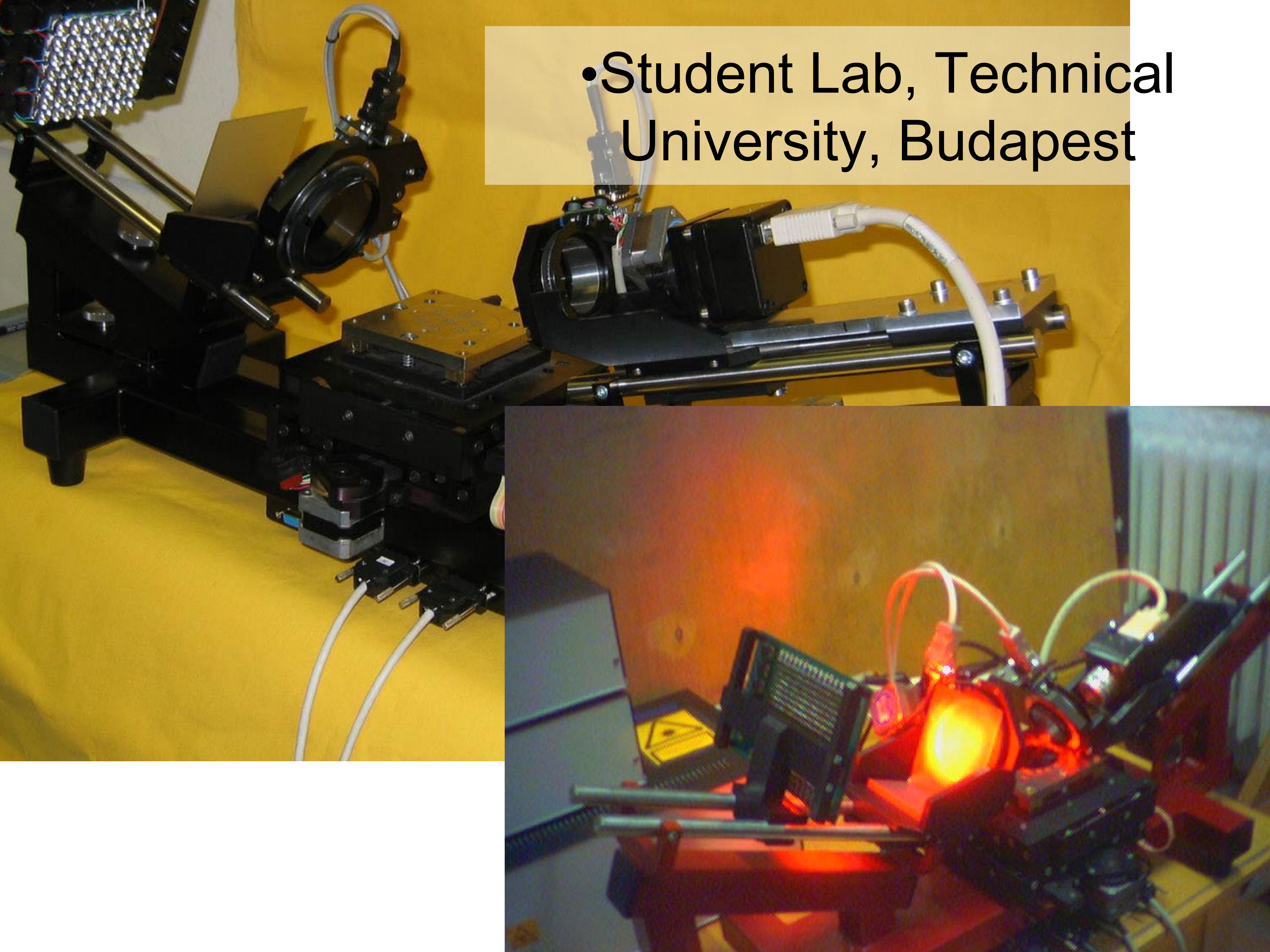

Application on large surface (ver. 2)

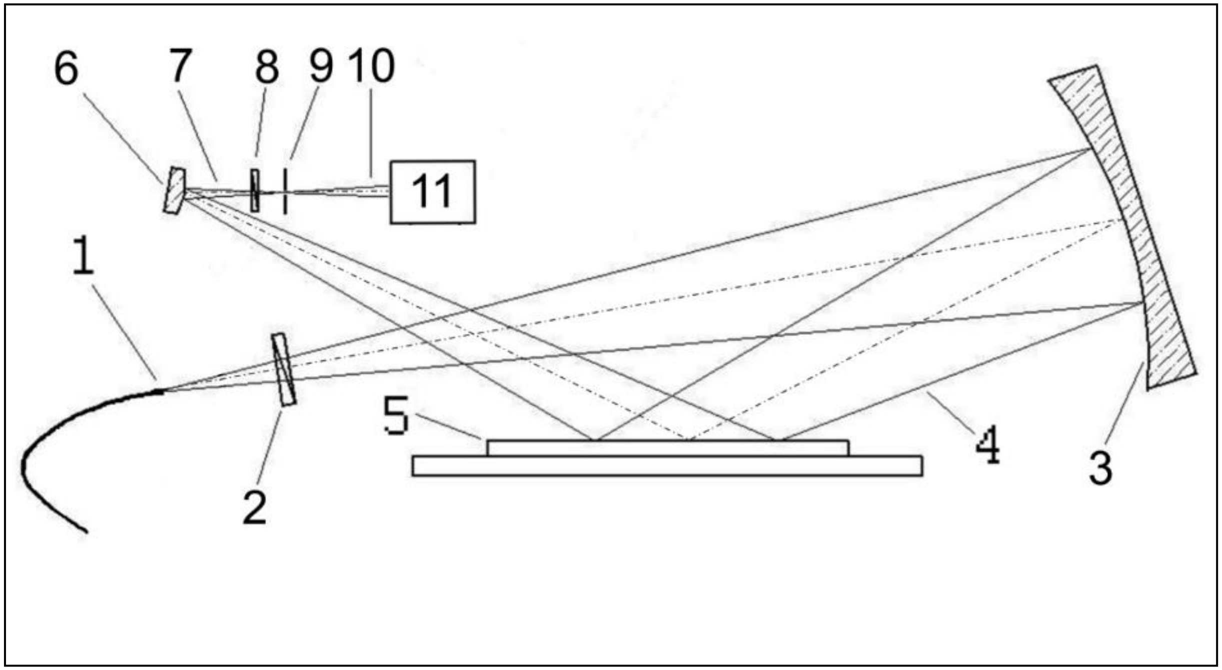

(1) Source, (2) polarizer, (3) spherical mirror, (4) convergent beam, (5) sample, (6) cylindrical (correction) mirror, (7) corrected beam, (8) analyzer, (9) pin-hole, (10) beam, (11) CCD

M. Fried, G. Juhász, C. Major, P. Petrik, O. Polgár, Z. Horváth, A. Nutsch, "Expanded beam (macro-imaging) ellipsometry", Thin Solid Films 519 (2011) 2730.

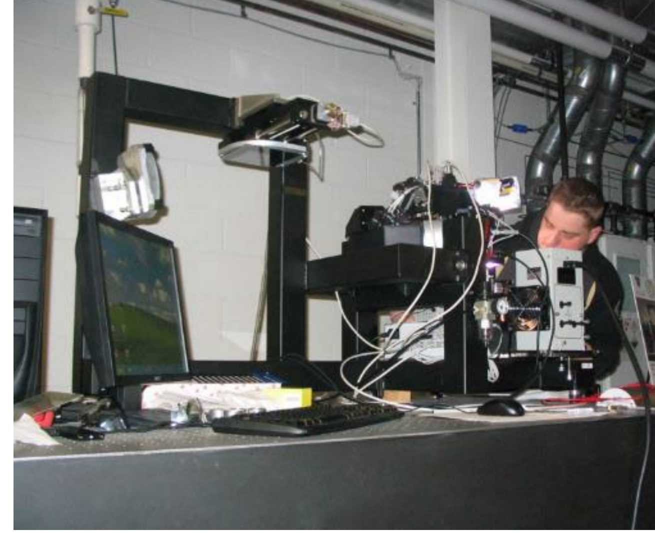

AccuMap MCS-23

thickness map [nm]

Expanded-Beam SE

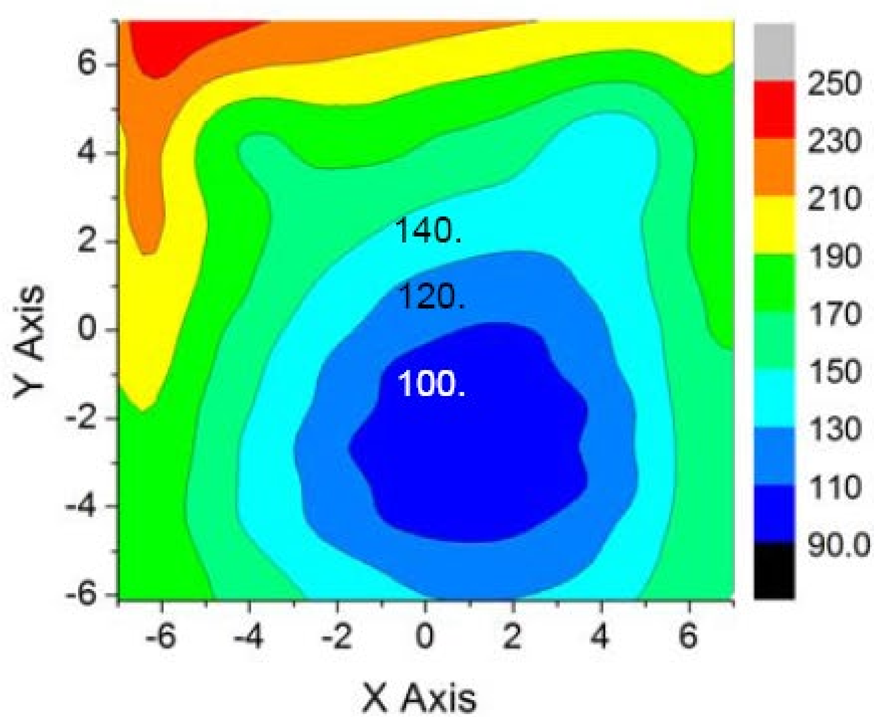

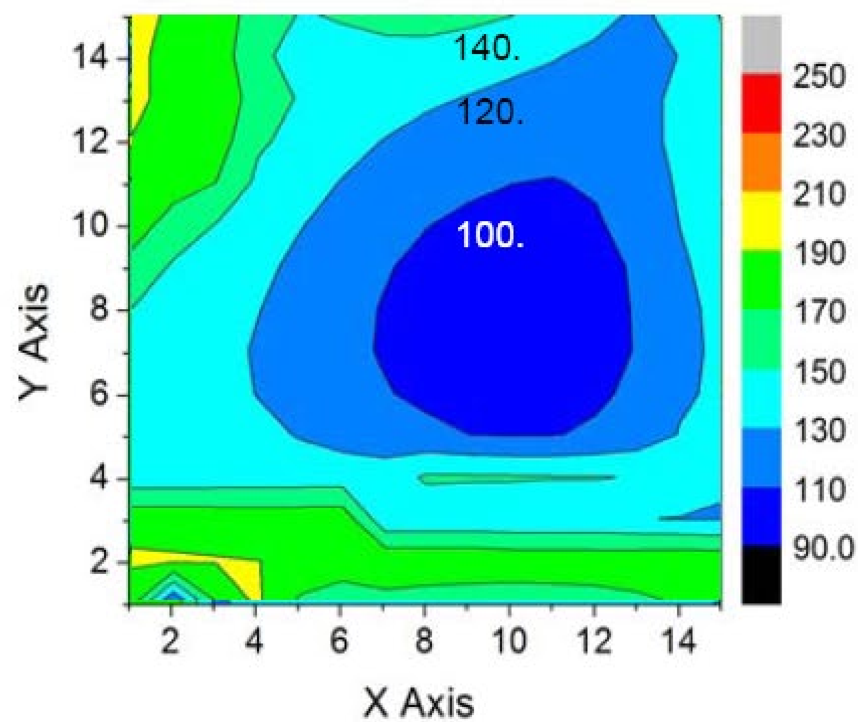

Psi-map of (nominally 110 nm) SiO_2/Si wafer

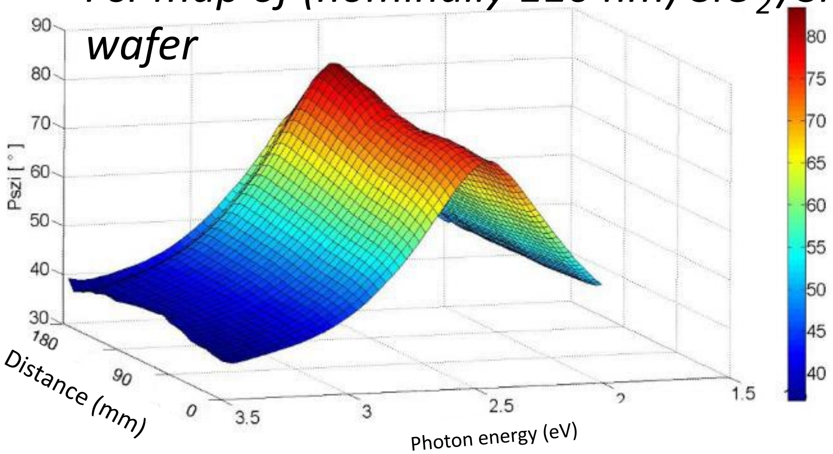

Moving the sample (wafer, panel, rolling foil) we get a map!

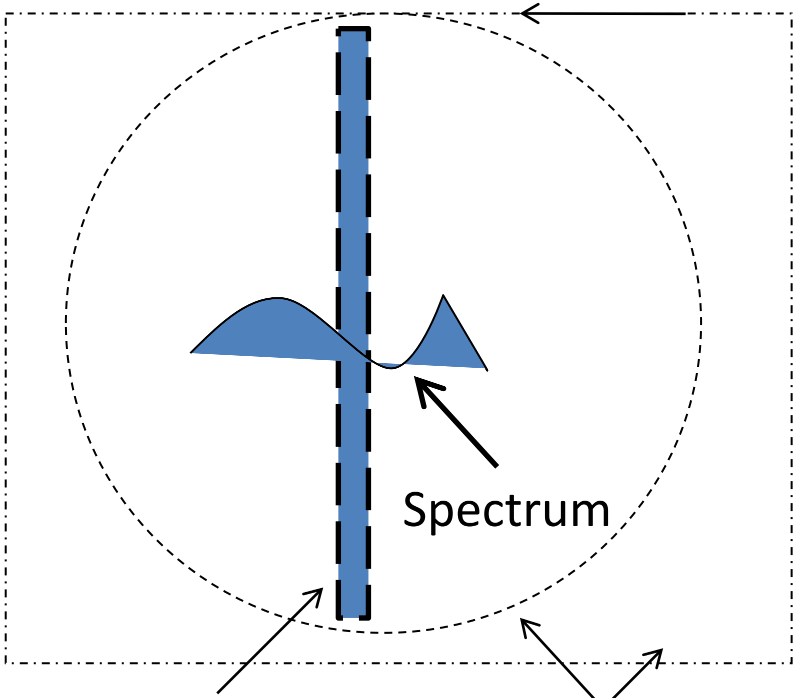

What is seen on the CCD-matrix?

5/10 mm periodic change (mask)

Test of the lateral & spectral resolution

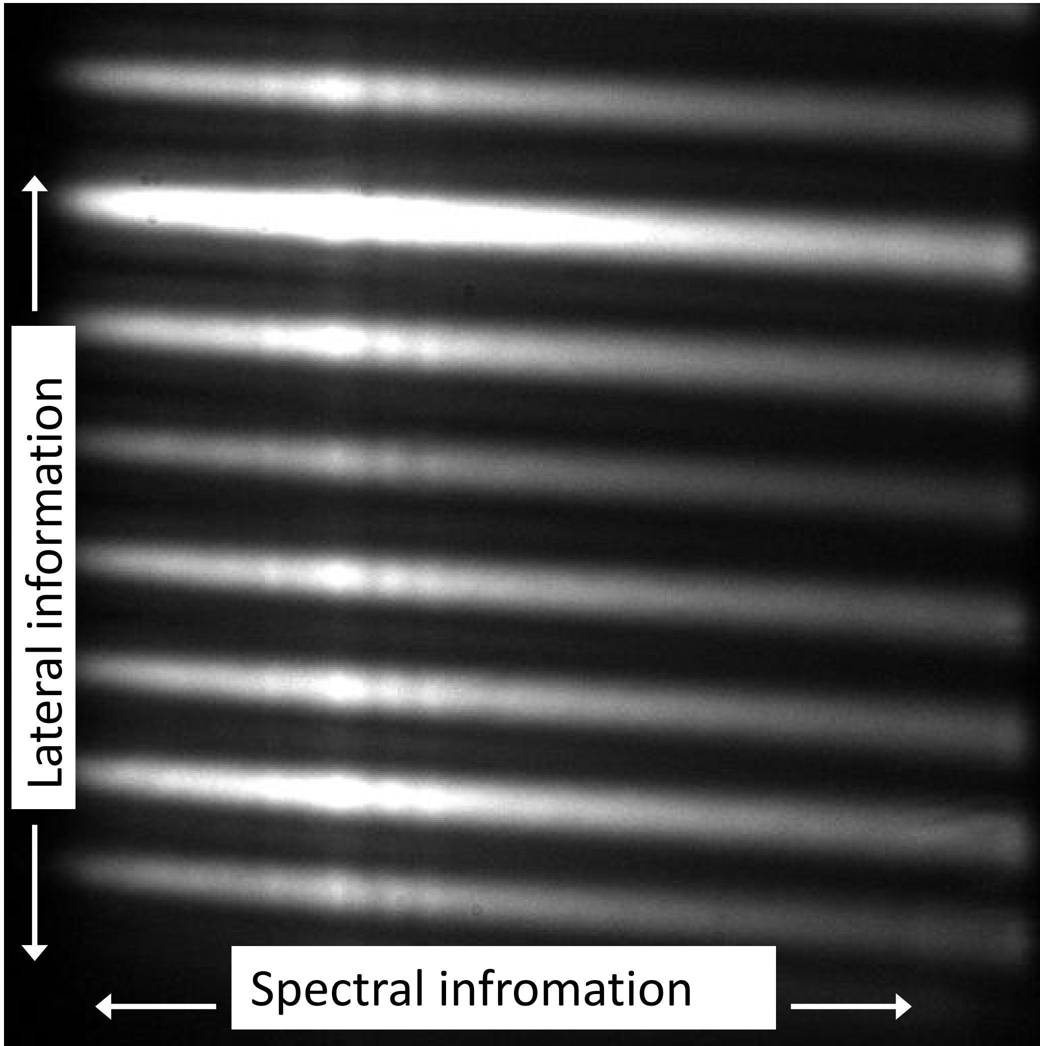

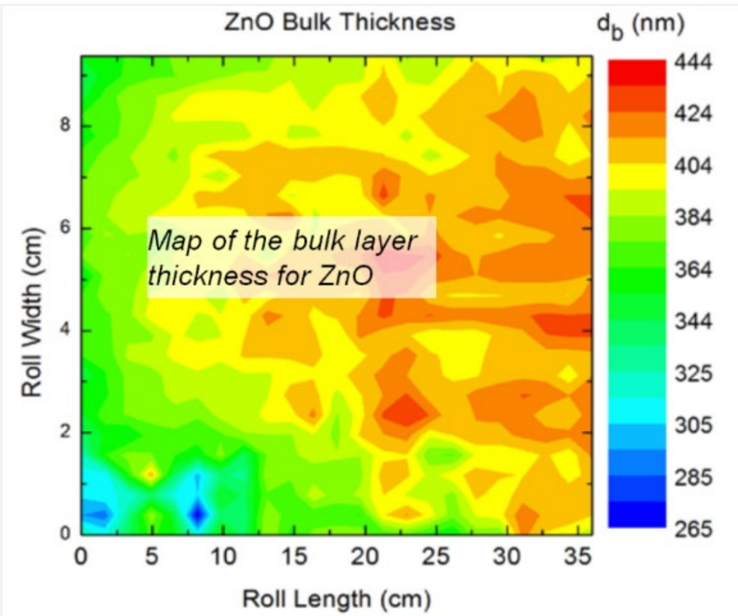
ZnO Bulk Thickness
d_b (nm)
444
424
404
384
364
344
325
305
285
265
Map of the bulk layer thickness for ZnO
Roll Width (cm)
Roll Length (cm)
0
2
4
6
8
0 5 10 15 20 25 30 35

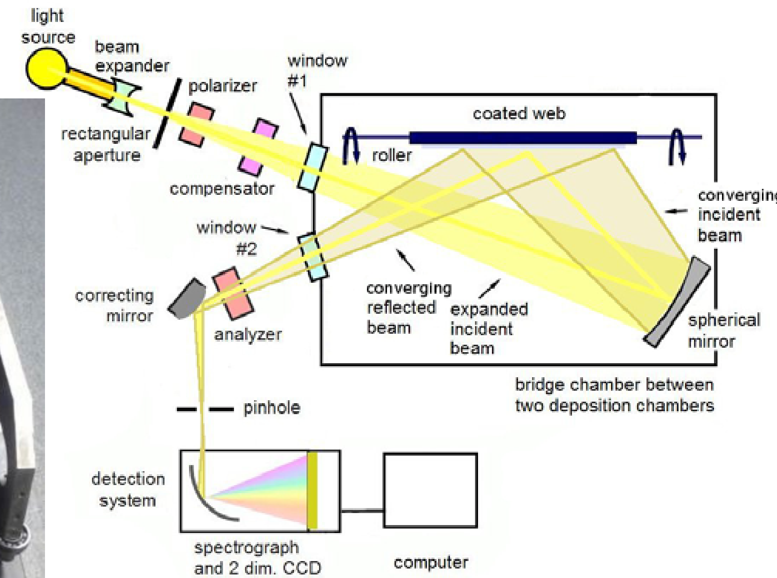
light source
beam expander
rectangular aperture
polarizer
compensator
window #1
coated web
roller
window #2
converging incident beam
converging reflected beam
expanded incident beam
correcting mirror
analyzer
spherical mirror
bridge chamber between two deposition chambers
pinhole
detection system
spectrograph and 2 dim. CCD
computer

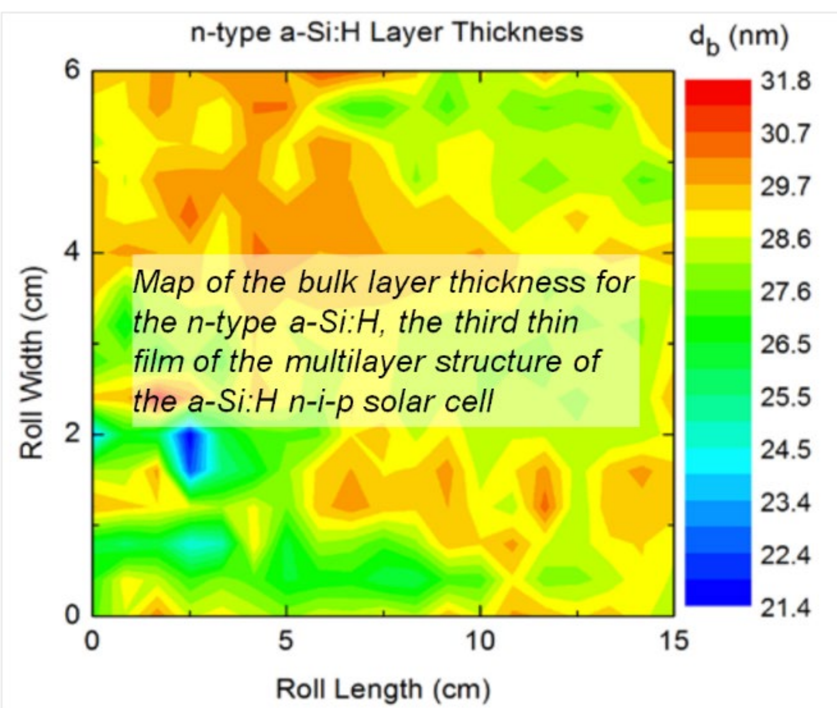
n-type a-Si:H Layer Thickness
d_b (nm)
31.8
30.7
29.7
28.6
27.6
26.5
25.5
24.5
23.4
22.4
21.4
Map of the bulk layer thickness for the n-type a-Si:H, the third thin film of the multilayer structure of the a-Si:H n-i-p solar cell
Roll Width (cm)
Roll Length (cm)
0
2
4
6
0 5 10 15

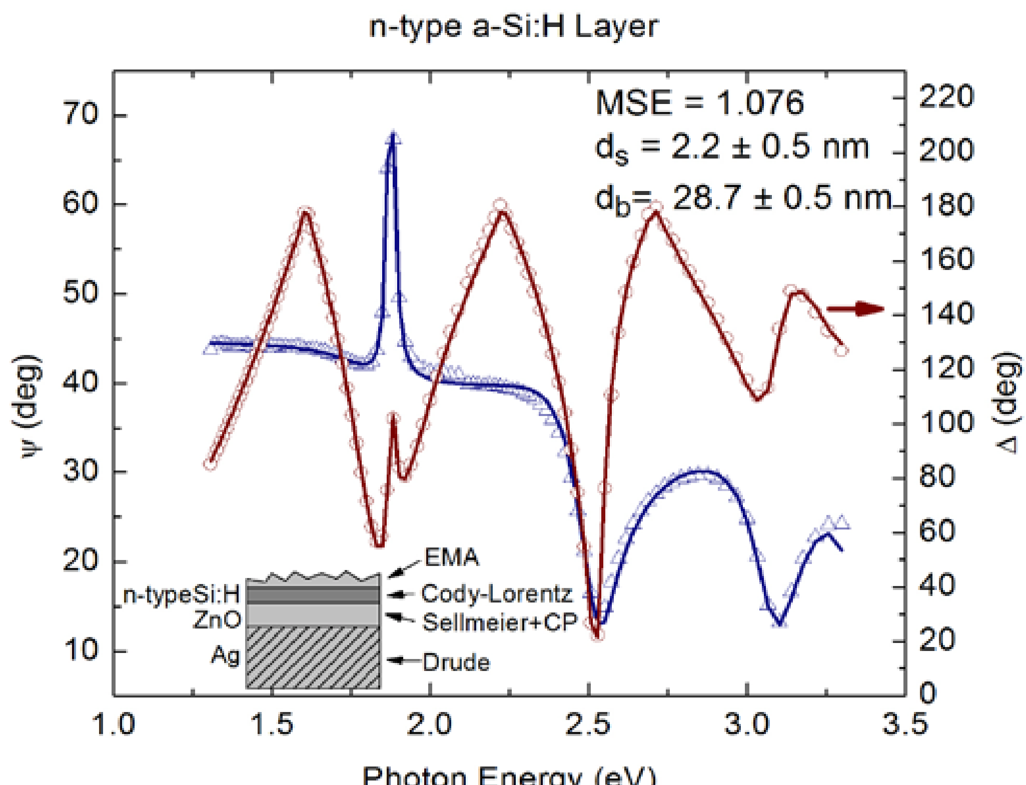
n-type a-Si:H Layer
MSE = 1.076
d_s = 2.2 ± 0.5 nm
d_b= 28.7 ± 0.5 nm
ψ (deg)
Δ (deg)
Photon Energy (eV)
10 20 30 40 50 60 70
0 20 40 60 80 100 120 140 160 180 200 220
1.0 1.5 2.0 2.5 3.0 3.5
EMA
n-typeSi:H
Cody-Lorentz
ZnO
Sellmeier+CP
Ag
Drude

•3 prototypes of expanded beam mapping spectroscopic ellipsometer

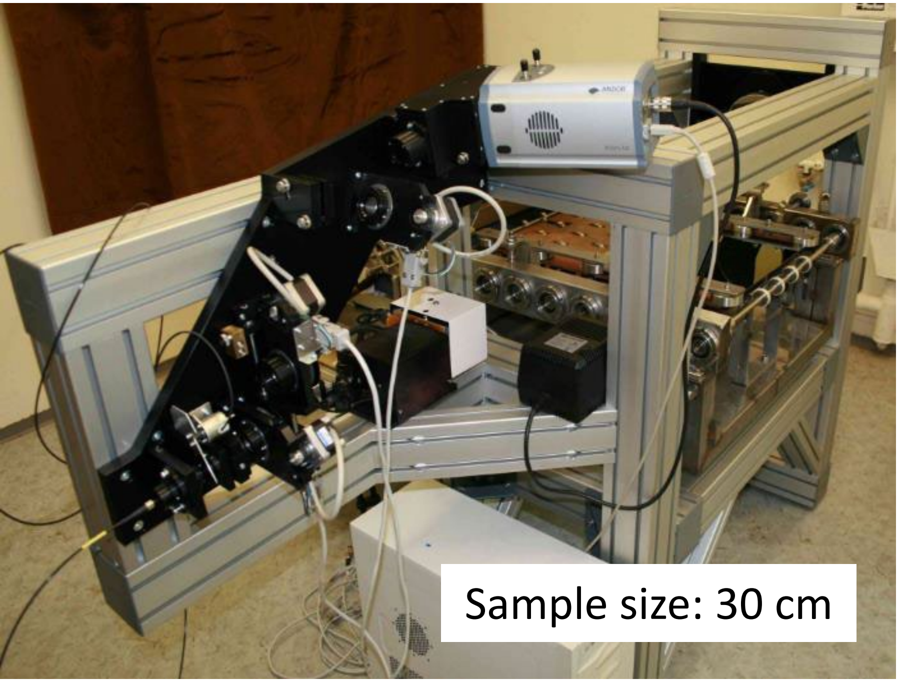

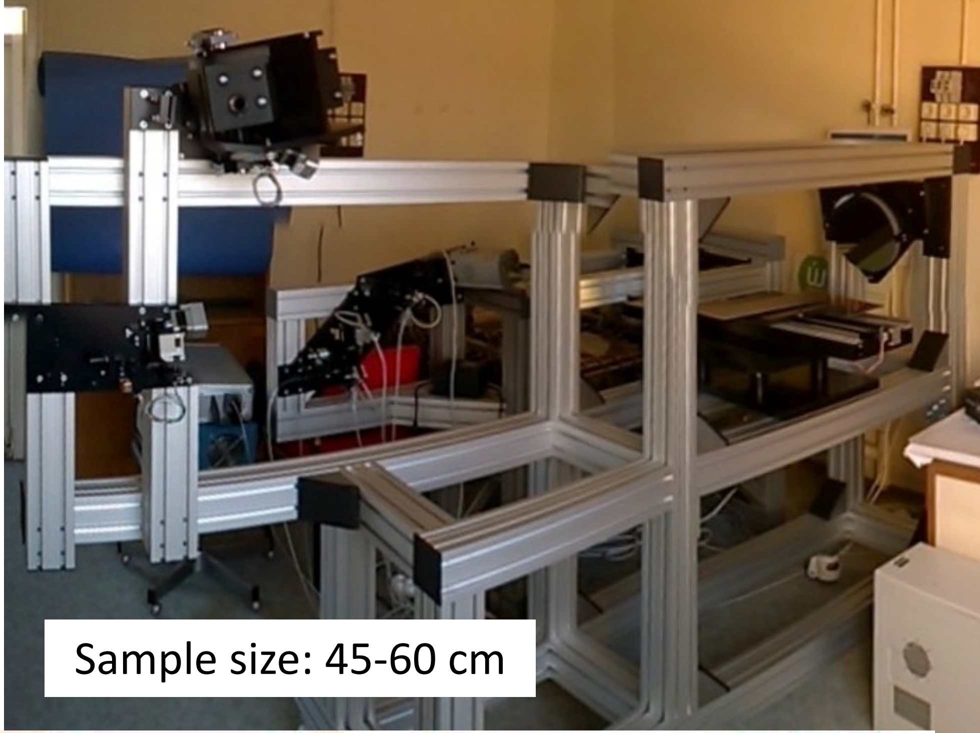

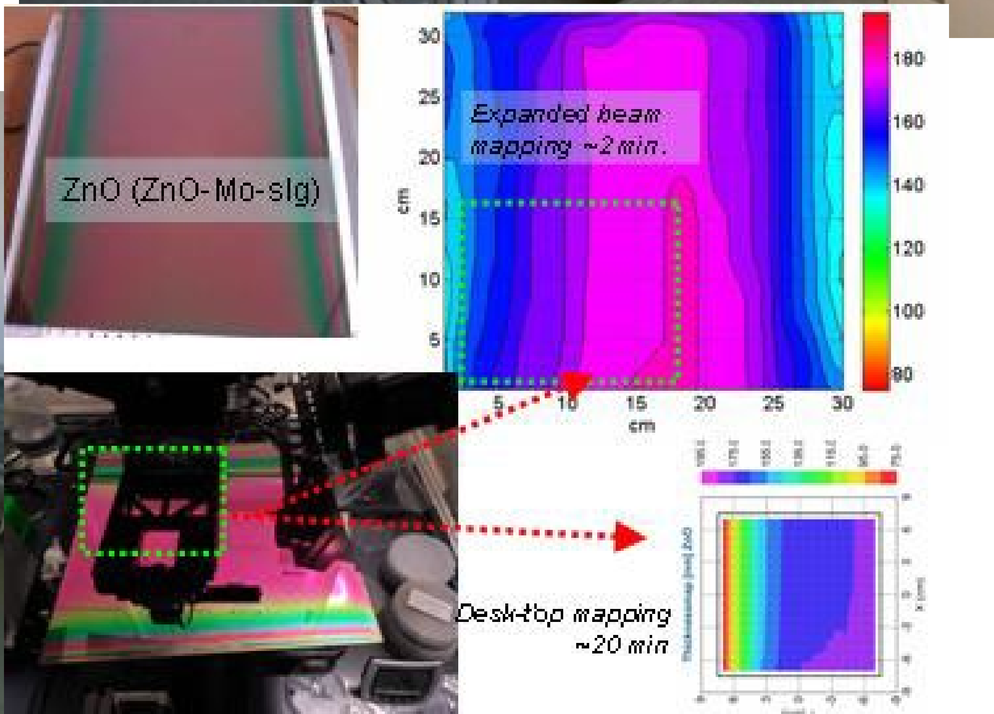

Mapping using complex models (a-Si/Al/Glass[subs.])

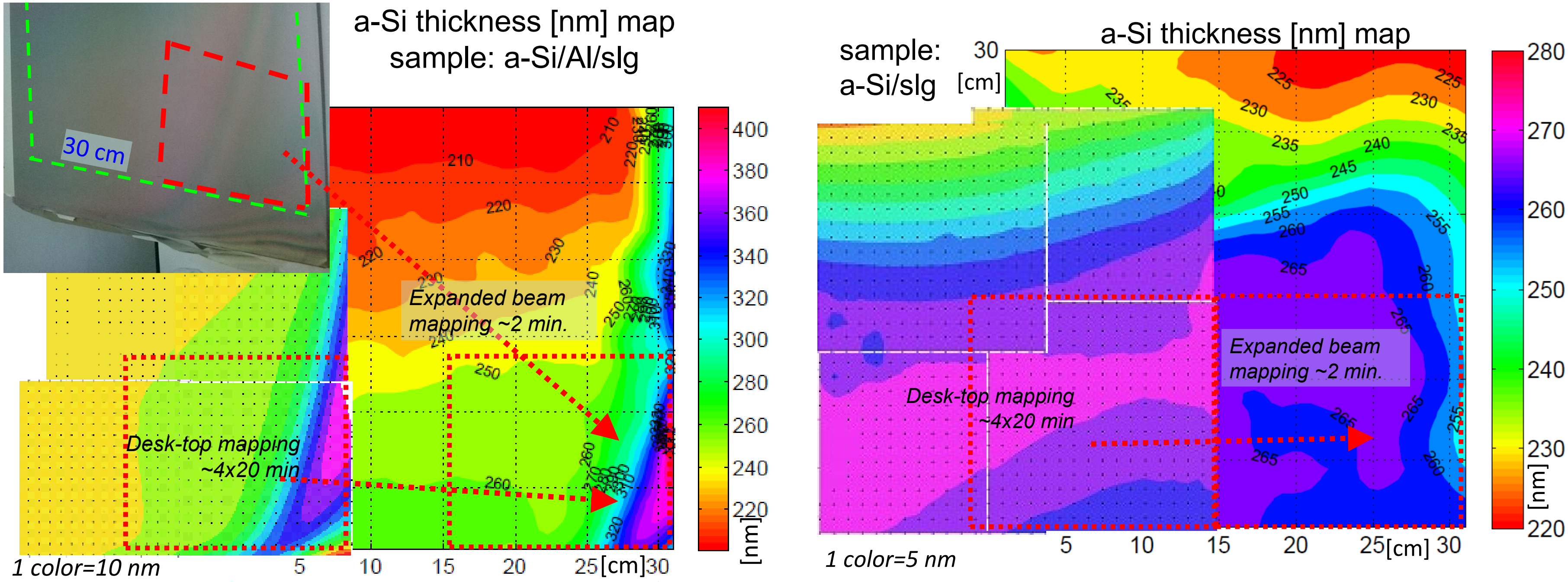

Thickness-maps of a-Si layers on 30x30 cm^2 a-Si/Al/glass (left) and a-Si/glass (right) samples by the 30 cm wide expanded beam device and by a commercial ellipsometer. 1 color = 10 nm. Maps by the commercial ellipsometer are merged from 4 independent 15x15 cm^2 maps (dashed rectangulars).

•The prototype is installed on the experimental vacuum chamber of the PhotoVoltaic Innovation and Commercialization Center at University of Toledo (Ohio).

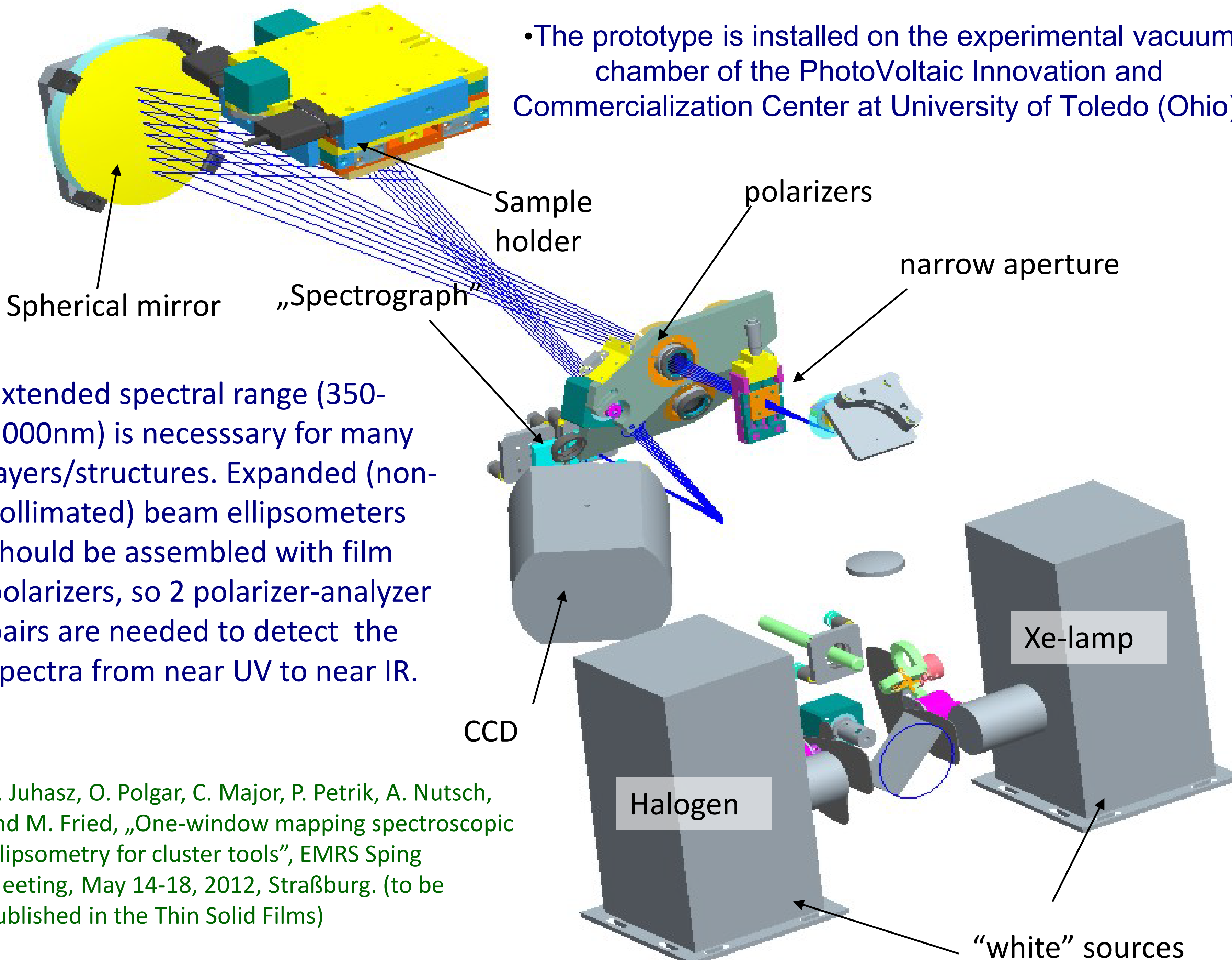

Extended spectral range (350-1000nm) is necesssary for many layers/structures. Expanded (non-collimated) beam ellipsometers should be assembled with film polarizers, so 2 polarizer-analyzer pairs are needed to detect the spectra from near UV to near IR.

G. Juhasz, O. Polgar, C. Major, P. Petrik, A. Nutsch, and M. Fried, „One-window mapping spectroscopic ellipsometry for cluster tools", EMRS Sping Meeting, May 14-18, 2012, Straßburg. (to be published in the Thin Solid Films)

Thin film silicon PV-cluster in PVIC

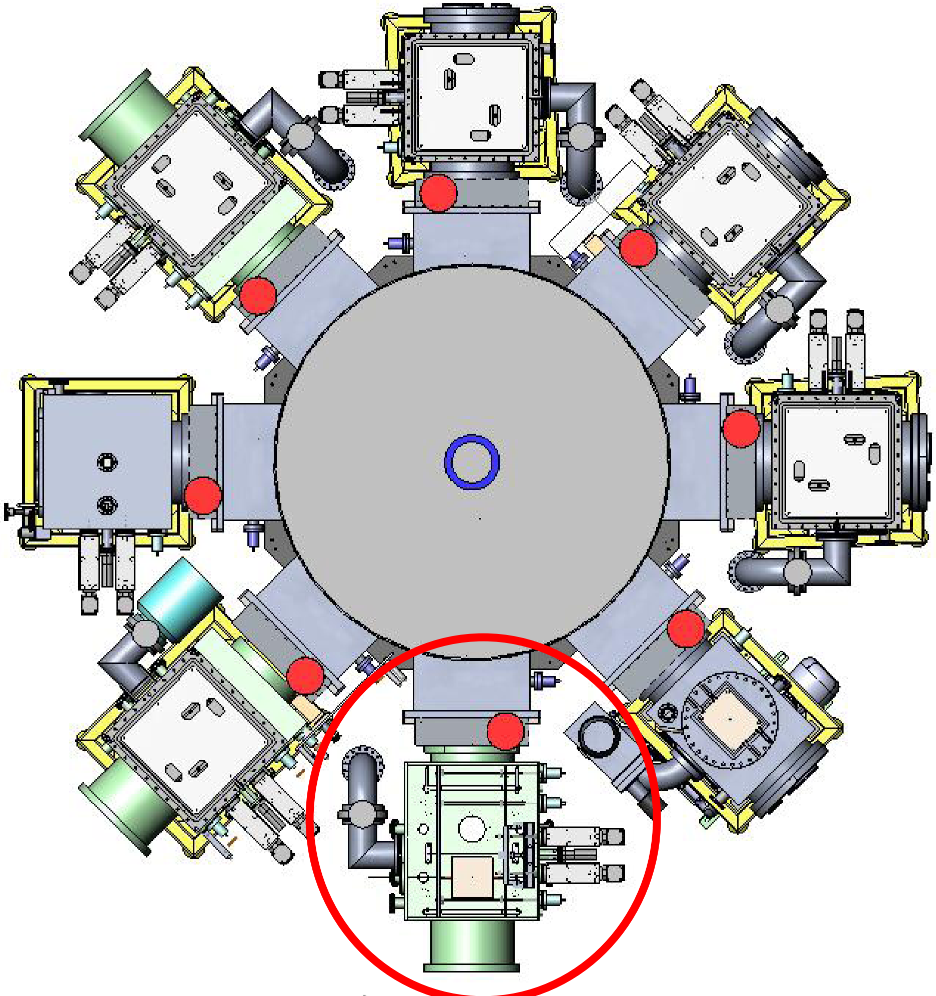

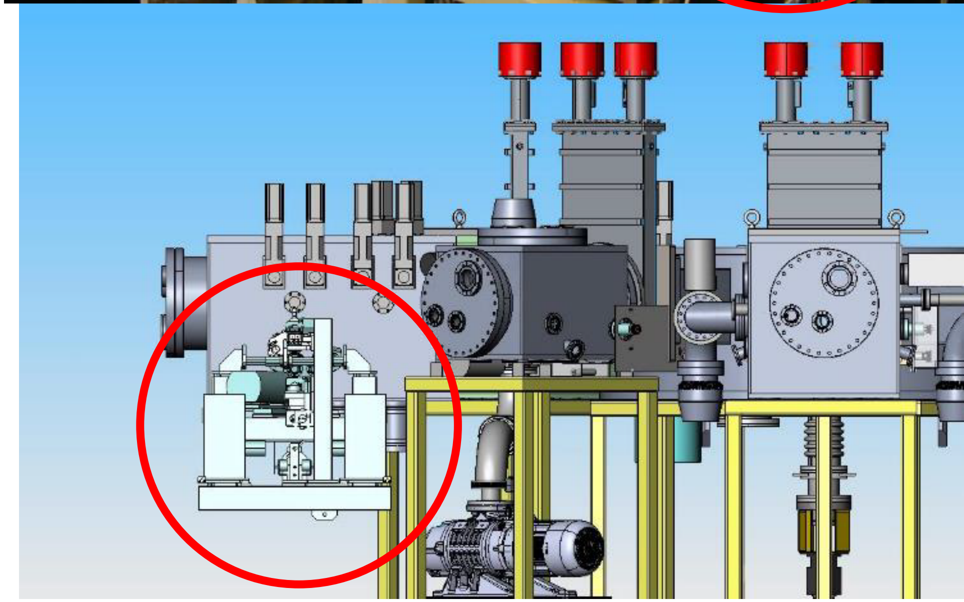

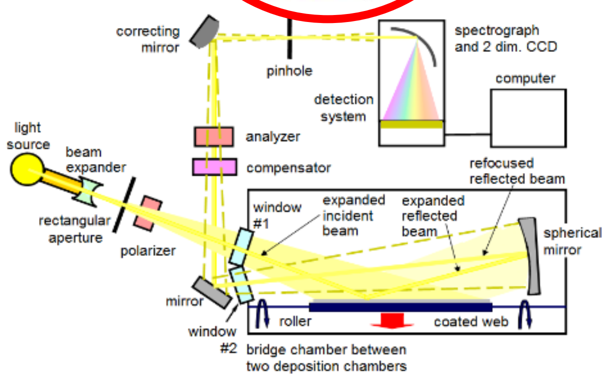

•Schematic view of the cluster integration

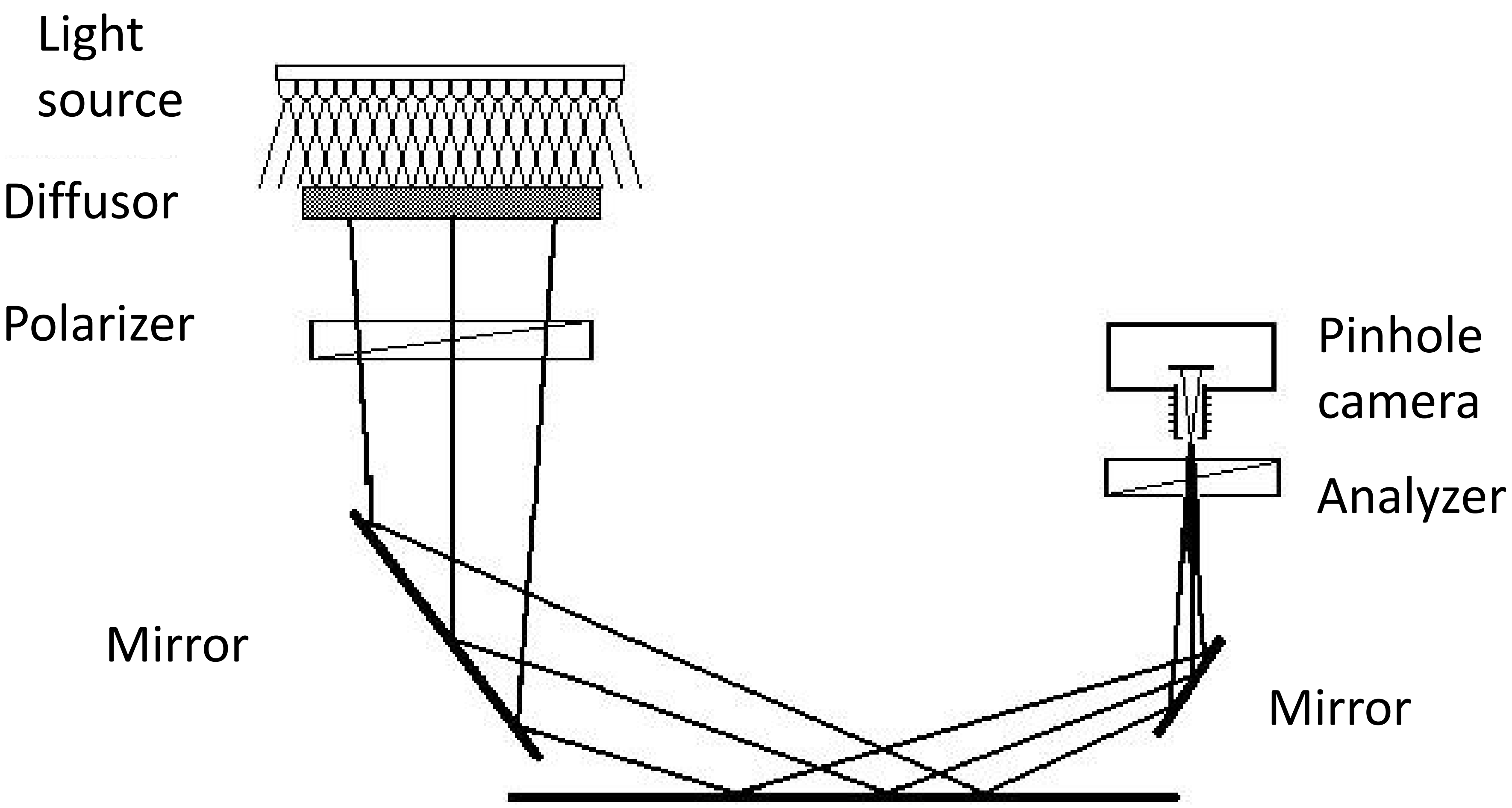

M. Fried, G. Juhász, C. Major, P. Petrik, O. Polgár, Z. Horváth, A. Nutsch, "Expanded beam (macro-imaging) ellipsometry", Thin Solid Films 519 (2011) 2730.

•New method for the integration of divergent light source ellipsometry into a cluster chamber

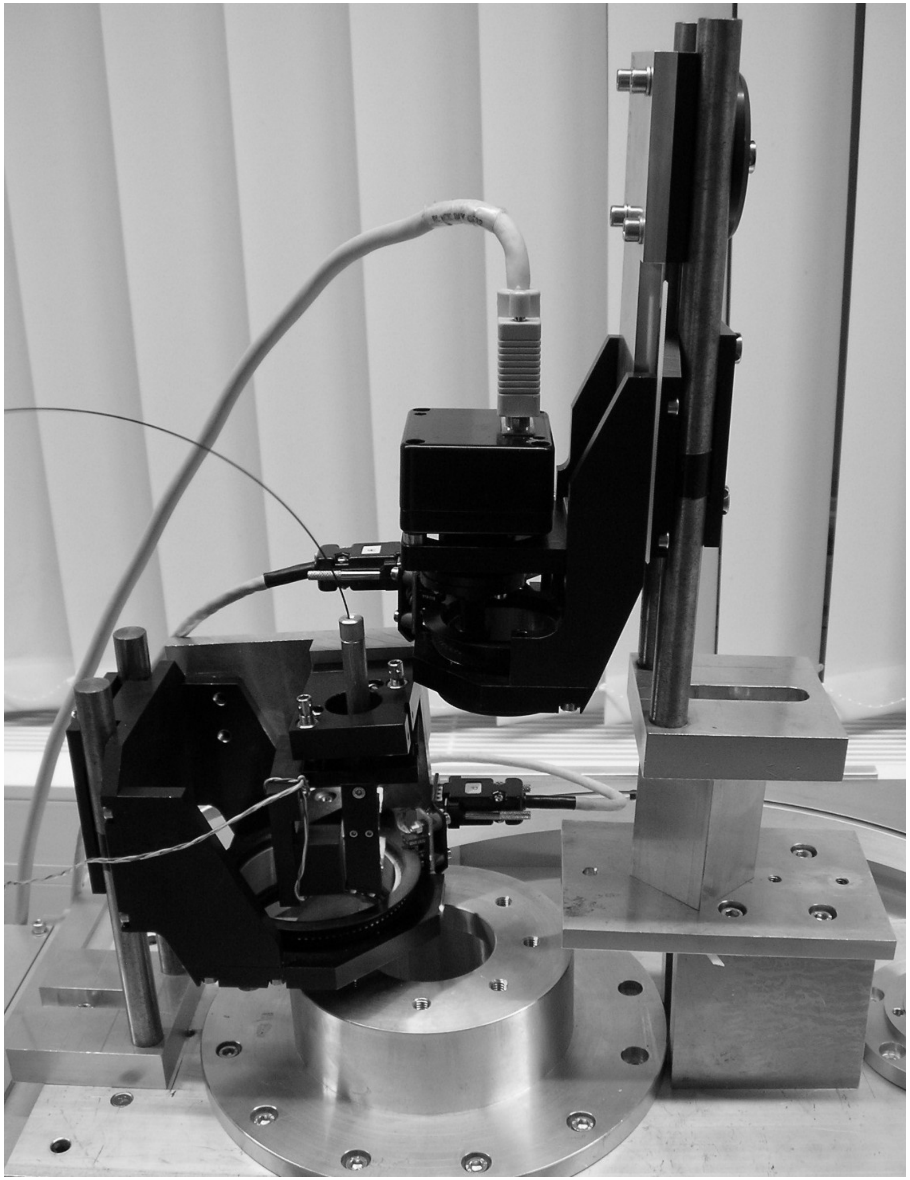

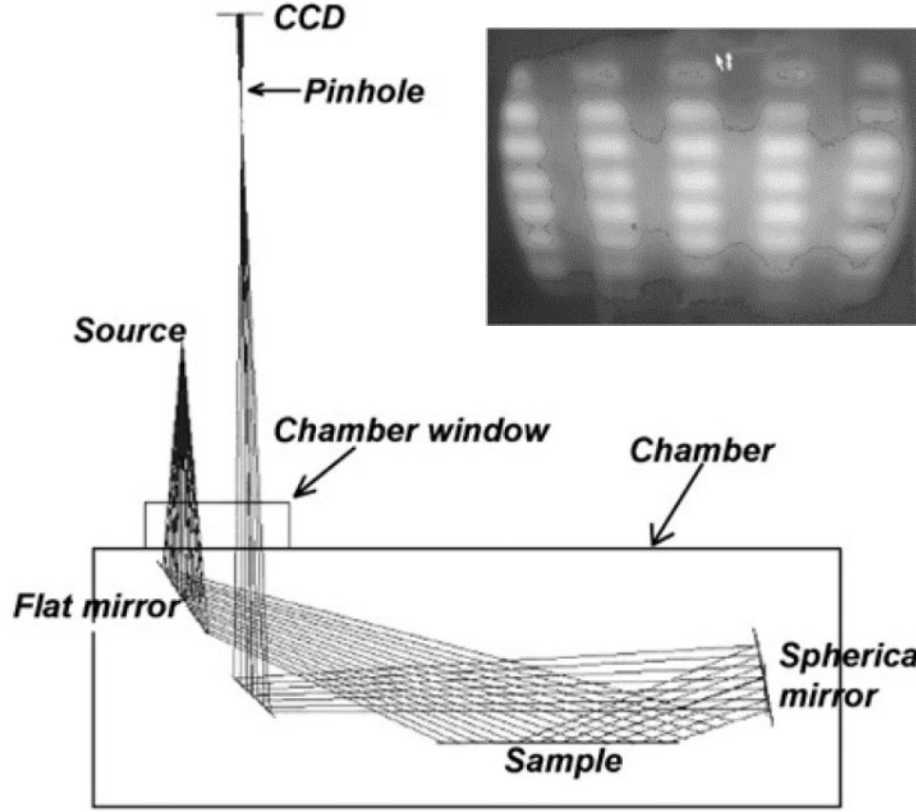

M. Fried, G. Juhász, C. Major, P. Petrik, O. Polgár, Z. Horváth, A. Nutsch, "Expanded beam (macro-imaging) ellipsometry", Thin Solid Films 519 (2011) 2730.

Nanocrystals in porous silicon

POROUS SILICON

Model	Substrate	Interface	Bulk layer	Surface	MSE
12	c-Si		d = 338.1 ± 0.1 nm c-Si + 0.43 ± 0.001 voids		27.3
13	c-Si		d = 340.1 ± 0.6 nm c-Si + 0.44 ± 0.001 voids + 0.17 ± 0.01 nc-Si		16.0
26	c-Si		d = 320.8 ± 0.9 nm c-Si + 0.46 ± 0.001 voids + 0.18 ± 0.004 nc-Si	d = 29.6 ± 1.0 nm c-Si + 0.44 ± 0.001 voids + 0.34 ± 0.01 nc-Si	11.2
39	c-Si	d = 19.1 ± 0.3 nm c-Si + 0.32 ± 0.02 voids + 2.22 ± 0.23 nc-Si	d = 313.0 ± 1.1 nm c-Si + 0.48 ± 0.001 voids + 0.21 ± 0.01 nc-Si	d = 38.0 ± 0.7 nm c-Si + 0.45 ± 0.001 voids + 0.29 ± 0.01 nc-Si	7.6

Effective Medium Approximation

R = 0.003 Ωcm

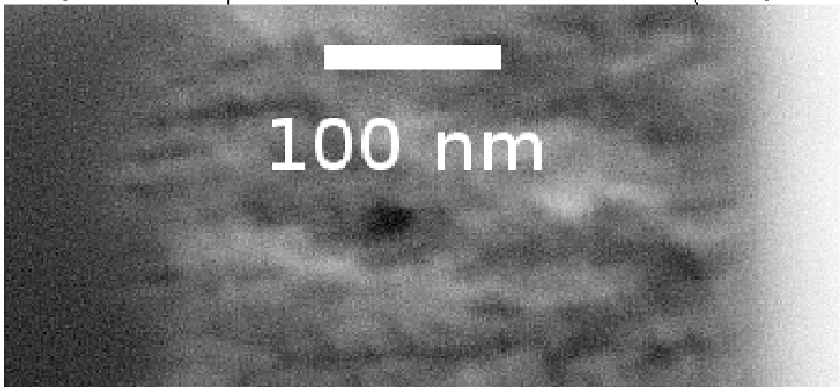

- nc-Si
- multilayer
- confidence

Fit of porous silicon using the effective medium method

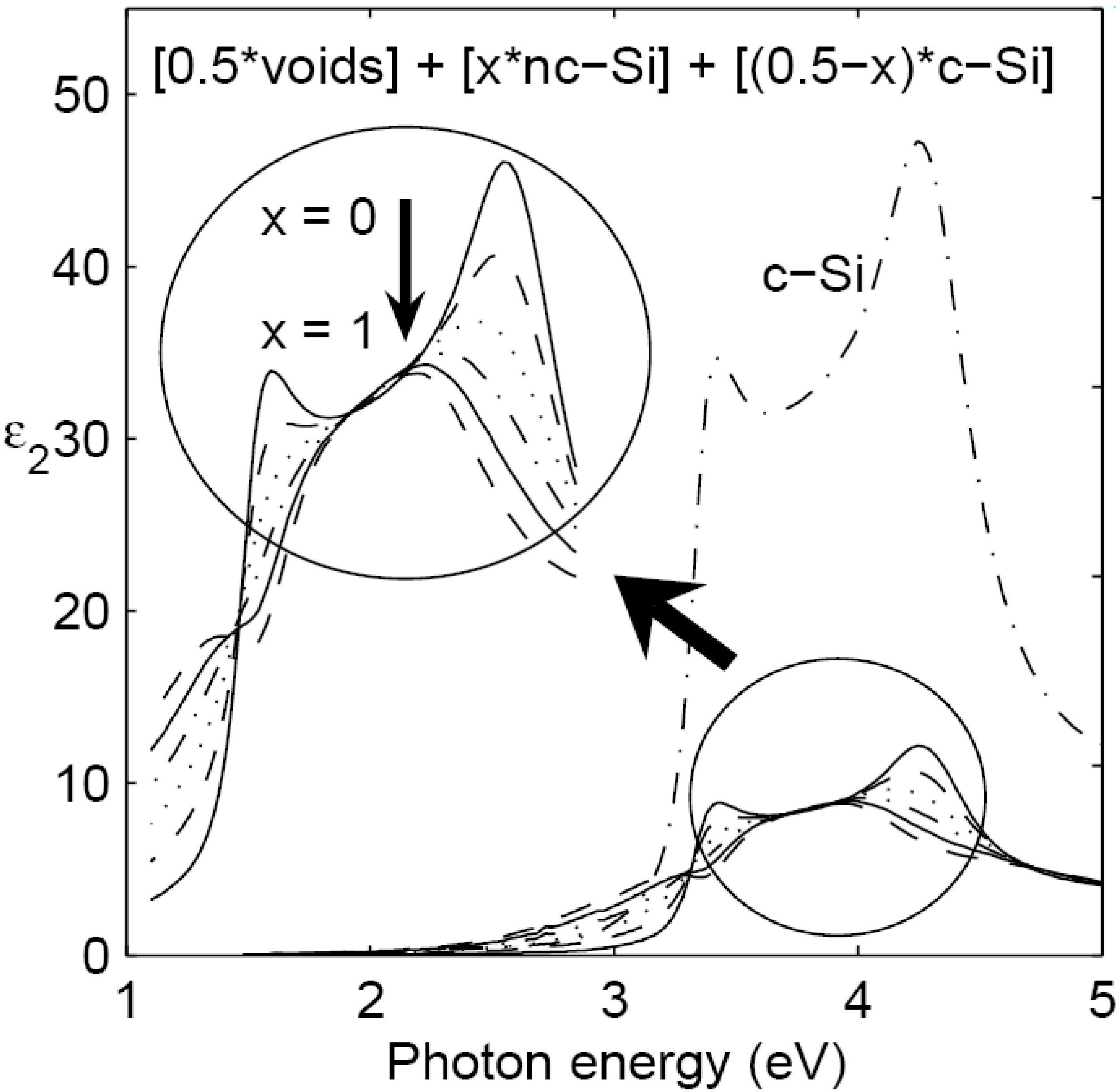

Imaginary part of dielectric function by Effective Medium Approximation

- decreasing amplitude
- red shift of peaks
- broadening

with increasing nc-Si fraction

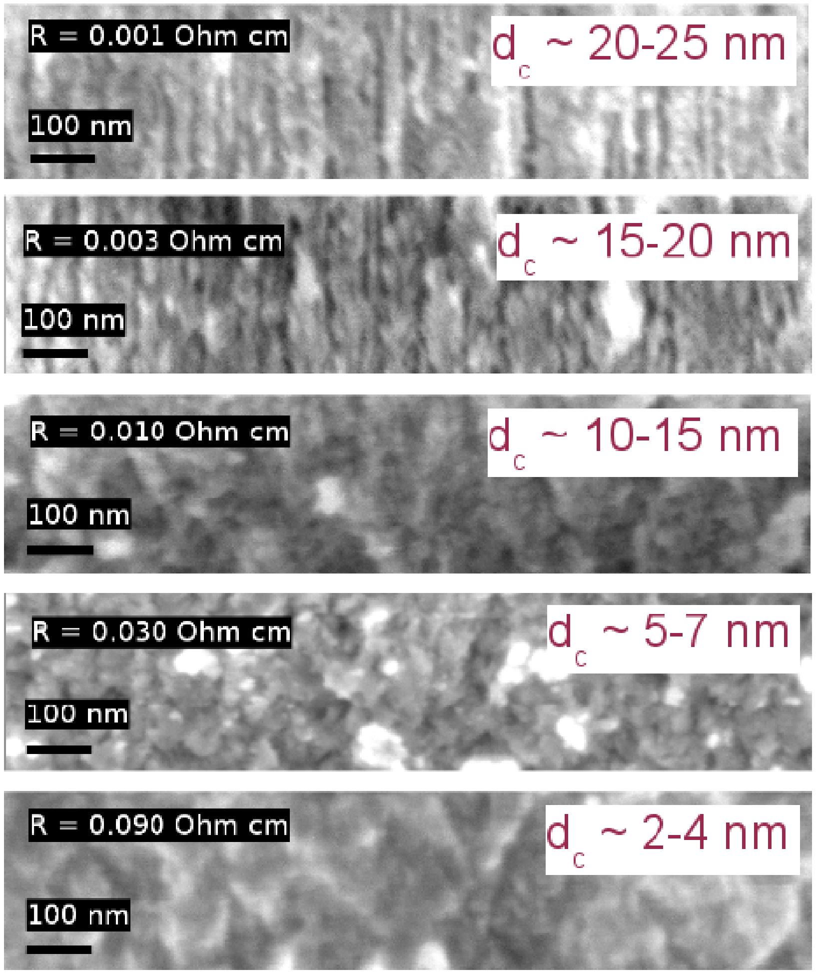

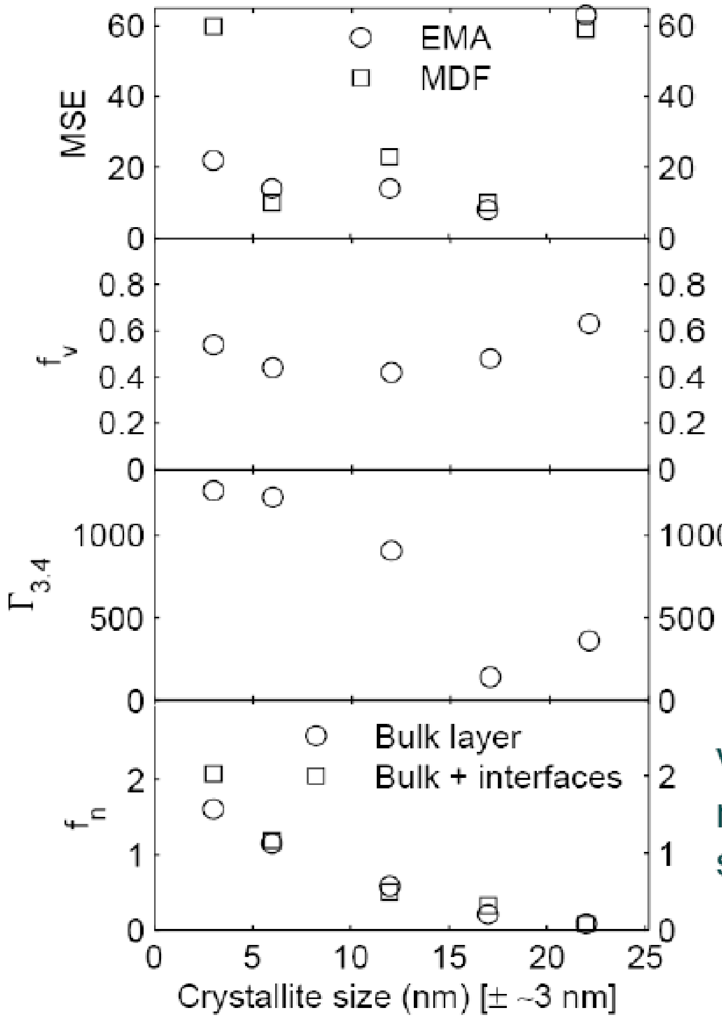

Quality of fit

Volume fraction of voids

Broadening of E_1

Volume fraction of nanocrystalline silicon

Parameterization of the dielectric function

Contributions of interband transitions to the imaginary part of the dielectric function of c-Si

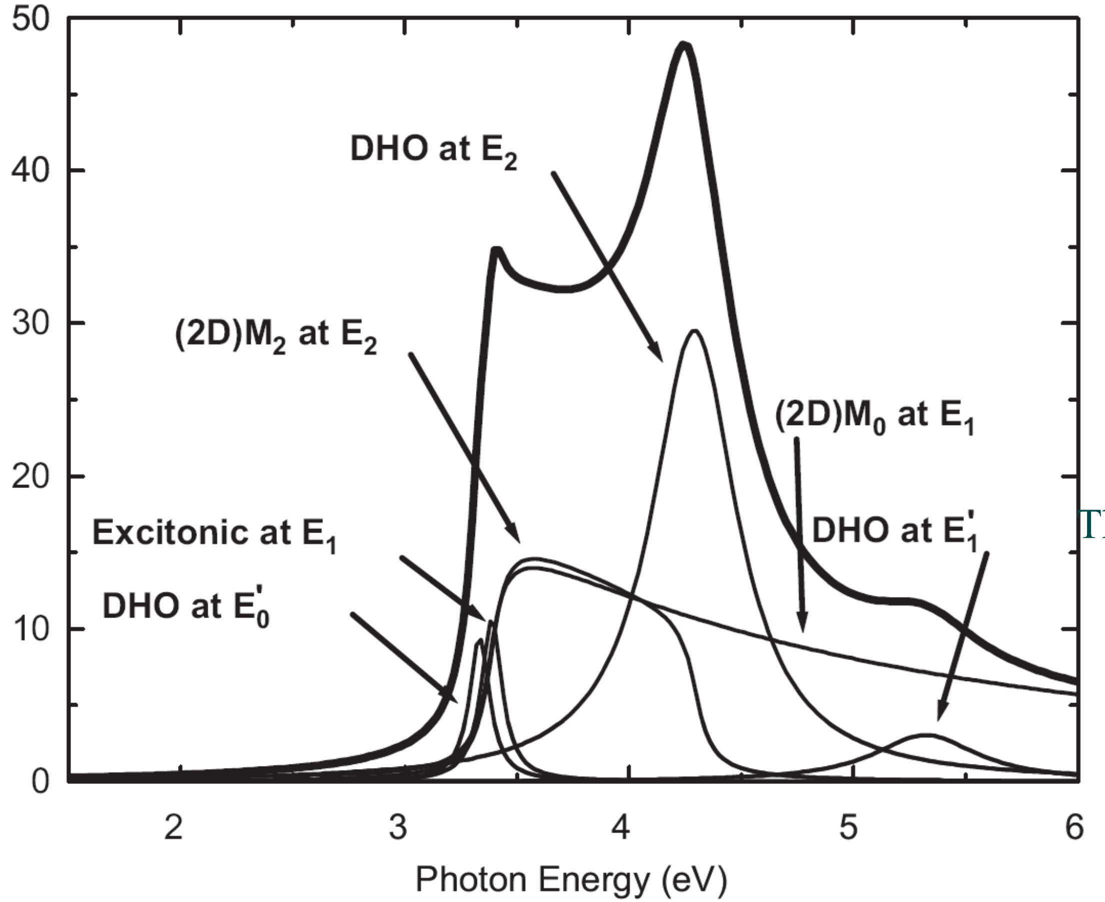

S. Adachi, Phys. Rev. B 38, 12966 (1988).

The 2D-CP at E_1 (3.4 eV) is described by

wher
e

Exciton at E_1:

Damped harmonic oscillators (DHO):

The 2D-CP at E_2 (4.2 eV) is described by

E: energies,
B, C, and F: strenghts,
Γ and γ: broadenings

Sensitive parameters can be identified by fitting the MDF model on reference data

	Fitted value for…		
	c-Si	nc-Si	a-Si
E_1	3.39±0.03	3.31±0.01	2.85±0.06
B_1	5.52±0.52	6.30±0.10	7.98±0.34
B_{1x}	0.60±0.57	—	—
γ	0.06±0.02	0.17±0.01	0.33±0.09
E_2	4.30±0.01	4.24±0.01	3.91±0.18
C_2	3.20±0.19	3.19±0.15	2.09±0.98
γ_2	0.11±0.01	0.19±0.01	0.38±0.05
F	3.68±0.26	3.89±0.26	0.99±1.38
E'_0	3.33±0.04	3.09±0.04	2.54±0.07
C'_0	0.31±0.49	0.35±0.14	1.32±0.65
γ'_0	0.03±0.02	0.13±0.03	0.28±0.04
E'_1	5.33±0.08	—	—
C'_1	0.33±0.14	—	—
γ'_1	0.11±0.05	—	—
MSE	0.34	0.32	0.34

Fit of MDF on nc-Si

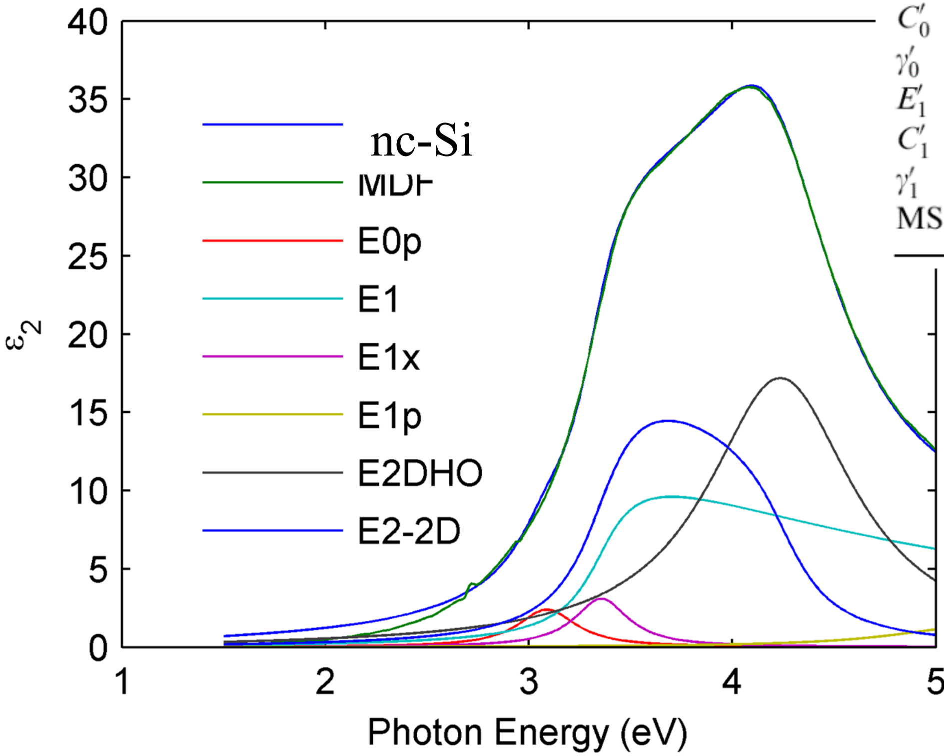

P. Basa, P. Petrik, M. Fried, L. Dobos, B. Pécz, L. Tóth, Physica E 38 (2007) 76.

Setup table of parameters to fit

- To set fitted and fixed parameters

- To define coupling

Multi point random search:

- MSE of 100000 random sets calculated

- Gradient search starting from sets of the 50 best MSEs

- Best-MSE gradient search result chosen as final result

Couple ↓ Ratio

Parname	Lower	Param	Upper	Fit	C	X
d1 (nm)	37.0000	41.0000	41.000	1	0	0.000
d2 (nm)	318.0000	318.3226	322.000	1	0	0.000
d3 (nm)	22.0000	22.9648	26.000	1	0	0.000
fv1 (%)	0.4200	0.4468	0.460	1	0	0.000
fv2 (%)	0.4600	0.4932	0.510	1	0	0.000
fv3 (%)	0.5500	0.6000	0.600	1	0	0.000
E_0p (eV)	3.2500	3.3500	3.500	0	0	0.000
C_0p	0.0200	0.0700	0.270	0	0	0.000
gm_0p	0.0200	0.0900	0.190	0	0	0.000
E_1 (eV)	3.3200	3.3612	3.400	1	0	0.000
A_1	3.7000	3.9833	4.000	1	0	0.000
A_1x	0.8000	1.1153	1.300	0	11	0.280
Gm_1 (eV)	0.0800	0.0970	0.120	1	0	0.000
E_1p (eV)	5.3300	5.3300	5.330	0	0	0.000
C_1p	0.3000	0.3000	0.300	0	0	0.000
gm_1p	0.1200	0.1200	0.120	0	0	0.000
E_2 (eV)	4.1900	4.2600	4.260	1	0	0.000
A_2	4.2600	4.3379	4.380	1	0	0.000
C_2	3.5200	3.2534	3.520	0	18	0.750
Gm_2 (eV)	0.0600	0.0871	0.120	1	0	0.000
gm_2	0.1200	0.1722	0.200	1	0	0.000
ei	0.0000	0.4371	1.000	1	0	0.000

Solar cell research

Durvított üveg

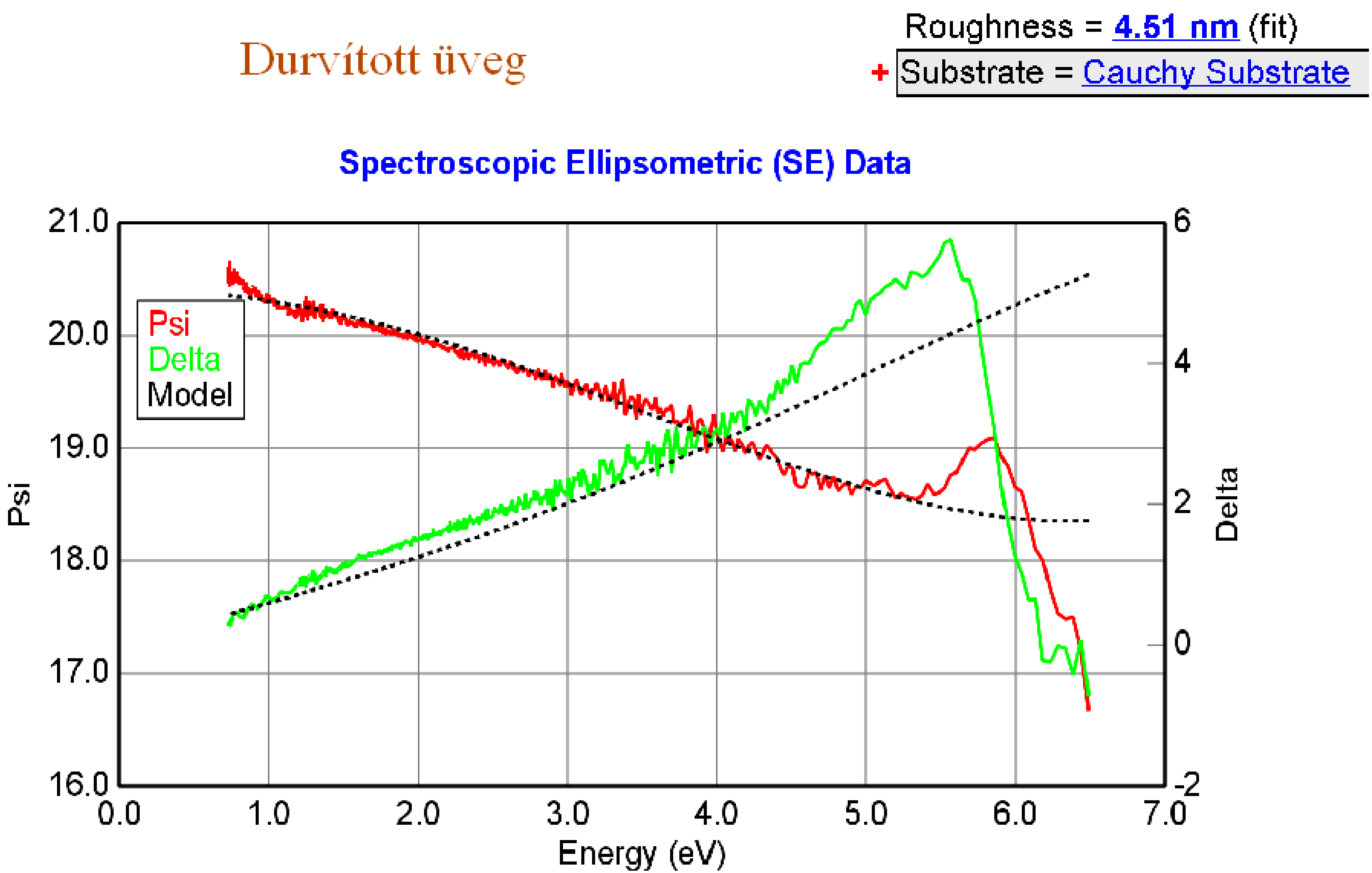

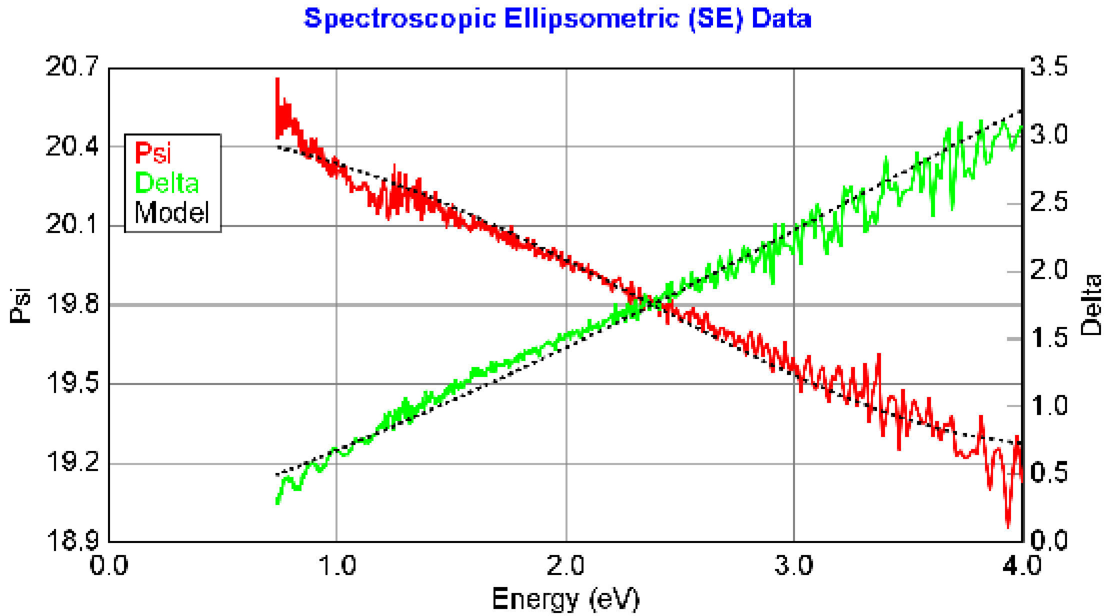

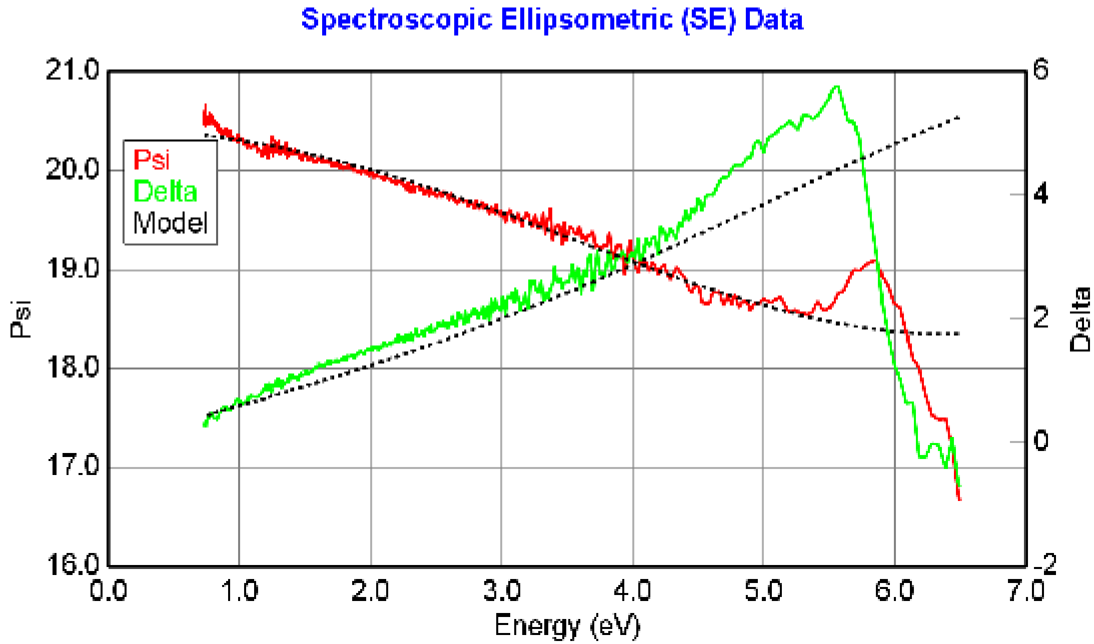

Durvított üveg

MSE = 1.377
Roughness = 5.13 ± 0.029 nm
A = 1.507 ± 0.0002
B = 0.00975 ± 0.000164
C = -0.00043 ± 0.000019
n @ 1.960 eV = 1.528

- forgó kompenzátor!
- forgó polarizátorral nem mérhető

	RCE	RAE	RPE
Measure all Ψ/Δ accurately	Yes	No	No
Measure Δ handedness	Yes	No	No
Combine with fast CCD detection	Yes	Yes	Yes

Model of amorphous silicon for solar cells

- Layer # 3 = a-Si parameterized Thickness # 3 = **668.48 nm** (fit)
  - Add Oscillator Show Dialog
  - Einf = 1.000
  - 1: Type = Cody-Lorentz Amp. = **117.582** (fit)
    - Br = **2.302** (fit) Eo = 3.594 Eg = **1.610** (fit)
    - Ep = 1.943 Et = 0.000 Eu = 0.500 Common Eg = OFF

Layer # 2 = SIO2_JAW Thickness # 2 = **137.24 nm** (fit)

Layer # 1 = INTR_JAW Thickness # 1 = 1.00 nm

Substrate = SI_JAW

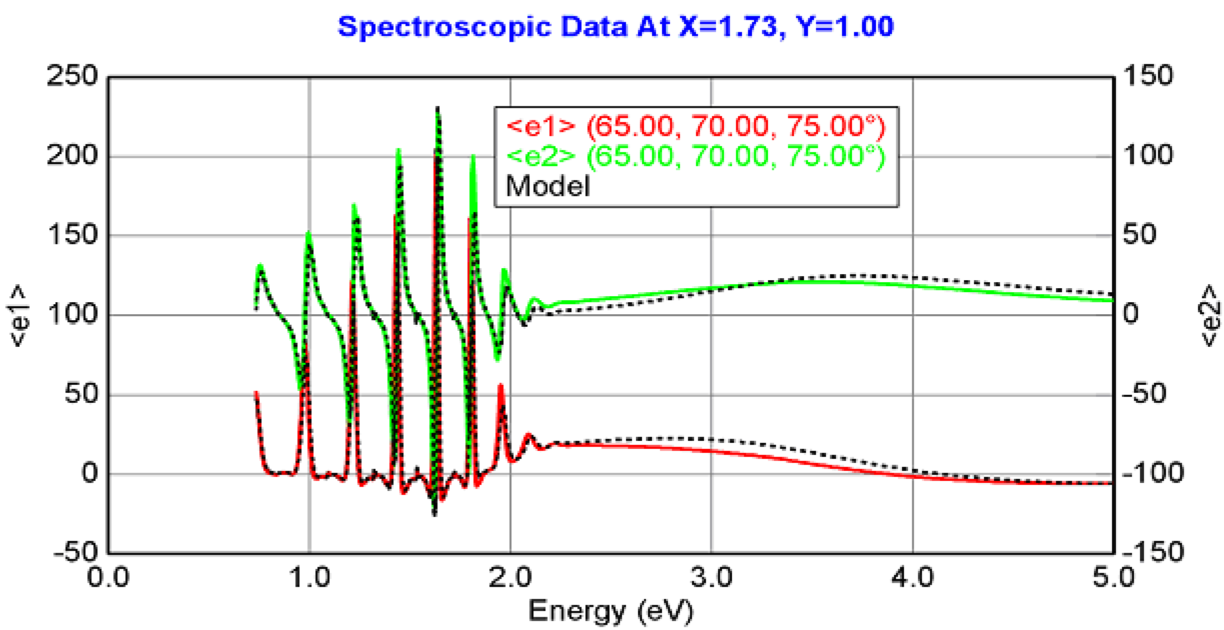

Error of the fit

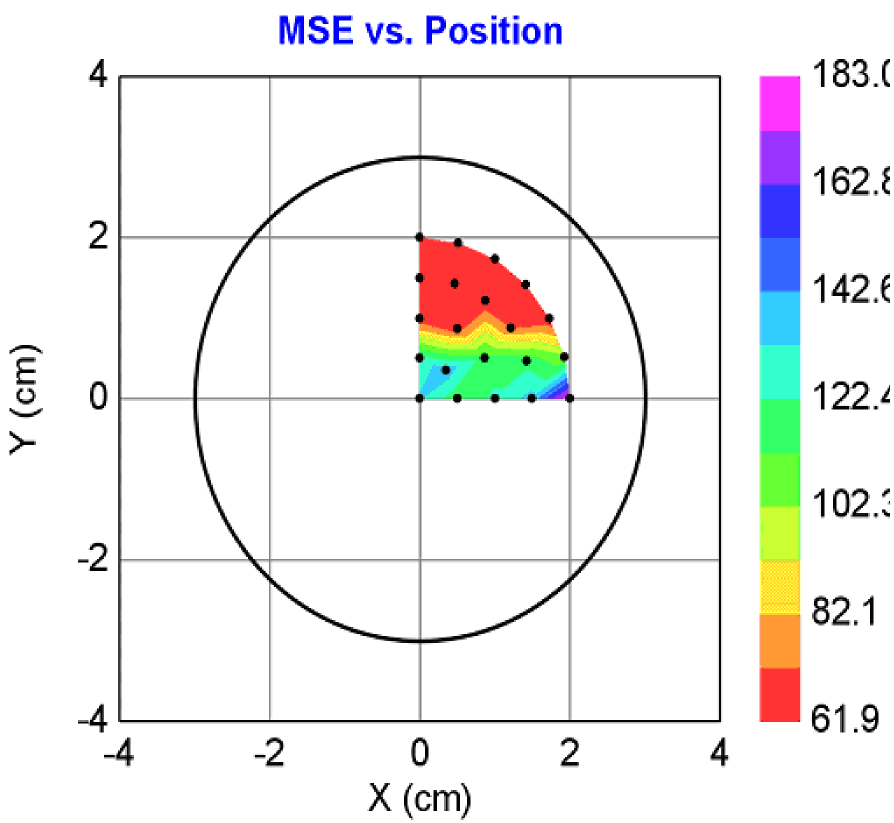

Thickness of the amorphous layer

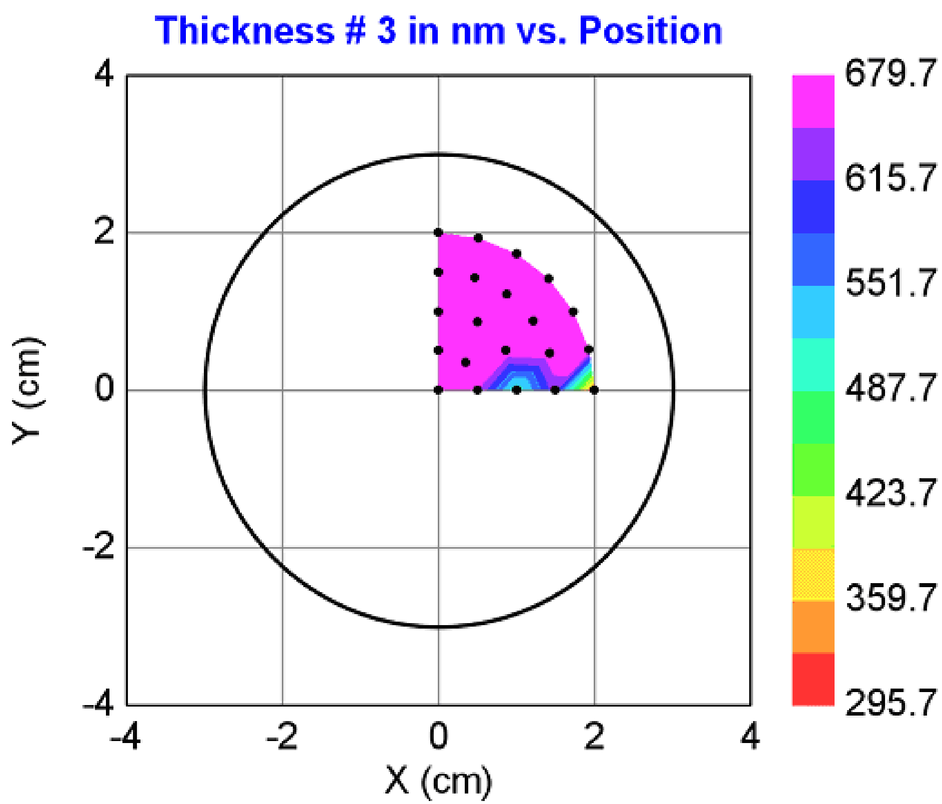

Broadening

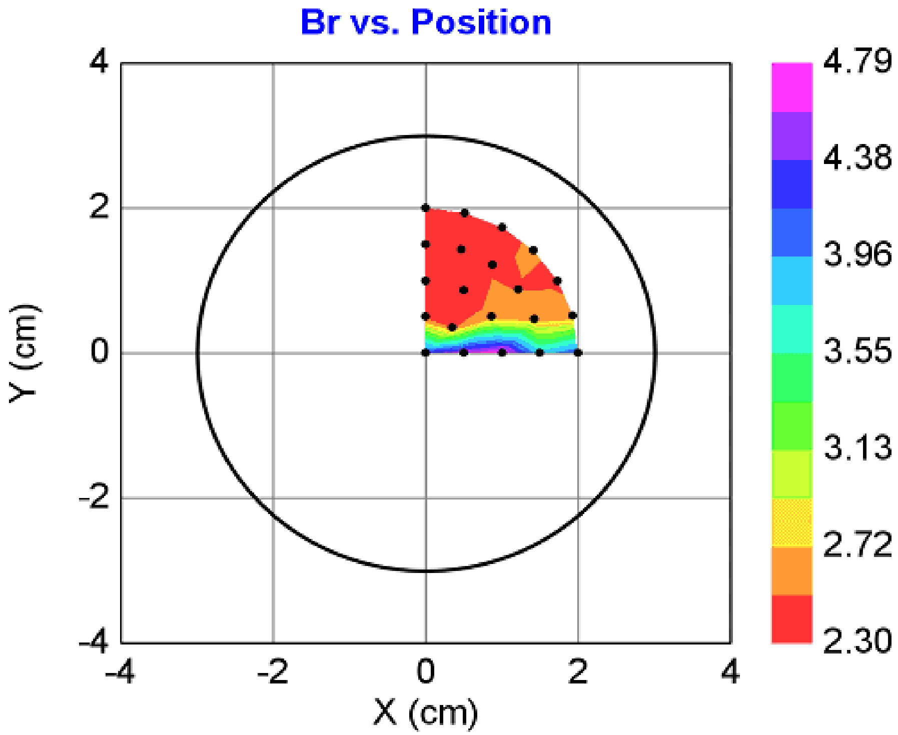

Gap

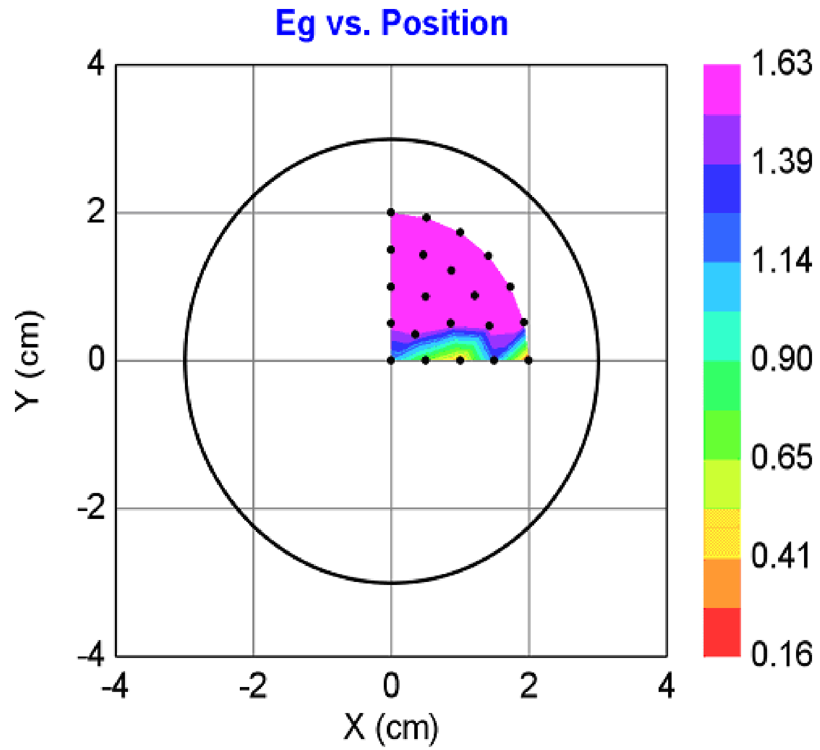

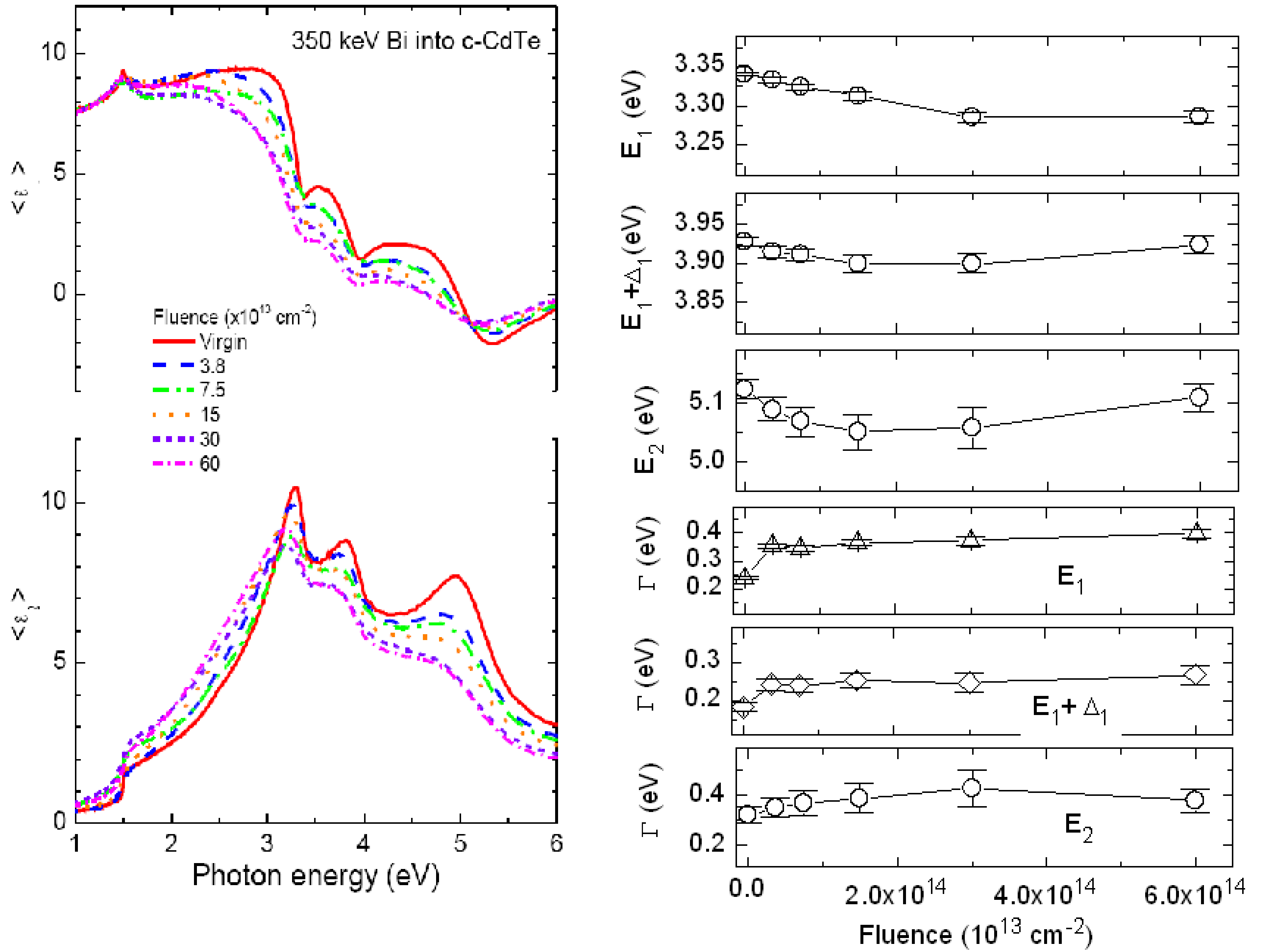

350 keV Bi into c-CdTe
Fluence (x10^13 cm^-2)
Virgin
3.8
7.5
15
30
60
Photon energy (eV)
E1 (eV)
E1+Δ1 (eV)
E2 (eV)
Γ (eV)
E1
E1+ Δ1
E2
Fluence (10^13 cm^-2)
0.0
2.0x10^14
4.0x10^14
6.0x10^14

Bioellipsometry

•Liquid cell

Capacity	0.2 ml
Angle of incidence	75°
Flow rate	Below 0.5 ml/min
Solution amount for 1 hour (at least)	30 ml
Windows diameter	4 mm
Sample size (O-ring)	27x7 mm

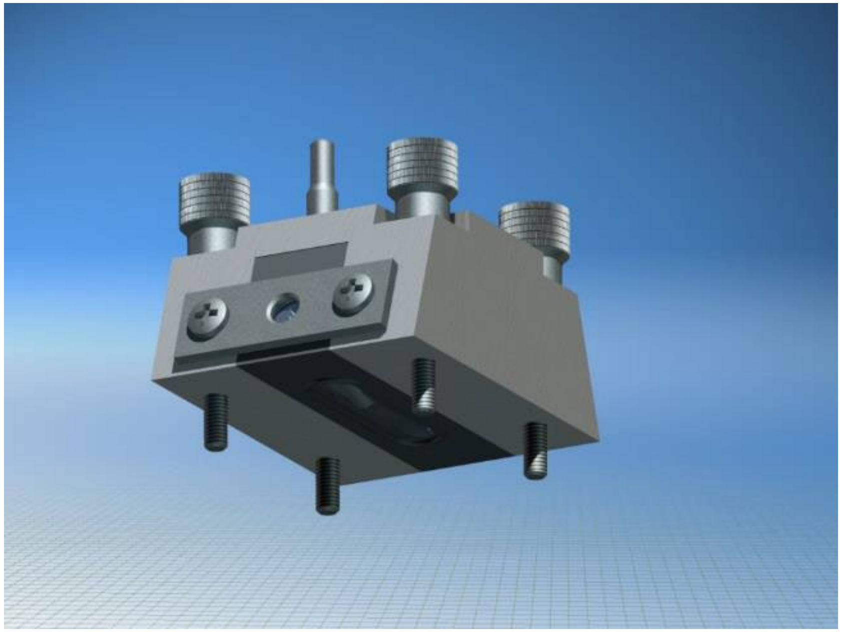

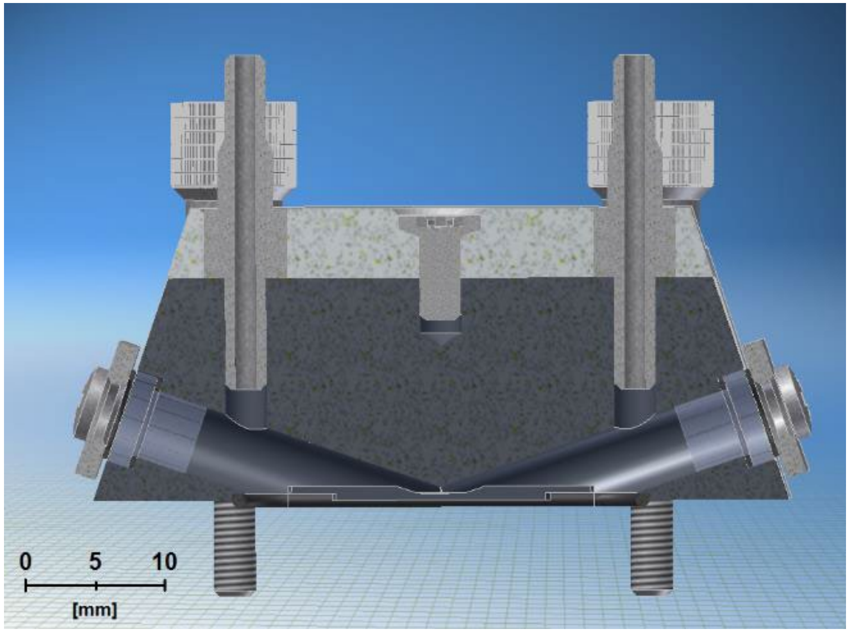

S. Kurunczi, A. Nemeth, T. Hulber, P. Kozma, P. Petrik, H. Jankovics, A. Sebestyen, F. Vonderviszt, M. Fried, I. Bársony, "In situ ellipsometric study of surface immobilization of flagellar filaments", Applied Surface Science 257 (2010) 319.

Immobilization in a liquid cell using a SOPRA ES4G ellipsometer

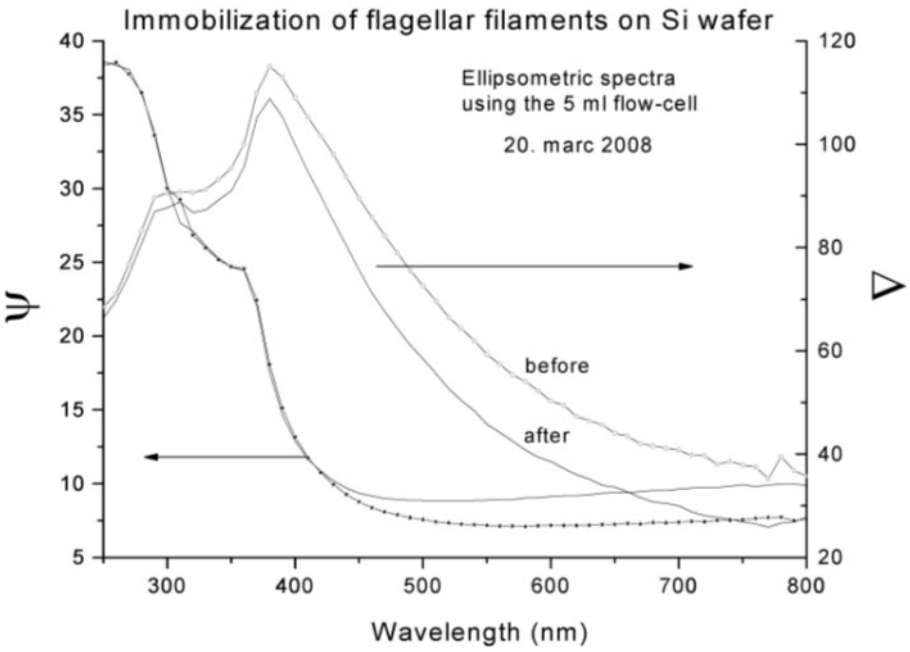

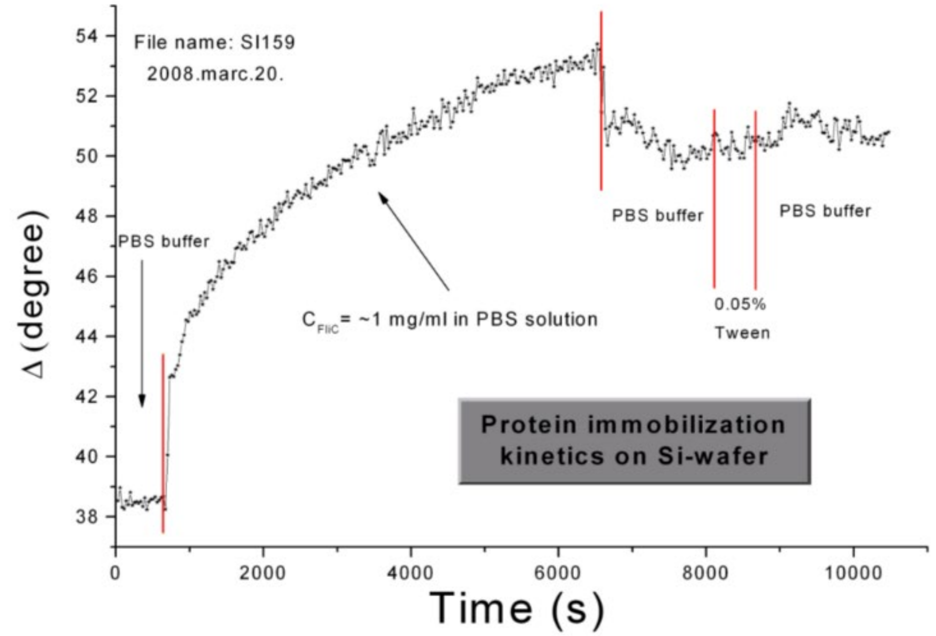

•Surface morphology

- Applying log-normal lenght distribution (x_m = 285 nm, w = 1.24 nm), 600 particles:

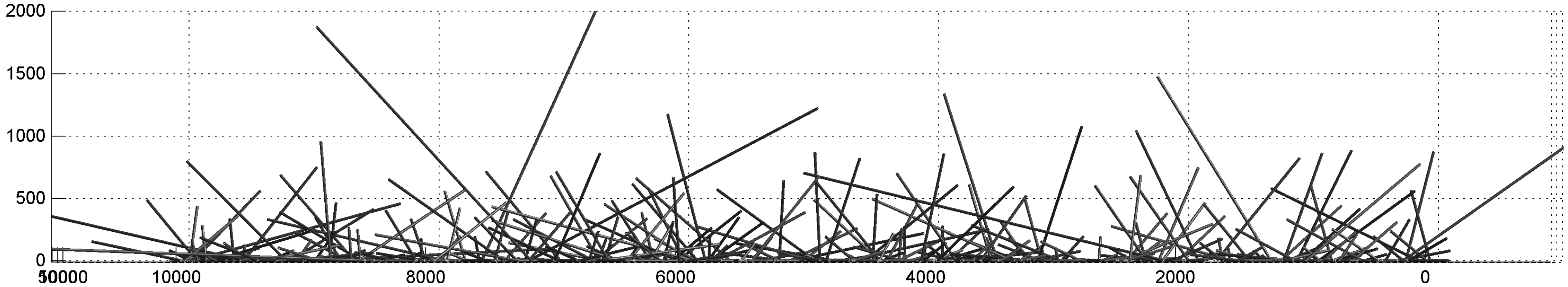

- Applying normal lenght distribution (x_m = 600 nm, w = 100 nm), 600 particles:

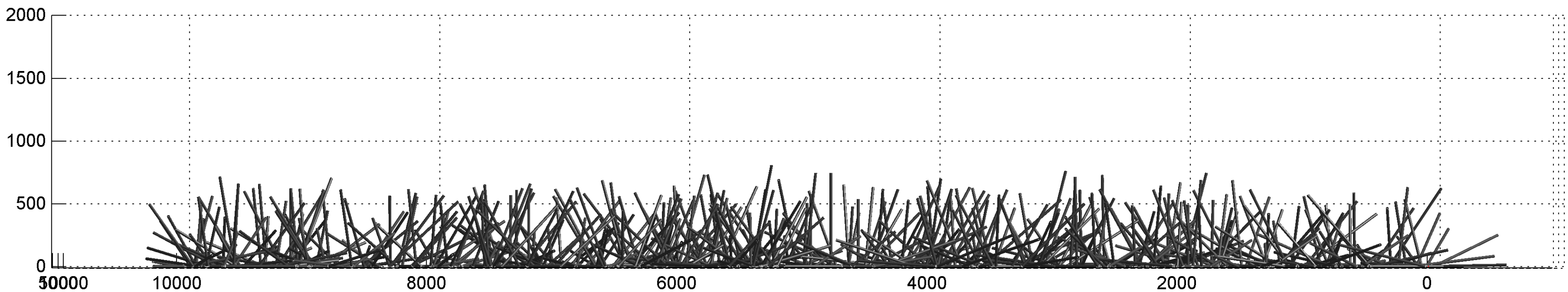

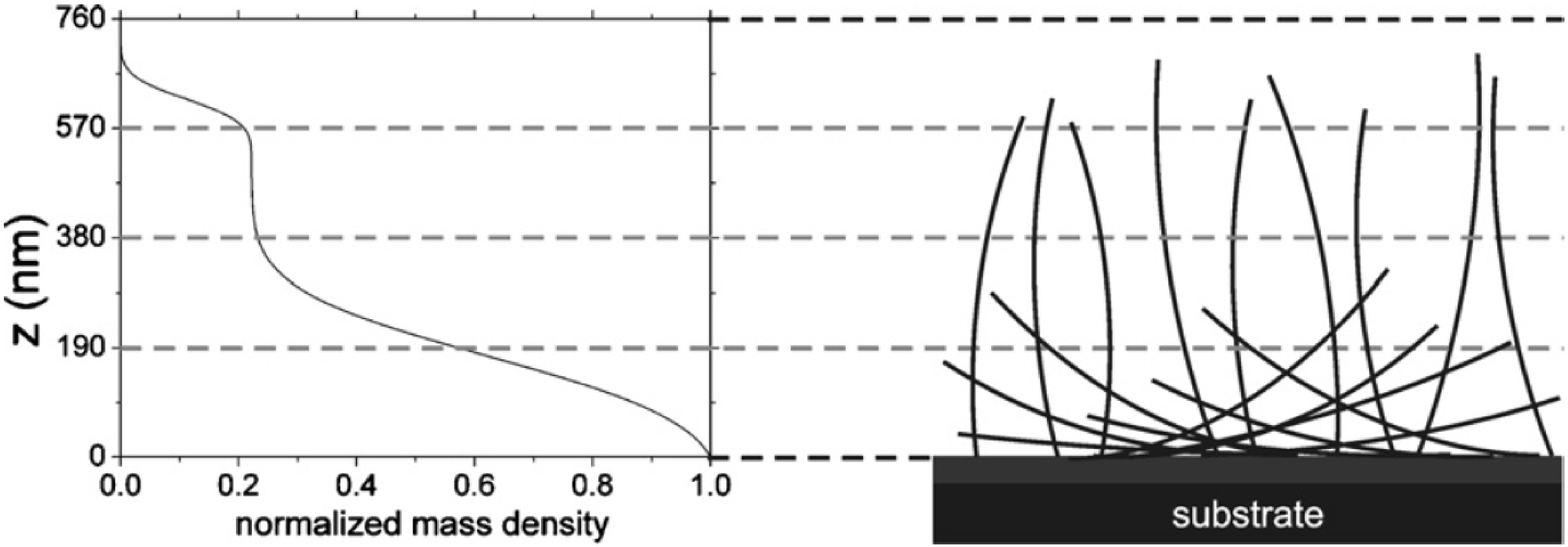

P. Kozma, D. Kozma, A. Nemeth, H. Jankovics, S. Kurunczi, R. Horvath, F. Vonderviszt, M. Fried, P. Petrik, In-depth characterization and computational 3D reconstruction of flagellar filament protein layer structure based on in situ spectroscopic ellipsometry, Applied Surface Science 257 (2011) 7160.

•Simulation

SE

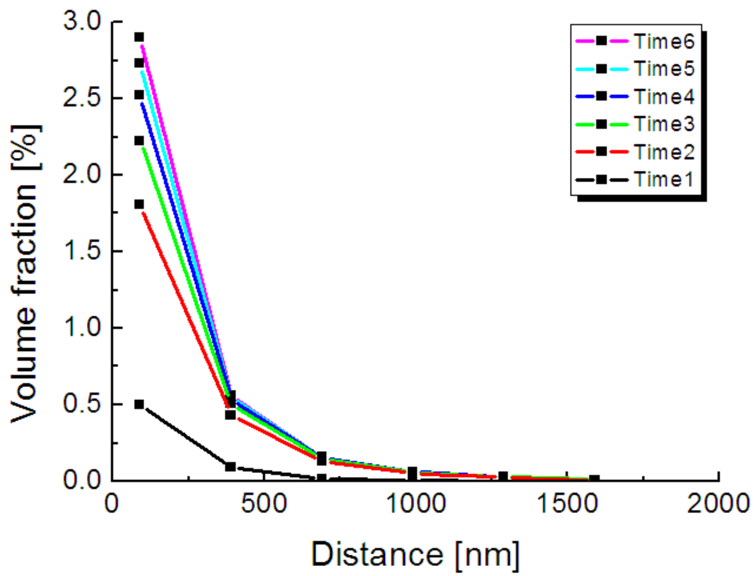

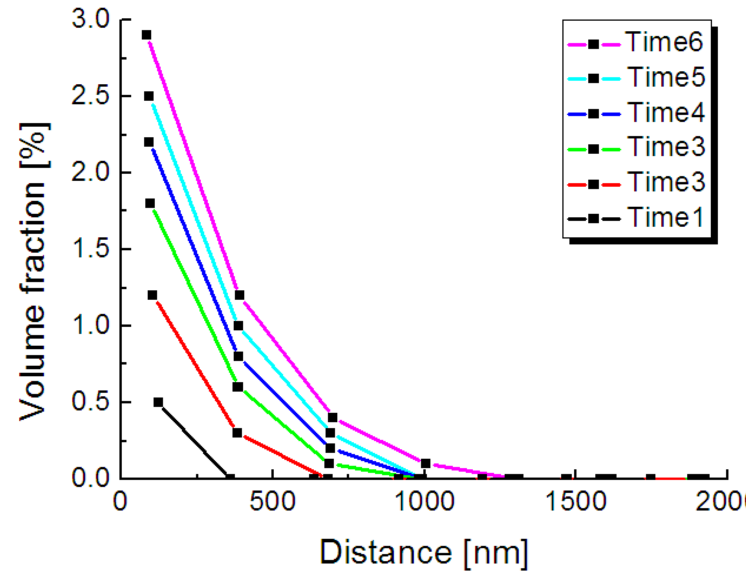

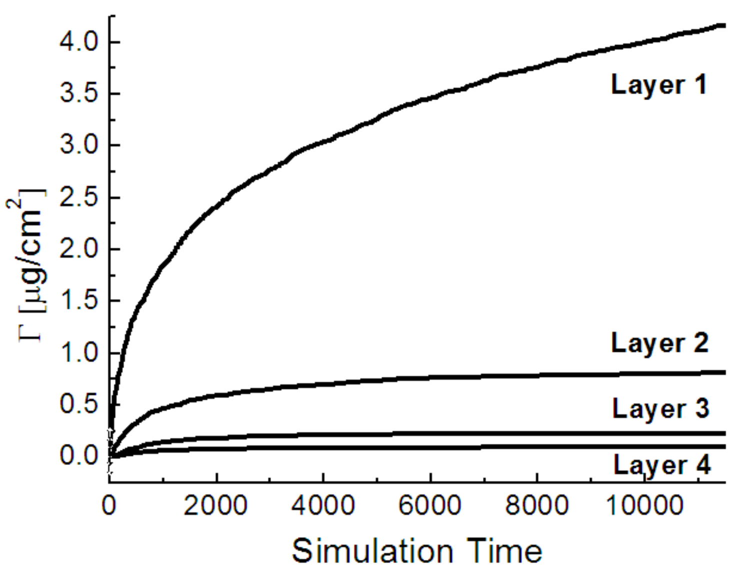

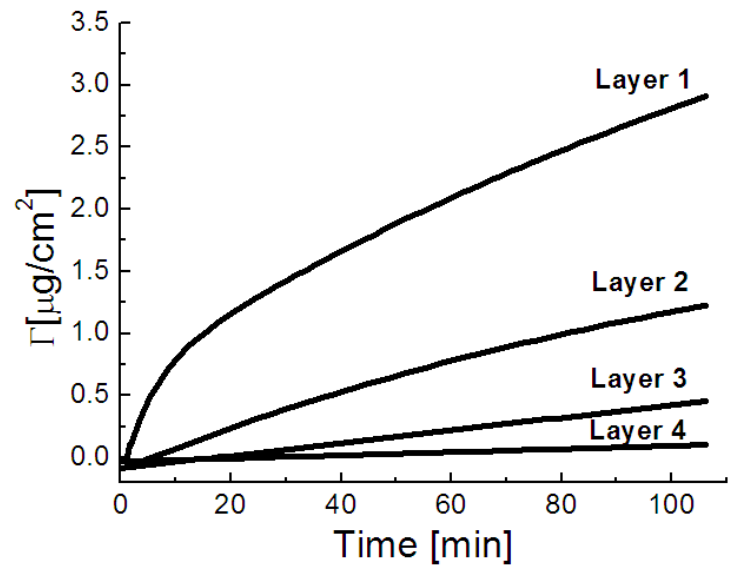

Combination of grating coupled interferometry with spectroscopic ellipsometry

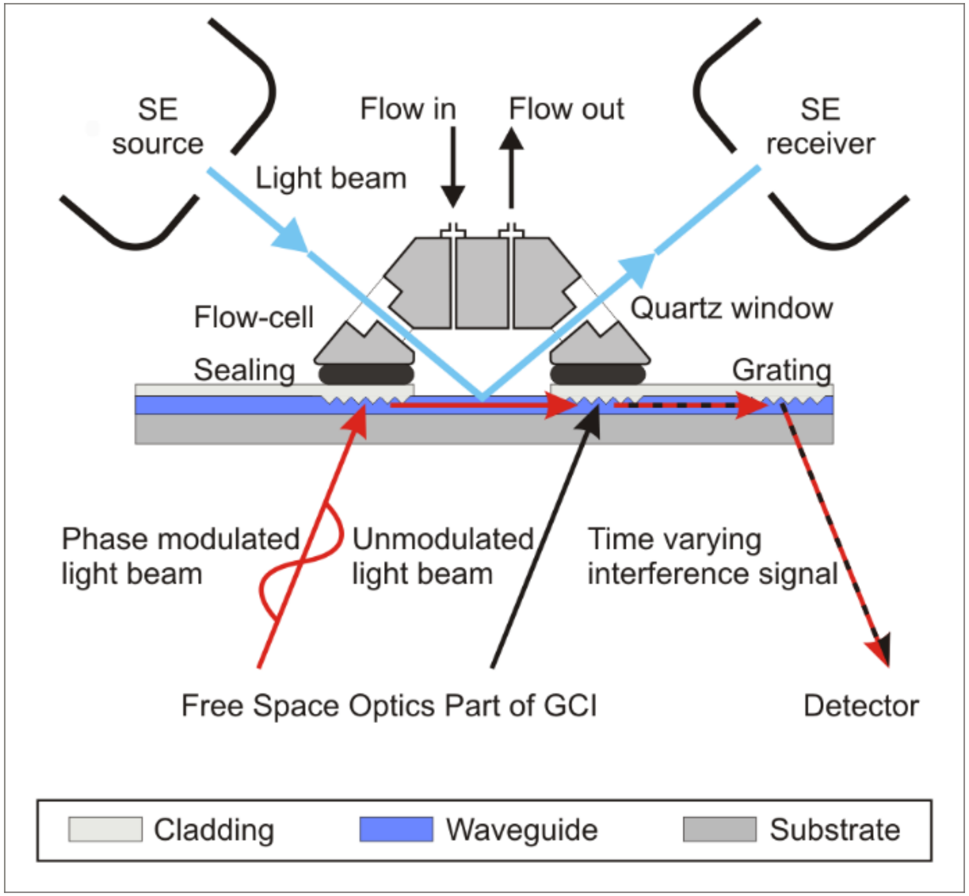

THE INTERFEROMETER:

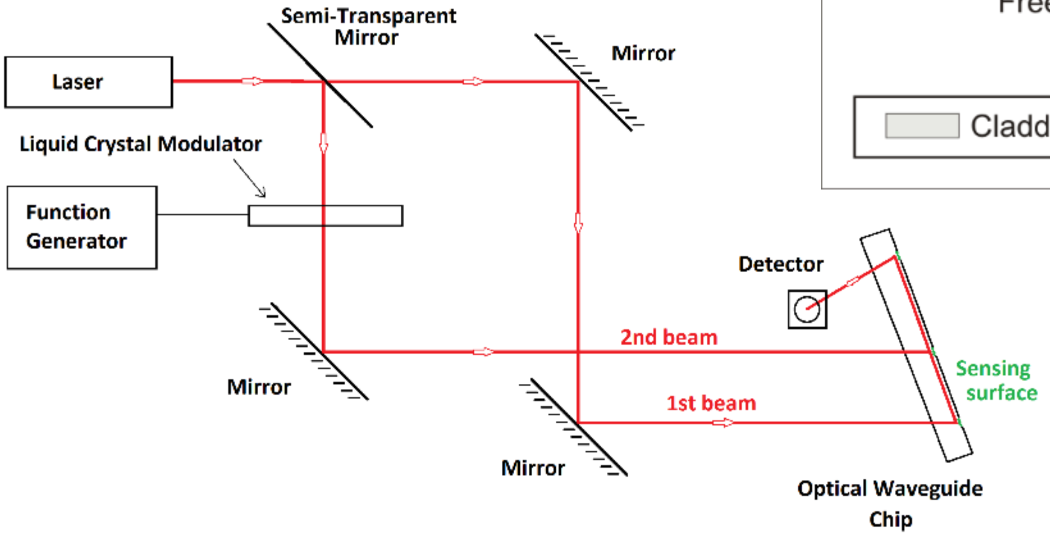

E. Agocs, P. Kozma, J. Nador, B. Kalas, A. Hamori, M. Janosov, S. Kurunczi, B. Fodor, M. Fried, R. Horvath, P. Petrik, “In-situ simultaneous monitoring of layer adsorption in aqueous solutions using grating coupled optical waveguide interferometry combined with spectroscopic ellipsometry“, to be published.

Combination of grating coupled interferometry with spectroscopic ellipsometry

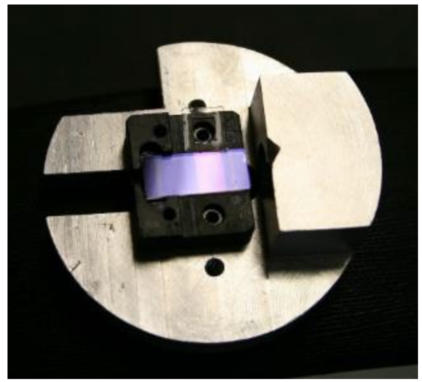

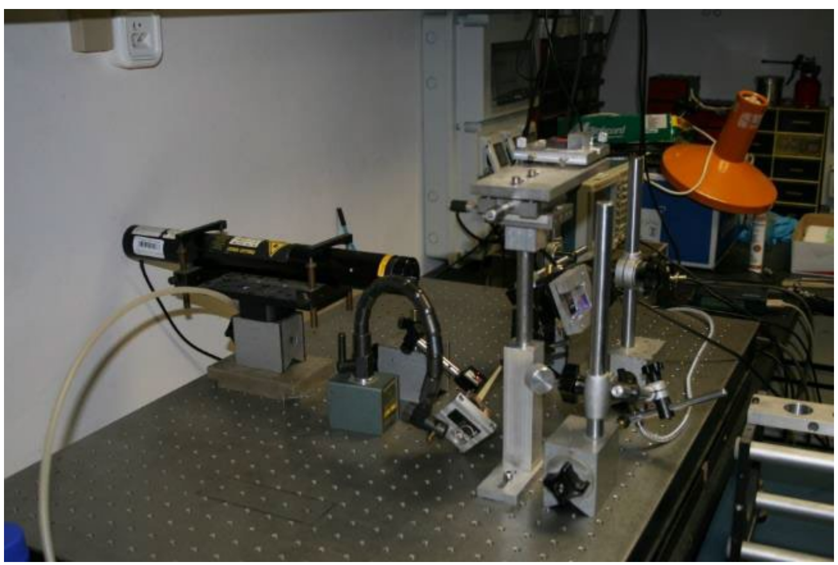

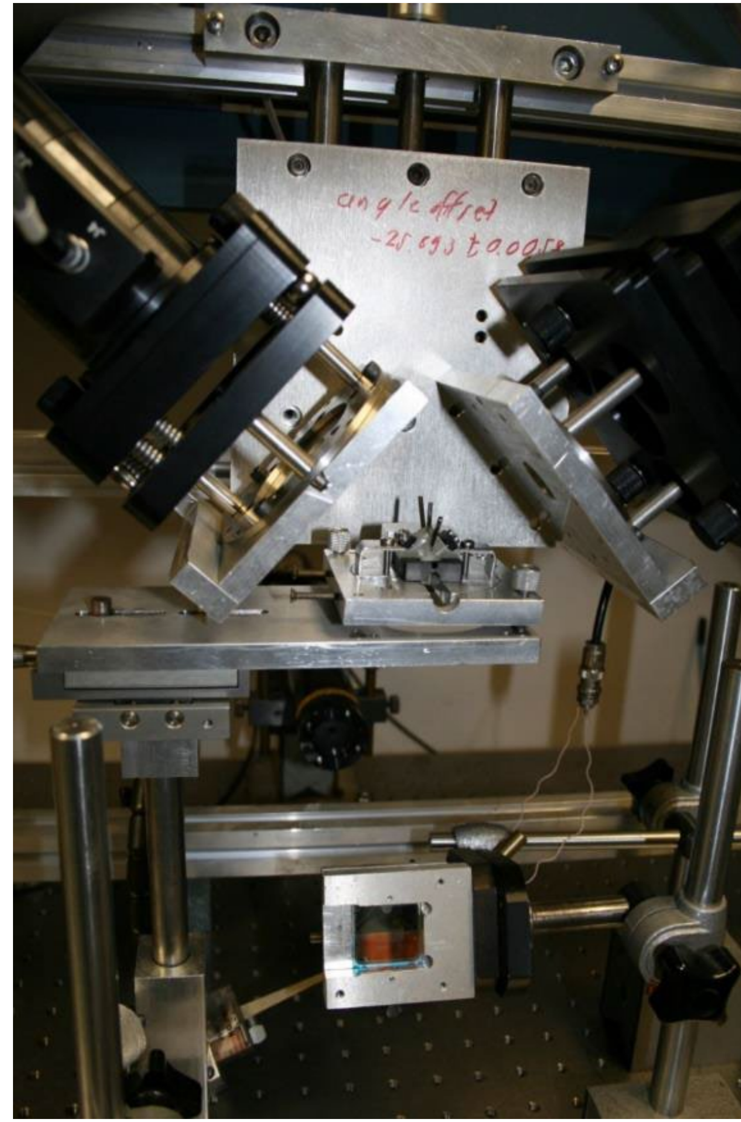

GCI + SE on protein deposition

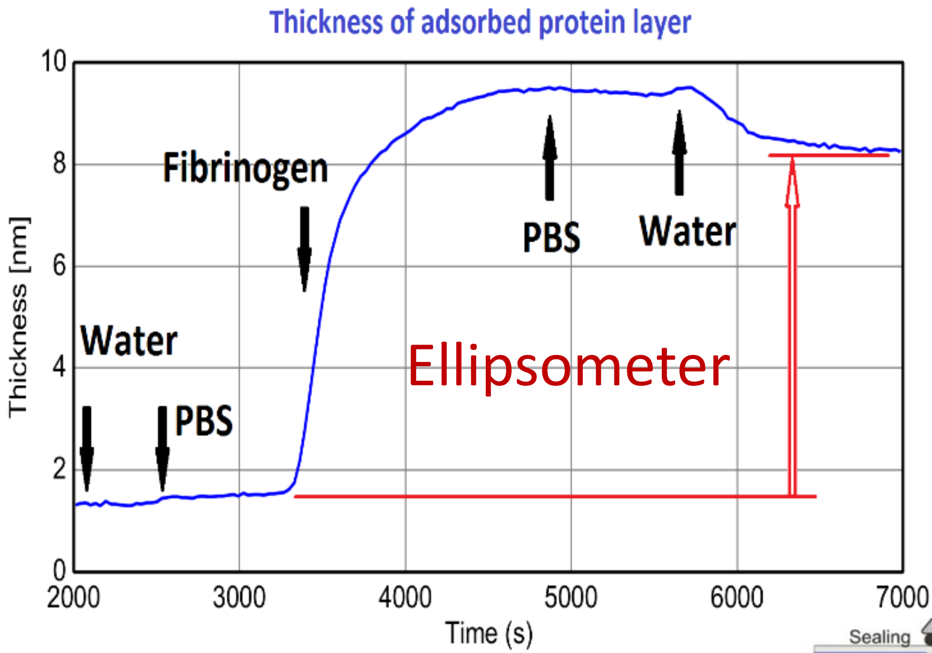

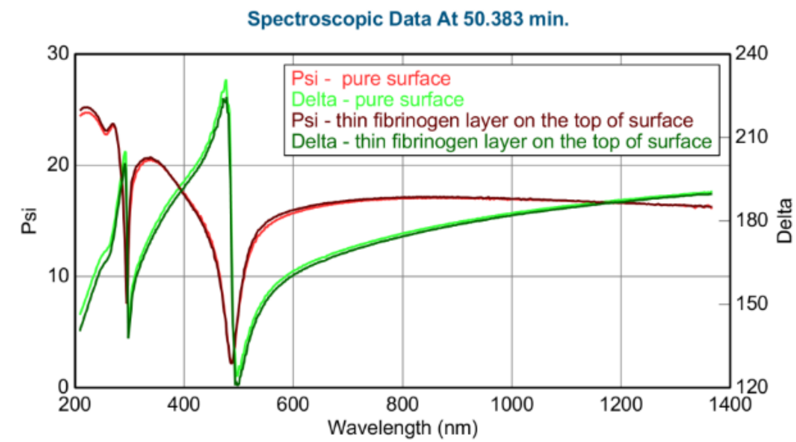

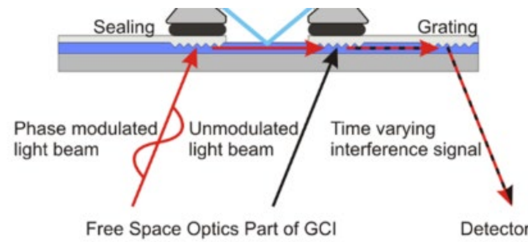

Interferometer

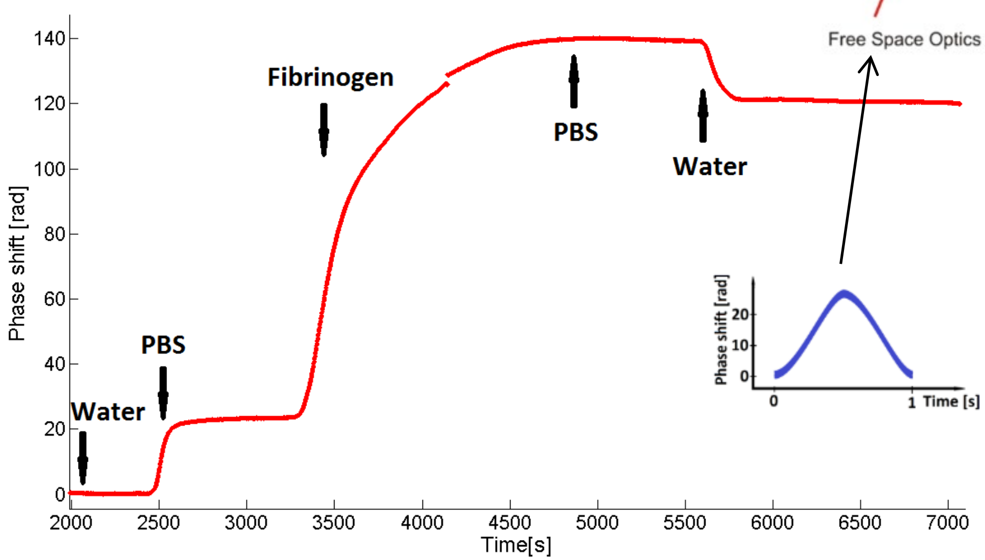

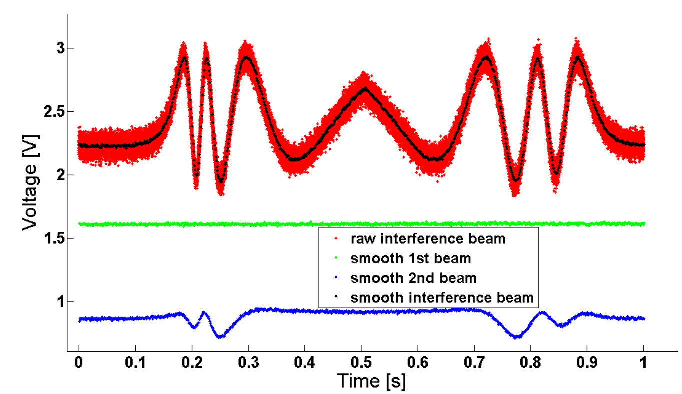

Combined GCI-SE test measurements

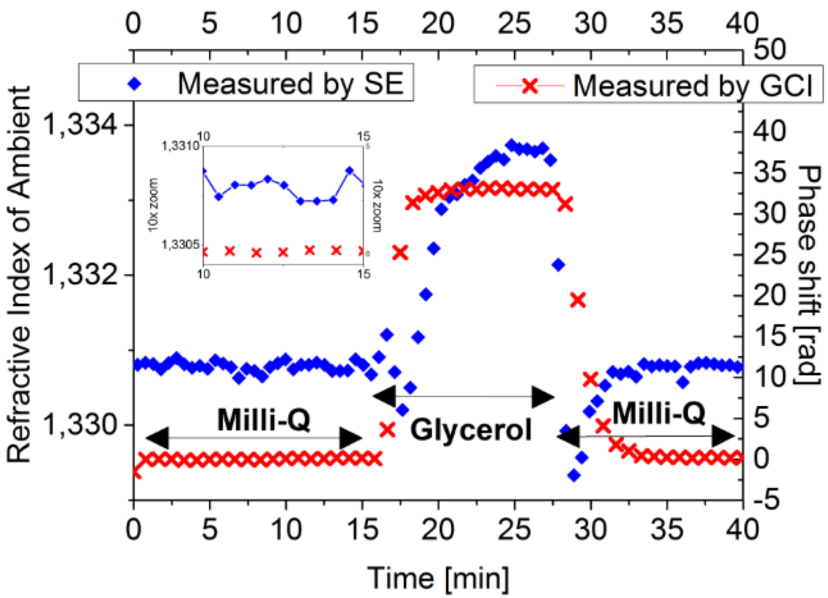

Polyelectrolite deposition

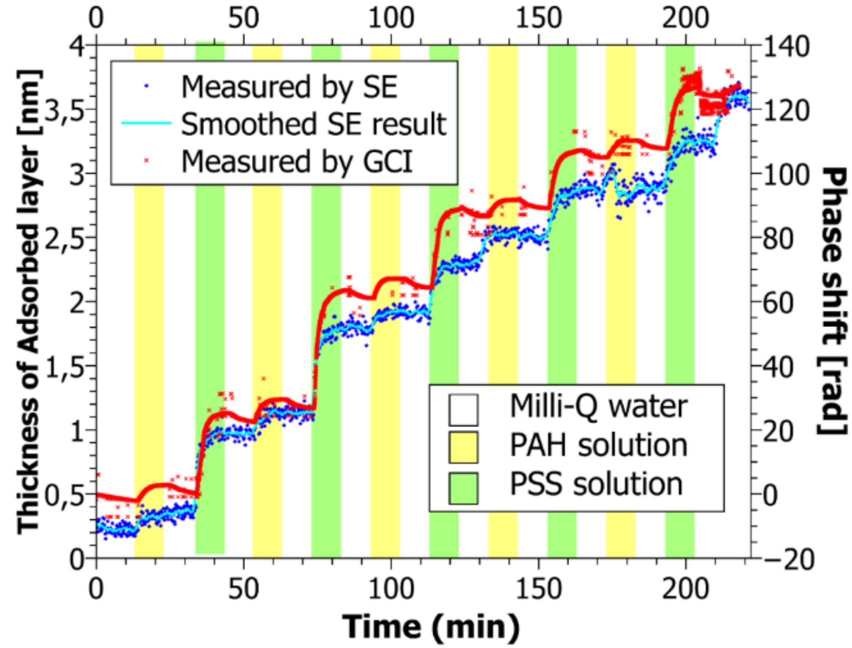

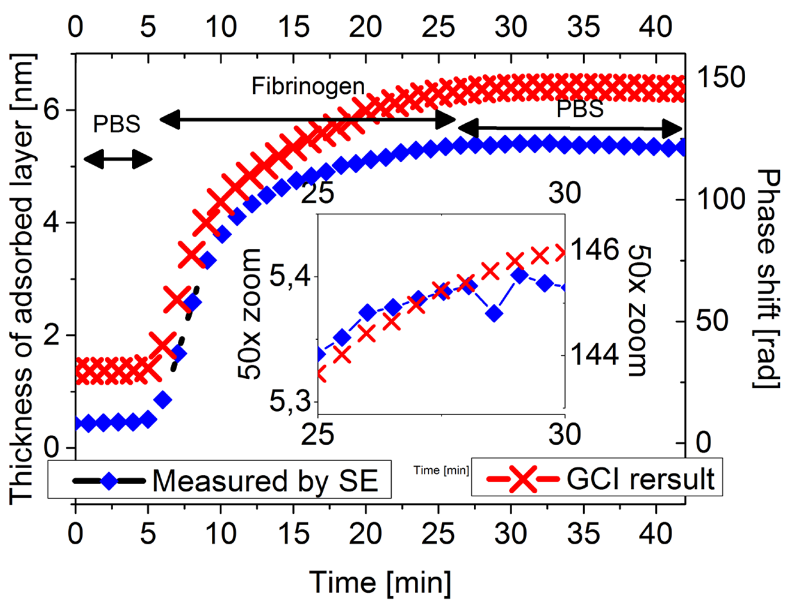

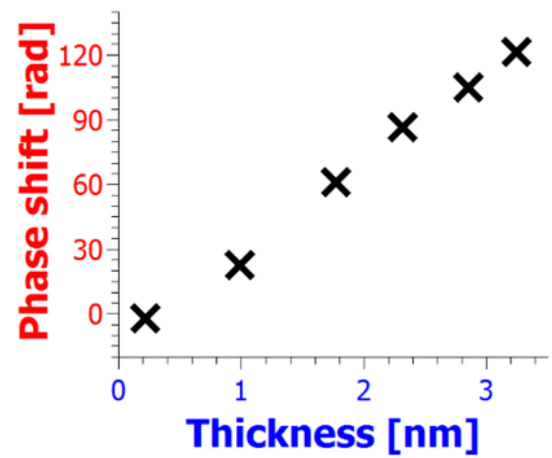

Standard flow cell configuration

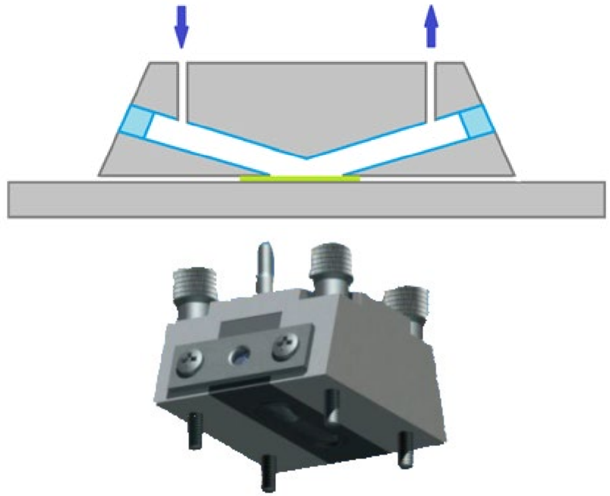

Kretschmann configuration

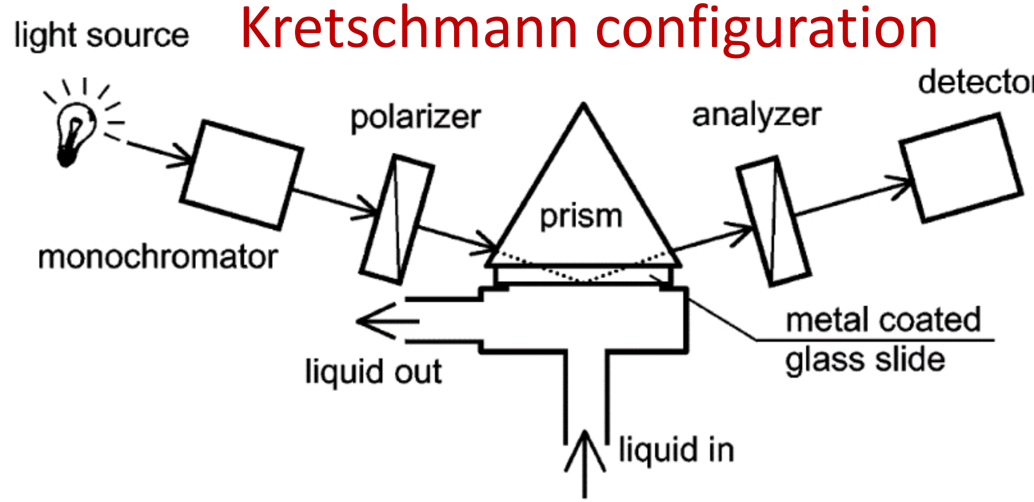

M.Poksinski, H.Arwin, “Protein monolayers monitored by internal reflection ellipsometry”, Thin Solid Films 455 –456 (2004) 716–721.

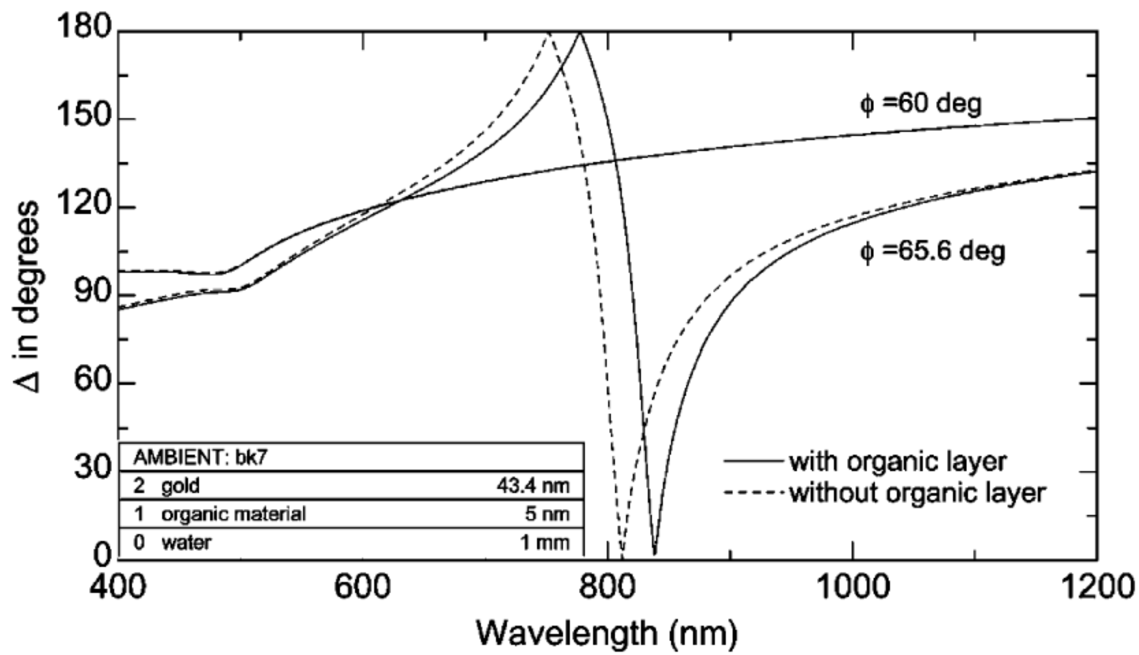

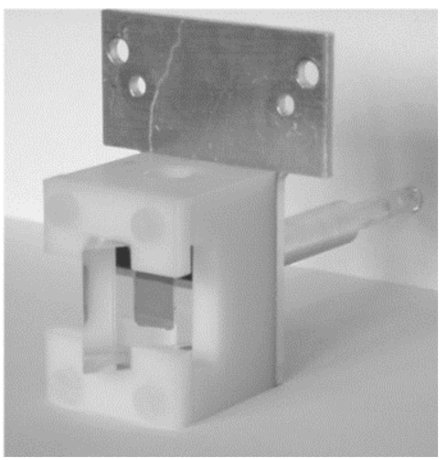

Another Kretschmann configuration

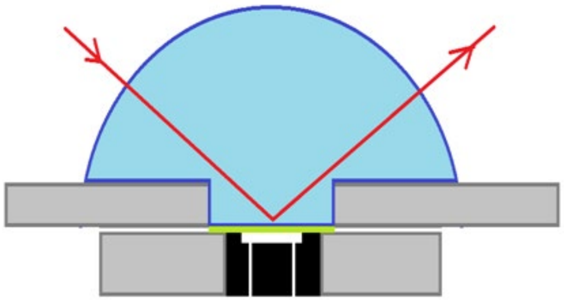

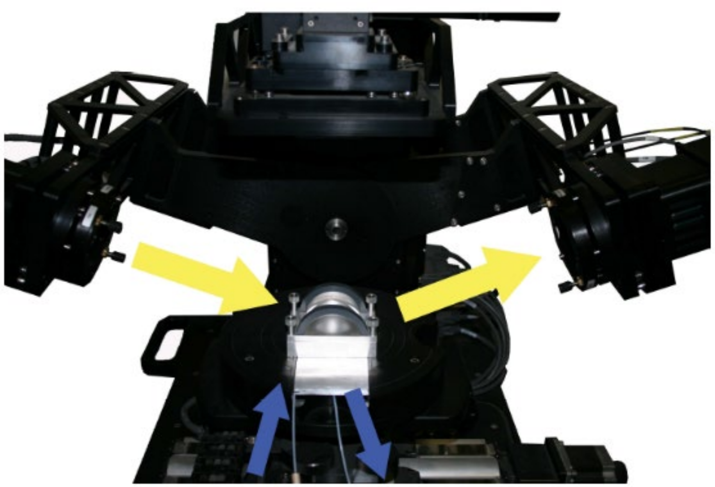

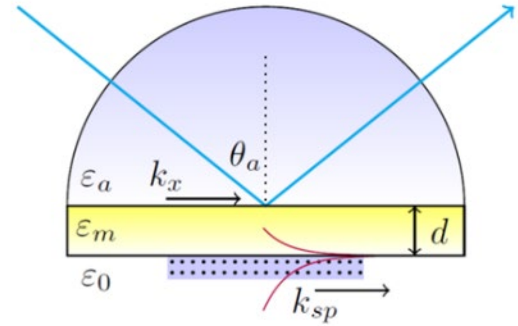

Plot of
abs(r_p/r_s)

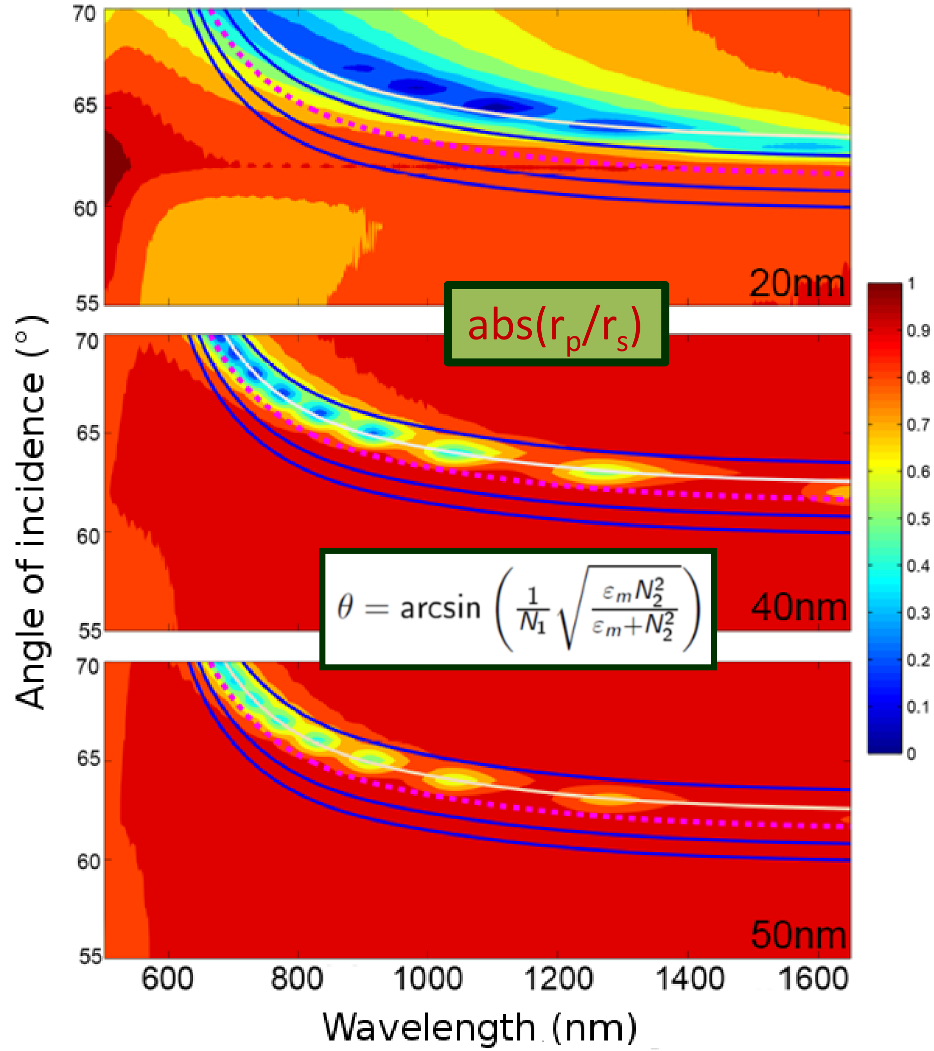

Measurement with the hemi-spherical Kretschmann setup

DIFFERENCE WITH AND WITHOUT A FIBRINOGEN LAYER

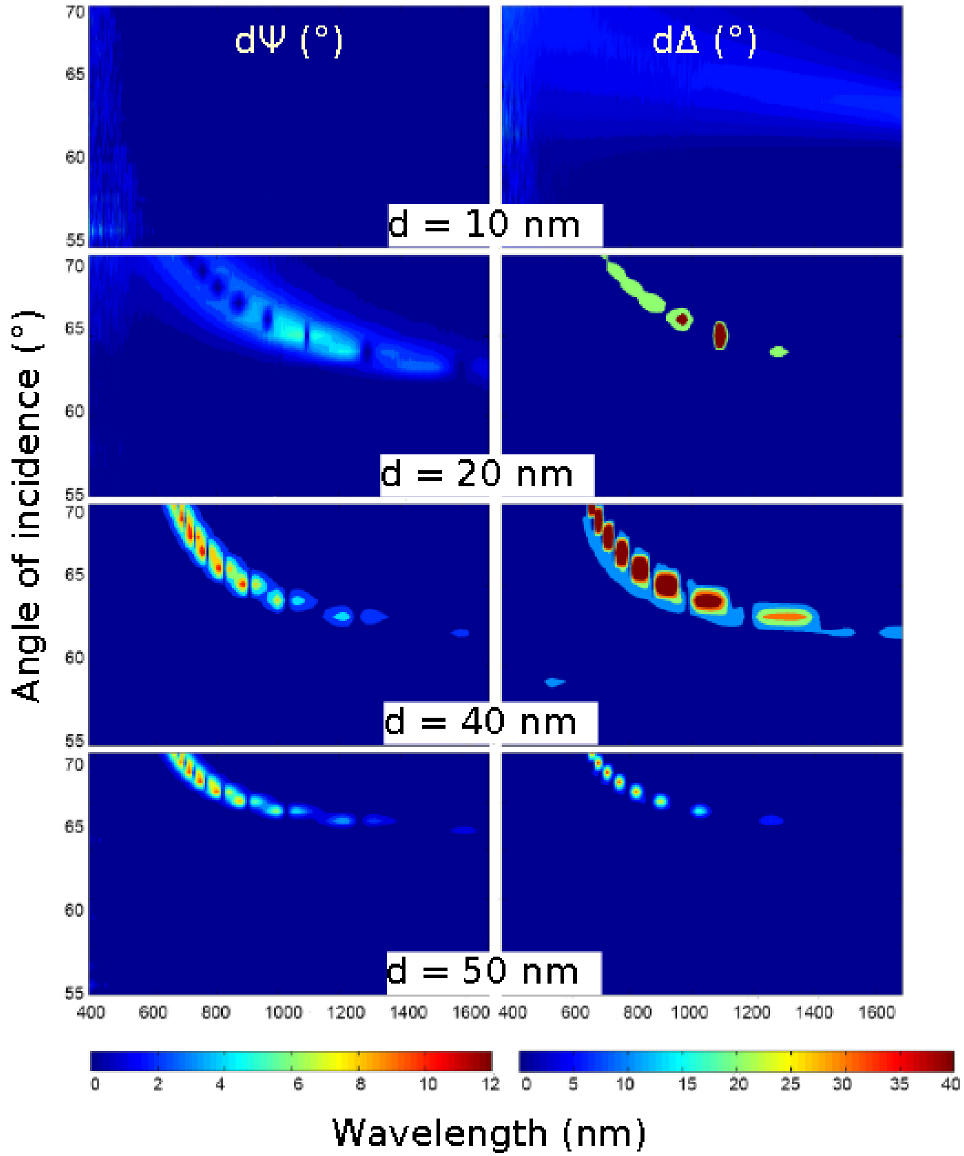

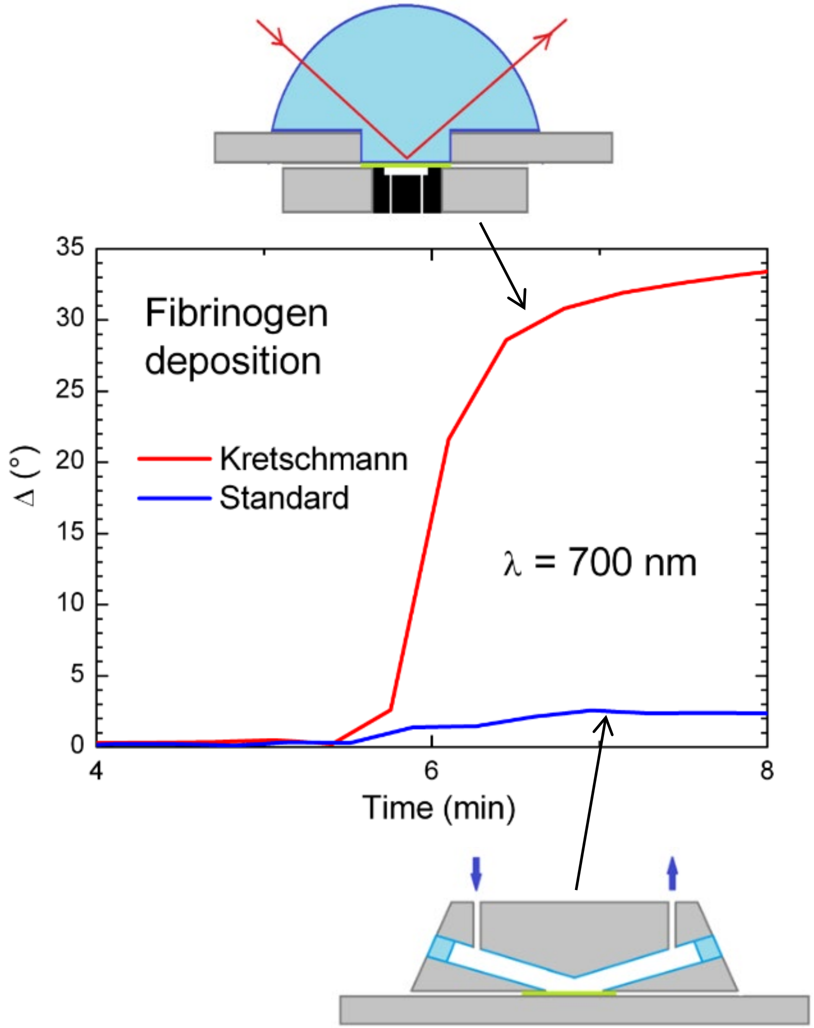

E. Agocs, B. Kalas, P. Kozma, P. Petrik, "Plasmon enhanced adsorption monitoring by multiple angle of incidence spectroscopic ellipsometry in the Kretschmann geometry", to be published.

•Glazed ceramic layers by SE, RBS and in-air PIXE

T. Lohner, E. Agócs, P. Petrik, Z. Zolnai, E. Szilágyi, I. Kovács, Z. Szőkefalvi-Nagy, L. Tóth, A. L. Tóth, L. Illés, I. Bársony, “Spectroellipsometric and ion beam analytical studies on a glazed ceramic object with metallic lustre decoration”, Thin Solid FIlms 571 (2014) 715.

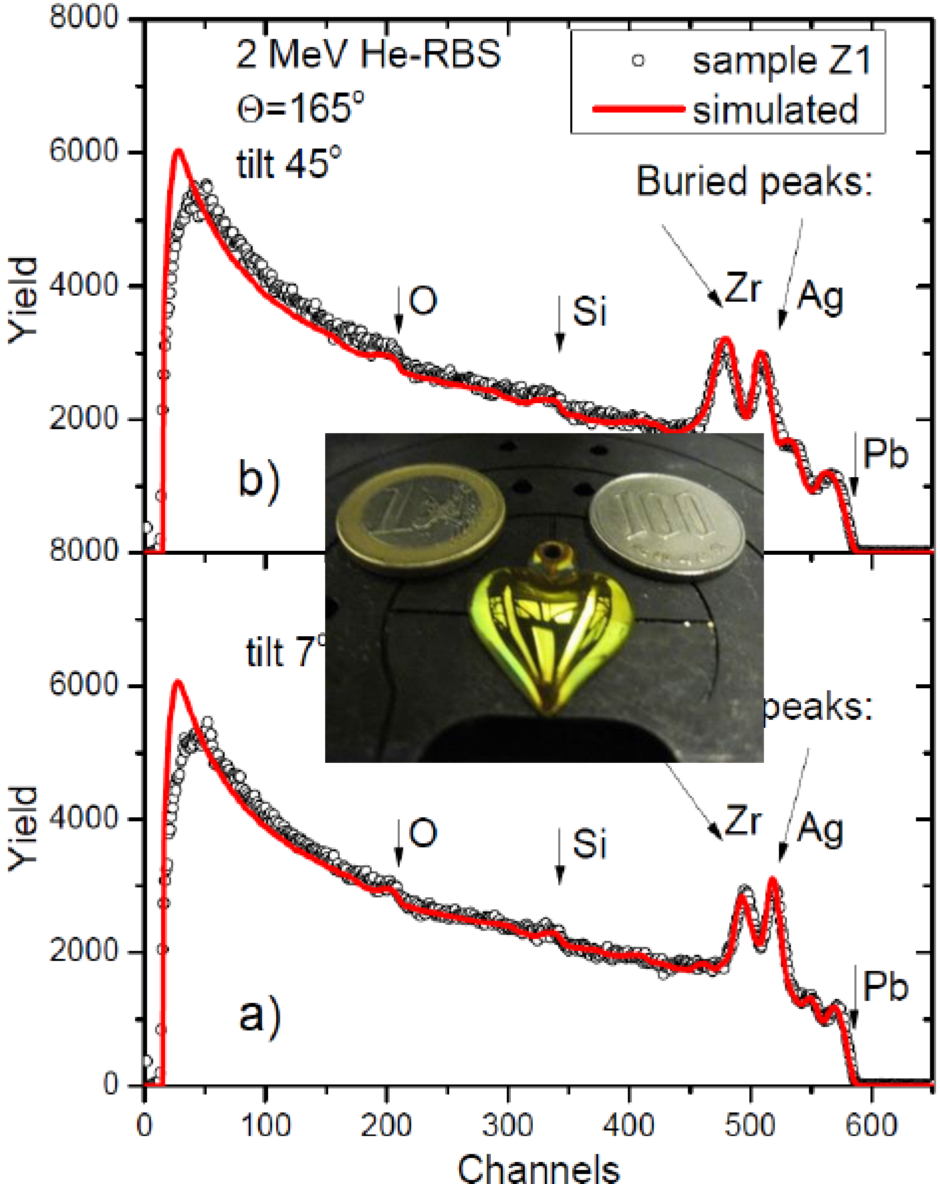

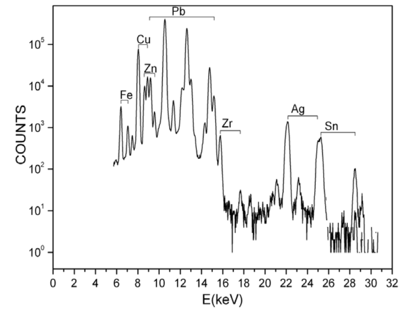

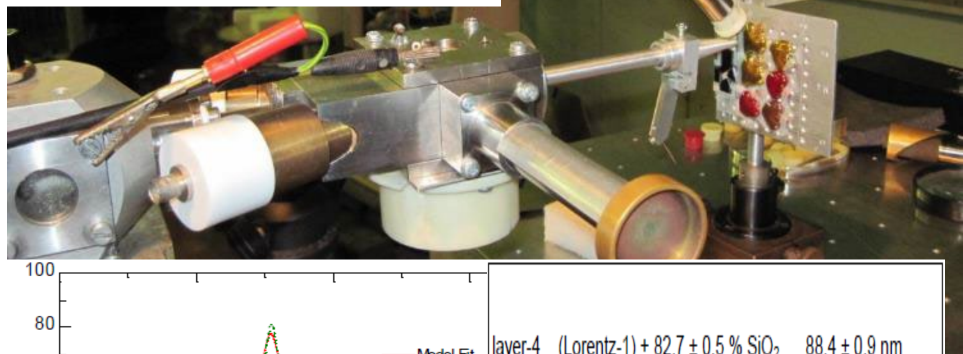

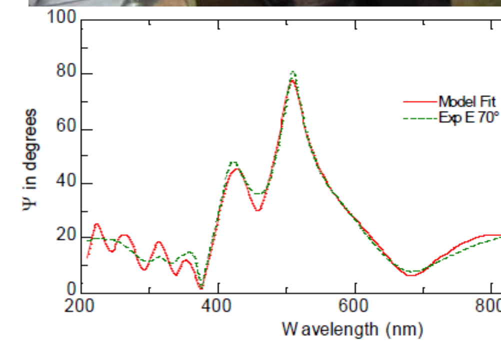

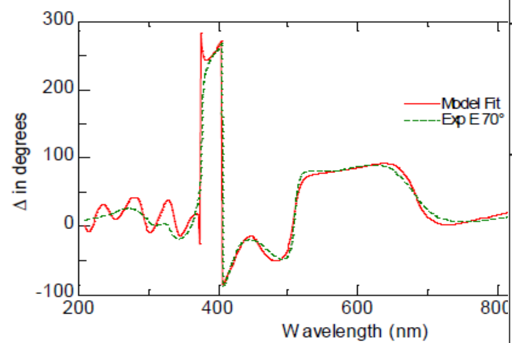

layer-4	(Lorentz-1) + 82.7 ± 0.5 % SiO_2	88.4 ± 0.9 nm
layer-3	(Lorentz-2) + 15.1 ± 1 % Ag	9.8 ± 0.2 nm
layer-2	(Lorentz-2) + 99.1 ± 0.2 % ZrO_2	85.1 ± 0.8 nm
layer-1	(Lorentz-2)	100 ± 3 nm
	(Lorentz-1) substrate	